Stability analysis of Fuzzy-Model-Based control systems and its application to control of continuum manipulators

Yu, Yan

Awarding institution:
King's College London

A thesis submitted for the degree of
Doctor of Philosophy

Stability Analysis of Fuzzy-Model-Based Control Systems and its Application to Control of Continuum Manipulators

Author : Yan Yu
Student Number : 1468372
First Supervisor : Dr. Hak-Keung Lam
Second Supervisor : Dr. Hongbin Liu

01/01/2019

Ph.D. in Robotics
Department of Informatics
Faculty of Natural & Mathematical Sciences
King's College London

Acknowledgment

First, I would like to express my sincere gratitude to my supervisor Dr. Hak-keung Lam for his continuous support during my Ph.D study. His patience, motivation and expert knowledge help me to overcome the difficulties all over the research and thesis writing stages. His enthusiasm on research gives us the best example and influences me all the time.

Besides my supervisor, I also would like to thank my colleagues who cooperate with me during my research. Without them, my research process could have been much harder and slower.

Last but not least, I would like to express my deepest gratitude to my parents who always support me spiritually and financially.

Abstract

This thesis is to investigate the stability analysis problem of fuzzy-model-based (FMB) control systems and its application to continuum manipulator. The stability analysis of T-S FMB control system is conducted on the basis of Lyapunov stability theory relaxed by membership-function-dependent (MFD) approach and extended to some practical control problems, such as control input saturation and guaranteed cost of system indexes, where numerical examples are raised to verify the effectiveness of each proposed fuzzy control method. An example of continuum manipulator is developed to show the process and advantage of applying fuzzy logic and fuzzy-model-based control method to a real complex practical system. The main works and contributions of the thesis are summarized in the following three parts:

1) The first part of work is presented in Chapter 3. It aims to consider the output feedback tracking control with control input saturation problem under the framework of Takagi-Sugeno (T-S) FMB control. A fuzzy controller is employed to close the feedback loop, which aims to drive the system states to follow those of a stable reference model subject to $\mathcal{H}_\infty$ performance. To enhance the fuzzy controller design flexibility, the number of rules and premise membership functions are not necessarily required to be the same as those of fuzzy model. To address the control input saturation problem, linear sectors are created by local upper and lower bounds to include the possible control area such that the nonlinear saturation problem can be tackled. Then, the membership-function-dependent (MFD) technique is used to embed the information of membership functions to the stability conditions in the form of linear matrix inequalities (LMIs). A numerical example is given to demonstrate the effectiveness of proposed method dealing with different levels of control input saturation problems.

2) The second part of the thesis work is presented in Chapter 4. It considers the guaranteed cost stability analysis in the T-S FMB control system. A weighted quadratic cost function is considered as the cost index to measure the performance of the closed-loop system in terms of the system states, system outputs and control signals. The stability of the FMB control system is investigated by the Lyapunov stability theory subject to the minimization of cost index for performance realization. An MFD approach using the piecewise linear membership

functions (PLMFs) technique is employed to include the information of membership functions into the stability analysis. MFD stability conditions in terms of LMIs are obtained to determine the system stability and feedback gains with the consideration of the system performance measured by the cost function. An numerical example is raised to demonstrate the effectiveness and merits of proposed method.

3) The third part of the work focuses on applying fuzzy logic and FMB control to a practical example of nonlinear systems. Based on the curve geometry of a continuum manipulator, the kinetic and potential energies can be calculated as the integration of the energies regarding to each slice perpendicular to the backbone of the manipulator. By applying Euler-Lagrangian equation of motion, we can obtain the dynamic model of continuum manipulator with the capabilities of bending and contractile. Two traditional nonlinear control methods, namely inverse dynamic control and sliding mode control, are implemented to drive the system states to follow the desired trajectory of a stable reference system. In order to improve the tracking performance and solve the chattering problem particularly in sliding mode control, a fuzzy sliding mode controller is proposed by applying fuzzy logic theory, which varies the value of feedback gains adaptively to the manipulator configurations and successfully attenuates the chattering problem in the traditional sliding mode control method. In order to further apply the FMB control on the practical example of nonlinear systems, the dynamic model of continuum manipulator needs to be transformed to a polynomial fuzzy model, where the fuzzy model of two-link rigid body manipulator is developed preparatively as a relatively simple practical nonlinear system. Then the development polynomial fuzzy model of continuum manipulator is proceeded with necessary simplifications.

Contents

Acknowledgment **2**

Abstract **3**

Contents **5**

Author's Publications **8**

List of Figures **9**

List of Tables **12**

Acronyms **13**

1 Overview **14**

1.1 Introduction 14

1.2 Literature Review 16

1.2.1 Fuzzy-Model-Based Control System 16

1.2.2 Relaxation of the Stability Conditions 17

1.2.3 Extension of Fuzzy-Model-Based Control Strategy 20

1.2.4 The Continuum Manipulator 21

1.3 Research Objectives 22

1.4 Organization of the Works 22

1.5 Contributions of the Thesis 24

2 Background **25**

2.1 Fuzzy Model Construction 25

2.1.1 Fuzzy Logic 25

2.1.2 Sector Nonlinearity 26

2.2 T-S Fuzzy-Model-Based Control System 28

2.3 Lyapunov Stability Analysis 30

2.4 Euler-Lagrangian Equation 31

2.5 Useful Lemmas 32

3 T-S Fuzzy-Model-Based Output Feedback Tracking Control with Control Input Saturation 34
3.1 Introduction . . . 34
3.2 Preliminary . . . 36
3.2.1 T-S Fuzzy Model . . . 36
3.2.2 Reference Model . . . 37
3.2.3 Output Feedback Fuzzy Controller . . . 37
3.2.4 Control Input Saturation . . . 38
3.3 Stability Analysis . . . 39
3.3.1 $\mathcal{H}_\infty$ Performance . . . 41
3.3.2 Control Input Saturation . . . 43
3.3.3 Tracking Control $\mathcal{H}_\infty$ Performance with Control Input Saturation . . . 45
3.3.4 Piecewise Linear Membership Functions . . . 53
3.4 Simulation Example . . . 55
3.5 Conclusions . . . 59

4 Membership-Function-Dependent Stability Analysis and Control Synthesis of Guaranteed Cost Fuzzy-Model-Based Control System 79
4.1 Introduction . . . 79
4.2 Preliminaries . . . 81
4.2.1 Fuzzy Controller . . . 81
4.2.2 Fuzzy-Model-Based Control System . . . 82
4.3 Stability Analysis . . . 82
4.3.1 Lyapunov Function . . . 82
4.3.2 Weighting Matrix . . . 83
4.3.3 Piecewise Linear Membership Functions . . . 86
4.4 Simulation Examples . . . 88
4.5 Conclusion . . . 92

5 Applications of Fuzzy Logic and Fuzzy-Model-Based Control to a Continuum Manipulator 100
5.1 Introduction . . . 101
5.2 Dynamic Model of Rigid Manipulator . . . 103
5.3 Kinematics of Continuum Manipulator . . . 104
5.4 Dynamic Model of Continuum Manipulator . . . 107
5.4.1 Kinetic Energy . . . 107
5.4.2 Potential Energy . . . 108
5.4.3 Lagrange Representation . . . 109
5.5 Nonlinear Control Method . . . 112
5.5.1 Inverse Dynamic Control . . . 112

5.5.2 Sliding Mode Control . . . 113
5.6 Application of Fuzzy Logic to Sliding Mode Control . . . 116
5.6.1 Fuzzy Sets . . . 116
5.6.2 Stability Analysis . . . 116
5.7 Fuzzy Model of Robot Manipulator . . . 118
5.7.1 Fuzzy Model of Rigid Manipulator . . . 119
5.7.2 Fuzzy Model of Continuum Manipulator . . . 123
5.7.3 Application of Fuzzy-model-based Control to Continuum Manipulator . . . 125
5.8 Simulation Results . . . 126
5.9 Conclusions . . . 137

6 Conclusion and Future Work Plans **140**
6.1 Conclusion . . . 140
6.2 Future Work . . . 142

A Awarded Poster **143**

Bibliography **144**

Author's Publications

[1] **Yan Yu** and H.K. Lam, "T-S fuzzy-model-based output feedback tracking control with control input saturation," *IEEE Transactions on Fuzzy Systems*, vol. 26, no.6, pp. 3514-3523, Dec. 2018.

[2] **Yan Yu**, Peng Qi, Kaspar Althoefer and H.K. Lam, "Lagrangian dynamics and nonlinear control of a continuum manipulator," *2015 IEEE International Conference on Robotics and Biomimetics (ROBIO)*, pp. 1912-1917, Dec. 6-9, 2015.

[3] **Yan Yu**, Shi Qian and H.K. Lam, "Fuzzy sliding mode control of a continuum manipulator," *2018 IEEE International Conference on Robotics and Biomimetics (ROBIO)*, pp. 2057-2062, Dec. 12-15, 2018.

[4] Bo Xiao, H.K. Lam, **Yan Yu** and Yuandi Li, "Sampled-data output-feedback tracking control for interval type-2 polynomial fuzzy systems," *IEEE Transactions on Fuzzy Systems*, 2019.

[5] Bo Xiao, H.K. Lam, Xiaozhan Yang, **Yan Yu**, Hongliang Ren, "Tracking control design of interval type-2 polynomial-fuzzy-model-based systems with time-varying delay," *Engineering Applications of Artificial Intelligence*, vol. 75, pp. 76-87, 2018.

[6] H.K. Lam, Bo Xiao, **Yan Yu**, Xunhe Yin, Hugang Han, Shun-Hung Tsai and Chin-Sheng Chen, "Membership-function-dependent stability analysis and control synthesis of guaranteed cost fuzzy-model-based control systems," *International Journal of Fuzzy Systems*, vol. 18, no. 4, pp. 537-549, 2016.

[7] Aiwen Meng, H.K. Lam, **Yan Yu**, Xiaomiao Li and Fucai Liu, "Static output feedback stabilization of positive polynomial fuzzy systems," *IEEE Transactions on Fuzzy Systems*, vol. 26, no. 3, pp. 1600-1612, Jun. 2018.

List of Figures

1.1 Membership-function-independent (MFI) and membership-function-dependent (MFD) techniques for stability condition relaxation [1]. . . 17
1.2 Three types of membership-function matching [2]. 19
1.3 Thesis overall structure and techniques used in different chapters. . . 23

2.1 Fuzzy model construction. 26
2.2 Fuzzy logic temperature. 27
2.3 Sector nonlinearity. 28
2.4 T-S FMB control system. 28
2.5 The boundary information for $y = f(x)$. 31

3.1 The control input saturation. 38
3.2 Block diagram of the T-S FMB output feedback tracking control system with control input saturation. 40
3.3 Tracking control result for Theorem 3.1 with $\sigma_1 = 10$ and $\sigma_2 = 10$. . . 60
3.4 Tracking control result for Theorem 3.1 with $\sigma_1 = 4.1323$ and $\sigma_2 = 0.51299$. 61
3.5 Tracking control result for Theorem 3.2 with $\sigma_1 = 10$ and $\sigma_2 = 10$. . . 62
3.6 Tracking control result for Theorem 3.2 with $\sigma_1 = 3.7067$ and $\sigma_2 = 0.26733$. 63
3.7 Tracking control result for Theorem 3.1 with $\sigma_1 = 10$ and $\sigma_2 = 10$. . . 64
3.8 Tracking control result for Theorem 3.1 with $\sigma_1 = 4.1323$ and $\sigma_2 = 0.51299$. 65
3.9 Tracking control result for Theorem 3.2 with $\sigma_1 = 10$ and $\sigma_2 = 10$. . . 66
3.10 Tracking control result for Theorem 3.2 with $\sigma_1 = 3.7067$ and $\sigma_2 = 0.26733$. 67
3.11 Tracking control result for Theorem 3.1 with $\sigma_1 = 10$ and $\sigma_2 = 10$. . . 68
3.12 Tracking control result for Theorem 3.1 with $\sigma_1 = 4.0872$ and $\sigma_2 = 0.51569$. 69
3.13 Tracking control result for Theorem 3.2 with $\sigma_1 = 10$ and $\sigma_2 = 10$. . . 70
3.14 Tracking control result for Theorem 3.2 with $\sigma_1 = 3.6982$ and $\sigma_2 = 0.22660$. 71
3.15 Tracking control result for Theorem 3.1 with $\sigma_1 = 10$ and $\sigma_2 = 10$. . . 72

3.16 Tracking control result for Theorem 3.1 with $\sigma_1 = 4.1799$ and $\sigma_2 = 0.53704$. 73
3.17 Tracking control result for Theorem 3.2 with $\sigma_1 = 10$ and $\sigma_2 = 10$. . . . 74
3.18 Tracking control result for Theorem 3.2 with $\sigma_1 = 3.7959$ and $\sigma_2 = 0.29619$. 75

4.1 Response of state $x_1(t)$ for Cases 1 (solid line), 2 (dashed line) and 3 (dotted line). 94
4.2 Response of state $x_2(t)$ for Cases 1 (solid line), 2 (dashed line) and 3 (dotted line). 94
4.3 Control signal $u(t)$ for Cases 1 (solid line), 2 (dashed line) and 3 (dotted line). 95
4.4 Response of output $y(t)$ for Cases 1 (solid line), 2 (dashed line) and 3 (dotted line). 95
4.5 Response of state $x_1(t)$ for Cases 4 (solid line), 5 (dashed line) and 6 (dotted line). 96
4.6 Response of state $x_2(t)$ for Cases 4 (solid line), 5 (dashed line) and 6 (dotted line). 96
4.7 Control signal $u(t)$ for Cases 4 (solid line), 5 (dashed line) and 6 (dotted line). 97
4.8 Response of output $y(t)$ for Cases 4 (solid line), 5 (dashed line) and 6 (dotted line). 97
4.9 Response of state $x_1(t)$ for Cases 7 (solid line), 8 (dashed line) and 9 (dotted line). 98
4.10 Response of state $x_2(t)$ for Cases 7 (solid line), 8 (dashed line) and 9 (dotted line). 98
4.11 Control signal $u(t)$ for Cases 7 (solid line), 8 (dashed line) and 9 (dotted line). 99
4.12 Response of output $y(t)$ for Cases 7 (solid line), 8 (dashed line) and 9 (dotted line). 99

5.1 Two-link robot arm. 103
5.2 Diagram of a continuum manipulator bending geometry in 3D space with coordinate frames illustrated. 105
5.3 The process of developing dynamic model of continuum manipulator. 110
5.4 Block diagram of nonlinear control system. 112
5.5 Sliding mode control in error state-space. 115
5.6 Block diagram of polynomial fuzzy model control system for continuum manipulator. 126
5.7 Block diagram of continuum manipulator control system with noise. . 127

5.8 Block diagram of the closed-loop inverse dynamic control system in MATLAB Simulink environment. 128
5.9 The step response of the inverse dynamic control. 129
5.10 The sine wave response of the inverse dynamic control. 129
5.11 The step response of the inverse dynamic control with noise. 130
5.12 Block diagram of the closed-loop sliding mode control system in MATLAB Simulink environment. 131
5.13 The step response results of the sliding mode control. 131
5.14 The sine wave response results of the sliding mode control. 132
5.15 The step response results of the sliding mode control with noise. . . . 132
5.16 Fuzzy sliding mode control membership function of s_1. 133
5.17 Fuzzy sliding mode control membership function of s_2. 134
5.18 Fuzzy sliding mode control membership function of $\dot{s}_1$. 134
5.19 Fuzzy sliding mode control membership function of $\dot{s}_2$. 135
5.20 Block diagram of the closed-loop fuzzy sliding mode control system in MATLAB Simulink environment. 135
5.21 The step response of fuzzy sliding mode control. 136
5.22 The sine wave response of fuzzy sliding mode control. 136
5.23 The step response of fuzzy sliding mode control with noise. 137

List of Tables

3.1 Simulation parameters for $\mathbf{H}_1 = [0.8]$ and $\mathbf{H}_2 = [1.0]$. 76
3.2 Simulation parameters for $\mathbf{H}_2 = [1.0]$ and $\tilde{\mathbf{u}}_{\max\,/\,\min} = \pm 3.7$. 76
3.3 Feedback gains for Table 3.1. 77
3.4 Feedback gains for Table 3.2. 78

4.1 Weighting matrices $\mathbf{W}_x$, $\mathbf{W}_y$ and $\mathbf{W}_u$ for the 9 cases. 90
4.2 Feedback gains $\mathbf{G}_j$ for the 9 cases. 93
4.3 Costs J, J_{x_1}, J_y and J_u for the 9 cases. 93

5.1 The rule table for fuzzy sliding mode control. 118
5.2 The continuum manipulator parameter setting. 127
5.3 Fuzzy output value gains for $\mathbf{K}$. 133

Acronyms

FMB	Fuzzy-model-based
LMI	Linear matrix inequality
MFD	Membership-function-dependent
MFI	Membership-function-independent
PDC	Parallel distributed compensation
PFMB	Polynomial-fuzzy-model-based
PLMF	Piecewise linear membership function
SOS	Sum-of-Squares
T-S	Takagi-Sugeno

Chapter 1

Overview

1.1 Introduction

Linear control theory has been well developed during the past five decades [3–9]. Although most models in the field are currently presented as linear systems, most real-world applications show the characteristics of nonlinearity. People now find that the dynamics of linear system is not rich enough to represent many phenomenons, suggesting that nonlinear control theory is needed to deal with nonlinear systems [10]. Therefore, researchers become more intended to use nonlinear models to express physical process and represent practical dynamics [11,12]. Consequently, more complex control laws are required for nonlinear systems with stringent design specifications. There are also many other reasons to use nonlinear control systems, such as for improving system performance, dealing with nonlinearities and tackling system uncertainty problems. In recent years, many practical applications have been developed by using nonlinear control systems, for example biomedical engineering [13], power system engineering [14], robotics [15] and aerospace technology [16].

Although nonlinear system now plays an important role in system modeling and control, there are many difficulties existing in the process of nonlinear system design. The complexity of nonlinear system can increase the difficulty of system representation and computational cost to realize the system control.

Thanks to the fuzzy logic theory proposed by Prof. Lotfi A. Zadeh [17] that the fuzzy control theory now becomes one of the most effective and systematic approaches for nonlinear system modelling and nonlinear control system stability analysis. Fuzzy control is used to solve the difficult task of modelling and simulating complex real-world nonlinear systems. It provides a formal methodology to mimic humans' heuristic knowledge for representing, manipulating and controlling the system. The transformation from conventional control to fuzzy control gives us more computational capability to deal with complex nonlinear control system problems.

Fuzzy logic was firstly proposed by Prof. Lotfi A. Zadeh of the University of

California at Berkeley in 1965 [17]. In 1973 [18] and 1975 [19], Prof. Lotfi A. Zadeh elaborated his idea to introduce the concept of "linguistic variables" with fuzzy set. The idea of fuzzy control was proposed between early 1970s to late 1980s [20, 21]. During this period, the process of fuzzy control was developed to consist of four steps, namely fuzzification, fuzzy rule base, fuzzy inference engine and defuzzification. The fuzzy logic controller is used to handle the complex and ill-defined nonlinear system with restricted or even without the knowledge on the mathematical model. At this stage, it worked as so called model-free fuzzy control method [22]. However, the heuristic design process of model-free fuzzy control method can be time-consuming and heavily relying on the empirical data. Thus, it normally lacks of theoretical derivation and cannot guarantee the system stability. That is why fuzzy-model-based (FMB) control theory later became an important control method from 1990s [23]. One of the typical representatives of FMB control theory is the Takagi-Sugeno (T-S) fuzzy model which was proposed in 1985 [24]. It uses an average membership-function weighted sum of local linear subsystems to express the complex nonlinear system. Based on the T-S fuzzy model, the state-feedback fuzzy controller is proposed to close the feedback loop to complete the structure of FMB control system.

After obtaining the FMB control system, the stability analysis can be processed under the framework of linear matrix inequalities (LMIs), where a feasible solution of system stability conditions (if there exists) can be found by applying convex programming techniques. The concept of parallel distributed compensation (PDC) [25] was proposed to relax the system conservativeness by suggesting that the fuzzy controller employs the same premise membership function as in the T-S fuzzy model. Until this stage, the stability analysis of FMB control system was referred to as the membership-function-independent (MFI) [26] approach, where although the group of linear subsystems were considered, the membership functions were not. From mid-2000s, researcher turned to draw a great attention on membership-function-dependent (MFD) [27] stability analysis. Since it includes the information of membership function during the stability analysis, the MFD approach effectively alleviates the conservativeness in the stability conditions compared to MFI approach. Therefore, many techniques have been developed for the MFD approach, such as global boundary information, regional boundary information and approximated membership functions [1]. Because of the advantages brought by MFD technique, the FMB control method is still a developing topic.

In this thesis, the stability analysis is investigated based on T-S FMB control system with the consideration of practical control problems, such as control input saturation and guaranteed cost on system index. The stability conditions are relaxed by MFD approach and derived according to Lyapunov stability theory. The fuzzy logic and FMB control methods are applied to the practical example of a com-

plex nonlinear control system, where a dynamic model of continuum manipulator is developed with the capabilities of bending and contractile to be driven to follow the reference signals of length and curvature.

1.2 Literature Review

This section aims to present the literature review of related works in this thesis. The review starts from the knowledge of FMB control systems including T-S fuzzy model, Lyapunov functions and LMIs. Then regarding to FMB control stability analysis, some methods are introduced in order to relax the stability conditions, such as different types of membership-function matching and MFD stability analysis. As an extension, guaranteed cost, output feedback and control input saturation techniques are involved in the stability analysis to extend the applications of FMB control strategy. At last, the general information of continuum manipulator is presented as a practical example for the application of fuzzy logic and FMB control methods.

1.2.1 Fuzzy-Model-Based Control System

Since FMB control attracts people's attention at the time of introducing model-free fuzzy control, T-S fuzzy model has played an important role in fuzzy control system design and system stability analysis. T-S fuzzy model approximates the nonlinear system as a weighted sum of linear subsystems which are weighted by membership functions. The accuracy of T-S fuzzy model depends on the number of rules, the types of membership functions and the choice of linear subsystems. After using T-S fuzzy model to represent the original nonlinear system, the state-feedback controller can be designed to connect the T-S fuzzy model so that the closed loop T-S FMB control system can be formed.

The stability analysis of T-S FMB control system can be investigated by Lyapunov stability theory which was proposed by, also named after, a Russian mathematician Aleksandr Mikhailovich Lyapunov around 1890 [28]. In the Lyapunov stability theory, the Lyapunov function is proposed to test the stability of a nonlinear system. This method was first applied to a practical problem in control engineering in 1940s by Lur'e [29] and others. The inequality produced by Lyapunov stability theory can be formulated in the convex form of LMIs, which means a feasible solution of system stability conditions can be numerically solved from a set of linear equations. Now, the problem of LMIs can be solved by many programming software, such as MATLAB.

In this thesis, a quadratic Lyapunov function is used to develop LMI-based stability conditions for FMB control systems. In literature, there are also some other types of Lyapunov functions proposed to generate the nonlinear system stability conditions, such as polynomial Lyapunov function [30], piecewise-linear Lyapunov

function [31], fuzzy Lyapunov function [32] and higher-order Lyapunov function [33]. Generally speaking, the more complex types of Lyapunov functions are applied, the more relaxed stability conditions can be potentially obtained, while more advanced mathematical techniques are required to support the analysis.

1.2.2 Relaxation of the Stability Conditions

Benefited from the advantages of FMB control system, researchers have been keen on the study of the relaxation of stability conditions. The stability analysis for FMB control system is generally classified into two methods, namely membership-function-independent (MFI) and membership-function-dependent (MFD) techniques, which are presented in Fig.1.1.

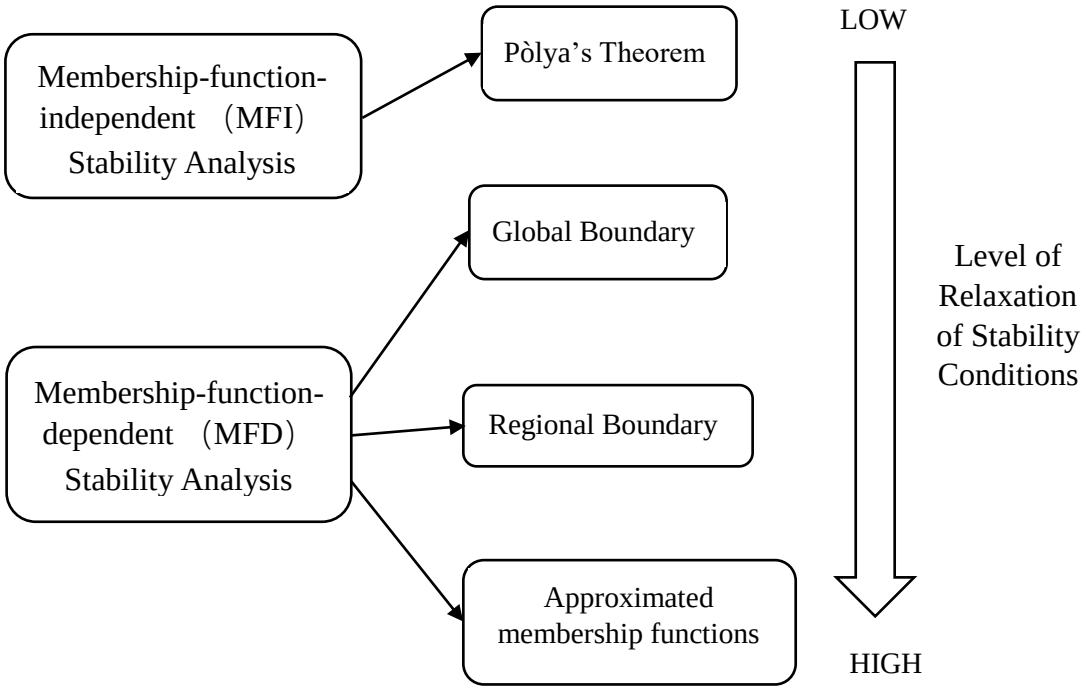

Figure 1.1: Membership-function-independent (MFI) and membership-function-dependent (MFD) techniques for stability condition relaxation [1].

The stability analysis using MFI technique investigates the stability conditions of FMB control system without the information of membership functions. The MFI technique simplifies the stability analysis process and reduces the computational cost, which makes it more applicable in practical engineering. However, because the information of membership functions is not considered, the stability conditions can be conservative which implies that the feasible solutions of MFI stability conditions can be restricted or even does not exist. Some researchers proposed specific techniques to relax the stability conditions under MFI method. In [34], the authors expanded the dimensions of fuzzy summation and applied Pólya's Theorem to realize the relaxation of the stability conditions. Another researcher improved this

relaxation by applying Finsler lemma in [35]. Considering about the large LMIs size in [34], [36] proposed a Sum-of-Squares (SOS) method to optimize the relaxation process in stability conditions.

Since the membership functions can contain a lot of information of the nonlinear system, choosing MFI approach to develop the stability conditions will inevitably lead to conservativeness. In contrast to MFI approach, MFD method includes the specific information of membership functions to investigate system stability conditions, which significantly alleviates the conservativeness in the stability analysis. The authors used the global boundary information of membership functions to relax the stability conditions in [26], where the boundary information was presented in the form of slack matrices. The relaxation of stability conditions was further improved in [37] where regional boundary information was considered rather than global boundary information. In this method, the membership functions were divided into a number of sub-domains where the regional information of upper and lower bounds information are collected separately. Thus, benefited by more specific information in regional boundary, it further relaxes the stability conditions with MFD approach. On the other hand, due to the continuity property of membership functions, there could be infinite number of MFD stability conditions involved in stability analysis. Fortunately, the approximated membership functions technique can successfully solve the problem by using certain types of membership functions to approximate the continuous information and maximize the information utilization in the membership functions [38]. Researchers proposed the staircase membership functions [39], piecewise linear membership functions (PLMFs) [40] and polynomial membership functions [41] as the approximation of original membership functions.

Apart from the methods mentioned in the previous sections, applying different types of membership-function matching can also affect the conservativeness and relaxation level of stability conditions for FMB control system. By comparing the membership functions and the number of rules used in T-S fuzzy model $\{w_1, \cdots, w_p\}$ and fuzzy controller $\{m_1, \cdots, m_c\}$ respectively, there can be three types of membership-function matching, namely perfectly matched premises, partially matched premises and imperfect matched premises [1]. Fig.1.2 illustrates the relationship between these three types of membership-function matching scenarios.

For perfectly matched premises [42], the T-S fuzzy model and fuzzy controller are required to share the same set of premise membership functions, which means the condition $\{w_1, \cdots, w_p\} = \{m_1, \cdots, m_c\}$ must be held. This is also known as PDC technique. Since the choice of membership functions is strictly restricted, the conservativeness of stability condition can be effectively relaxed, although the flexibility of fuzzy controller design may be reduced.

For partially matched premises [43], the T-S fuzzy model and fuzzy controller are not required to share the same set of premises membership functions, but the number

of rules must be the same, which can be written as $\{w_1, \cdots, w_p\} \neq \{m_1, \cdots, m_c\}$ and $c = p$. Generally speaking, the membership functions of T-S fuzzy model sometimes can be very complex in order to have a good approximation on the nonlinear system. But this may increase the computational cost and difficulty during the stability analysis. Under partially matched premises, although the number of rules cannot be changed, some membership functions with simple structure can be adopted by the fuzzy controller, which can reduce the computation and implementation costs of FMB control system in some extent.

For imperfectly matched premises [42], the restrictions on the premise membership functions and number of rules between the T-S fuzzy model and fuzzy controller are completely removed, which means $\{w_1, \cdots, w_p\} \neq \{m_1, \cdots, m_c\}$ and $c \neq p$. This strategy enables the fuzzy controller design with more flexibility, lower computational cost and higher applicability. Under the imperfectly matched premises, the premise membership functions can be applied with simple shape and the number of rules can be small. However, under imperfectly matched premises, the conservativeness of stability conditions is potentially increased compared to perfectly and partially matched premises. Also, more advanced stability analysis techniques are needed to be applied to deal with the mismatched premise membership functions.

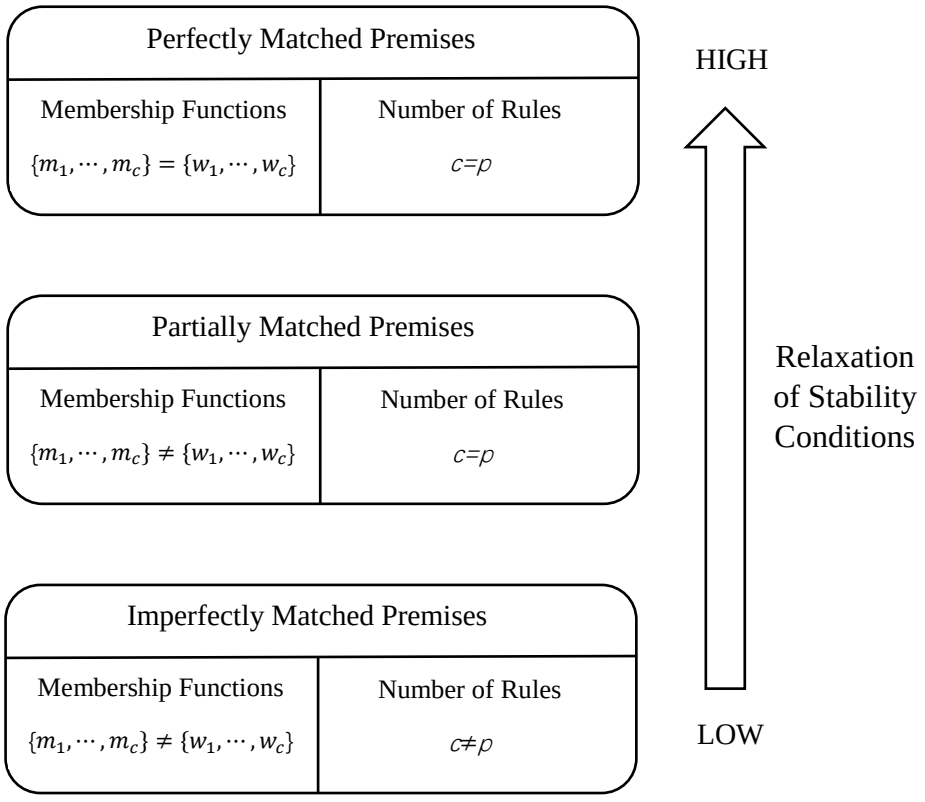

Figure 1.2: Three types of membership-function matching [2].

1.2.3 Extension of Fuzzy-Model-Based Control Strategy

There are many useful techniques in the nonlinear control system design, which can be further extended to FMB control strategies. These include tracking control system, guaranteed cost technique, output feedback control system, time-delay control system [44], control input saturation and sampled-data based control system [45], etc. They can effectively improve the applicability of FMB control methods in the practical control system design. In this thesis, guaranteed cost technique, tracking output feedback control and control input saturation are investigated as the extensions for FMB control strategies.

1.2.3.1 Guaranteed Cost

The nonlinear system stability conditions developed by Lyapunov stability theory depends only on the convergence to the equilibrium point and the problem formulation. However, the specific system performance indexes, such as system state, system output or control signal, are not included in the consideration. Therefore, the guaranteed cost technique is introduced aiming to guarantee the cost of specific system performance index. Generally, the guaranteed cost approach pre-defines a cost function which contains the performance index that needs to be monitored and controlled. In [46], the performance index has been limited with an upper boundary such that the system performances can be guaranteed to be capped by some certain values. Later in [47], this method has been extended to T-S FMB control system with time delays. In FMB control system, the pre-defined cost function is written as a quadratic function involved as a slack matrix in stability analysis [48].

1.2.3.2 Output Feedback Tracking Control

Tracking control is a popular topic in the nonlinear control system design. It has been widely applied to practical engineering systems, such as robot manipulator [49], autopilot control [50] and power system control [51]. It basically requires the controller having the ability of controlling the states of nonlinear system to follow the state trajectory of a stable reference system. Encouraged by the advantages and successful applications of FMB control system, the work in [52] investigated the fuzzy control stability conditions with tracking control method, where $\mathcal{H}_\infty$ performance is used to optimize the state tracking errors. Then, the authors proposed the output feedback control to combine the tracking control method to build the closed loop control system in [53]. In fuzzy output feedback tracking control, the orthogonal complement is introduced to mathematically construct a convex LMI-based stability conditions [54] such that the feasible solution can be found. In addition, the output feedback control only requires the information of the output signal used for feedback compensation, which is more applicable than the state feedback control method.

1.2.3.3 Control Input Saturation

In the practical application, there could be many challenges for the control system, for example parameter uncertainties [55], time-delay problem [56] and dead-zone input threshold [57]. Control input saturation is one of the most common problems discussed in practical engineering control system design. In real applications, the practical actuator is limited by physical constraints. In other words, it is not possible to expect the actuator to work perfectly in all operation domains. This is where the control input saturation may occur. An unexpected control input saturation could result in severe performance deterioration which is intolerable for practical engineering applications. Researchers suggested to use low-gain control law to limit the control input signal in a certain region to avoid saturation in [58]. However, this method may restrict the ability of the controller and worsen the system performance. A smooth function was proposed to approximate the input saturation condition in [59]. However, it is very difficult to involve the mathematical form of nonlinear saturation function into the stability analysis since the LMIs expression could be non-convex.

1.2.4 The Continuum Manipulator

One of the advantages using fuzzy logic and FMB control methods is to deal with complex or ill-defined nonlinear system. The fuzzy logic concept gives us the possibility of relating the nonlinear system and nonlinear control strategies to linear system and linear control methods. The continuum manipulator is a typical practical example that consists of highly nonlinear and complex terms in its dynamics. The continuum manipulator is initially invented from the inspiration of animal features, such as snakes and elephant trunks. There are obviously many advantages to apply continuum manipulators in practical engineer applications than to use conventional rigid-link manipulators. The better maneuverability and flexibility encourage researchers to contribute more passion and effort on the study of continuum manipulator control system. In 1994, [60] proposed the research about hyper-redundant manipulator which was then extended in [61] and [62]. Later in 2002, [63] was able to control the manipulator with improved hyper-flexibility and the ability of bending and contracting. However, most of the previous studies build the dynamic model of continuum manipulator as it consists of infinite number of rigid-link robot arms and then use summation to obtain the overall structure. The complex and nonlinear characteristics of continuum manipulator bring a lot of challenges in the process of model building, stability analysis and control design. However, as mentioned in Section 1.1, fuzzy logic theory can use an average membership-function weighted sum of subsystems to represent the complex nonlinear system, which brings a lot of conveniences to realize the control of continuum manipulator. Therefore, the fuzzy

logic theory and FMB control methods can be an appropriate choice to be applied on continuum manipulator.

1.3 Research Objectives

The main research objectives of this thesis are to investigate and relax the stability conditions of T-S FMB control systems under the MFD framework and consider practical extensions for FMB control strategies. The continuum manipulator is used as a practical example for the application of fuzzy logic and FMB control method to realize the control of complex nonlinear system and improve control system performance. The details are presented as follows:

1) The first aim is to develop the stability analysis of the FMB control systems based on Lyapunov stability theory. Then, the system stability conditions can be relaxed by MFD method with PLMFs technique under the framework of imperfectly/perfectly matched membership functions. After the investigation of Lyapunov stability conditions, the extensions of FMB control strategy can be further applied according to the requirements of practical applications, including guaranteed cost control and control input saturation.

2) In addition to the theoretical stability analysis of FMB control systems with numerical simulation examples, another objective in this thesis is to develop a practical engineer example for the application of fuzzy logic and FMB control methods. The dynamic model of continuum manipulator is a complex and highly nonlinear system. It could be challenging to achieve good control performance by using traditional nonlinear control methods. Therefore, the fuzzy logic and FMB control methods are advantageous to be implemented.

1.4 Organization of the Works

The overall structure of the thesis is illustrated in Fig 1.3 and the details are presented as follows.

- In Chapter 2, the preliminary knowledge is presented, including fuzzy logic control theory, T-S FMB control system, Lyapunov stability analysis, classic model of robot manipulator and some useful lemmas.

- In Chapter 3, the stability analysis for T-S FMB output feedback tracking control with control input saturation is investigated. The control input saturation problem will be tackled by local linear upper and lower bounds technique. Also, the $\mathcal{H}_\infty$ performance is introduced to attenuate the tracking error of tracking control system.

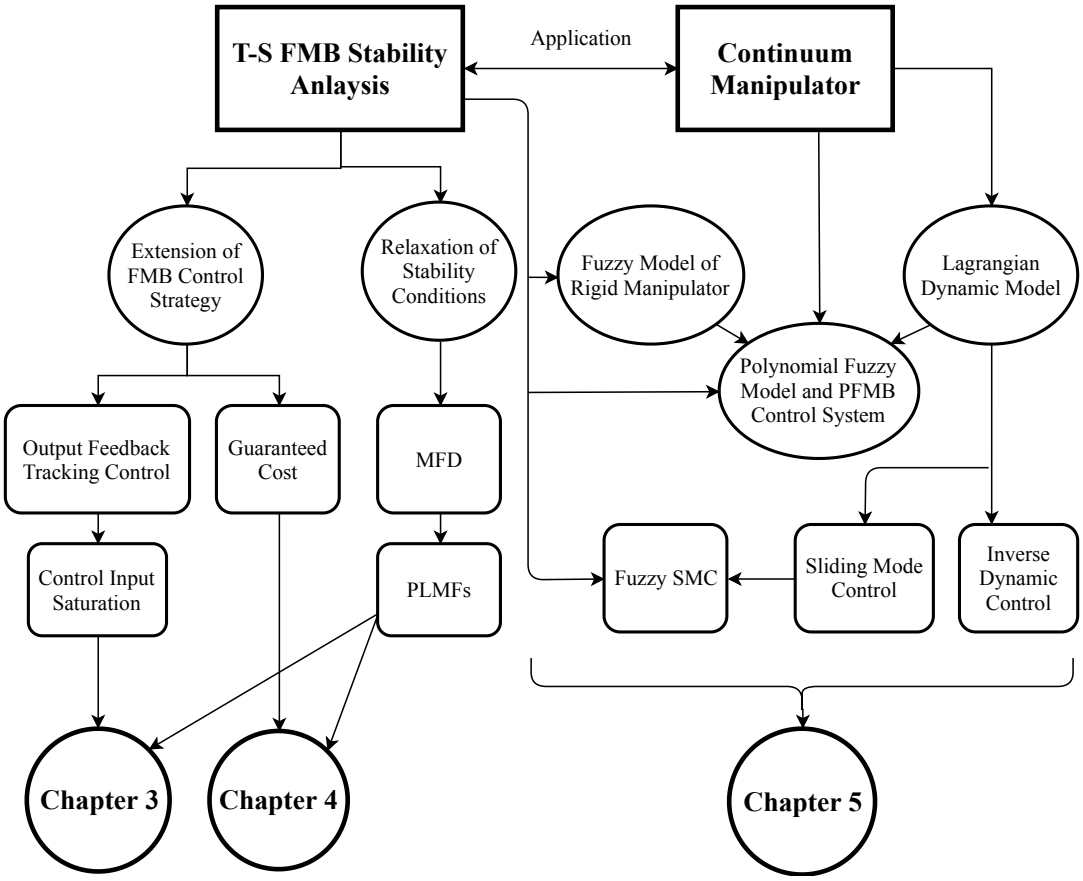

Figure 1.3: Thesis overall structure and techniques used in different chapters.

- In Chapter 4, the system performance index, namely system states, system output and control signal, is considered in stability analysis of FMB control system by using guaranteed cost technique. The stability conditions are relaxed by using MFD approach with PLMFs method to approximate the continuous membership functions.

- In Chapter 5, the continuum manipulator is used as a practical example for the application of fuzzy logic and FMB control method. The dynamic model of continuum manipulator constructed based on Euler-Lagrangian equation of motion appears to be complex and high nonlinear, which brings the challenge for traditional control strategies. Two nonlinear control methods, namely inverse dynamic control and sliding mode control, are tested to realize the state tracking control of the continuum manipulator. Then, in order to improve the control performance of the traditional control methods, fuzzy logic is applied to sliding mode control and the polynomial fuzzy model of continuum manipulator is expected to be built in order to apply FMB control strategies.

- In Chapter 6, the conclusion of the thesis is drawn and the future work plan is discussed.

1.5 Contributions of the Thesis

The contributions of the thesis are summarized as follows:

1. The stability conditions of output feedback control of the T-S FMB control system with control input saturation are successfully developed and simulation results are conducted to verify the effectiveness of control strategy and stability analysis results. The results have been published in "T-S fuzzy model based output feedback tracking control with control input saturation," *IEEE Transactions on Fuzzy Systems*, vol. 26, no.6, pp. 3514-3523, Dec. 2018.

2. The control system performance index is successfully included in the consideration of T-S FMB control system stability analysis by using guaranteed cost technique. The results have been published in "Membership-function-dependent stability analysis and control synthesis of guaranteed cost fuzzy-model-based control systems," *International Journal of Fuzzy Systems*, vol. 18, no. 4, pp. 537-549, 2016.

3. The dynamic model of continuum manipulator with bending and contracting abilities is first developed based on Euler-Lagrangian equation of motion. Two nonlinear control methods are successfully applied to the dynamic model. The fuzzy logic control theory is applied to traditional sliding mode control in order to improve the system performance. The results have been published in "Lagrangian dynamics and nonlinear control of a continuum manipulator," *2015 IEEE International Conference on Robotics and Biomimetics (ROBIO)*, pp. 1912-1917, Dec. 6-9, 2015, and "Fuzzy sliding mode control of a continuum manipulator," *2018 IEEE International Conference on Robotics and Biomimetics (ROBIO)*, Dec. 12-15, 2018, respectively.

4. The continuum manipulator is selected as an application of T-S and polynomial FMB control methods in order to improve the control performance from traditional nonlinear control methods. The research results have been published in poster "Fuzzy Control of Continuum Manipulator" attached in the Appendix has been awarded "The Winner of the Poster Competition" in *2018 IEEE UK & IRELAND Robotics & Automation Society (RAS) Conference* on 22 Feb, 2018.

Chapter 2

Background

In this chapter, the background of the research topics will be presented and briefly explained. The first part is the basic knowledge, including the concepts of fuzzy logic theory and the sector nonlinearity approach for constructing fuzzy-model-based system. Secondly, the T-S FMB control system will be introduced, where the details of T-S fuzzy model and fuzzy controller, especially PDC control method, will be explained. In the third part, the basic knowledge of Lyapunov stability theory on nonlinear system stability analysis will be introduced. In the fourth part, the Euler-Lagrangian equation of motion is derived based on least action principle, which will be used in the constructing of continuum manipulator. Lastly, some useful lemmas to be applied in this thesis will be listed.

2.1 Fuzzy Model Construction

The first step of developing a FMB control system is to build the fuzzy model corresponding to the nonlinear system. Taking T-S fuzzy model as an example, it uses a set of membership functions to weight local linear subsystems summarized to describe the nonlinear system. Specifically, on the basis of fuzzy logic theory, fuzzy model uses IF-THEN rules to map the input value from the fuzzifier to output value which will then be sent to defuzzifier to obtain the approximated nonlinear features. This process can be illustrated in Fig. 2.1.

2.1.1 Fuzzy Logic

In classic logic, also called Boolean logic, the value of variables should either be true or false denoted by integer 0 or 1. However, fuzzy logic is a many-valued logic which returns the truth value of variables with a real number between 0 to 1.

The history of fuzzy logic can be traced back to 1965 when Prof. Lotfi A. Zadeh first proposes the fuzzy logic theory in [17]. From that time, people start to realize the advantages of fuzzy logic and apply fuzzy logic theory to a wide range of areas, such as mechanical engineering [64] and control theory.

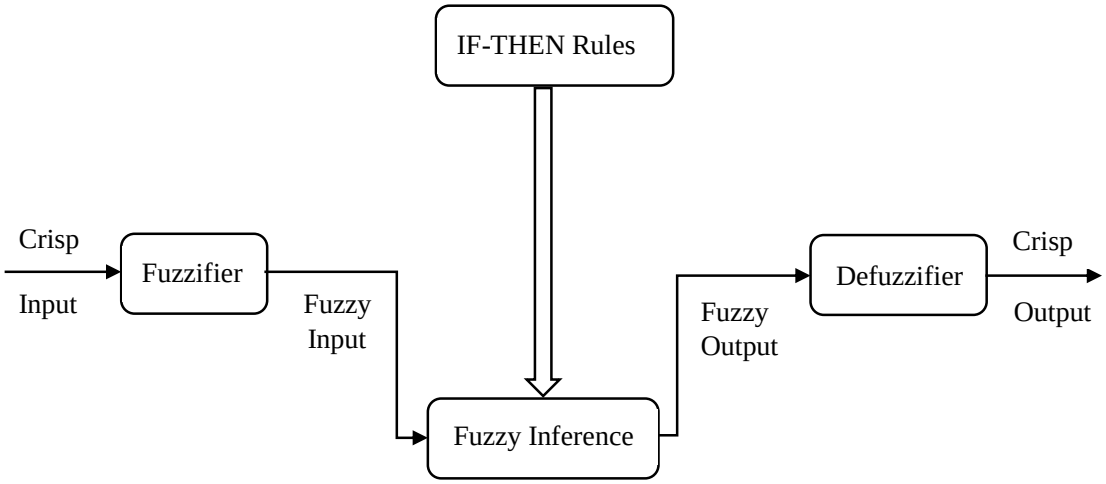

Figure 2.1: Fuzzy model construction.

In order to make better explanation of the fuzzy logic theory, the model of temperature can be a good example to illustrate the difference between classic logic and fuzzy logic. In classic logic, suppose there are three expressions for feeling of temperature which are "COLD","WARM" and "HOT". However, feeling "COLD", "WARM" or "HOT" is not a definite expression, which can be various from person to person and case to case. Therefore, fuzzy logic is useful to provide a mathematical way to express the vagueness and imprecise information in a more accurate way. According to the reference [65] from a biological anthropologist A. R. Frisancho, human starts to feel "COLD" by shivering in an unclothed condition from 25℃, while starts to feel "HOT" by sweating from 28°C. The "WARM" concept is even more vague, which is set between 10°C and 37°C. Fig. 2.2 presents the fuzzy logic temperature scale with three membership functions of "COLD","WARM" and "HOT". At each particular degree of temperature, there are three truth values to describe the feeling. Instead of one truth value in the classic logic, fuzzy logic expresses the feeling of temperature as the summation of membership function weighted "COLD", "WARM" and "HOT". The shape of membership functions is normally presented as triangle or trapezoid shape, peaking at 1 and decreasing in slope drop.

2.1.2 Sector Nonlinearity

Sector nonlinearity is a useful approach to deal with the nonlinearity in the way of fuzzy logic. The main purpose of sector nonlinearity is to find the global/local sector such that the nonlinear terms can be represented by the summation of membership functions weighted linear functions.

Consider the nonlinear system $\dot{\mathbf{x}}(t) = f(\mathbf{x}(t))$, where $\mathbf{x}(t)$ is the system state, $f(\mathbf{x}(t))$ is nonlinear and $f(0) = 0$. It can be seen from Fig. 2.3 that the sector nonlinearity approach uses two linear functions $a_1\mathbf{x}(t)$ and $a_2\mathbf{x}(t)$ to form a

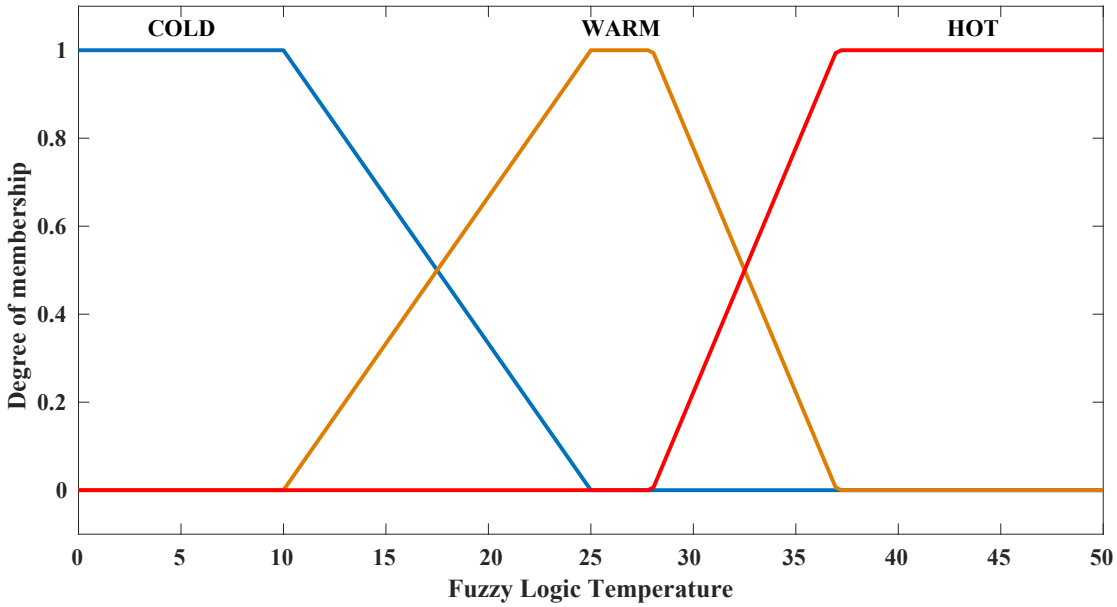

Figure 2.2: Fuzzy logic temperature.

global section to include the nonlinear function $\dot{\mathbf{x}}(t)$, which can be written as $f(\mathbf{x}(t)) \in [a_1\mathbf{x}(t) \quad a_2\mathbf{x}(t)]$. Thus, the nonlinear function $f(\mathbf{x}(t))$ can be mathematically represented by the combination of two linear functions as follow:

$$f(\mathbf{x}(t)) = h_1(x)a_1\mathbf{x}(t) + h_2(x)a_2\mathbf{x}(t), \tag{2.1}$$

where $h_1(x)$ and $h_2(x)$ are the membership functions, which means $h_1(x)+h_2(x) = 1$ and $h_1(x), h_2(x) > 0$. The details of membership functions $h_1(x)$ and $h_2(x)$ can be written as:

$$h_1(x) = \frac{f(\mathbf{x}(t)) - a_2\mathbf{x}(t)}{(a_1 - a_2)\mathbf{x}(t))}; \tag{2.2}$$

$$h_2(x) = \frac{a_1\mathbf{x}(t) - f(\mathbf{x}(t))}{(a_1 - a_2)\mathbf{x}(t))}. \tag{2.3}$$

Thus, the nonlinear function $f(\mathbf{x}(t))$ can be represented by the summation of two membership-function weighted linear functions $a_1\mathbf{x}(t)$ and $a_2\mathbf{x}(t)$. In case that the nonlinear term is not suitable to be globally expressed by linear functions, the local sector nonlinearity approach can be considered. Instead of considering the global value of nonlinear function, local sector nonlinearity only considers a specific region, such as $0 \leq \mathbf{x}(t) \leq d$. When the nonlinear term operates in this local area, it can be represented by the combination of linear functions in the same way of global sector nonlinearity approach.

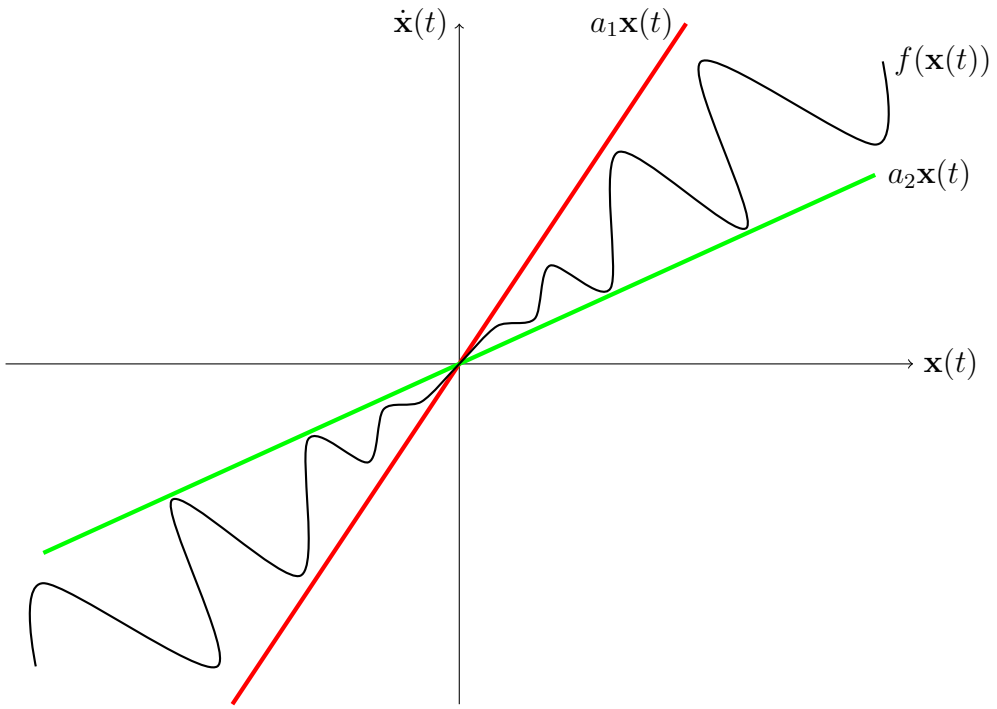

Figure 2.3: Sector nonlinearity.

2.2 T-S Fuzzy-Model-Based Control System

The T-S FMB control system generally consists of T-S fuzzy model and fuzzy controller, which can be described by Fig. 2.4. Similarly to classic control theory, the typical output feedback FMB control system uses the error signal $\mathbf{e}(t)$ calculated from reference signal $\mathbf{r}(t)$ and system state $\mathbf{x}(t)$ for fuzzy controller to generate the control signal $\mathbf{u}(t)$ to stabilize the system. The mathematical express can be written as follows.

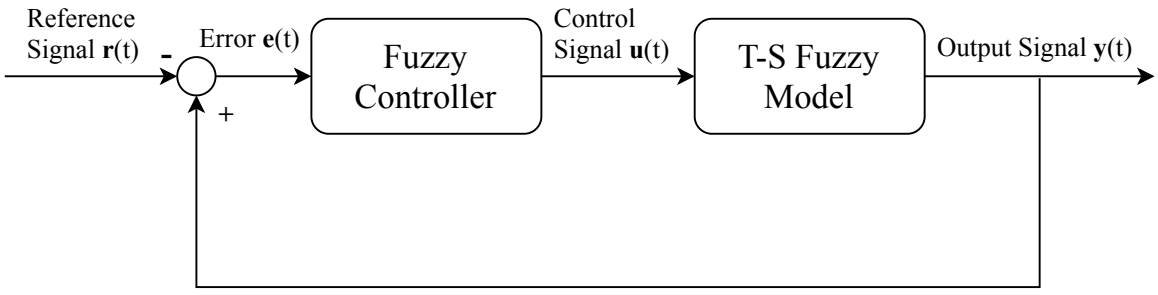

Figure 2.4: T-S FMB control system.

Consider a nonlinear system represented by T-S fuzzy model [24] with p IF-THEN rules as follow:

$$\begin{aligned} &\text{Rule } i\text{: IF } f_1(\mathbf{x}(t)) \text{ is } M_1^i \text{ AND } \cdots \text{ AND } f_\Psi(\mathbf{x}(t)) \text{ is } M_\Psi^i \\ &\text{THEN } \dot{\mathbf{x}}(t) = \mathbf{A}_i\mathbf{x}(t) + \mathbf{B}_i\mathbf{u}(t) \end{aligned} \tag{2.4}$$

where M_α^i is the fuzzy term of ith rule corresponding to the function $f_\alpha(\mathbf{x}(t))$ with α

$= 1, 2, \ldots, \Psi$; $i = 1, 2, \ldots, p$; Ψ is a positive integer; $\mathbf{x}(t) \in \mathbb{R}^n$ is the system state vector; $\mathbf{A}_i \in \mathbb{R}^{n\times n}$ and $\mathbf{B}_i \in \mathbb{R}^{n\times m}$ are known system, input matrices; $\mathbf{u}(t) \in \mathbb{R}^m$ is the control input vector.

The system dynamics and output are defined as follows:

$$\dot{\mathbf{x}}(t) = \sum_{i=1}^{p} w_i(\mathbf{x}(t))\big(\mathbf{A}_i\mathbf{x}(t) + \mathbf{B}_i\mathbf{u}(t)\big), \tag{2.5}$$

$$\mathbf{y}(t) = \sum_{i=1}^{p} w_i(\mathbf{x}(t))\mathbf{C}_i\mathbf{x}(t), \tag{2.6}$$

where

$$w_i(\mathbf{x}(t)) \geq 0 \;\forall\; i, \sum_{i=1}^{p} w_i(\mathbf{x}(t)) = 1, \tag{2.7}$$

$$w_i(\mathbf{x}(t)) = \frac{\prod_{l=1}^{\Psi} \mu_{M_l^i}(f_l(\mathbf{x}(t)))}{\sum_{k=1}^{p} w_i \prod_{l=1}^{\Psi} \mu_{M_l^k}} \tag{2.8}$$

$w_i(\mathbf{x}(t))$, $i = 1, 2, \ldots, p$, are the normalized membership grades, $\mu_{M_\alpha^i}(f_\alpha(\mathbf{x}(t)))$, $\alpha = 1, 2, \ldots, \Psi$, are the membership grades corresponding to the fuzzy term M_α^i.

Use PDC approach to develop the fuzzy controller. The IF-THEN rules for fuzzy controller can be written as

$$\begin{aligned} &\text{Rule } j\text{: IF } f_1(\mathbf{x}(t)) \text{ is } M_1^j \text{ AND } \cdots \text{ AND } f_\Psi(\mathbf{x}(t)) \text{ is } M_\Psi^j \\ &\quad \text{THEN } \mathbf{u}(t) = \mathbf{G}_j\mathbf{x}(t) \end{aligned} \tag{2.9}$$

where $\mathbf{G}_j \in \mathbb{R}^{m\times n}$ is the PDC fuzzy control gain. Thus, the PDC fuzzy controller can be expressed as

$$\mathbf{u}(t) = \sum_{j=1}^{p} w_j(\mathbf{x}(t))\mathbf{G}_j\mathbf{x}(t). \tag{2.10}$$

It is worth mentioning that PDC approach requires the fuzzy controller to share the same type of membership functions and same number of rules, which can be reflected from equations (2.5) and (2.10) with the same membership function shape $w(\mathbf{x}(t))$ and same number of rules p. Thanks for the strict constraint in PDC approach, the stability conditions can be relaxed effectively. However, the design flexibility and applicability may be sacrificed. Fig. 1.2 shows that the fuzzy controller can be designed with partially or imperfectly matched premises, which means the membership functions of fuzzy controller and the number of rules have the flexibility to be different from the T-S fuzzy model.

Therefore, combining equations (2.5) and (2.10), the T-S FMB control system

using PDC approach can be written as follows:

$$\dot{\mathbf{x}}(t) = \sum_{i=1}^{p}\sum_{j=1}^{p} w_i(\mathbf{x}(t))w_j(\mathbf{x}(t))\big(\mathbf{A}_i + \mathbf{B}_i\mathbf{G}_j\big)\mathbf{x}(t). \tag{2.11}$$

2.3 Lyapunov Stability Analysis

The Lyapunov stability theory provides a solution of stability at equilibrium point regarding to the nonlinear system represented by differential equations. Consider the Lyapunov function $V(\mathbf{x}(t)) \in \mathbb{R}^n$, the system is guaranteed to be asymptotically stable by the Lyapunov stability theory when the following conditions are held:

$$\begin{aligned} V(\mathbf{x}(t)) = 0 &\iff \mathbf{x}(t) = 0; \\ V(\mathbf{x}(t)) > 0 &\iff \mathbf{x}(t) \neq 0; \\ \dot{V}(\mathbf{x}(t)) < 0 &\iff \mathbf{x}(t) \neq 0. \end{aligned}$$

In fact, the Lyapunov function reflects the level of system energy which should always be a positive value or 0. In order to guarantee the system stability, the trend of system energy needs to be negative. There are many types of Lyapunov functions as they are introduced in Section 1.2.1, such as piecewise linear Lyapunov function, multiple Lyapunov function and fuzzy Lyapunov function. In this thesis, the quadratic Lyapunov function is considered to investigate nonlinear and FMB control system stability conditions.

After the stability conditions are developed from Lyapunov stability theory, it can be transformed in the form of LMIs, which is then applicable to be solved by numerical software such as MATLAB. For example, consider a linear system in the following form:

$$\dot{\mathbf{x}}(t) = \mathbf{A}\mathbf{x}(t). \tag{2.12}$$

The Lyapunov function is chosen as

$$V(\mathbf{x}(t)) = \mathbf{x}(t)^T\mathbf{P}\mathbf{x}(t). \tag{2.13}$$

According to the Lyapunov stability theory, we have

$$\begin{aligned} \dot{V}(\mathbf{x}(t)) &= \dot{\mathbf{x}}(t)^T\mathbf{P}\mathbf{x}(t) + \mathbf{x}(t)^T\mathbf{P}\dot{\mathbf{x}}(t) \\ &= \mathbf{x}(t)^T\mathbf{A}^T\mathbf{P}\mathbf{x}(t) + \mathbf{x}(t)^T\mathbf{P}\mathbf{A}\mathbf{x}(t) \\ &= \mathbf{x}(t)^T(\mathbf{A}^T\mathbf{P} + \mathbf{P}\mathbf{A})\mathbf{x}(t) < 0. \end{aligned} \tag{2.14}$$

Thus, the Lyapunov stability conditions can be expressed as

$$\mathbf{P} > 0; \tag{2.15}$$

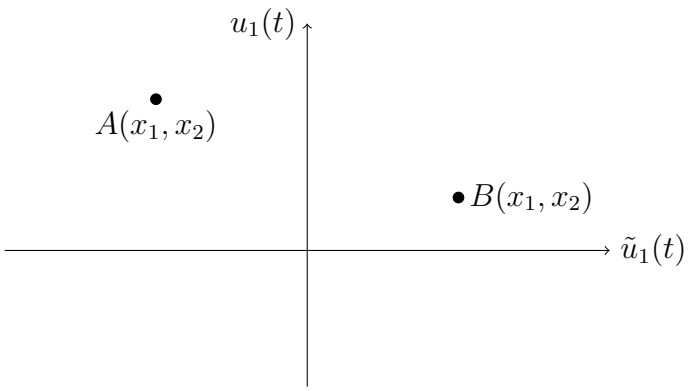

Figure 2.5: The boundary information for $y = f(x)$.

$$\mathbf{A}^T\mathbf{P} + \mathbf{P}\mathbf{A} < 0. \tag{2.16}$$

Since the inequalities in stability conditions are convex to $\mathbf{P}$, the LMIs techniques can be used to find the feasible solution to guarantee the system stability.

2.4 Euler-Lagrangian Equation

According to the least action principle that any physical system will follow a path of least length, we can use Euler-Lagrangian equation to obtain the equation of motion for mechanical system. The Euler-Lagrangian equation is a second order partial differential equation who can find the stationary function of a functional function.

Suppose we need to find a function $y = f(x)$, such that equation $I = \int_{x_1}^{x_2} F(x, y, \dot{y})dx$ is stationary, where the function F is assumed to be twice differentiable [122].

Define two points $A(x_1, y_1)$ and $B(x_2, y_2)$ as shown in Fig. 2.5, such that the boundary conditions can be written as follows

$$y(x_1) = y_1; \tag{2.17}$$

$$y(x_2) = y_2. \tag{2.18}$$

Define a function $\eta(x)$ such that $\eta(x_1) = \eta(x_2) = 0$. A family of curves represented by $\bar{y}(x)$ can be written by

$$\bar{y}(x) = y(x) + \epsilon\eta(x), \tag{2.19}$$

where ϵ is a small arbitrary function.

Therefore, $\bar{y}(x)$ shares the same boundary conditions as $y(x)$. The original problem can be transformed to find a particular curve $\bar{y}(x)$ such that $I(\epsilon) = \int_{x_1}^{x_2} F(x, y, \dot{y})dx$ is stationary.

Since I only depends on ϵ, in order to make I stationary, we need to satisfy

$$\left.\frac{dI}{d\epsilon}\right|_{\epsilon=0} = 0, \tag{2.20}$$

which means

$$\begin{aligned}
&\left.\frac{d}{d\epsilon}\right|_{\epsilon=0} \int_{x_2}^{x_1} F(x,y,\dot{y})dx \\
= &\int_{x_1}^{x_2} \left.\frac{\partial}{\partial\epsilon}F(x,y,\dot{y})\right|_{\epsilon=0} dx \\
= &\int_{x_1}^{x_2} \left.\left[\frac{\partial F}{\partial \bar{y}}\frac{\partial \bar{y}}{\partial \epsilon} + \frac{\partial F}{\partial \dot{\bar{y}}}\frac{\partial \dot{\bar{y}}}{\partial \epsilon}\right]\right|_{\epsilon=0} dx \\
= &\int_{x_1}^{x_2} \left.\left[\frac{\partial F}{\partial \bar{y}}\eta + \frac{\partial F}{\partial \dot{\bar{y}}}\dot{\eta}\right]\right|_{\epsilon=0} dx \\
= &\int_{x_1}^{x_2} \left.\left[\frac{\partial F}{\partial \bar{y}} - \frac{d}{dx}\Big(\frac{\partial F}{\partial \dot{\bar{y}}}\Big)\right]\eta\right|_{\epsilon=0} dx \\
= &\int_{x_1}^{x_2} \left[\frac{\partial F}{\partial y} - \frac{d}{dx}\Big(\frac{\partial F}{\partial \dot{y}}\Big)\right]\eta dx.
\end{aligned} \tag{2.21}$$

Thus, if $y(x)$ makes function I stationary, then it must satisfy the Euler-Lagrangian equation as follows:

$$\frac{\partial F}{\partial y} - \frac{d}{dx}\Big(\frac{\partial F}{\partial \dot{y}}\Big) = 0. \tag{2.22}$$

2.5 Useful Lemmas

In this thesis, the following lemmas are introduced, which play vital roles during the analysis.

Lemma 1 (S-Procedure)**.** *[66]*

Consider two symmetric matrices $\mathbf{A} \in \mathbb{R}^{n\times n}$, $\mathbf{B} \in \mathbb{R}^{n\times n}$ and matrix $\mathbf{x} \in \mathbb{R}^n$. By assuming that the quadratic in equality

$$\mathbf{x}^T\mathbf{A}\mathbf{x} \geq 0 \tag{2.23}$$

is strictly feasible, we can have the consequence quadratic inequality

$$\mathbf{x}^T\mathbf{B}\mathbf{x} \geq 0, \tag{2.24}$$

if and only if there exists a non-negative λ such that

$$\mathbf{B} \geq \lambda\mathbf{A}. \tag{2.25}$$

Lemma 2 (Schur complement)**.** *[67]*

Suppose we have $\mathbf{A} \in \mathbb{R}^{p\times p}$, $\mathbf{B} \in \mathbb{R}^{p\times q}$ *and* $\mathbf{C} \in \mathbb{R}^{q\times q}$, *where the matrix* $\mathbf{C}$ *is invertible. Let* $\mathbf{Q} \in \mathbb{R}^{(p+q)\times(p+q)}$ *be a symmetric matrix given by*

$$\mathbf{Q} = \begin{bmatrix} \mathbf{A} & \mathbf{B} \\ \mathbf{B}^T & \mathbf{C} \end{bmatrix}. \tag{2.26}$$

The Schur complement [68] of $\mathbf{C}$ *in* $\mathbf{X}$ *is defined as* $\mathbf{A} - \mathbf{B}\mathbf{C}^{-1}\mathbf{B}^T$. *If* $\mathbf{C} > 0$, *then* $\mathbf{Q} \geq 0$ *if and only if* $\mathbf{A} - \mathbf{B}\mathbf{C}^{-1}\mathbf{B}^T \geq 0$.

Chapter 3

T-S Fuzzy-Model-Based Output Feedback Tracking Control with Control Input Saturation

In this chapter, the stability analysis of output feedback tracking control for FMB system is conducted when the control input is saturated, where the FMB is developed based on a T-S fuzzy model and a fuzzy controller. The fuzzy controller is employed to close the feedback loop and generate the system states to trace the trajectory of the states of a stable reference model subject to $\mathcal{H}_\infty$ performance. To enhance the design flexibility of the fuzzy controller, the number of rules and premise membership functions can be adjusted. Stability analysis for the FMB control system is performed based on Lyapunov stability theory. To address the input saturation, linear sectors are created by local linear upper bound and lower bound to include the possible control input saturation area. Hence the nonlinear saturation problem can be tackled by the stability analysis of linear sectors. MFD technique is used to bring the information and address the nonlinearity of embedded membership functions into the stability analysis. A numerical simulation example demonstrates the effectiveness of proposed approach and discusses the effect of $\mathcal{H}_\infty$ performance and control input saturation rate to tracking result.

3.1 Introduction

In recent years, fuzzy control system has been rapidly developed among fundamental research and control applications. Its increasing popularity and control effectiveness are encouraging researchers to explore further study in this topic. A fuzzy model proposed by Takagi and Sugeno, namely T-S fuzzy model, can facilitate that any smooth nonlinear control systems can be approximated with linear rule consequence [24,69]. The motor control system and the regulation of DC-DC power converters are two of numerous successful examples that use T-S fuzzy model to apply control theory

on practical systems [70–73]. Similar to the fuzzy models, the smooth nonlinear controller can also be approximated by the PDC-based fuzzy controller [74–80]. A key point of current research focuses on the stability analysis of FMB control system which consists of a T-S fuzzy model and a fuzzy controller. There are fruitful results proposed by researchers around this topic [34, 74–83].

In order to obtain a feasible fuzzy controller that can effectively stabilize the T-S fuzzy model, the Lyapunov stability condition is commonly used, which can be represented by a class of LMIs. On the basis of the Lyapunov stability theory, further researches have been devoted on the determination of more relaxed LMIs based stability condition. In general, there are mainly two ways. The first one is to focus on developing more appropriate Lyapunov functions to alleviate the conservativeness of stability analysis. For example, [85] and [86] tried to develop the piecewise Lyapunov functions which are a more general form and contain much richer class of Lyapunov function candidates so that it is capable to handle a larger set of fuzzy systems. Another way to relax the stability conditions is to apply more information of membership functions to stability analysis [26].

In general, the stability conditions of FMB control systems are investigated with MFI stability analysis approach and then MFD stability analysis approach [1, 26, 27, 87, 88] is used to reduce the conservativeness by involving more specific information of the membership functions. In the literature, the staircase-membership-function method is introduced in [39], where the continuous membership functions of both fuzzy model and fuzzy controller are approximated by the staircase functions with finite number of levels. The original FMB control system is stable if the stability of the FMB control system at all levels of the staircase membership functions is guaranteed with the consideration of approximation error. The novelty of this technique is that it proposes a new concept for MFD stability analysis which brings the staircase membership functions into stability conditions and approximates the infinite number of MFD stability conditions with finite ones. However, the number of MFD stability conditions depends on the approximation errors. To reduce the approximate error, the method of PLMFs was proposed for continuous membership function approximation [89], which requires less number of MFD stability conditions to achieve the same level of stability analysis results. This concept was then generalized through the use of Taylor series approximation [90].

In this Chapter, we attempt to investigate the stability issues of using output feedback tracking control to drive the nonlinear system to trace the state trajectory of a reference model when the control input saturation exists. Since the nonlinear system is represented by T-S fuzzy model, in order to reduce the conservativeness of system analysis, the stability condition of FMB control system is proceeded on the basis of MFD approach. Due to the continuity property of MFD method, the PLMF is conducted to reduce the approximation error when approximating the

infinite number of MFD stability conditions as finite ones. On the basis of MFD stability analysis, the system stability is significantly dependant on its tracking performance, where $\mathcal{H}_\infty$ performance technique needs to be considered. The $\mathcal{H}_\infty$ method is combined wit MFD stability analysis to suppress the system tracking error to a desired level. Therefore, the Lyapunov-based MFD stability conditions can be developed with $\mathcal{H}_\infty$ method to guarantee the system tracking performance. Furthermore, the control input saturation problem can also be solved by satisfying a corresponding developed inequality condition. Thus, the overall input saturation MFD tracking control stability condition can be transformed into the form of LMIs. By solving the LMIs problem, a common positive definite matrix and feedback gains can be used to construct an output feedback T-S fuzzy controller such that the system is stabilized subject to $\mathcal{H}_\infty$ performance with the consideration of control input saturation.

3.2 Preliminary

This section provides the preliminary knowledge of T-S fuzzy model and fuzzy controller, as well as the control input saturation which are engaged with the proposed approach.

3.2.1 T-S Fuzzy Model

Consider a nonlinear plant described by the T-S fuzzy model [24, 104] with p rules of the following IF-THEN format.

$$\begin{aligned} &\text{Rule } i\text{: IF } f_1(\mathbf{x}(t)) \text{ is } M_1^i \text{ AND } \cdots \text{ AND } f_\Psi(\mathbf{x}(t)) \text{ is } M_\Psi^i \\ &\quad \text{THEN } \dot{\mathbf{x}}(t) = \mathbf{A}_i\mathbf{x}(t) + \mathbf{B}_i\mathbf{u}(t), \mathbf{y}(t) = \mathbf{C}\mathbf{x}(t) \end{aligned} \tag{3.1}$$

where M_α^i is a fuzzy term of rule i corresponding to the function $f_\alpha(\mathbf{x}(t))$ with $\alpha =$ 1, 2, ..., Ψ; $i =$ 1, 2, ..., p; Ψ is a positive integer; $\mathbf{x}(t) \in \mathbb{R}^n$ is the system state vector; $\mathbf{y}(t) \in \mathbb{R}^l$ is the system output vector; $\mathbf{A}_i \in \mathbb{R}^{n\times n}$, $\mathbf{B}_i \in \mathbb{R}^{n\times m}$ and $\mathbf{C} \in \mathbb{R}^{l\times n}$ are known system, input and output matrices, respectively; $\mathbf{u}(t) \in \mathbb{R}^m$ is the control input vector used to tackle the system saturation. The system dynamics and output are defined as follows:

$$\dot{\mathbf{x}}(t) = \sum_{i=1}^{p} w_i(\mathbf{x}(t))\big(\mathbf{A}_i\mathbf{x}(t) + \mathbf{B}_i\mathbf{u}(t)\big), \tag{3.2}$$

$$\mathbf{y}(t) = \mathbf{C}\mathbf{x}(t) \tag{3.3}$$

where

$$w_i(\mathbf{x}(t)) \geq 0 \; \forall \; i, \sum_{i=1}^{p} w_i(\mathbf{x}(t)) = 1, \tag{3.4}$$

$$w_i(\mathbf{x}(t)) = \frac{\prod_{l=1}^{\Psi} \mu_{M_l^i}(f_l(\mathbf{x}(t)))}{\sum_{k=1}^{p} w_i \prod_{l=1}^{\Psi} \mu_{M_l^k}} \tag{3.5}$$

$w_i(\mathbf{x}(t))$, $i = 1, 2, \ldots, p$, are the normalized membership grades, $\mu_{M_\alpha^i}(f_\alpha(\mathbf{x}(t)))$, $\alpha = 1, 2, \ldots, \Psi$, are the membership grades corresponding to the fuzzy term M_α^i.

Remark 3.1. *Given that* $\mathbf{u}(t) = [u_1(t), u_2(t), \ldots, u_m(t)]^T$, $\mathbf{u}_{\min}(t) = [u_{1_{\min}}(t), u_{2_{\min}}(t), \ldots, u_{m_{\min}}(t)]^T$ *and* $\mathbf{u}_{\max}(t) = [u_{1_{\max}}(t), u_{2_{\max}}(t), \ldots, u_{m_{\max}}(t)]^T$ *are denoted as the lower and upper bounds of* $\mathbf{u}(t)$ *respectively, regarding to the system saturation.*

3.2.2 Reference Model

A stable reference model is defined as follows:

$$\dot{\mathbf{x}}_\mathbf{r}(t) = \mathbf{A}_\mathbf{r}\mathbf{x}_\mathbf{r}(t) + \mathbf{B}_\mathbf{r}\mathbf{r}(t), \tag{3.6}$$

$$\mathbf{y}_\mathbf{r}(t) = \mathbf{C}\mathbf{x}_\mathbf{r}(t) \tag{3.7}$$

where $\mathbf{x}_\mathbf{r}(t) \in \mathbb{R}^N$ denotes the state vector of reference model, $\mathbf{A}_\mathbf{r} \in \mathbb{R}^{n\times n}$ and $\mathbf{B}_\mathbf{r} \in \mathbb{R}^{n\times m}$ are the constant system and input matrices respectively, $\mathbf{r}(t) \in \mathbb{R}^m$ is the input vector of reference system, $\mathbf{y}_\mathbf{r}(t) \in \mathbb{R}^l$ is the reference model output vector.

3.2.3 Output Feedback Fuzzy Controller

The output feedback fuzzy controller attempts to control the system states (3.2) to track the state trajectory of the stable reference model (3.6). The error between the system states and reference states is defined by

$$\mathbf{e}(t) = \mathbf{x}(t) - \mathbf{x}_\mathbf{r}(t). \tag{3.8}$$

In the same way, the output error is defined as

$$\mathbf{e}_\mathbf{y}(t) = \mathbf{y}(t) - \mathbf{y}_\mathbf{r}(t) = \mathbf{C}\mathbf{e}(t). \tag{3.9}$$

The output feedback fuzzy controller consists of c rules of which is give as:

$$\begin{aligned} &\text{Rule } j\text{: IF } g_1(\mathbf{y}(t)) \text{ is } N_1^j \text{ AND } \cdots \text{ AND } g_\Omega(\mathbf{y}(t)) \text{ is } N_\Psi^j \\ &\text{THEN } \tilde{\mathbf{u}}(t) = \mathbf{F}_j\mathbf{e}_\mathbf{y}(t) + \mathbf{G}_j\mathbf{y}_\mathbf{r}(t) \end{aligned} \tag{3.10}$$

where N_α^j is a fuzzy term of rule j corresponding to the function $g_\beta(\mathbf{x}(t))$, $\beta = 1, 2, \ldots, \Omega$; $j = 1, 2, \ldots, c$; Ω is a positive integer; $\mathbf{F}_j \in \mathbb{R}^{m\times l}$ and $\mathbf{G}_j \in \mathbb{R}^{m\times l}$, $j = 1, 2,$

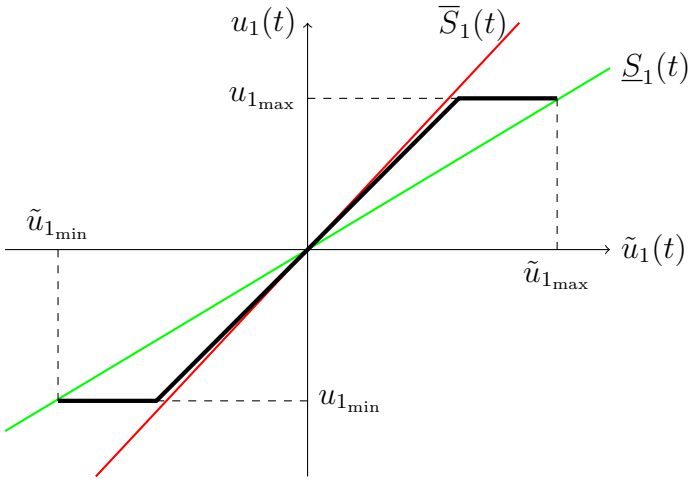

Figure 3.1: The control input saturation.

..., c, are the feedback gains to be determined.

Considering (3.8) and (3.9), the output feedback fuzzy controller can be formulated as follows:

$$\begin{aligned}\tilde{\mathbf{u}}(t) &= \sum_{j=1}^{c} m_j(\mathbf{x}(t))(\mathbf{F}_j\mathbf{C}\mathbf{e}(t) + \mathbf{G}_j\mathbf{C}\mathbf{x}_\mathbf{r}(t)) \\ &= \sum_{j=1}^{c} m_j(\mathbf{x}(t))(\mathbf{F}_j\mathbf{C}\mathbf{x}(t) + (\mathbf{G}_j - \mathbf{F}_j)\mathbf{C}\mathbf{x}_\mathbf{r}(t)) \end{aligned} \tag{3.11}$$

where

$$m_j(\mathbf{x}(t)) \geq 0 \; \forall \; j, \sum_{j=1}^{c} m_j(\mathbf{x}(t)) = 1, \tag{3.12}$$

$$m_j(\mathbf{x}(t)) = \frac{\prod_{l=1}^{\Omega} \mu_{N_l^j}(g_l(\mathbf{x}(t)))}{\sum_{k=1}^{c} m_j \prod_{l=1}^{\Omega} \mu_{N_l^k}} \tag{3.13}$$

$m_j(\mathbf{x}(t))$, $j = 1, 2, \ldots, c$, are the normalized membership grades, $\mu_{N_\beta^j}(g_\beta(\mathbf{x}(t)))$, $\beta = 1, 2, \ldots, \Omega$, are the membership grades corresponding to the fuzzy term N_β^j.

Remark 3.2. *Denoting that* $\tilde{\mathbf{u}}(t) = [\tilde{u}_1(t), \tilde{u}_2(t), \ldots, \tilde{u}_m(t)]^T$, $\tilde{\mathbf{u}}(t)$ *is assumed to work within the lower bounds* $\tilde{\mathbf{u}}_{\min}(t) = [\tilde{u}_{1_{\min}}(t), \tilde{u}_{2_{\min}}(t), \ldots, \tilde{u}_{m_{\min}}(t)]^T$ *and upper bounds* $\tilde{\mathbf{u}}_{\max}(t) = [\tilde{u}_{1_{\max}}(t), \tilde{u}_{2_{\max}}(t), \ldots, \tilde{u}_{m_{\max}}(t)]^T$.

3.2.4 Control Input Saturation

The concept of control input saturation is depicted in Fig. 3.1. Aforementioned that $\tilde{\mathbf{u}}(t) = [\tilde{u}_1(t), \tilde{u}_2(t), \ldots, \tilde{u}_m(t)]^T$ is the control signal given by the ideal output feedback fuzzy controller and $\mathbf{u}(t) = [u_1(t), u_2(t), \ldots, u_m(t)]^T$ is the practical control signal, which are used to address saturation problem. For illustration purposes, Fig. 3.1 only shows the control input saturation characteristics of the first element between $\tilde{\mathbf{u}}(t)$ and $\mathbf{u}(t)$, i.e., $\tilde{u}_1(t)$ and $u_1(t)$.

In ideal situation, the control signal vector $\tilde{\mathbf{u}}(t)$ is equal to the practical control vector $\mathbf{u}(t)$. Fig. 3.1 shows that there exists a linear relationship between $\tilde{u}_1(t)$ and $u_1(t)$ in a certain range. After the ideal control signal $\tilde{u}_1(t)$ reaches either the limit value of $u_{1_{\max}}$ or $u_{1_{\min}}$, the practical control input $u_1(t)$ no longer follows the increasing or decreasing trend of $\tilde{u}_1(t)$, but saturates at the value, i.e., $u_{1_{\max}}$ or $u_{1_{\min}}$. In general, the following relationship stands: $u_{i_{\max}} = -u_{i_{\min}}, i = 1, 2, \ldots, m$, which is also denoted as $\mathbf{u}_{\max} = -\mathbf{u}_{\min}$. $\tilde{u}_{1_{\max}}$ and $\tilde{u}_{1_{\min}}$ are the intersection points between the saturated control signal $u_1(t)$ and the control input lower bound $\underline{S}_1(t)$.

Based on [95], The control input saturation can be formulated as

$$(\mathbf{u}(t) - \underline{\mathbf{S}}(t))^T \mathbf{\Lambda}^{-1} (\overline{\mathbf{S}}(t) - \mathbf{u}(t)) \geq 0 \tag{3.14}$$

where $\overline{\mathbf{S}}(t) = [\overline{S}_1(t), \overline{S}_2(t), \ldots, \overline{S}_m(t)]^T$ and $\underline{\mathbf{S}}(t) = [\underline{S}_1(t), \underline{S}_2(t), \ldots, \underline{S}_m(t)]^T$ are the upper bound and lower bound of control input which create a region of space where the stability analysis can be further investigated; $\mathbf{\Lambda} \in \mathbb{R}^{m \times m}$ is a positive semi-definite diagonal matrix to be determined, i.e., $\mathbf{\Lambda} = \text{diag}\{\tau_1, \ldots, \tau_m\} \geq 0$ and $\mathbf{\Lambda}^{-1} \geq 0$.

Remark 3.3. *In order to guarantee the stability of nonlinear system under all saturation conditions, in Fig. 3.1, the slope of all elements in $\underline{\mathbf{S}}(t)$ should be chosen as zero to include the whole area. However, in practical applications, the output signal is limited, for example, no more than $\mathbf{u}_{max}$. Therefore, the slope of lower bound can be adjusted to a larger value in order to reduce the estimated area. An over-estimated area will generate conservative analysis result. Therefore, the saturation area used in stability analysis should be as small as possible in order to satisfy the practical requirements.*

3.3 Stability Analysis

This section presents the stability analysis of T-S FMB tracking control system with control input saturation based on Lyapunov stability theory. An $\mathcal{H}_\infty$ performance is introduced to evaluate the tracking error. Through approximating the membership functions using PLMFs [89], with the consideration of approximation error, MFD stability conditions in terms of LMIs are obtained. The block diagram of the T-S FMB output feedback tracking control system with control input saturation is shown in Fig. 3.2.

From (3.2), (3.6) and (3.8), the dynamics of error system is obtained as follows:

$$\begin{aligned} \dot{\mathbf{e}}(t) &= \dot{\mathbf{x}}(t) - \dot{\mathbf{x}}_{\mathbf{r}}(t) \\ &= \sum_{i=1}^{p} w_i(\mathbf{x}(t))(\mathbf{A}_i \mathbf{x}(t) + \mathbf{B}_i \mathbf{u}(t)) - \mathbf{A}_{\mathbf{r}} \mathbf{x}_{\mathbf{r}}(t) - \mathbf{B}_{\mathbf{r}} \mathbf{r}(t). \end{aligned} \tag{3.15}$$

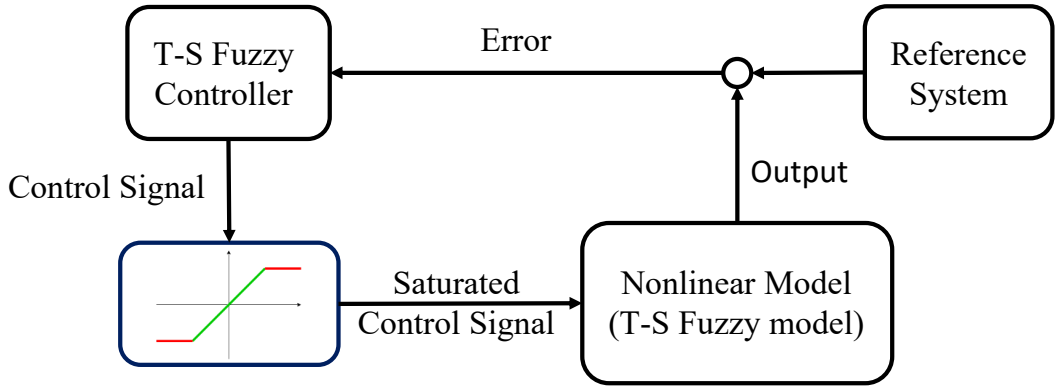

Figure 3.2: Block diagram of the T-S FMB output feedback tracking control system with control input saturation.

The control objective is to determine the feedback gains $\mathbf{F}_j$ and $\mathbf{G}_j$ in the output feedback fuzzy controller (3.11) under the existence of control input saturation such that the state error $\mathbf{e}(t)$ is attenuated subject to an $\mathcal{H}_\infty$ performance index.

For brevity, t in the time-varying variables is omitted, e.g., $\mathbf{x}(t)$ is written as $\mathbf{x}$.

To investigate the stability of the error system (3.15), the following Lyapunov function candidate is deployed.

$$V = \mathbf{e}^T \mathbf{X}^{-1} \mathbf{e} \tag{3.16}$$

where $0 < \mathbf{X} = \mathbf{X}^T \in \mathbb{R}^{n \times n}$ is to be determined. Then (3.8) and (3.15) can be rewritten, respectively, as follows:

$$\mathbf{e} = \begin{bmatrix} \mathbf{X} & -\mathbf{X} & \mathbf{0} & \mathbf{0} \end{bmatrix} \begin{bmatrix} \mathbf{X}^{-1}\mathbf{x} \\ \mathbf{X}^{-1}\mathbf{x_r} \\ \mathbf{X}^{-1}\mathbf{u} \\ \mathbf{X}^{-1}\mathbf{r} \end{bmatrix}, \tag{3.17}$$

$$\dot{\mathbf{e}} = \sum_{i=1}^{p} w_i(\mathbf{x}) \begin{bmatrix} \mathbf{A}_i\mathbf{X} & -\mathbf{A_r}\mathbf{X} & \mathbf{B}_i\mathbf{X} & -\mathbf{B_r}\mathbf{X} \end{bmatrix} \begin{bmatrix} \mathbf{X}^{-1}\mathbf{x} \\ \mathbf{X}^{-1}\mathbf{x_r} \\ \mathbf{X}^{-1}\mathbf{u} \\ \mathbf{X}^{-1}\mathbf{r} \end{bmatrix}. \tag{3.18}$$

From (3.16), (3.17) and (3.18), we have

$$\dot{V} = \dot{\mathbf{e}}^T \mathbf{X}^{-1} \mathbf{e} + \mathbf{e}^T \mathbf{X}^{-1} \dot{\mathbf{e}}$$

$$
\begin{aligned}
&= \sum_{i=1}^{p} w_i(\mathbf{x}) \begin{bmatrix} \mathbf{X}^{-1}\mathbf{x} \\ \mathbf{X}^{-1}\mathbf{x_r} \\ \mathbf{X}^{-1}\mathbf{u} \\ \mathbf{X}^{-1}\mathbf{r} \end{bmatrix}^T \begin{bmatrix} \mathbf{A}_i\mathbf{X} \\ -\mathbf{A_r}\mathbf{X} \\ \mathbf{B}_i\mathbf{X} \\ -\mathbf{B_r}\mathbf{X} \end{bmatrix} \mathbf{X}^{-1} \begin{bmatrix} \mathbf{X} \\ -\mathbf{X} \\ \mathbf{0} \\ \mathbf{0} \end{bmatrix}^T \begin{bmatrix} \mathbf{X}^{-1}\mathbf{x} \\ \mathbf{X}^{-1}\mathbf{x_r} \\ \mathbf{X}^{-1}\mathbf{u} \\ \mathbf{X}^{-1}\mathbf{r} \end{bmatrix} \\
&\quad + \sum_{i=1}^{p} w_i(\mathbf{x}) \begin{bmatrix} \mathbf{X}^{-1}\mathbf{x} \\ \mathbf{X}^{-1}\mathbf{x_r} \\ \mathbf{X}^{-1}\mathbf{u} \\ \mathbf{X}^{-1}\mathbf{r} \end{bmatrix}^T \begin{bmatrix} \mathbf{X} \\ -\mathbf{X} \\ \mathbf{0} \\ \mathbf{0} \end{bmatrix} \mathbf{X}^{-1} \begin{bmatrix} \mathbf{A}_i\mathbf{X} \\ -\mathbf{A_r}\mathbf{X} \\ \mathbf{B}_i\mathbf{X} \\ -\mathbf{B_r}\mathbf{X} \end{bmatrix}^T \begin{bmatrix} \mathbf{X}^{-1}\mathbf{x} \\ \mathbf{X}^{-1}\mathbf{x_r} \\ \mathbf{X}^{-1}\mathbf{u} \\ \mathbf{X}^{-1}\mathbf{r} \end{bmatrix} \\
&= \sum_{i=1}^{p} w_i(\mathbf{x}) \begin{bmatrix} \mathbf{X}^{-1}\mathbf{x} \\ \mathbf{X}^{-1}\mathbf{x_r} \\ \mathbf{X}^{-1}\mathbf{u} \\ \mathbf{X}^{-1}\mathbf{r} \end{bmatrix}^T \begin{bmatrix} \mathbf{X}\mathbf{A}_i^T & -\mathbf{X}\mathbf{A}_i^T & \mathbf{0} & \mathbf{0} \\ -\mathbf{X}\mathbf{A_r}^T & \mathbf{X}\mathbf{A_r}^T & \mathbf{0} & \mathbf{0} \\ \mathbf{X}\mathbf{B}_i^T & -\mathbf{X}\mathbf{B}_i^T & \mathbf{0} & \mathbf{0} \\ -\mathbf{X}\mathbf{B_r}^T & \mathbf{X}\mathbf{B_r}^T & \mathbf{0} & \mathbf{0} \end{bmatrix} \begin{bmatrix} \mathbf{X}^{-1}\mathbf{x} \\ \mathbf{X}^{-1}\mathbf{x_r} \\ \mathbf{X}^{-1}\mathbf{u} \\ \mathbf{X}^{-1}\mathbf{r} \end{bmatrix} \\
&\quad + \sum_{i=1}^{p} w_i(\mathbf{x}) \begin{bmatrix} \mathbf{X}^{-1}\mathbf{x} \\ \mathbf{X}^{-1}\mathbf{x_r} \\ \mathbf{X}^{-1}\mathbf{u} \\ \mathbf{X}^{-1}\mathbf{r} \end{bmatrix}^T \begin{bmatrix} \mathbf{A}_i\mathbf{X} & -\mathbf{A_r}\mathbf{X} & \mathbf{B}_i\mathbf{X} & -\mathbf{B_r}\mathbf{X} \\ -\mathbf{A}_i\mathbf{X} & \mathbf{A_r}\mathbf{X} & -\mathbf{B}_i\mathbf{X} & \mathbf{B_r}\mathbf{X} \\ \mathbf{0} & \mathbf{0} & \mathbf{0} & \mathbf{0} \\ \mathbf{0} & \mathbf{0} & \mathbf{0} & \mathbf{0} \end{bmatrix} \begin{bmatrix} \mathbf{X}^{-1}\mathbf{x} \\ \mathbf{X}^{-1}\mathbf{x_r} \\ \mathbf{X}^{-1}\mathbf{u} \\ \mathbf{X}^{-1}\mathbf{r} \end{bmatrix} \\
&= \sum_{i=1}^{p} w_i(\mathbf{x}) \begin{bmatrix} \mathbf{X}^{-1}\mathbf{x} \\ \mathbf{X}^{-1}\mathbf{x_r} \\ \mathbf{X}^{-1}\mathbf{u} \\ \mathbf{X}^{-1}\mathbf{r} \end{bmatrix}^T \\
&\quad \times \begin{bmatrix} \mathbf{X}\mathbf{A}_i^T + \mathbf{A}_i\mathbf{X} & -\mathbf{X}\mathbf{A}_i^T - \mathbf{A_r}\mathbf{X} & \mathbf{B}_i\mathbf{X} & -\mathbf{B_r}\mathbf{X} \\ -\mathbf{A}_i\mathbf{X} - \mathbf{X}\mathbf{A_r}^T & \mathbf{X}\mathbf{A_r}^T + \mathbf{A_r}\mathbf{X} & -\mathbf{B}_i\mathbf{X} & \mathbf{B_r}\mathbf{X} \\ \mathbf{X}\mathbf{B}_i^T & -\mathbf{X}\mathbf{B}_i^T & \mathbf{0} & \mathbf{0} \\ -\mathbf{X}\mathbf{B_r}^T & \mathbf{X}\mathbf{B_r}^T & \mathbf{0} & \mathbf{0} \end{bmatrix} \begin{bmatrix} \mathbf{X}^{-1}\mathbf{x} \\ \mathbf{X}^{-1}\mathbf{x_r} \\ \mathbf{X}^{-1}\mathbf{u} \\ \mathbf{X}^{-1}\mathbf{r} \end{bmatrix}. \quad (3.19)
\end{aligned}
$$

3.3.1 $\mathcal{H}_\infty$ Performance

The $\mathcal{H}_\infty$ performance is to require the closed loop feedback gain to stabilize the control system and minimize the $\mathcal{L}_2$ gain which is defined as follows [105]:

$$
\mathcal{L}_2[0,T] := \{\mathbf{u}, T] \in \mathbb{R}^n | \int_0^T ||\mathbf{u}||^2 dt < \infty\}. \quad (3.20)
$$

Suppose the control signal $\mathbf{u}$ is a function in $\mathcal{L}_2[0,\infty)$. The dissipation inequality of $\mathcal{H}_\infty$ performance in time interval $[0,T]$ with initial condition $\mathbf{x}(0)$ can be written

as follows [106]:

$$V(\mathbf{x}(T)) \leq V(\mathbf{x}(0)) + \gamma^2 \int_0^T ||\mathbf{u}||^2 dt - \int_0^T ||\mathbf{y}||^2 dt, \tag{3.21}$$

where $\gamma > 0$ is a fixed number.

Remark 3.4. *The dissipation inequality in* (3.21) *indicates that with the input* $\mathbf{u} \in \mathcal{L}_2[0, \infty)$*, the system responses from initial condition* $\mathbf{x}(0)$ *producing the output* $\mathbf{y} \in \mathcal{L}_2[0, \infty)$*. The ratio between* $\mathcal{L}_2$ *norms of the output* $\mathbf{y}$ *and the input* $\mathbf{u}$ *is bounded by* γ*. In other words, the system signal produces finite energy during the infinite time interval* $[0, \infty])$ *and the ratio between input energy and output energy can be interpreted by* γ*.*

Remark 3.5. *The main objective of* $\mathcal{H}_\infty$ *control is to minimize the* $\mathcal{H}_\infty$ *norm of the system energy, which can be understood as the minimization of the maximum singular value in any direction and any frequency in the system function including the noises and disturbances. Comparatively, the linear quadratic regulator (LQR) applied in Chapter 4 aims to design a controller to minimize a quadratic cost function subject to linear system dynamics.*

Since the reference model (3.6) is a stable system, the state error can be bounded by the reference state $\mathbf{x_r}$ and the reference input $\mathbf{r}$ in the following analysis when the H_∞ performance is used as the performance metric.

From (3.19), we have

$$\dot{V} = \mathbf{\Xi} - \mathbf{e}^T\mathbf{e} + \sigma_1^2 {\mathbf{x_r}}^T\mathbf{x_r} + \sigma_2^2 \mathbf{r}^T\mathbf{r} \tag{3.22}$$

where σ_1 and σ_2 are scalars to be determined and

$$\begin{aligned}
\mathbf{\Xi} &= \dot{V} + \mathbf{e}^T\mathbf{e} - \sigma_1^2 {\mathbf{x_r}}^T\mathbf{x_r} - \sigma_2^2 \mathbf{r}^T\mathbf{r} \\
&= \sum_{i=1}^{p} w_i(\mathbf{x}) \begin{bmatrix} \mathbf{X}^{-1}\mathbf{x} \\ \mathbf{X}^{-1}\mathbf{x_r} \\ \mathbf{X}^{-1}\mathbf{u} \\ \mathbf{X}^{-1}\mathbf{r} \end{bmatrix}^T \\
&\quad \times \begin{bmatrix} \mathbf{X}\mathbf{A}_i^T + \mathbf{A}_i\mathbf{X} + \mathbf{X}\mathbf{X} & * & * & * \\ -\mathbf{A}_i\mathbf{X} - \mathbf{X}{\mathbf{A}_\mathbf{r}}^T - \mathbf{X}\mathbf{X} & \mathbf{X}{\mathbf{A}_\mathbf{r}}^T + \mathbf{A}_\mathbf{r}\mathbf{X} + \mathbf{X}\mathbf{X} - \sigma_1^2\mathbf{X}\mathbf{X} & * & * \\ \mathbf{X}\mathbf{B}_i^T & -\mathbf{X}\mathbf{B}_i^T & \mathbf{0} & * \\ -\mathbf{X}{\mathbf{B}_\mathbf{r}}^T & \mathbf{X}{\mathbf{B}_\mathbf{r}}^T & \mathbf{0} & -\sigma_2^2\mathbf{X}\mathbf{X} \end{bmatrix}
\end{aligned}$$

$$\times \begin{bmatrix} \mathbf{X}^{-1}\mathbf{x} \\ \mathbf{X}^{-1}\mathbf{x_r} \\ \mathbf{X}^{-1}\mathbf{u} \\ \mathbf{X}^{-1}\mathbf{r} \end{bmatrix}. \tag{3.23}$$

Considering

$$\mathbf{\Xi} = \dot{V} + \mathbf{e}^T\mathbf{e} - \sigma_1^2 {\mathbf{x_r}}^T\mathbf{x_r} - \sigma_2^2\mathbf{r}^T\mathbf{r} < 0, \tag{3.24}$$

we have

$$\dot{V} < -\mathbf{e}^T\mathbf{e} + \sigma_1^2 {\mathbf{x_r}}^T\mathbf{x_r} + \sigma_2^2\mathbf{r}^T\mathbf{r}. \tag{3.25}$$

Define T as the terminal time of control [54] and integrate both sides of (3.25) with respect to time t. The $\mathcal{H}_\infty$ performance regarding to tracking error can be expressed as

$$\frac{\int_0^T \mathbf{e}^T\mathbf{e}\, dt - V(0)}{\int_0^T (\sigma_1^2 {\mathbf{x_r}}^T\mathbf{x_r} + \sigma_2^2\mathbf{r}^T\mathbf{r})\, dt} < 1. \tag{3.26}$$

Therefore, in order to control the nonlinear system formulated by the T-S fuzzy model (3.2) to trace the state trajectory of the stable reference system (3.6) subject to H_∞ performance (3.26), the inequality (3.24) is necessary to be satisfied.

Remark 3.6. *The physical meaning of* (3.26) *is that the system tracking error* $\mathbf{e}$ *is attenuated below a prescribed level which is determined by two scalars* σ_1 *and* σ_2 *from the view of energy. With a set of smaller values of* σ_1 *and* σ_2*, the tracking performance can be improved with less tracking error. Furthermore, the inequality (3.24) has not been presented in convex form, since the stability condition can further be investigated with control input saturation. If necessary, the method used in later sections will transfer the inequality (3.24) to an LMI form.*

3.3.2 Control Input Saturation

In this section, the property of control input saturation is discussed. Fig. 3.1 shows that the fuzzy controller designed in (3.11) outputs the control signal vector $\tilde{\mathbf{u}}$, demonstrating the property of saturation. The control input vector $\mathbf{u}$ will be nonlinear to $\tilde{\mathbf{u}}$ and hold its value at $\mathbf{u}_{max}$ while $\tilde{\mathbf{u}}$ increases to a predefined level.

Referring to (3.14), it represents the information in the region bounded between the upper bound $\overline{\mathbf{S}}$ and lower bound $\underline{\mathbf{S}}$ as shown in Fig. 3.1 [89]. The stability analysis can be conducted to address control input saturation by taking (3.14) into account.

Assume that there exist the diagonal matrices $\mathbf{H}_1 \in \mathbb{R}^{m\times m}$ and $\mathbf{H}_2 \in \mathbb{R}^{m\times m}$ such that $\mathbf{H}_2 \geq \mathbf{I} > \mathbf{H}_1 \geq 0$. According to (3.11), the upper bound $\overline{\mathbf{S}}$ and lower bound $\underline{\mathbf{S}}$ of the control input are defined by

$$\overline{\mathbf{S}} = \sum_{j=1}^{c} m_j(\mathbf{x})(\mathbf{H}_2\mathbf{F}_j\mathbf{C}\mathbf{x} + \mathbf{H}_2(\mathbf{G}_j - \mathbf{F}_j)\mathbf{C}\mathbf{x}_\mathbf{r}), \tag{3.27}$$

$$\underline{\mathbf{S}} = \sum_{j=1}^{c} m_j(\mathbf{x})(\mathbf{H}_1\mathbf{F}_j\mathbf{C}\mathbf{x} + \mathbf{H}_1(\mathbf{G}_j - \mathbf{F}_j)\mathbf{C}\mathbf{x}_\mathbf{r}). \tag{3.28}$$

Remark 3.7. *In this method, it requires the information of saturation area between upper bound and lower bound in order to choose a proper lower bound* $\underline{\mathbf{S}}$ *which attempts to increase the feasibility of stability condition. Additionally, as mentioned in Introduction, the saturation is just a particular case to control input nonlinearities. The expression of upper bound and lower bound in (3.27) can be generalized as other nonlinear boundaries [90].*

Remark 3.8. $\mathbf{H}_1$ *represents the slope of* $\underline{\mathbf{S}}$*. In order to let the control signal operated in designed saturation area, the following condition has to be satisfied* $\frac{\mathbf{u}_{\max/\min}}{\bar{\mathbf{u}}_{\max/\min}} > \mathbf{H}_1$.

Therefore, the sector nonlinearity inequality (3.14) can be expanded as

$$\begin{aligned}&\sum_{j=1}^{c}\sum_{k=1}^{c} m_j(\mathbf{x})m_k(\mathbf{x})\left[\mathbf{u} - \mathbf{H}_1\mathbf{F}_j\mathbf{C}\mathbf{x} - \mathbf{H}_1(\mathbf{G}_j - \mathbf{F}_j)\mathbf{C}\mathbf{x}_\mathbf{r}\right]^T \\ &\mathbf{\Lambda}^{-1}\left[\mathbf{H}_2\mathbf{F}_k\mathbf{C}\mathbf{x} + \mathbf{H}_2(\mathbf{G}_k - \mathbf{F}_k)\mathbf{C}\mathbf{x}_\mathbf{r} - \mathbf{u}\right] \geq 0.\end{aligned} \tag{3.29}$$

The inequality equation (3.29) is reformualted as below before being applied to stability analysis:

$$\begin{aligned}&\sum_{j=1}^{c}\sum_{k=1}^{c} m_j(\mathbf{x})m_k(\mathbf{x})[\mathbf{u}^T\mathbf{\Lambda}^{-1}\mathbf{H}_2\mathbf{F}_k\mathbf{C}\mathbf{x} + \mathbf{u}^T\mathbf{\Lambda}^{-1}\mathbf{H}_2(\mathbf{G}_k - \mathbf{F}_k)\mathbf{C}\mathbf{x}_\mathbf{r} - \mathbf{u}^T\mathbf{\Lambda}\mathbf{u} \\ &-\mathbf{x}^T\mathbf{C}^T\mathbf{F}_j^T\mathbf{H}_1\mathbf{\Lambda}^{-1}\mathbf{H}_2\mathbf{F}_k\mathbf{C}\mathbf{x} - \mathbf{x}^T\mathbf{C}^T\mathbf{F}_j^T\mathbf{H}_1\mathbf{\Lambda}^{-1}\mathbf{H}_2(\mathbf{G}_k - \mathbf{F}_k)\mathbf{C}\mathbf{x}_\mathbf{r} \\ &+\mathbf{x}^T\mathbf{C}^T\mathbf{F}_j^T\mathbf{H}_1\mathbf{\Lambda}^{-1}\mathbf{u} - \mathbf{x}_\mathbf{r}{}^T\mathbf{C}^T(\mathbf{G}_j - \mathbf{F}_j)^T\mathbf{H}_1\mathbf{\Lambda}^{-1}\mathbf{H}_2\mathbf{F}_k\mathbf{C}\mathbf{x} \\ &-\mathbf{x}_\mathbf{r}{}^T\mathbf{C}^T(\mathbf{G}_j - \mathbf{F}_j)^T\mathbf{H}_1\mathbf{\Lambda}^{-1}\mathbf{H}_2(\mathbf{G}_k - \mathbf{F}_k)\mathbf{C}\mathbf{x}_\mathbf{r} \\ &+\mathbf{x}_\mathbf{r}{}^T\mathbf{C}^T(\mathbf{G}_j - \mathbf{F}_j)^T\mathbf{H}_1\mathbf{\Lambda}^{-1}\mathbf{u}] \geq 0.\end{aligned} \tag{3.30}$$

Then reformulate (3.30) in the matrix form as follows:

$$\begin{bmatrix}\mathbf{X}^{-1}\mathbf{x} \\ \mathbf{X}^{-1}\mathbf{x}_\mathbf{r} \\ \mathbf{X}^{-1}\mathbf{u}\end{bmatrix}^T \mathbf{M} \begin{bmatrix}\mathbf{X}^{-1}\mathbf{x} \\ \mathbf{X}^{-1}\mathbf{x}_\mathbf{r} \\ \mathbf{X}^{-1}\mathbf{u}\end{bmatrix} \geq 0 \tag{3.31}$$

where

$$\mathbf{M} = \sum_{j=1}^{c}\sum_{k=1}^{c} m_j(\mathbf{x})m_k(\mathbf{x}) \begin{bmatrix}\mathbf{M}_{jk}^{(11)} & * & * \\ \mathbf{M}_{jk}^{(21)} & \mathbf{M}_{jk}^{(22)} & * \\ \mathbf{M}_{jk}^{(31)} & \mathbf{M}_{jk}^{(32)} & -\mathbf{X}\mathbf{\Lambda}^{-1}\mathbf{X}\end{bmatrix}$$

where

$$\begin{aligned}
\mathbf{M}_{jk}^{(11)} &= -\mathbf{X}\mathbf{C}^T\mathbf{F}_j^T\mathbf{H}_1\mathbf{\Lambda}^{-1}\mathbf{H}_2\mathbf{F}_k\mathbf{C}\mathbf{X};\\
\mathbf{M}_{jk}^{(21)} &= -\mathbf{X}\mathbf{C}^T(\mathbf{G}_j-\mathbf{F}_j)^T\mathbf{H}_1\mathbf{\Lambda}^{-1}\mathbf{H}_2\mathbf{F}_k\mathbf{C}\mathbf{X};\\
\mathbf{M}_{jk}^{(22)} &= -\mathbf{X}\mathbf{C}^T(\mathbf{G}_j-\mathbf{F}_j)^T\mathbf{H}_1\mathbf{\Lambda}^{-1}\mathbf{H}_2(\mathbf{G}_k-\mathbf{F}_k)\mathbf{C}\mathbf{X};\\
\mathbf{M}_{jk}^{(31)} &= \mathbf{X}\mathbf{\Lambda}^{-1}\frac{\mathbf{H}_1+\mathbf{H}_2}{2}\mathbf{F}_j\mathbf{C}\mathbf{X};\\
\mathbf{M}_{jk}^{(32)} &= \mathbf{X}\mathbf{\Lambda}^{-1}\frac{\mathbf{H}_1+\mathbf{H}_2}{2}(\mathbf{G}_j-\mathbf{F}_j)\mathbf{C}\mathbf{X}.
\end{aligned}$$

Remark 3.9. *As* $\mathbf{H}_1$, $\mathbf{H}_2$ *and* $\mathbf{\Lambda}$ *are all diagonal matrices, it gives* $\mathbf{H}_1\mathbf{\Lambda}^{-1}\mathbf{H}_2 = \mathbf{H}_2\mathbf{\Lambda}^{-1}\mathbf{H}_1$. *Thus,* (3.30) *can be written in the form of* (3.31) *where matrix* $\mathbf{M}$ *is symmetric.*

3.3.3 Tracking Control $\mathcal{H}_\infty$ Performance with Control Input Saturation

Based on the analysis in the previous three sections: tracking control, $\mathcal{H}_\infty$ performance and control input saturation, we include the information of control input saturation specified in (3.14) to be expressed in the matrix form in (3.31) into (3.24).

When (3.14) is considered, by applying S-procedure in Lemma 1, the holding of (3.25) is implied by the holding of the following inequality:

$$\dot{V} + \mathbf{e}^T\mathbf{e} - \sigma_1^2{\mathbf{x_r}}^T\mathbf{x_r} - \sigma_2^2\mathbf{r}^T\mathbf{r} + (\mathbf{u}-\underline{\mathbf{S}})^T\mathbf{\Lambda}^{-1}(\overline{\mathbf{S}}-\mathbf{u}) < 0. \tag{3.32}$$

Substituting (3.23) and (3.31) into (3.32), it gives

$$\begin{aligned}
&\sum_{i=1}^{p}\sum_{j=1}^{c}\sum_{k=1}^{c} w_i(\mathbf{x})m_j(\mathbf{x})m_k(\mathbf{x}) \begin{bmatrix} \mathbf{X}^{-1}\mathbf{x} \\ \mathbf{X}^{-1}\mathbf{x_r} \\ \mathbf{X}^{-1}\mathbf{u} \\ \mathbf{X}^{-1}\mathbf{r} \end{bmatrix}^T \\
&\times \begin{bmatrix} \mathbf{\Delta}_{ijk}^{(11)} & * & * & * \\ \mathbf{\Delta}_{ijk}^{(21)} & \mathbf{\Delta}_{jk}^{(22)} & * & * \\ \mathbf{\Delta}_{ij}^{(31)} & \mathbf{\Delta}_{ij}^{(32)} & -\mathbf{X}\mathbf{\Lambda}^{-1}\mathbf{X} & * \\ -\mathbf{X}{\mathbf{B_r}}^T & \mathbf{X}{\mathbf{B_r}}^T & \mathbf{0} & -\sigma_2^2\mathbf{X}\mathbf{X} \end{bmatrix} \begin{bmatrix} \mathbf{X}^{-1}\mathbf{x} \\ \mathbf{X}^{-1}\mathbf{x_r} \\ \mathbf{X}^{-1}\mathbf{u} \\ \mathbf{X}^{-1}\mathbf{r} \end{bmatrix} < 0
\end{aligned} \tag{3.33}$$

where

$$\mathbf{\Delta}_{ijk}^{(11)} = \mathbf{X}\mathbf{A}_i^T + \mathbf{A}_i\mathbf{X} + \mathbf{X}\mathbf{X} - \mathbf{X}\mathbf{C}^T\mathbf{F}_j^T\mathbf{H}_1\mathbf{\Lambda}^{-1}\mathbf{H}_2\mathbf{F}_k\mathbf{C}\mathbf{X}; \tag{3.34}$$

$$\boldsymbol{\Delta}_{ijk}^{(21)} = -\mathbf{A}_i\mathbf{X} - \mathbf{X}\mathbf{A_r}^T - \mathbf{X}\mathbf{X} - \mathbf{X}\mathbf{C}^T(\mathbf{G}_j - \mathbf{F}_j)^T\mathbf{H}_1\boldsymbol{\Lambda}^{-1}\mathbf{H}_2\mathbf{F}_k\mathbf{C}\mathbf{X}; \quad (3.35)$$

$$\begin{aligned}\boldsymbol{\Delta}_{jk}^{(22)} &= \mathbf{X}\mathbf{A_r}^T + \mathbf{A_r}\mathbf{X} + \mathbf{X}\mathbf{X} - \sigma_1^2\mathbf{X}\mathbf{X} \\ &\quad -\mathbf{X}\mathbf{C}^T(\mathbf{G}_j - \mathbf{F}_j)^T\mathbf{H}_1\boldsymbol{\Lambda}^{-1}\mathbf{H}_2(\mathbf{G}_k - \mathbf{F}_k)\mathbf{C}\mathbf{X}; \end{aligned} \quad (3.36)$$

$$\boldsymbol{\Delta}_{ij}^{(31)} = \mathbf{X}\mathbf{B}_i^T + \mathbf{X}\boldsymbol{\Lambda}^{-1}\frac{\mathbf{H}_1 + \mathbf{H}_2}{2}\mathbf{F}_j\mathbf{C}\mathbf{X}; \quad (3.37)$$

$$\boldsymbol{\Delta}_{ij}^{(32)} = -\mathbf{X}\mathbf{B}_i^T + \mathbf{X}\boldsymbol{\Lambda}^{-1}\frac{\mathbf{H}_1 + \mathbf{H}_2}{2}(\mathbf{G}_j - \mathbf{F}_j)\mathbf{C}\mathbf{X}. \quad (3.38)$$

To further proceed the analysis for obtaining the stability conditions in convex form guaranteeing the holding of (3.33), the Schur complement Lemma [68] is introduced.

By applying Schur complement in Lemma 2 to (3.33), the holding of (3.33) is equivalent to the holding of the inequality below:

$$\begin{aligned}\boldsymbol{\Phi} &\equiv \sum_{i=1}^{p}\sum_{j=1}^{c}\sum_{k=1}^{c} w_i(\mathbf{x})m_j(\mathbf{x})m_k(\mathbf{x}) \begin{bmatrix} \boldsymbol{\Delta}_{ijk}^{(11)} & * \\ \boldsymbol{\Delta}_{ijk}^{(21)} & \boldsymbol{\Delta}_{jk}^{(22)} \end{bmatrix} \\ &+ \left(\sum_{i=1}^{p}\sum_{j=1}^{c} w_i(\mathbf{x})m_j(\mathbf{x}) \begin{bmatrix} \boldsymbol{\Delta}_{ij}^{(31)} & \boldsymbol{\Delta}_{ij}^{(32)} \\ -\mathbf{X}\mathbf{B_r}^T & \mathbf{X}\mathbf{B_r}^T \end{bmatrix}\right)^T \\ &\times \begin{bmatrix} \mathbf{X}^{-1}\boldsymbol{\Lambda}\mathbf{X}^{-1} & * \\ 0 & \sigma_2^{-2}\mathbf{X}^{-1}\mathbf{X}^{-1} \end{bmatrix} \left(\sum_{r=1}^{p}\sum_{s=1}^{c} w_l(\mathbf{x})m_s(\mathbf{x}) \begin{bmatrix} \boldsymbol{\Delta}_{ls}^{(31)} & \boldsymbol{\Delta}_{ls}^{(32)} \\ -\mathbf{X}\mathbf{B_r}^T & \mathbf{X}\mathbf{B_r}^T \end{bmatrix}\right) \\ = &\sum_{i=1}^{p}\sum_{j=1}^{c}\sum_{k=1}^{c} w_i(\mathbf{x})m_j(\mathbf{x})m_k(\mathbf{x}) \begin{bmatrix} \boldsymbol{\Delta}_{ijk}^{(11)} & * \\ \boldsymbol{\Delta}_{ijk}^{(21)} & \boldsymbol{\Delta}_{jk}^{(22)} \end{bmatrix} \\ &+ \sum_{i=1}^{p}\sum_{j=1}^{c}\sum_{l=1}^{p}\sum_{s=1}^{c} w_i(\mathbf{x})m_j(\mathbf{x})w_l(\mathbf{x})m_s(\mathbf{x}) \begin{bmatrix} \boldsymbol{\Theta}_{ijls}^{(11)} & * \\ \boldsymbol{\Theta}_{ijls}^{(21)} & \boldsymbol{\Theta}_{ijls}^{(22)} \end{bmatrix} < 0 \end{aligned} \quad (3.39)$$

where

$$\begin{aligned}\boldsymbol{\Theta}_{ijls}^{(11)} &= \mathbf{B}_i\boldsymbol{\Lambda}\mathbf{B}_l^T + \mathbf{X}\mathbf{C}^T\mathbf{F}_j^T\frac{\mathbf{H}_1 + \mathbf{H}_2}{2}\boldsymbol{\Lambda}^{-1}\frac{\mathbf{H}_1 + \mathbf{H}_2}{2}\mathbf{F}_s\mathbf{C}\mathbf{X} + \mathbf{X}\mathbf{C}^T\mathbf{F}_j^T\frac{\mathbf{H}_1 + \mathbf{H}_2}{2}\mathbf{B}_l^T \\ &\quad +\mathbf{B}_i\frac{\mathbf{H}_1 + \mathbf{H}_2}{2}\mathbf{F}_s\mathbf{C}\mathbf{X} + \mathbf{B_r}\sigma_2^{-2}\mathbf{B_r}^T; \end{aligned} \quad (3.40)$$

$$\begin{aligned}\boldsymbol{\Theta}_{ijls}^{(21)} &= -\mathbf{B}_i\boldsymbol{\Lambda}\mathbf{B}_l^T + \mathbf{X}\mathbf{C}^T(\mathbf{G}_j-\mathbf{F}_j)^T\frac{\mathbf{H}_1+\mathbf{H}_2}{2}\boldsymbol{\Lambda}^{-1}\frac{\mathbf{H}_1+\mathbf{H}_2}{2}\mathbf{F}_s\mathbf{C}\mathbf{X}\\ &\quad +\mathbf{X}\mathbf{C}^T(\mathbf{G}_j-\mathbf{F}_j)^T\frac{\mathbf{H}_1+\mathbf{H}_2}{2}\mathbf{B}_l^T - \mathbf{B}_i\frac{\mathbf{H}_1+\mathbf{H}_2}{2}\mathbf{F}_s\mathbf{C}\mathbf{X}\\ &\quad -\mathbf{B}_{\mathbf{r}}\sigma_2^{-2}\mathbf{B}_{\mathbf{r}}{}^T; \end{aligned} \tag{3.41}$$

$$\begin{aligned}\boldsymbol{\Theta}_{ijls}^{(22)} &= \mathbf{B}_i\boldsymbol{\Lambda}\mathbf{B}_l^T + \mathbf{X}\mathbf{C}^T(\mathbf{G}_j-\mathbf{F}_j)^T\frac{\mathbf{H}_1+\mathbf{H}_2}{2}\boldsymbol{\Lambda}^{-1}\frac{\mathbf{H}_1+\mathbf{H}_2}{2}(\mathbf{G}_s-\mathbf{F}_s)\mathbf{C}\mathbf{X}\\ &\quad -\mathbf{X}\mathbf{C}^T(\mathbf{G}_j-\mathbf{F}_j)^T\frac{\mathbf{H}_1+\mathbf{H}_2}{2}\mathbf{B}_l^T - \mathbf{B}_i\frac{\mathbf{H}_1+\mathbf{H}_2}{2}(\mathbf{G}_s-\mathbf{F}_s)\mathbf{C}\mathbf{X}\\ &\quad +\mathbf{B}_{\mathbf{r}}\sigma_2^{-2}\mathbf{B}_{\mathbf{r}}{}^T. \end{aligned} \tag{3.42}$$

Referring to (3.39), the following mathematical terms can be further combined:

$$\begin{aligned}&\sum_{j=1}^{c}\sum_{k=1}^{c} m_j(\mathbf{x})m_k(\mathbf{x})\left(-\mathbf{X}\mathbf{C}^T\mathbf{F}_j^T\mathbf{H}_1\boldsymbol{\Lambda}^{-1}\mathbf{H}_2\mathbf{F}_k\mathbf{C}\mathbf{X}\right)\\ &+\sum_{j=1}^{c}\sum_{s=1}^{c} m_j(\mathbf{x})m_s(\mathbf{x})\left(\mathbf{X}\mathbf{C}^T\mathbf{F}_j^T\frac{\mathbf{H}_1+\mathbf{H}_2}{2}\boldsymbol{\Lambda}^{-1}\frac{\mathbf{H}_1+\mathbf{H}_2}{2}\mathbf{F}_s\mathbf{C}\mathbf{X}\right)\\ =&\sum_{j=1}^{c}\sum_{k=1}^{c} m_j(\mathbf{x})m_k(\mathbf{x})\mathbf{X}\mathbf{C}^T\mathbf{F}_j^T\Bigg(-4\times\frac{\mathbf{H}_1}{2}\boldsymbol{\Lambda}^{-1}\frac{\mathbf{H}_2}{2}+\frac{\mathbf{H}_1}{2}\boldsymbol{\Lambda}^{-1}\frac{\mathbf{H}_1}{2}+\frac{\mathbf{H}_2}{2}\boldsymbol{\Lambda}^{-1}\frac{\mathbf{H}_2}{2}\\ &+\frac{\mathbf{H}_1}{2}\boldsymbol{\Lambda}^{-1}\frac{\mathbf{H}_2}{2}+\frac{\mathbf{H}_2}{2}\boldsymbol{\Lambda}^{-1}\frac{\mathbf{H}_1}{2}\Bigg)\mathbf{F}_k\mathbf{C}\mathbf{X}\\ =&\sum_{j=1}^{c}\sum_{k=1}^{c} m_j(\mathbf{x})m_k(\mathbf{x})\mathbf{X}\mathbf{C}^T\mathbf{F}_j^T\Bigg(\frac{\mathbf{H}_1}{2}\boldsymbol{\Lambda}^{-1}\frac{\mathbf{H}_1}{2}+\frac{\mathbf{H}_2}{2}\boldsymbol{\Lambda}^{-1}\frac{\mathbf{H}_2}{2}-\frac{\mathbf{H}_1}{2}\boldsymbol{\Lambda}^{-1}\frac{\mathbf{H}_2}{2}\\ &-\frac{\mathbf{H}_1}{2}\boldsymbol{\Lambda}^{-1}\frac{\mathbf{H}_2}{2}\Bigg)\mathbf{F}_k\mathbf{C}\mathbf{X}\\ =&\sum_{j=1}^{c}\sum_{k=1}^{c} m_j(\mathbf{x})m_k(\mathbf{x})\left(\mathbf{X}\mathbf{C}^T\mathbf{F}_j^T\frac{\mathbf{H}_1-\mathbf{H}_2}{2}\boldsymbol{\Lambda}^{-1}\frac{\mathbf{H}_1-\mathbf{H}_2}{2}\mathbf{F}_k\mathbf{C}\mathbf{X}\right); \end{aligned} \tag{3.43}$$

$$\begin{aligned}&\sum_{j=1}^{c}\sum_{k=1}^{c} m_j(\mathbf{x})m_k(\mathbf{x})\left(-\mathbf{X}\mathbf{C}^T(\mathbf{G}_j-\mathbf{F}_j)^T\mathbf{H}_1\boldsymbol{\Lambda}^{-1}\mathbf{H}_2\mathbf{F}_k\mathbf{C}\mathbf{X}\right)\\ &+\sum_{j=1}^{c}\sum_{s=1}^{c} m_j(\mathbf{x})m_s(\mathbf{x})\left(\mathbf{X}\mathbf{C}^T(\mathbf{G}_j-\mathbf{F}_j)^T\frac{\mathbf{H}_1+\mathbf{H}_2}{2}\boldsymbol{\Lambda}^{-1}\frac{\mathbf{H}_1+\mathbf{H}_2}{2}\mathbf{F}_s\mathbf{C}\mathbf{X}\right)\\ =&\sum_{j=1}^{c}\sum_{k=1}^{c} m_j(\mathbf{x})m_k(\mathbf{x})\\ &\left(\mathbf{X}\mathbf{C}^T(\mathbf{G}_j-\mathbf{F}_j)^T\frac{\mathbf{H}_1-\mathbf{H}_2}{2}\boldsymbol{\Lambda}^{-1}\frac{\mathbf{H}_1-\mathbf{H}_2}{2}\mathbf{F}_k\mathbf{C}\mathbf{X}\right); \end{aligned} \tag{3.44}$$

$$
\begin{aligned}
&\sum_{j=1}^{c}\sum_{k=1}^{c} m_j(\mathbf{x})m_k(\mathbf{x})\left(-\mathbf{X}\mathbf{C}^T(\mathbf{G}_j-\mathbf{F}_j)^T\mathbf{H}_1\mathbf{\Lambda}^{-1}\mathbf{H}_2(\mathbf{G}_k-\mathbf{F}_k)\mathbf{C}\mathbf{X}\right)\\
&+\sum_{j=1}^{c}\sum_{s=1}^{c} m_j(\mathbf{x})m_s(\mathbf{x})\\
&\left(\mathbf{X}\mathbf{C}^T(\mathbf{G}_j-\mathbf{F}_j)^T\frac{\mathbf{H}_1+\mathbf{H}_2}{2}\mathbf{\Lambda}^{-1}\frac{\mathbf{H}_1+\mathbf{H}_2}{2}(\mathbf{G}_s-\mathbf{F}_s)\mathbf{C}\mathbf{X}\right)\\
=\ &\sum_{j=1}^{c}\sum_{k=1}^{c} m_j(\mathbf{x})m_k(\mathbf{x})\\
&\left(\mathbf{X}\mathbf{C}^T(\mathbf{G}_j-\mathbf{F}_j)^T\frac{\mathbf{H}_1-\mathbf{H}_2}{2}\mathbf{\Lambda}^{-1}\frac{\mathbf{H}_1-\mathbf{H}_2}{2}(\mathbf{G}_k-\mathbf{F}_k)\mathbf{C}\mathbf{X}\right). \qquad (3.45)
\end{aligned}
$$

Integrating (3.43), (3.44) and (3.45) into (3.39), (3.39) can be reformulated in a compact form as below:

$$
\mathbf{\Phi}=\sum_{i=1}^{p}\sum_{j=1}^{c}\sum_{l=1}^{p}\sum_{k=1}^{c} w_i(\mathbf{x})m_j(\mathbf{x})w_l(\mathbf{x})m_k(\mathbf{x})\begin{bmatrix}\mathbf{\Phi}_{ijlk}^{(11)} & *\\ \mathbf{\Phi}_{ijlk}^{(21)} & \mathbf{\Phi}_{ijlk}^{(22)}\end{bmatrix}<0 \qquad (3.46)
$$

where

$$
\begin{aligned}
\mathbf{\Phi}_{ijlk}^{(11)} =\ &\mathbf{X}\mathbf{A}_i^T+\mathbf{A}_i\mathbf{X}+\mathbf{X}\mathbf{X}+\mathbf{X}\mathbf{C}^T\mathbf{F}_j^T\frac{\mathbf{H}_1-\mathbf{H}_2}{2}\mathbf{\Lambda}^{-1}\frac{\mathbf{H}_1-\mathbf{H}_2}{2}\mathbf{F}_k\mathbf{C}\mathbf{X}+\mathbf{B}_i\mathbf{\Lambda}\mathbf{B}_l^T\\
&+\mathbf{X}\mathbf{C}^T\mathbf{F}_j^T\frac{\mathbf{H}_1+\mathbf{H}_2}{2}\mathbf{B}_i^T+\mathbf{B}_i\frac{\mathbf{H}_1+\mathbf{H}_2}{2}\mathbf{F}_j\mathbf{C}\mathbf{X}+\mathbf{B}_\mathbf{r}\sigma_2^{-2}\mathbf{B}_\mathbf{r}{}^T; \qquad (3.47)
\end{aligned}
$$

$$
\begin{aligned}
\mathbf{\Phi}_{ijlk}^{(21)} =\ &-\mathbf{A}_i\mathbf{X}-\mathbf{X}\mathbf{A}_\mathbf{r}{}^T-\mathbf{X}\mathbf{X}+\mathbf{X}\mathbf{C}^T(\mathbf{G}_j-\mathbf{F}_j)^T\frac{\mathbf{H}_1-\mathbf{H}_2}{2}\mathbf{\Lambda}^{-1}\frac{\mathbf{H}_1-\mathbf{H}_2}{2}\mathbf{F}_k\mathbf{C}\mathbf{X}\\
&-\mathbf{B}_i\mathbf{\Lambda}\mathbf{B}_l^T+\mathbf{X}\mathbf{C}^T(\mathbf{G}_j-\mathbf{F}_j)^T\frac{\mathbf{H}_1+\mathbf{H}_2}{2}\mathbf{B}_i^T-\mathbf{B}_i\frac{\mathbf{H}_1+\mathbf{H}_2}{2}\mathbf{F}_j\mathbf{C}\mathbf{X}\\
&-\mathbf{B}_\mathbf{r}\sigma_2^{-2}\mathbf{B}_\mathbf{r}{}^T; \qquad (3.48)
\end{aligned}
$$

$$
\begin{aligned}
\mathbf{\Phi}_{ijlk}^{(22)} =\ &\mathbf{A}_\mathbf{r}\mathbf{X}+\mathbf{X}\mathbf{A}_\mathbf{r}{}^T+\mathbf{X}(\mathbf{I}-\sigma_1^2)\mathbf{X}\\
&+\mathbf{X}\mathbf{C}^T(\mathbf{G}_j-\mathbf{F}_j)^T\frac{\mathbf{H}_1-\mathbf{H}_2}{2}\mathbf{\Lambda}^{-1}\frac{\mathbf{H}_1-\mathbf{H}_2}{2}(\mathbf{G}_k-\mathbf{F}_k)\mathbf{C}\mathbf{X}+\mathbf{B}_i\mathbf{\Lambda}\mathbf{B}_l^T\\
&-\mathbf{X}\mathbf{C}^T(\mathbf{G}_j-\mathbf{F}_j)^T\frac{\mathbf{H}_1+\mathbf{H}_2}{2}\mathbf{B}_i^T-\mathbf{B}_i\frac{\mathbf{H}_1+\mathbf{H}_2}{2}(\mathbf{G}_j-\mathbf{F}_j)\mathbf{C}\mathbf{X}\\
&+\mathbf{B}_\mathbf{r}\sigma_2^{-2}\mathbf{B}_\mathbf{r}{}^T. \qquad (3.49)
\end{aligned}
$$

In order to eliminate the non-convex issue brought by output feedback control,

$\mathbf{\Gamma} \in \mathbb{R}^{n\times n}$ [45] is defined as

$$\mathbf{\Gamma} = \begin{bmatrix} \mathbf{C}^T(\mathbf{C}\mathbf{C}^T)^{-1} & ortc(\mathbf{C}^T) \end{bmatrix}, \tag{3.50}$$

then

$$\mathbf{C}\mathbf{\Gamma} = \begin{bmatrix} \mathbf{I}_l & \mathbf{0} \end{bmatrix} \tag{3.51}$$

where $ortc(\mathbf{C}^T)$ stands for the orthogonal complement of $\mathbf{C}^T$ and $\mathbf{I}_l \in \mathbb{R}^{l\times l}$ is an identity matrix.

In order to proceed further analysis, we assume that $\mathbf{\Gamma}^{-1}$ exists and choose

$$\mathbf{X} = \begin{bmatrix} \mathbf{X}_{11} & \mathbf{0} \\ \mathbf{0} & \mathbf{X}_{22} \end{bmatrix} \tag{3.52}$$

where $\mathbf{X}_{11} \in \mathbb{R}^{l\times l}$ and $\mathbf{X}_{22} \in \mathbb{R}^{(n-l)\times(n-l)}$.

The feedback gains are designed as

$$\mathbf{F} = \mathbf{M}(\mathbf{\Gamma}^{-1}\mathbf{X})^{-1}; \tag{3.53}$$

$$\mathbf{G} = \mathbf{N}(\mathbf{\Gamma}^{-1}\mathbf{X})^{-1} \tag{3.54}$$

where $\mathbf{M}_j \in \mathbb{R}^{m\times l}$ and $\mathbf{N}_j \in \mathbb{R}^{m\times l}$.

From (3.51), (3.53) and (3.54), we can obtain that

$$\mathbf{F}_j\mathbf{C}\mathbf{X} = \mathbf{F}_j\mathbf{C}\mathbf{\Gamma}\mathbf{\Gamma}^{-1}\mathbf{X} = \begin{bmatrix} \mathbf{M}_j & \mathbf{0} \end{bmatrix}; \tag{3.55}$$

$$\mathbf{G}_j\mathbf{C}\mathbf{X} = \mathbf{G}_j\mathbf{C}\mathbf{\Gamma}\mathbf{\Gamma}^{-1}\mathbf{X} = \begin{bmatrix} \mathbf{N}_j & \mathbf{0} \end{bmatrix}; \tag{3.56}$$

$$(\mathbf{G}_j - \mathbf{F}_j)\mathbf{C}\mathbf{X} = \begin{bmatrix} \mathbf{N}_j - \mathbf{M}_j & \mathbf{0} \end{bmatrix}. \tag{3.57}$$

Using (3.55), (3.56) and (3.57), (3.46) can be rewritten in the form as follows where the output feedback terms are transformed into a convex form:

$$\mathbf{\Phi} = \sum_{i=1}^{p}\sum_{j=1}^{c}\sum_{l=1}^{p}\sum_{k=1}^{c} w_i(\mathbf{x})m_j(\mathbf{x})w_l(\mathbf{x})m_k(\mathbf{x}) \begin{bmatrix} \mathbf{\Phi}_{ijlk}^{(new11)} & * \\ \mathbf{\Phi}_{ijlk}^{(new21)} & \mathbf{\Phi}_{ijlk}^{(new22)} \end{bmatrix} < 0 \tag{3.58}$$

where

$$\begin{aligned} \mathbf{\Phi}_{ijlk}^{(new11)} &= \mathbf{X}\mathbf{A}_i^T + \mathbf{A}_i\mathbf{X} + \mathbf{X}\mathbf{X} + \begin{bmatrix} \mathbf{M}_j & \mathbf{0} \end{bmatrix}^T \frac{\mathbf{H}_1 - \mathbf{H}_2}{2}\mathbf{\Lambda}^{-1}\frac{\mathbf{H}_1 - \mathbf{H}_2}{2}\begin{bmatrix} \mathbf{M}_k & \mathbf{0} \end{bmatrix} \\ &\quad + \mathbf{B}_i\mathbf{\Lambda}\mathbf{B}_l^T + \begin{bmatrix} \mathbf{M}_j & \mathbf{0} \end{bmatrix}^T \frac{\mathbf{H}_1 + \mathbf{H}_2}{2}\mathbf{B}_i^T + \mathbf{B}_i\frac{\mathbf{H}_1 + \mathbf{H}_2}{2}\begin{bmatrix} \mathbf{M}_j & \mathbf{0} \end{bmatrix} \\ &\quad + \mathbf{B}_\mathbf{r}\sigma_2^{-2}\mathbf{B}_\mathbf{r}{}^T; \end{aligned} \tag{3.59}$$

$$\begin{aligned}\boldsymbol{\Phi}_{ijlk}^{(new21)} &= -\mathbf{A}_i\mathbf{X} - \mathbf{X}{\mathbf{A}_\mathbf{r}}^T - \mathbf{X}\mathbf{X} \\ &+ \begin{bmatrix}\mathbf{N}_j - \mathbf{M}_j & \mathbf{0}\end{bmatrix}^T \frac{\mathbf{H}_1 - \mathbf{H}_2}{2}\boldsymbol{\Lambda}^{-1}\frac{\mathbf{H}_1 - \mathbf{H}_2}{2}\begin{bmatrix}\mathbf{M}_k & \mathbf{0}\end{bmatrix} - \mathbf{B}_i\boldsymbol{\Lambda}\mathbf{B}_l^T \\ &+ \begin{bmatrix}\mathbf{N}_j - \mathbf{M}_j & \mathbf{0}\end{bmatrix}^T \frac{\mathbf{H}_1 + \mathbf{H}_2}{2}\mathbf{B}_i^T - \mathbf{B}_i\frac{\mathbf{H}_1 + \mathbf{H}_2}{2}\begin{bmatrix}\mathbf{M}_j & \mathbf{0}\end{bmatrix} \\ &- \mathbf{B}_\mathbf{r}\sigma_2^{-2}{\mathbf{B}_\mathbf{r}}^T; \end{aligned} \tag{3.60}$$

$$\begin{aligned}\boldsymbol{\Phi}_{ijlk}^{(new22)} &= \mathbf{A}_\mathbf{r}\mathbf{X} + \mathbf{X}{\mathbf{A}_\mathbf{r}}^T + \mathbf{X}(\mathbf{I} - \sigma_1^2)\mathbf{X} \\ &+ \begin{bmatrix}\mathbf{N}_j - \mathbf{M}_j & \mathbf{0}\end{bmatrix}^T \frac{\mathbf{H}_1 - \mathbf{H}_2}{2}\boldsymbol{\Lambda}^{-1}\frac{\mathbf{H}_1 - \mathbf{H}_2}{2}\begin{bmatrix}\mathbf{N}_k - \mathbf{M}_k & \mathbf{0}\end{bmatrix} + \mathbf{B}_i\boldsymbol{\Lambda}\mathbf{B}_l^T \\ &- \begin{bmatrix}\mathbf{N}_j - \mathbf{M}_j & \mathbf{0}\end{bmatrix}^T \frac{\mathbf{H}_1 + \mathbf{H}_2}{2}\mathbf{B}_i^T - \mathbf{B}_i\frac{\mathbf{H}_1 + \mathbf{H}_2}{2}\begin{bmatrix}\mathbf{N}_j - \mathbf{M}_j & \mathbf{0}\end{bmatrix} \\ &+ \mathbf{B}_\mathbf{r}\sigma_2^{-2}{\mathbf{B}_\mathbf{r}}^T. \end{aligned} \tag{3.61}$$

Rearranging the terms in (3.58) before applying Schur complement, (3.58) can be reformulated as

$$\begin{aligned}\boldsymbol{\Phi} &= \sum_{i=1}^{p}\sum_{j=1}^{c} w_i(\mathbf{x})m_j(\mathbf{x})\begin{bmatrix}\tilde{\boldsymbol{\Phi}}_{ij}^{(11)} & * \\ \tilde{\boldsymbol{\Phi}}_{ij}^{(21)} & \tilde{\boldsymbol{\Phi}}_{ij}^{(22)}\end{bmatrix} + \sum_{j=1}^{c}\sum_{k=1}^{c} m_j(\mathbf{x})m_k(\mathbf{x}) \\ &\begin{bmatrix}\begin{bmatrix}\mathbf{M}_j & \mathbf{0}\end{bmatrix}^T \frac{\mathbf{H}_1 - \mathbf{H}_2}{2} \\ \begin{bmatrix}\mathbf{N}_j - \mathbf{M}_j & \mathbf{0}\end{bmatrix}^T \frac{\mathbf{H}_1 - \mathbf{H}_2}{2}\end{bmatrix}\boldsymbol{\Lambda}^{-1}\begin{bmatrix}\frac{\mathbf{H}_1 - \mathbf{H}_2}{2}\begin{bmatrix}\mathbf{M}_k & \mathbf{0}\end{bmatrix} & \frac{\mathbf{H}_1 - \mathbf{H}_2}{2}\begin{bmatrix}\mathbf{N}_k - \mathbf{M}_k & \mathbf{0}\end{bmatrix}\end{bmatrix} \\ &+ \sum_{i=1}^{p}\sum_{l=1}^{p} w_i(\mathbf{x})w_l(\mathbf{x})\begin{bmatrix}\mathbf{B}_i\boldsymbol{\Lambda} \\ -\mathbf{B}_i\boldsymbol{\Lambda}\end{bmatrix}\boldsymbol{\Lambda}^{-1}\begin{bmatrix}\boldsymbol{\Lambda}\mathbf{B}_l^T & -\boldsymbol{\Lambda}\mathbf{B}_l^T\end{bmatrix} \\ &+ \begin{bmatrix}\mathbf{B}_\mathbf{r} \\ -\mathbf{B}_\mathbf{r}\end{bmatrix}\sigma_2^{-2}\begin{bmatrix}{\mathbf{B}_\mathbf{r}}^T & -{\mathbf{B}_\mathbf{r}}^T\end{bmatrix} + \begin{bmatrix}\mathbf{X} \\ -\mathbf{X}\end{bmatrix}\mathbf{I}\begin{bmatrix}\mathbf{X} & -\mathbf{X}\end{bmatrix} \\ &+ \begin{bmatrix}\mathbf{0} & \mathbf{0} \\ \mathbf{0} & -\sigma_1^2\mathbf{X}\mathbf{X}\end{bmatrix} < 0 \end{aligned} \tag{3.62}$$

where

$$\begin{aligned}\tilde{\boldsymbol{\Phi}}_{ij}^{(11)} &= \mathbf{X}\mathbf{A}_i^T + \mathbf{A}_i\mathbf{X} + \begin{bmatrix}\mathbf{M}_j & \mathbf{0}\end{bmatrix}^T \frac{\mathbf{H}_1 + \mathbf{H}_2}{2}\mathbf{B}_i^T \\ &+ \mathbf{B}_i\frac{\mathbf{H}_1 + \mathbf{H}_2}{2}\begin{bmatrix}\mathbf{M}_j & \mathbf{0}\end{bmatrix}; \end{aligned} \tag{3.63}$$

$$\tilde{\boldsymbol{\Phi}}_{ij}^{(21)} = -\mathbf{A}_i\mathbf{X} - \mathbf{X}{\mathbf{A}_\mathbf{r}}^T + \begin{bmatrix}\mathbf{N}_j - \mathbf{M}_j & \mathbf{0}\end{bmatrix}^T \frac{\mathbf{H}_1 + \mathbf{H}_2}{2}\mathbf{B}_i^T$$

$$-\mathbf{B}_i\frac{\mathbf{H}_1+\mathbf{H}_2}{2}\begin{bmatrix}\mathbf{M}_j & \mathbf{0}\end{bmatrix}; \tag{3.64}$$

$$\begin{aligned}\tilde{\mathbf{\Phi}}_{ij}^{(22)} &= \mathbf{A_r X} + \mathbf{X}{\mathbf{A_r}}^T - \begin{bmatrix}\mathbf{N}_j - \mathbf{M}_j & \mathbf{0}\end{bmatrix}^T \frac{\mathbf{H}_1+\mathbf{H}_2}{2}\mathbf{B}_i^T \\ &\quad -\mathbf{B}_i\frac{\mathbf{H}_1+\mathbf{H}_2}{2}\begin{bmatrix}\mathbf{N}_j - \mathbf{M}_j & \mathbf{0}\end{bmatrix}.\end{aligned} \tag{3.65}$$

It can be seen from (3.62) that $-\sigma_1^{-2}\mathbf{XX}$ is still in non-convex form. Let ϵ be a pre-defined constant value, we have

$$(\mathbf{X}-\epsilon\mathbf{I})^T(\mathbf{X}-\epsilon\mathbf{I}) \geq 0. \tag{3.66}$$

The non-convex term in (3.62) can be handled by using the following property [93]

$$-\sigma_1^2\mathbf{X}^T\mathbf{X} \leq \sigma_1^2(\epsilon^2\mathbf{I}^2 - \epsilon\mathbf{X}^T - \epsilon\mathbf{X}). \tag{3.67}$$

Thus, we can further obtain the following:

$$\begin{aligned}\mathbf{\Phi} \leq\ & \sum_{i=1}^{p}\sum_{j=1}^{c} w_i(\mathbf{x})m_j(\mathbf{x})\begin{bmatrix}\tilde{\mathbf{\Phi}}_{ij}^{(11)} & * \\ \tilde{\mathbf{\Phi}}_{ij}^{(21)} & \tilde{\mathbf{\Phi}}_{ij}^{(22)}\end{bmatrix} \\ & + \sum_{j=1}^{c}\sum_{k=1}^{c} m_j(\mathbf{x})m_k(\mathbf{x}) \\ & \begin{bmatrix}\begin{bmatrix}\mathbf{M}_j & \mathbf{0}\end{bmatrix}^T \frac{\mathbf{H}_1-\mathbf{H}_2}{2} \\ \begin{bmatrix}\mathbf{N}_j - \mathbf{M}_j & \mathbf{0}\end{bmatrix}^T \frac{\mathbf{H}_1-\mathbf{H}_2}{2}\end{bmatrix} \mathbf{\Lambda}^{-1}\begin{bmatrix}\frac{\mathbf{H}_1-\mathbf{H}_2}{2}\begin{bmatrix}\mathbf{M}_k & \mathbf{0}\end{bmatrix} & \frac{\mathbf{H}_1-\mathbf{H}_2}{2}\begin{bmatrix}\mathbf{N}_k - \mathbf{M}_k & \mathbf{0}\end{bmatrix}\end{bmatrix} \\ & + \sum_{i=1}^{p}\sum_{l=1}^{p} w_i(\mathbf{x})w_l(\mathbf{x})\begin{bmatrix}\mathbf{B}_i\mathbf{\Lambda} \\ -\mathbf{B}_i\mathbf{\Lambda}\end{bmatrix}\mathbf{\Lambda}^{-1}\begin{bmatrix}\mathbf{\Lambda}\mathbf{B}_l^T & -\mathbf{\Lambda}\mathbf{B}_l^T\end{bmatrix} \\ & + \begin{bmatrix}\mathbf{B_r} \\ -\mathbf{B_r}\end{bmatrix}\sigma_2^{-2}\begin{bmatrix}{\mathbf{B_r}}^T & -{\mathbf{B_r}}^T\end{bmatrix} + \begin{bmatrix}\mathbf{X} \\ -\mathbf{X}\end{bmatrix}\mathbf{I}\begin{bmatrix}\mathbf{X} & -\mathbf{X}\end{bmatrix} \\ & + \begin{bmatrix}\mathbf{0} & \mathbf{0} \\ \mathbf{0} & \sigma_1^2(\epsilon^2\mathbf{I}^2 - \epsilon\mathbf{X}^T - \epsilon\mathbf{X})\end{bmatrix} < 0.\end{aligned} \tag{3.68}$$

By applying the lemma of Schur complement, the holding of (3.68) is implied by the holding of the following inequality:

$$\sum_{i=1}^{p}\sum_{j=1}^{c} w_i(\mathbf{x})m_j(\mathbf{x})\mathbf{H}_{ij} < 0 \tag{3.69}$$

where

$$\mathbf{H}_{ij} = \begin{bmatrix} \tilde{\mathbf{\Phi}}_{ij}^{(11)} & * & * & * & * & * \\ \tilde{\mathbf{\Phi}}_{ij}^{(21)} & \tilde{\mathbf{\Phi}}_{ij}^{(22)} + \sigma_1^2(\epsilon^2\mathbf{I}^2 - \epsilon\mathbf{X}^T - \epsilon\mathbf{X}) & * & * & * & * \\ \frac{\mathbf{H}_1-\mathbf{H}_2}{2}\begin{bmatrix}\mathbf{M}_j & \mathbf{0}\end{bmatrix} & \frac{\mathbf{H}_1-\mathbf{H}_2}{2}\begin{bmatrix}\mathbf{N}_j - \mathbf{M}_j & \mathbf{0}\end{bmatrix} & -\mathbf{\Lambda} & * & * & * \\ \mathbf{\Lambda}\mathbf{B}_i^T & -\mathbf{\Lambda}\mathbf{B}_i^T & \mathbf{0} & -\mathbf{\Lambda} & * & * \\ \mathbf{B_r}^T & -\mathbf{B_r}^T & \mathbf{0} & \mathbf{0} & -\sigma_2^2\mathbf{I} & * \\ \mathbf{X} & -\mathbf{X} & \mathbf{0} & \mathbf{0} & \mathbf{0} & -\mathbf{I} \end{bmatrix}. \tag{3.70}$$

Remark 3.10. *According to* (3.26)*, the generalized eigenvalue minimization problem (GEVP) under LMIs constraints is formulated to optimize the tracking control performance by minimizing two pre-defined scalars* σ_1 *and* σ_2*. In this research, as it involves two variables, an iterative approach is adopted. We first initialize* σ_2 *as a sufficiently large value and minimize* σ_1 *using the GEVP routine from Matlab. Then, turn back to minimize the value of* σ_2 *by using the found* σ_1*. Iteratively repeat the above steps (minimize one value at a time but keep another value found in the previous iteration as a constant) until a stopping criterion is met, e.g., the change of* σ_1 *and* σ_2 *is not significant or a predefined iteration number is reached, which is determined by the user.*

Theorem 3.1. *The output feedback fuzzy controller* (3.11) *is able to drive the states of the nonlinear system represented as a fuzzy model (3.2) to follow the state trajectory of a stable reference model (3.6) subject to the* $\mathcal{H}_\infty$ *performance (3.26) with the consideration of control input saturation* (3.14)*, if there exist matrix decision variables* $\mathbf{X} \in \mathbb{R}^{n\times n}$*,* $\mathbf{M}_j \in \mathbb{R}^{m\times l}$ *and* $\mathbf{N}_j \in \mathbb{R}^{m\times l}$*,* $j = 1, 2, \ldots, p$*, and scalar decision variables,* τ_k*,* $k = 1, 2, \ldots, m$*, which forms* $\mathbf{\Lambda} = diag\{\tau_1, \tau_2, \ldots, \tau_m\}$ *such that the following GEVP is feasible:*

$$\min \sigma_1, \sigma_2 \text{ (using the iterative method in Remark 3.10) subject to}$$

$$\sigma_1 > 0; \sigma_2 > 0;$$

$$\mathbf{X} > 0;$$

$$\mathbf{\Lambda} > 0;$$

$$\mathbf{H}_{ij} < 0, \forall\, i, j$$

where $\mathbf{\Lambda} \in \mathbb{R}^{m\times m}$*,* $\mathbf{H}_1 \in \mathbb{R}^{m\times m}$ *and* $\mathbf{H}_2 \in \mathbb{R}^{m\times m}$ *are all diagonal matrices and satisfy* $\mathbf{H}_2 \geq \mathbf{I} \geq \mathbf{H}_1 \geq 0$*; the feedback gains* $\mathbf{G}$ *and* $\mathbf{F}$ *are defined in* (3.53) *and* (3.54)*.*

3.3.4 Piecewise Linear Membership Functions

The stability conditions in Theorem 3.1 are developed when the information of membership functions are not engaged. In this section, the PLMFs technique [89] is applied and used to approximate the membership functions $h_{ij}(\mathbf{x}) \equiv w_i(\mathbf{x})m_j(\mathbf{x})$ so that they can be taken into account of the stability analysis for relaxing the conservativeness. In the PLMFs method, the membership functions will firstly be sampled. Based on the membership sample, the membership functions $h_{ij}(\mathbf{x})$ are approximated by linear interpolation method to obtain an approximated membership function, which is referred to as PLMFs.

Let the state space of interest Υ be divided into q sub-state spaces, expressed as Υ_k, $k = 1, 2, \ldots, q$. Thus, the original membership function $h_{ij}(\mathbf{x})$ approximated by the PLMF method can be expressed by

$$\hat{h}_{ij}(\mathbf{x}) = \sum_{k=1}^{q}\sum_{i_1=1}^{2}\cdots\sum_{i_n=1}^{2}\prod_{r=1}^{n} v_{ri_rk}(x_r)\delta_{iji_1i_2\ldots i_nk}, \quad \forall\, i, j, k, \tag{3.71}$$

$$0 \le \hat{h}_{ijl}(\mathbf{x}) \le 1, \tag{3.72}$$

$$0 \le \delta_{iji_1i_2\ldots i_nk} \le 1, \tag{3.73}$$

where $\delta_{iji_1i_2\ldots i_nk}$ is a constant scalar to be determined representing the sample point of the original membership function $h_{ij}(\mathbf{x})$ at each chosen point $\mathbf{x}$; $0 \le v_{ri_sk}(x_r) \le 1$ and $v_{r1k}(x_r) + v_{r2k}(x_r) = 1$ for $r, s = 1, 2, \ldots, n$; $i_r = 1, 2$; $\mathbf{x} \in \Phi_k$; otherwise, $v_{ri_sk}(x_r) = 0$. Based on the above settings, we have the following property:

$$\sum_{k=1}^{q}\sum_{i_1=1}^{2}\sum_{i_2=1}^{2}\cdots\sum_{i_n=1}^{2}\prod_{r=1}^{n} v_{ri_rk}(x_r) = 1. \tag{3.74}$$

The approximation error, $\Delta h_{ij}(\mathbf{x}) = h_{ij}(\mathbf{x}) - \hat{h}_{ij}(\mathbf{x})$, satisfies

$$\Delta\underline{h}_{ij} \le h_{ij}(\mathbf{x}) - \hat{h}_{ij}(\mathbf{x}) \le \Delta\overline{h}_{ij} \tag{3.75}$$

where $\Delta\underline{h}_{ij}$ and $\Delta\overline{h}_{ij}(\mathbf{x})$, representing respectively the lower and upper bounds of Δh_{ij}, are to be determined.

Based on (3.75), (3.69) can be reformulated as

$$\sum_{i=1}^{p}\sum_{j=1}^{c} h_{ij}(\mathbf{x})\mathbf{H}_{ij} = \sum_{i=1}^{p}\sum_{j=1}^{c} \hat{h}_{ij}(\mathbf{x})\mathbf{H}_{ij} + \sum_{i=1}^{p}\sum_{j=1}^{c}(h_{ij}(\mathbf{x}) - \hat{h}_{ij}(\mathbf{x}))\mathbf{H}_{ij}$$

$$
\begin{aligned}
&= \sum_{i=1}^{p}\sum_{j=1}^{c}\hat{h}_{ij}(\mathbf{x})\mathbf{H}_{ij} + \sum_{i=1}^{p}\sum_{j=1}^{c}(\Delta h_{ij}(\mathbf{x}) + \Delta\underline{h}_{ij} - \Delta\underline{h}_{ij})\mathbf{H}_{ij} \\
&= \sum_{i=1}^{p}\sum_{j=1}^{c}(\hat{h}_{ij}(\mathbf{x}) + \Delta\underline{h}_{ij})\mathbf{H}_{ij} + \sum_{i=1}^{p}\sum_{j=1}^{c}(\Delta h_{ij}(\mathbf{x}) - \Delta\underline{h}_{ij})\mathbf{H}_{ij} \\
&\leq \sum_{i=1}^{p}\sum_{j=1}^{c}(\hat{h}_{ij}(\mathbf{x}) + \Delta\underline{h}_{ij})\mathbf{H}_{ij} \\
&\quad + \sum_{i=1}^{p}\sum_{j=1}^{c}(\Delta\overline{h}_{ij} - \Delta\underline{h}_{ij})\mathbf{Y}_{ij} \qquad (3.76)
\end{aligned}
$$

where $\mathbf{Y}_{ij} \in \mathbb{R}^{(n+l+m)\times(n+l+m)}$ is a slack matrix satisfying $\mathbf{Y}_{ij} = \mathbf{Y}_{ij}^T \geq 0$ and $\mathbf{Y}_{ij} \geq \mathbf{H}_{ij}$ for all i and j.

Expanding $\hat{h}_{ij}(\mathbf{x})$ in (3.76), we have

$$
\begin{aligned}
&\sum_{i=1}^{p}\sum_{j=1}^{c}h_{ij}(\mathbf{x})\mathbf{H}_{ij} \leq \sum_{k=1}^{q}\sum_{i_1=1}^{2}\cdots\sum_{i_n=1}^{2}\prod_{r=1}^{n}v_{ri_rk}(x_r) \\
&\times\sum_{i=1}^{p}\sum_{j=1}^{c}\Big((\delta_{iji_1i_2\ldots i_nk} + \Delta\underline{h}_{ij})\mathbf{H}_{ij} + (\Delta\overline{h}_{ij} - \Delta\underline{h}_{ij})\mathbf{Y}_{ij}\Big). \qquad (3.77)
\end{aligned}
$$

Considering the property in (3.74), the satisfaction of inequality (3.76) guarantees the holding of (3.68) which further implies $\dot{V} \leq 0$ except $\mathbf{x} = 0$. The stability conditions obtained through PLMFs method are concluded as below.

Theorem 3.2. *The output feedback fuzzy controller* (3.11) *is able to drive the states of the nonlinear system represented as a fuzzy model (3.2) to follow the state trajectory of a stable reference model (3.6) subject to the $\mathcal{H}_\infty$ performance (3.26) with the consideration of control input saturation* (3.14)*, if there exist decision matrix variables $\mathbf{X} \in \mathbb{R}^{n\times n}$, $\mathbf{M}_j \in \mathbb{R}^{m\times l}$ and $\mathbf{N}_j \in \mathbb{R}^{m\times l}$, $j = 1, 2, \ldots, p$, and decision scalar variables τ_k, $k = 1, 2, \ldots, m$ forming diagonal matrix $\mathbf{\Lambda} \in \mathbb{R}^{m\times m} = diag\{\tau_1, \tau_2, \ldots, \tau_m\}$ such that the following GEVP is feasible:*

$$\min \sigma_1, \sigma_2 \text{ (using the iterative method in Remark 3.10) subject to}$$

$$\sigma_1 > 0; \sigma_2 > 0;$$

$$\mathbf{X} > 0;$$

$$\mathbf{\Lambda} > 0;$$

$$\mathbf{Y}_{ij} > 0, \forall\, i, j;$$

$$\mathbf{Y}_{ij} > \mathbf{H}_{ij}, \forall\, i, j;$$

$$\sum_{i=1}^{p}\sum_{j=1}^{c}(\hat{h}_{ij}(\mathbf{x})+\Delta\underline{h}_{ij})\mathbf{H}_{ij}+\sum_{i=1}^{p}\sum_{j=1}^{c}(\Delta\overline{h}_{ij}-\Delta\underline{h}_{ij})\mathbf{Y}_{ij}\leq 0$$
$$\forall\, i,j,k,i_1,i_2,\ldots,i_n$$

where $\delta_{iji_1i_2\ldots i_nk}$ *is a sample of the original membership function* $h_{ij}(\mathbf{x})$ *at a chosen point* $\mathbf{x}$*;* $\Delta\underline{h}_{ij}$ *and* $\Delta\overline{h}_{ij}$ *are the constant scalars satisfying* $\Delta\underline{h}_{ij}\leq h_{ij}(\mathbf{x})-\hat{h}_{ij}(\mathbf{x})\leq\Delta\overline{h}_{ij}$ *for all* i *and* j*; the diagonal matrices* $\mathbf{H}_1$ *and* $\mathbf{H}_2$ *satisfy* $\mathbf{H}_2\geq\mathbf{I}\geq\mathbf{H}_1\geq 0$*; and the feedback gain is given as* $\mathbf{F}_j=\mathbf{M}_j(\mathbf{\Gamma X})^{-1}$ *and* $\mathbf{G}_j=\mathbf{N}_j(\mathbf{\Gamma X})^{-1}$ *for all* j*.*

3.4 Simulation Example

A numerical example is presented to verify the stability condition and demonstrate the system performance. The 3-rule T-S fuzzy model inspired from [80] regarding to (3.2) is constructed where the system, input and output matrices are $\mathbf{A}_1=\begin{bmatrix}-4 & 5\\ 4 & -4.8\end{bmatrix}$, $\mathbf{A}_2=\begin{bmatrix}-4.5 & 6\\ 5.5 & -6.2\end{bmatrix}$, $\mathbf{A}_3=\begin{bmatrix}-2.5 & 4.3\\ 3 & -3.5\end{bmatrix}$, $\mathbf{B}_1=\begin{bmatrix}1\\ 0\end{bmatrix}$, $\mathbf{B}_2=\begin{bmatrix}8\\ 0\end{bmatrix}$, $\mathbf{B}_3=\begin{bmatrix}7\\ -1\end{bmatrix}$, $\mathbf{C}=\begin{bmatrix}1 & 0\end{bmatrix}$. The membership functions are chosen as below.

$$w_1(x_1)=\mu_{M_1^1}(x_1)=\begin{cases}1 & \text{for } x_1<-10\\ \frac{-x_1+2}{12} & \text{for } -10\leq x_1\leq 2\\ 0 & \text{for } x_1>2\end{cases} \tag{3.78}$$

$$w_2(x_1)=\mu_{M_1^2}(x_1)=1-w_1(x_1)-w_3(x_1) \tag{3.79}$$

$$w_3(x_1)=\mu_{M_1^3}(x_1)=\begin{cases}0 & \text{for } x_1<-2\\ \frac{x_1+2}{12} & \text{for } -2\leq x_1\leq 10\\ 1 & \text{for } x_1>10\end{cases}. \tag{3.80}$$

The 3-rule T-S fuzzy model is expressed as:

$$\dot{\mathbf{x}}=\sum_{i=1}^{3}w_i(x_1)(\mathbf{A}_i\mathbf{x}+\mathbf{B}_iu). \tag{3.81}$$

The output is obtained as

$$\mathbf{y}=\mathbf{C}\mathbf{x}. \tag{3.82}$$

The corresponding 2-rule fuzzy controller in the form of (3.11) used to close the

feedback loop can be written as:

$$m_1(x_1) = \mu_{N_1^1}(x_1) = 1 - \frac{1}{e^{\frac{-x_1}{2}}}; \tag{3.83}$$

$$m_2(x_1) = \mu_{N_1^2}(x_1) = 1 - m_1(x_1). \tag{3.84}$$

Thus, the 2-rule fuzzy controller is obtained as follows:

$$\mathbf{u} = \sum_{j=1}^{2} m_j(x_1)(\mathbf{F}_j\mathbf{C}\mathbf{x} + (\mathbf{G}_j - \mathbf{F}_j)\mathbf{C}\mathbf{x}_\mathbf{r}). \tag{3.85}$$

Note that, in this example, the fuzzy controller is applied with different number rules and different shape of membership functions from those of T-S fuzzy model. This is so called imperfectly matched premises [88, 107].

In order to apply Theorem 3.2, the membership function approximated by PLMFs method can be expressed as (3.71). Since the membership functions of both fuzzy model and fuzzy controller depend only on x_1, the PLMFs method constructed model can be built based only on x_1 as well. Considering $x_1 \in [-10, 10]$, δ_{iji_1k} is set as $h_{ij}(x_1)$ by considering the samples of x_1 at $\{-10, -9.5, \ldots, 9.5, 10\}$, e.g., $\delta_{iji_11} = h_{ij}(-10)$, $\delta_{iji_12} = h_{ij}(-9.5)$ and so on. The functions $v_{11k}(x_1) = \frac{x_1 - \underline{x}_{1k}}{\overline{x}_{1k} - \underline{x}_{1k}}$ and $v_{12k}(x_1) = 1 - v_{11k}(x_1)$ are used where $\overline{x}_{1k}$ and $\underline{x}_{1k}$ denote the lower and upper end points of x_1 at the k-th sub-region, e.g., $\overline{x}_{1k} = -10$ and $\underline{x}_{1k} = -9.5$ when $k = 1$, $\overline{x}_{1k} = -9.5$ and $\underline{x}_{1k} = -9$ when $k = 2$ and so on. It should be noted that $v_{11k}(x_1) = 0$ and $v_{12k}(x_1) = 0$ when x_1 is outside the k-th region. According to the chosen original membership functions and PLMF, it is found numerically that $\Delta\underline{h}_{11} = \Delta\underline{h}_{32} = -2.4426 \times 10^{-3}$, $\Delta\underline{h}_{12} = \Delta\underline{h}_{31} = -6.7708 \times 10^{-4}$, $\Delta\underline{h}_{21} = \Delta\underline{h}_{22} = -1.7826 \times 10^{-3}$, $\Delta\overline{h}_{11} = \Delta\overline{h}_{32} = 1.7839 \times 10^{-3}$, $\Delta\overline{h}_{12} = \Delta\overline{h}_{31} = 1.3139 \times 10^{-3}$, $\Delta\overline{h}_{21} = \Delta\overline{h}_{22} = 2.4622 \times 10^{-3}$ satisfying the inequality (3.75).

As mentioned in the previous section, $\mathbf{u}_{\max\,/\,\min}$ is the maximum (minimum) value where control signal can practically reach. The slope of control input lower bound $\mathbf{H}_1$ can be adjusted according to the requirement of practical application. The smaller value applied for $\mathbf{H}_1$, the more ability that the controller can guarantee system stability under the saturation, but harder to find a feasible solution by using Theorem 3.1 and Theorem 3.2. The pre-defined constant ϵ is selected as $\epsilon = 0.3$. The designed fuzzy controller (3.11) is employed to control the nonlinear fuzzy system (3.2) with the initial condition $\mathbf{x}(0) = \begin{bmatrix} 0 & 0 \end{bmatrix}^T$ and $\mathbf{x}_\mathbf{r}(0) = \begin{bmatrix} 0 & 0 \end{bmatrix}^T$.

The set of scalars σ_1 and σ_2 are initially chosen as $\sigma_1 = 10$ and $\sigma_2 = 10$, which gives a relatively more relaxed $\mathcal{H}_\infty$ performance constraint. Starting from the initial condition, the scalars σ_1 and σ_2 are minimized to optimize the $\mathcal{H}_\infty$ performance. Although the relationship between the scalar set σ_1 and σ_2 and the tracking error $\mathbf{e}$ can be directly shown in (3.26), due to the involvement of reference system state $\mathbf{x}_\mathbf{r}$ and input signal $\mathbf{r}$ as well as the limited computational power of MATLAB

software algorithm, in currently stage, the best we can do is to find the optimal minimum value for each of σ_1 and σ_2 iteratively according to the procedure in Remark 3.10. The MATLAB function "gevp", performing generalized eigenvalue minimization under LMI constraints, is applied to take turns finding the minimum feasible value of σ_1 and σ_2 iteratively. For example in Table 3.1a, first setting $\sigma_2 = 10$, we can obtain the minimum value of σ_1 from GEVP method which gives $\sigma_1 = 4.1323$. In the same way, setting $\sigma_1 = 4.1323$, the minimum feasible value for σ_2 from GEVP method is $\sigma_2 = 0.51299$. By repeating the mutual operations, we can use GEVP method to obtain the minimum value of σ_1 under the condition of $\sigma_2 = 0.51299$. The iteration stops until the values of σ_1 and σ_2 decrease under 1% in two consecutive generations.

The following simulations are conducted to verify and compare the effectiveness of Theorems 3.1 and 3.2 that the obtained feasible solution from system stability analysis can produce a fuzzy controller guaranteeing the system stability when the control signal is saturated at the certain level. Tables 3.1 and 3.2 show that the simulation is proceeded in four groups, where Tables 3.3 and 3.4 tabulate the details of feedback gains $\mathbf{F}_j$ and $\mathbf{G}_j$ regarding to Tables 3.1 and 3.2 respectively. In Table 3.1, the two slope values deciding the control signal saturation region in stability analysis, namely $\mathbf{H}_1$ and $\mathbf{H}_2$, are fixed at $\mathbf{H}_1 = [0.8]$ and $\mathbf{H}_2 = [1.0]$. In order to show the impact of control signal saturation to the tracking performance, two sub-tables are listed for comparison, where Table 3.1a shows the system tracking performance under an unsaturated condition and Table 3.1b is simulated under a designed saturation condition described in Fig. 3.1. In Table 3.2, the upper bound of control input $\mathbf{H}_2$ is fixed at $\mathbf{H}_2 = [1.0]$ and the control input signal $\tilde{\mathbf{u}}_{\max/\min}$ is limited at ± 3.7. In order to verify that the designed fuzzy controller can guarantee the system stability under certain saturation condition, Tables 3.2a and 3.2b present the system tracking performances by applying different lower bound values of control input saturation region. Moreover, according to Remark 3.6, the value of scalar set σ_1 and σ_2 can also affect the system tracking performance. Therefore, in each table, the simulations are run by applying Theorems 3.1 and 3.2 with optimized and unoptimized scalar set σ_1 and σ_2 respectively.

In Table 3.1a, the control signal limit is set as $\mathbf{u}_{\max/\min} = \pm 16$, so that the system stability and tracking performance can be observed in the unsaturated control signal condition. The system is tested first by applying Theorem 3.1 with the non-optimal scalars $\sigma_1 = 10$ and $\sigma_2 = 10$. Then using GEVP method, the value of σ_1 and σ_2 are minimized to the optimal values $\sigma_1 = 4.1323$ and $\sigma_2 = 0.51299$. Figs. 3.3a and 3.4a show that the system with optimized values of σ_1 and σ_2 can have smaller error in tracking control. After that, the system is applied with Theorem 3.2 to obtain the feasible solution. According to the theoretical analysis in Theorem 3.2, the PLMF method is capable to reduce the conservativeness of stability analysis

results. Therefore, the optimal values of σ_1 and σ_2 in Theorem 3.2 is smaller than those in Theorem 3.1. The comparison of Figs. 3.5a and 3.6a also proves that the smaller σ_1 and σ_2 can generate more effective the system tracking performance. By observing Fig. 3.6b, we set the maximum and minimum values of control input signal $\tilde{\mathbf{u}}_{\max/\min} = \pm 3.7$ and the control signal saturation value $\mathbf{u}_{\max/\min} = \pm 3.0$. Referring to the control signal in Table 3.1a, the control input signal $\left|\tilde{\mathbf{u}}_{\max/\min}\right|$ in Figs. 3.3b, 3.4b and 3.5b are all larger than 3.7, which means according to Remark 3.8 when $\left|\frac{\mathbf{u}_{\max/\min}}{\tilde{\mathbf{u}}_{\max/\min}}\right| < \mathbf{H}_1$, the system can no longer be guaranteed to be stable. The simulation result in Table 3.1b verifies the analysis. After setting the control signal saturation value $\mathbf{u}_{\max/\min} = \pm 3.0$, the tracking performance shown in Figs. 3.7a and 3.9a become unstable, while the system shown in Fig. 3.10a which has $\left|\frac{\mathbf{u}_{\max/\min}}{\tilde{\mathbf{u}}_{\max/\min}}\right| > \mathbf{H}_1$ guarantees the system stability.

Table 3.2 shows simulation conditions that can verify when applying different values of lower bound $\mathbf{H}_2$, the fuzzy controller developed from Theorems 3.1 and 3.2 can guarantee the system stability in different control input saturation condition referring to Remark 3.8. In Table 3.2, the control signal upper bound is assumed as $\mathbf{H}_1 = [1.0]$. The maximum and minimum values of control input signal are assumed as $\tilde{\mathbf{u}}_{\max/\min} = \pm 3.7$. Then in Tables 3.2a and 3.2b, different values of lower bound $\mathbf{H}_1$ are applied to Theorem 3.1 and 3.2 in order to test the effectiveness. In Table 3.2a, set $\mathbf{H}_1 = [0.9]$ which brings $\mathbf{u}_{\max/\min} = \pm 3.3$. Figs. 3.11a, 3.12a, 3.13a and 3.14a show that the simulation results are all stable, even though Figs. 3.11b and 3.13b show that the control signal is far greater than $\tilde{\mathbf{u}}_{\max/\min} = \pm 3.7$. However, Figs. 3.11a and 3.13a show that worse tracking results are obtained with large tracking errors compared with Figs. 3.12a and 3.14a, which again show the optimized scalar set σ_1 and σ_2 gives positive impact on system tracking performance. Similar with the simulation process in Tables 3.2a and 3.2b, we set $\mathbf{H}_1 = [0.7]$ and $\mathbf{u}_{\max/\min} = \pm 2.6$. The simulation result in Fig. 3.15a shows the system becomes unstable since the control signal in Fig. 3.15b fails to satisfy the condition in Remark 3.8. In contrast, when the control signal shown in Fig. 3.17b satisfies the condition $\left|\frac{\mathbf{u}_{\max/\min}}{\tilde{\mathbf{u}}_{\max/\min}}\right| > \mathbf{H}_1$, the system stability can always be guaranteed.

The above four groups of simulations demonstrate that Theorems 3.1 and 3.2 can offer stability conditions for output feedback tracking control systems under certain saturation condition. The simulation results of Figs. 3.8, 3.10, 3.12, 3.14, 3.16 and 3.18 further show that the feasible solution derived from Theorem 3.1 and 3.2 can guarantee the system stability when the control input signal satisfies the condition in Remark 3.8. If the condition is not satisfied, Figs. 3.7, 3.9, 3.11, 3.13, 3.15 and 3.17 show that the system stability is no longer can be guaranteed by Theorems 3.1 and 3.2. Moreover, the comparison indicates that the smaller value of scalar set σ_1 and σ_2 can improve the system tracking performance with smaller tracking error. And since Theorem 3.2 reduces the conservativeness in stability analysis, it

can produce a smaller values of σ_1 and σ_2 compared to Theorem 3.1.

3.5 Conclusions

In this chapter, the tracking control of a T-S fuzzy model based nonlinear system has been investigated to tackle the control input saturation problem. The output feedback fuzzy controller has been employed to drive the system state to trace the trajectory of a stable reference model state where tracking error is evaluated $\mathcal{H}_\infty$ performance. MFD stability analysis of T-S fuzzy model based control system has been investigated by Lyapunov stability theory where the control input saturation is addressed. The membership-function-dependent stability conditions are organised into an LMIs form which can be used to design the output feedback fuzzy controller if a feasible solution exists. Simulation examples are used to demonstrate the effectiveness of the output feedback fuzzy control scheme that can guarantee the system stability when satisfying a certain control input saturation condition. We further verify that the $\mathcal{H}_\infty$ performance has positive impact to the state tracking performance in terms of tracking error.

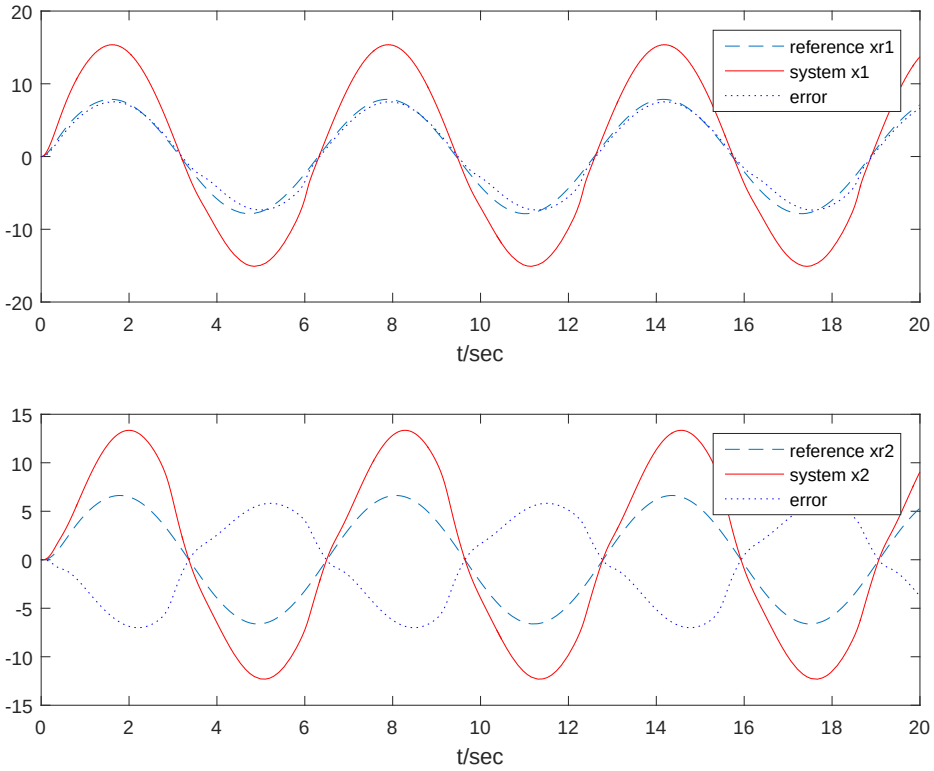

(a) State tracking result and tracking error.

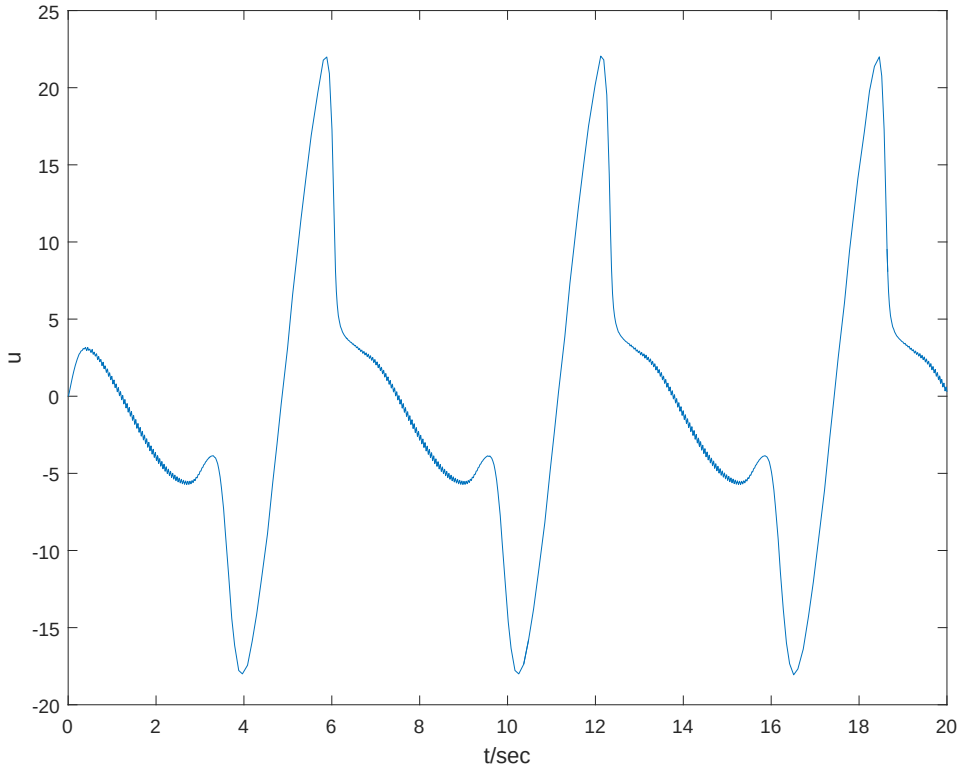

(b) Control signal without saturation.

Figure 3.3: Tracking control result for Theorem 3.1 with $\sigma_1 = 10$ and $\sigma_2 = 10$.

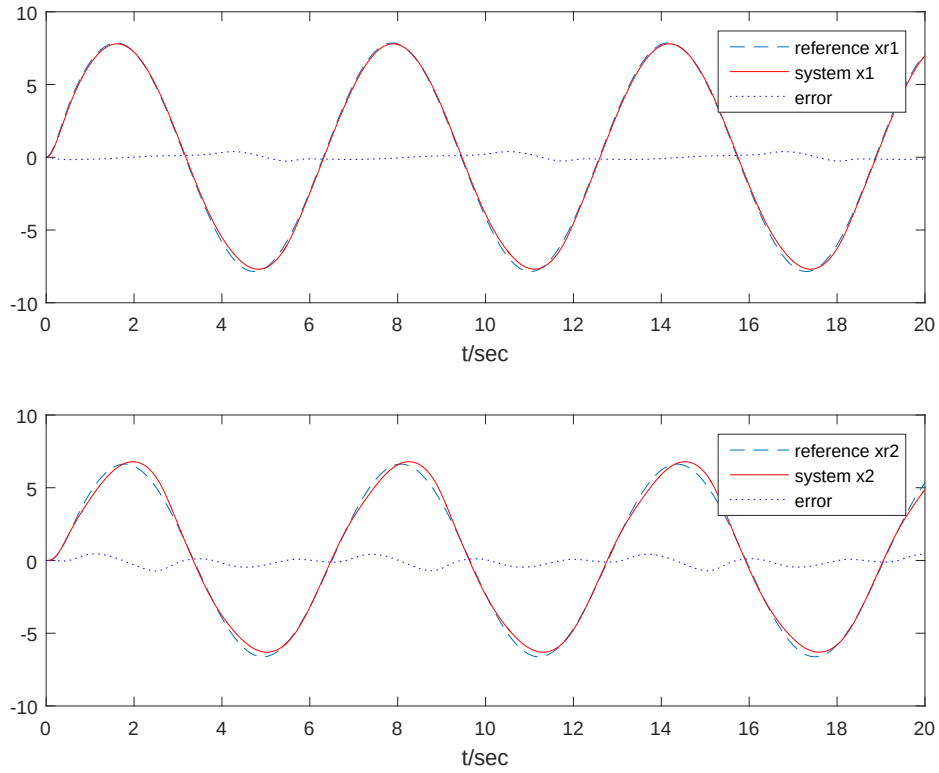

(a) State tracking result and tracking error.

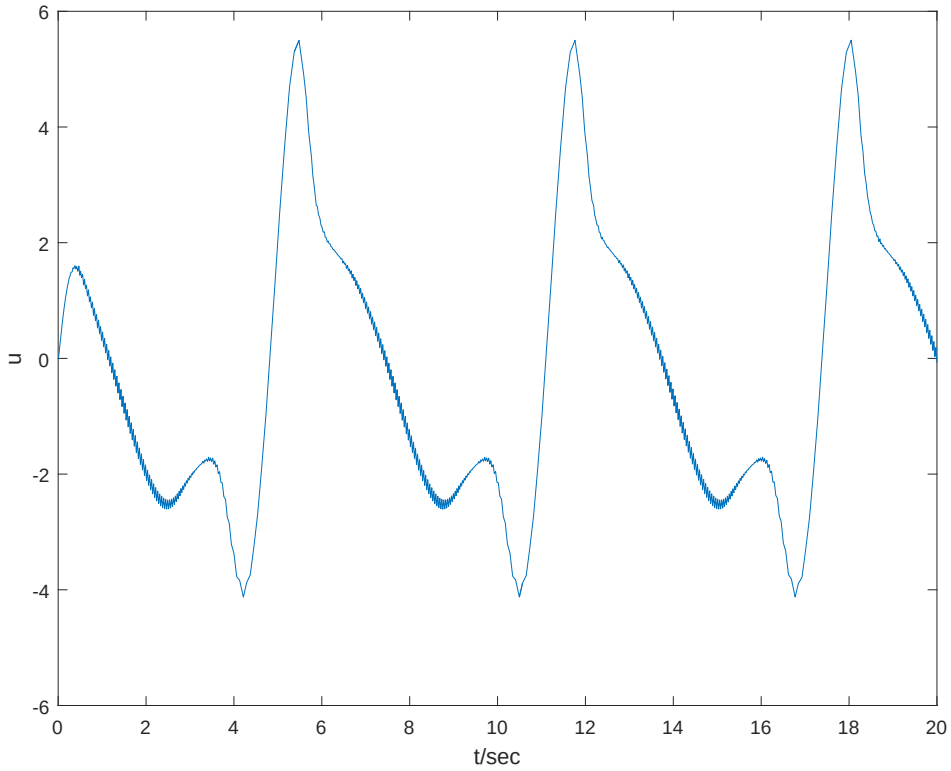

(b) Control signal without saturation.

Figure 3.4: Tracking control result for Theorem 3.1 with $\sigma_1 = 4.1323$ and $\sigma_2 = 0.51299$.

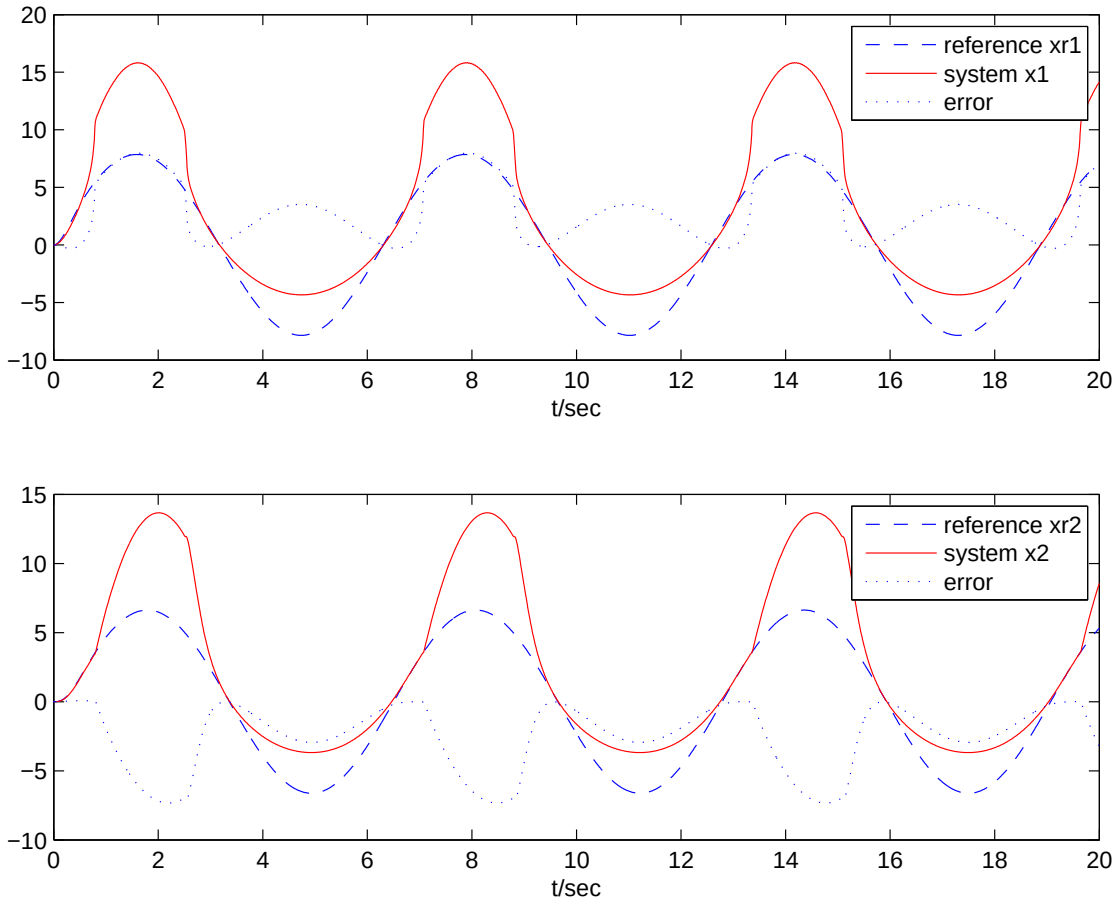

(a) State tracking result and tracking error.

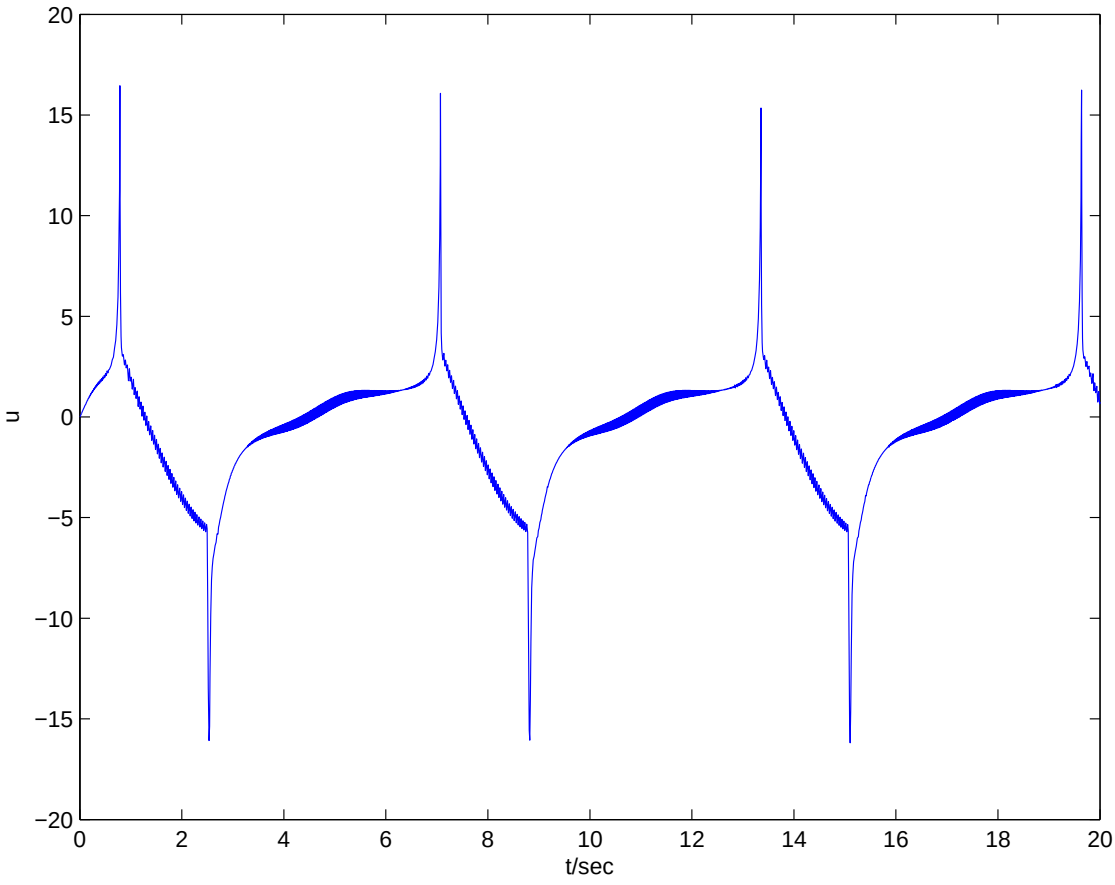

(b) Control signal without saturation.

Figure 3.5: Tracking control result for Theorem 3.2 with $\sigma_1 = 10$ and $\sigma_2 = 10$.

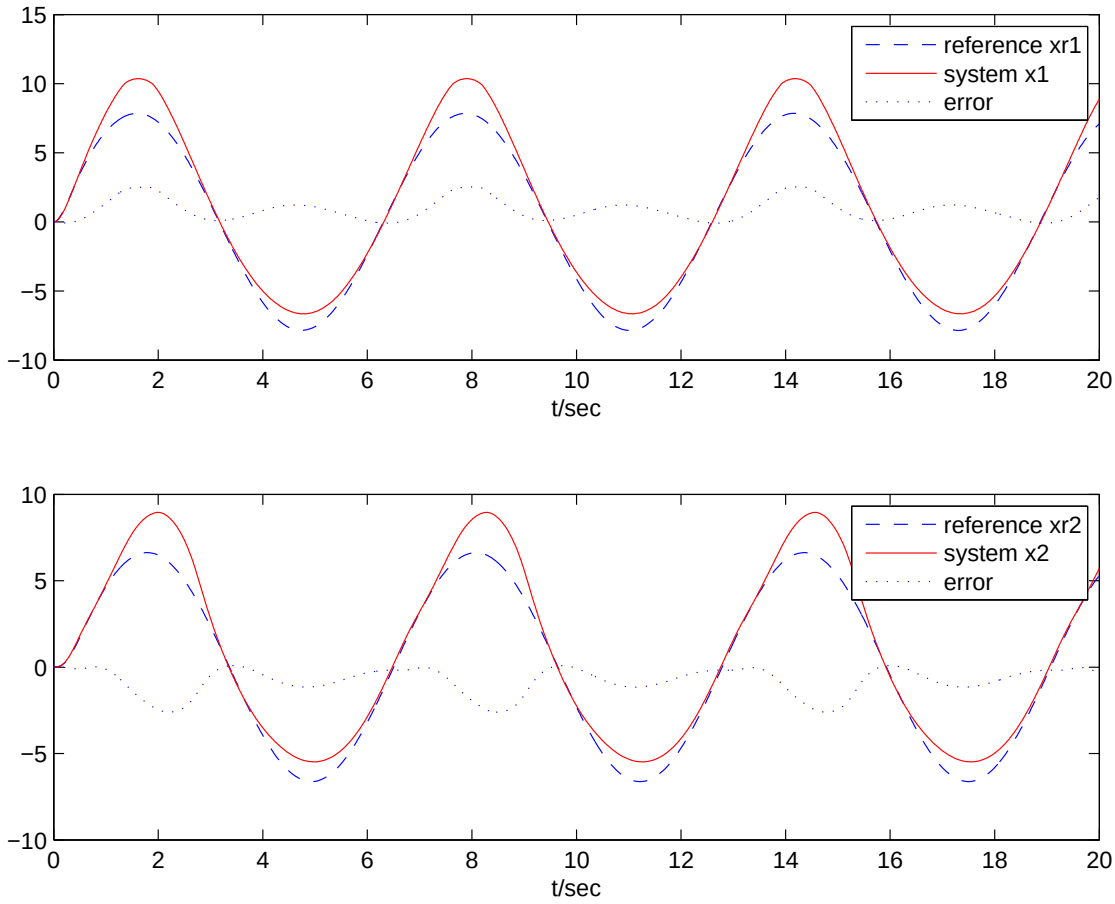

(a) State tracking result and tracking error.

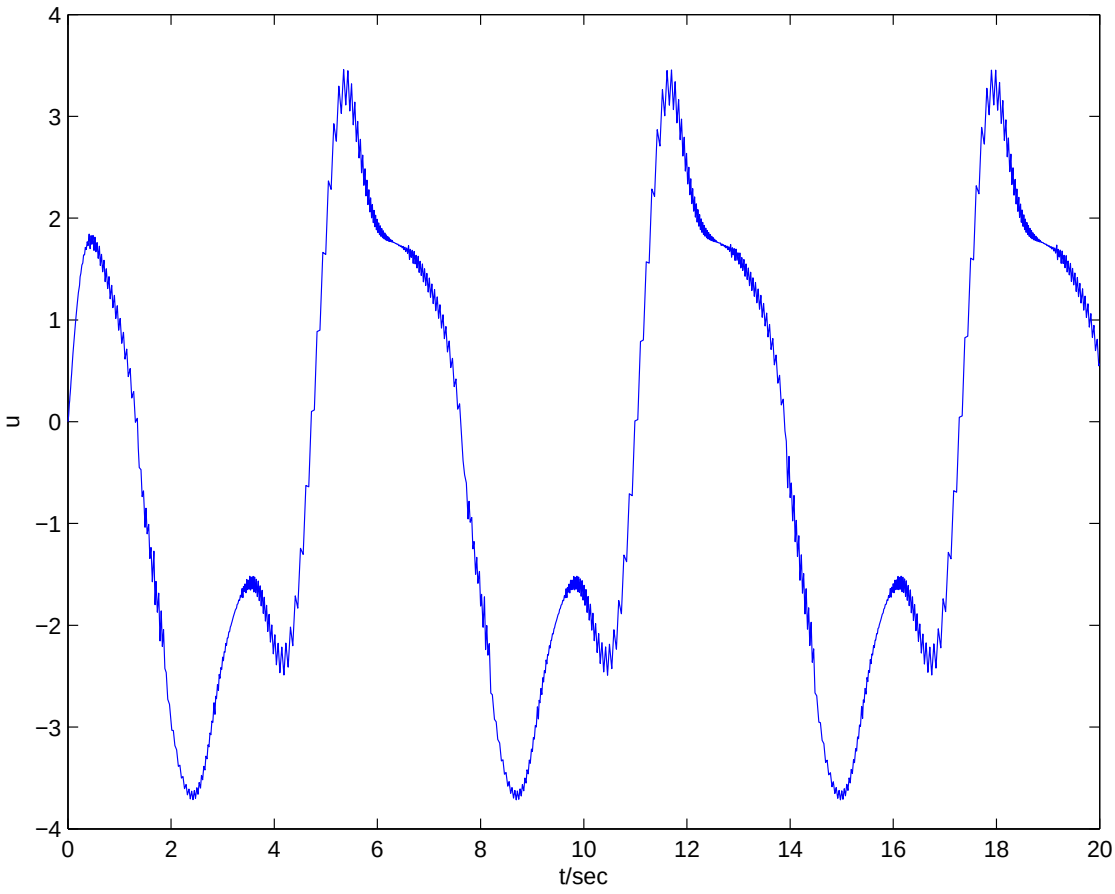

(b) Control signal without saturation.

Figure 3.6: Tracking control result for Theorem 3.2 with $\sigma_1 = 3.7067$ and $\sigma_2 = 0.26733$.

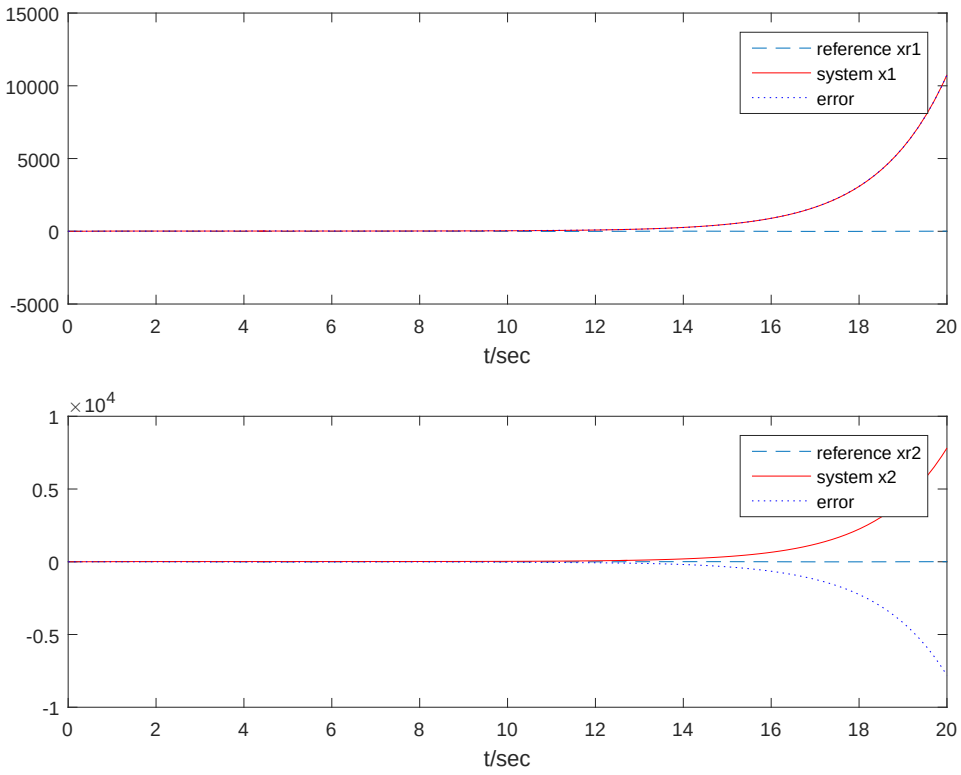

(a) State tracking result and tracking error.

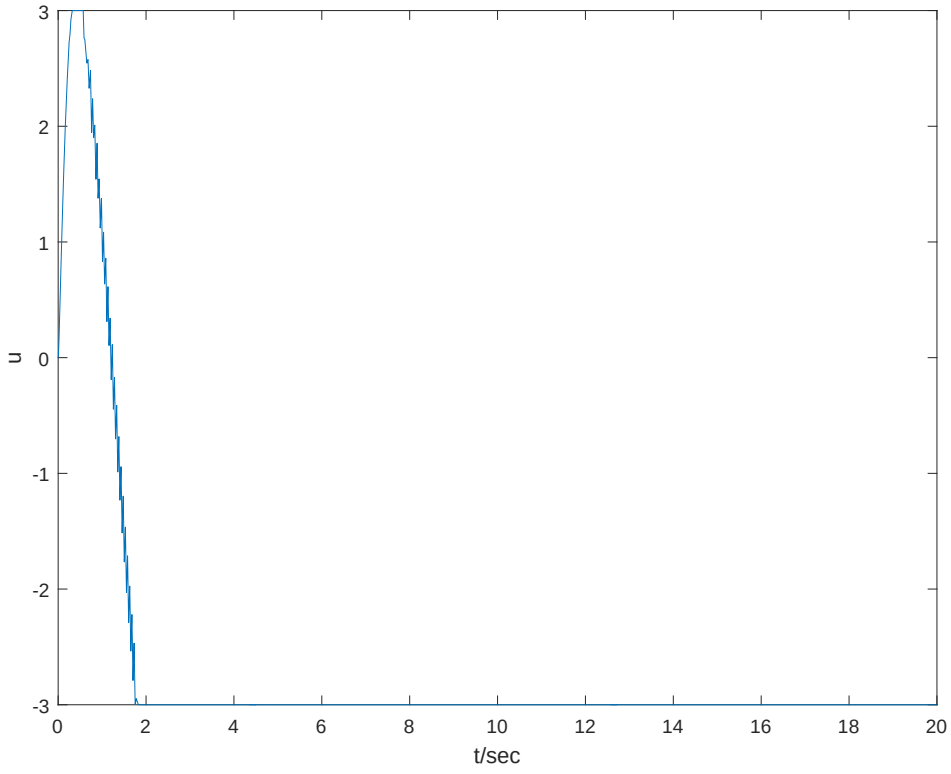

(b) Control signal saturated at ± 3.0.

Figure 3.7: Tracking control result for Theorem 3.1 with $\sigma_1 = 10$ and $\sigma_2 = 10$.

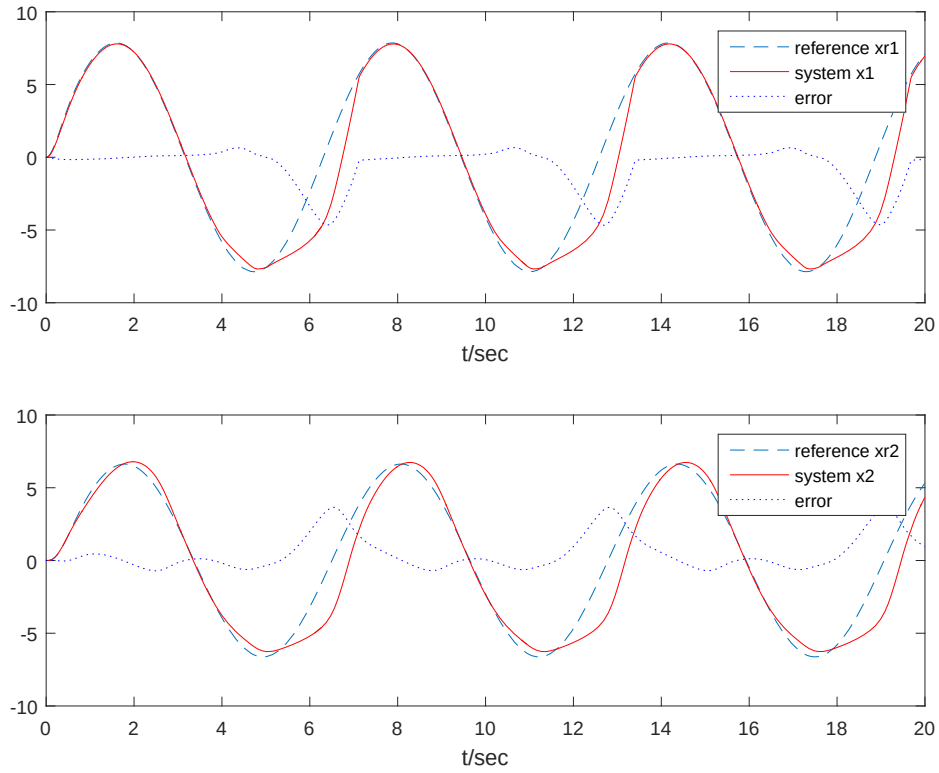

(a) State tracking result and tracking error.

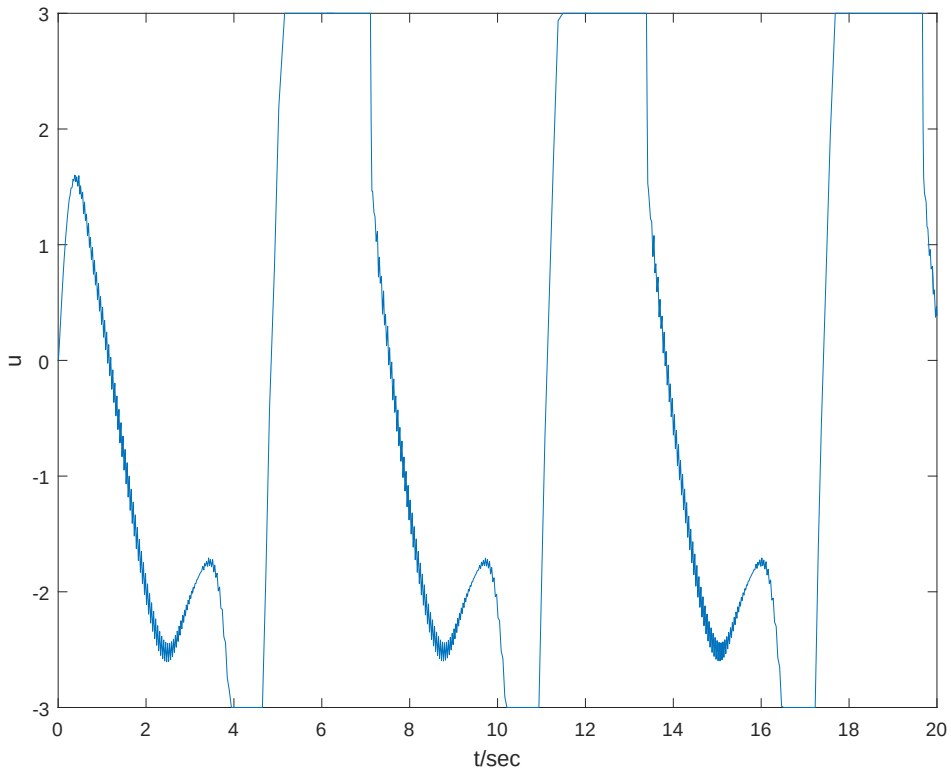

(b) Control signal saturated at ±3.0.

Figure 3.8: Tracking control result for Theorem 3.1 with $\sigma_1 = 4.1323$ and $\sigma_2 = 0.51299$.

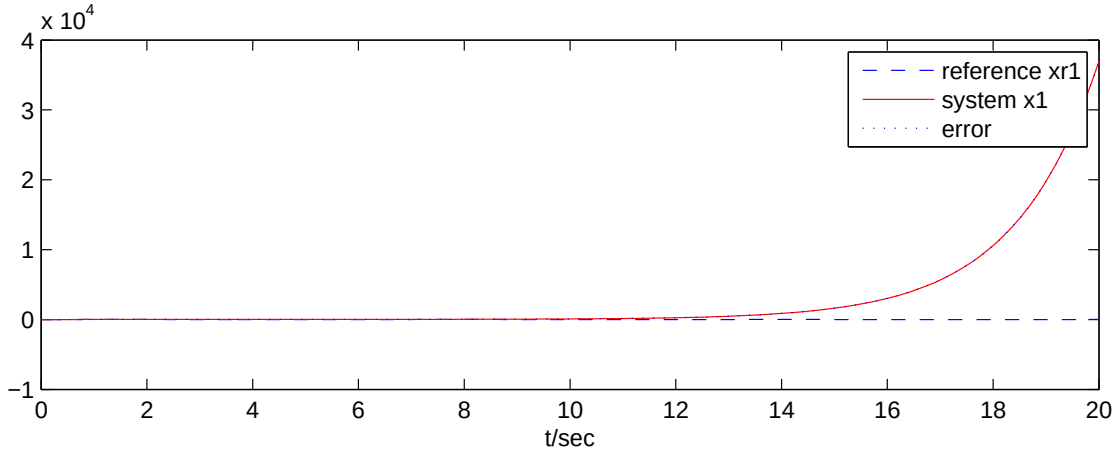

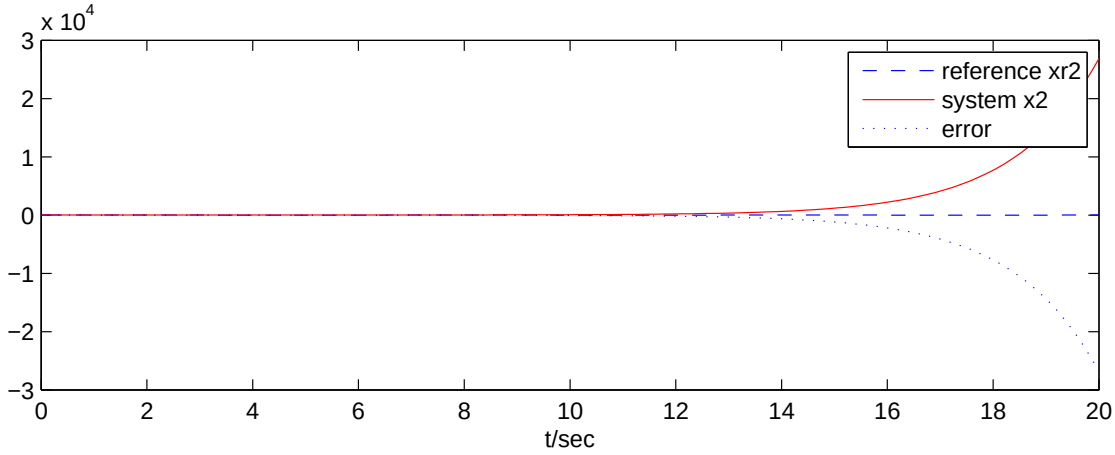

(a) State tracking result and tracking error.

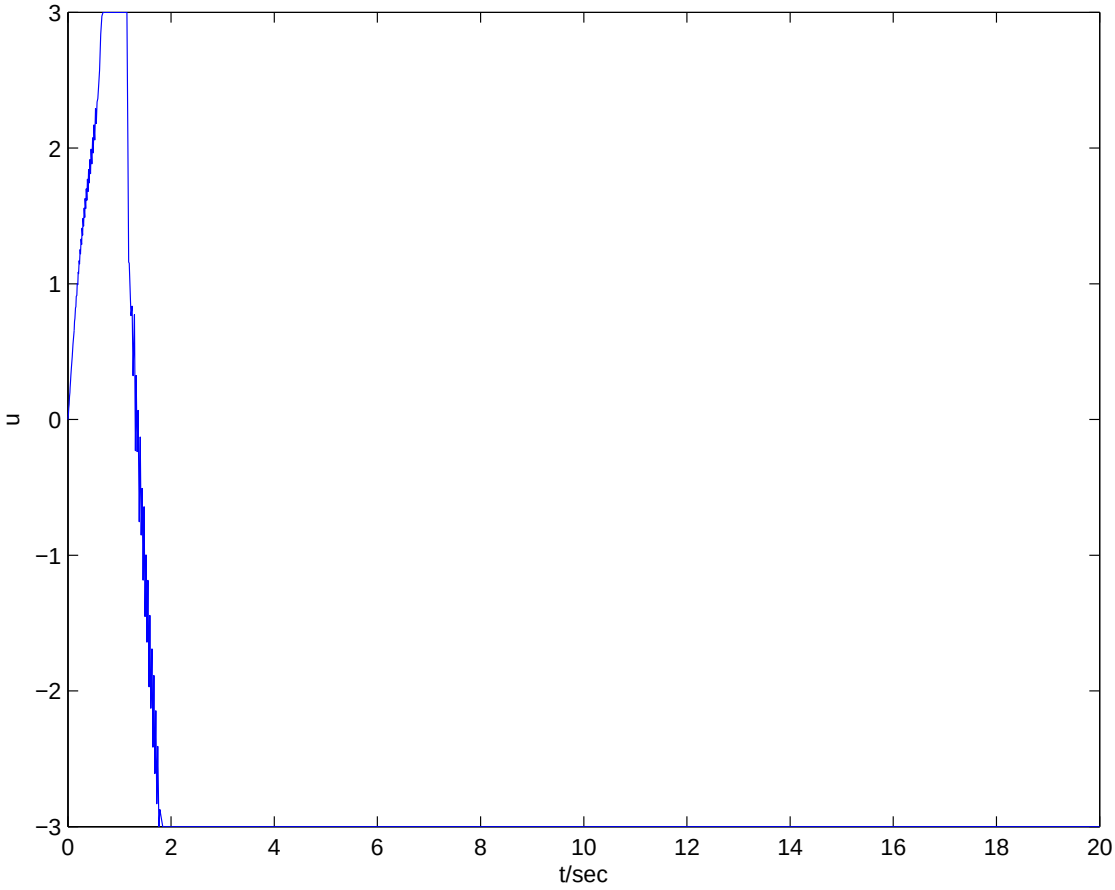

(b) Control signal saturated at ±3.0.

Figure 3.9: Tracking control result for Theorem 3.2 with $\sigma_1 = 10$ and $\sigma_2 = 10$.

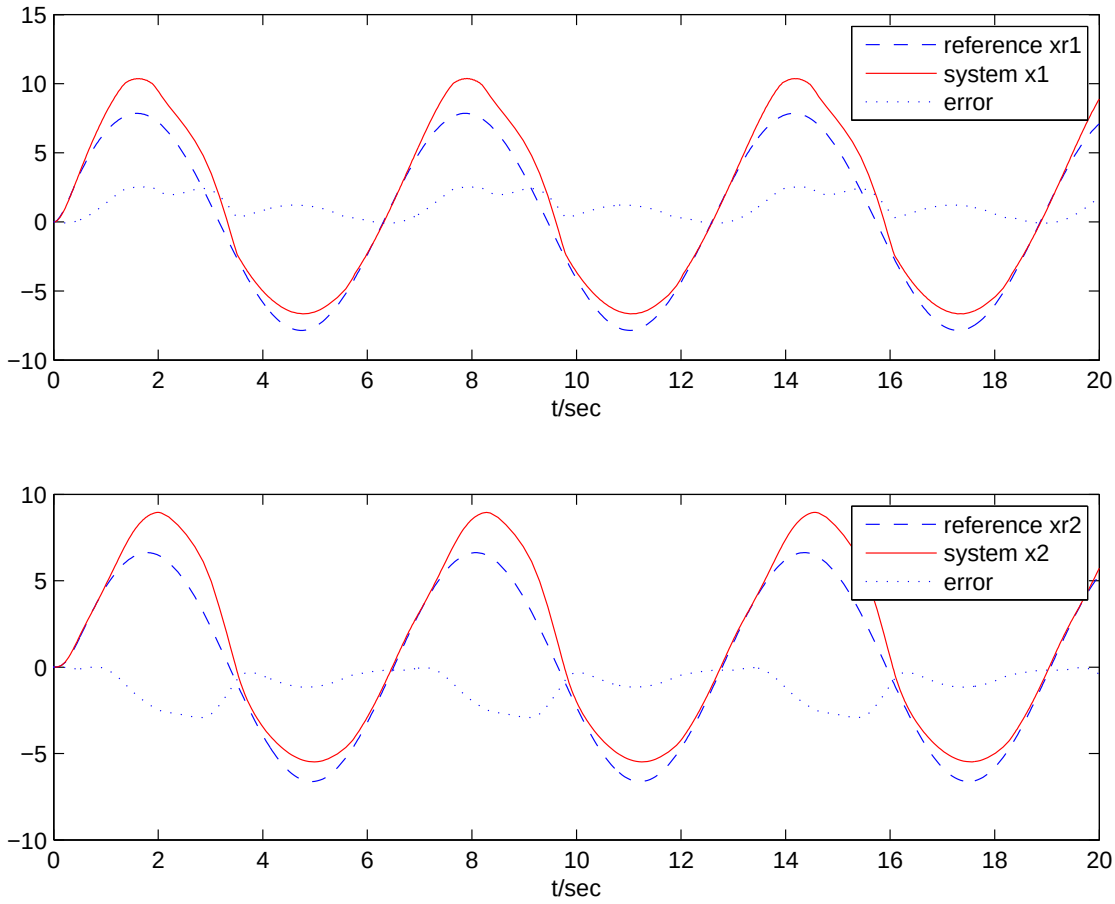

(a) State tracking result and tracking error.

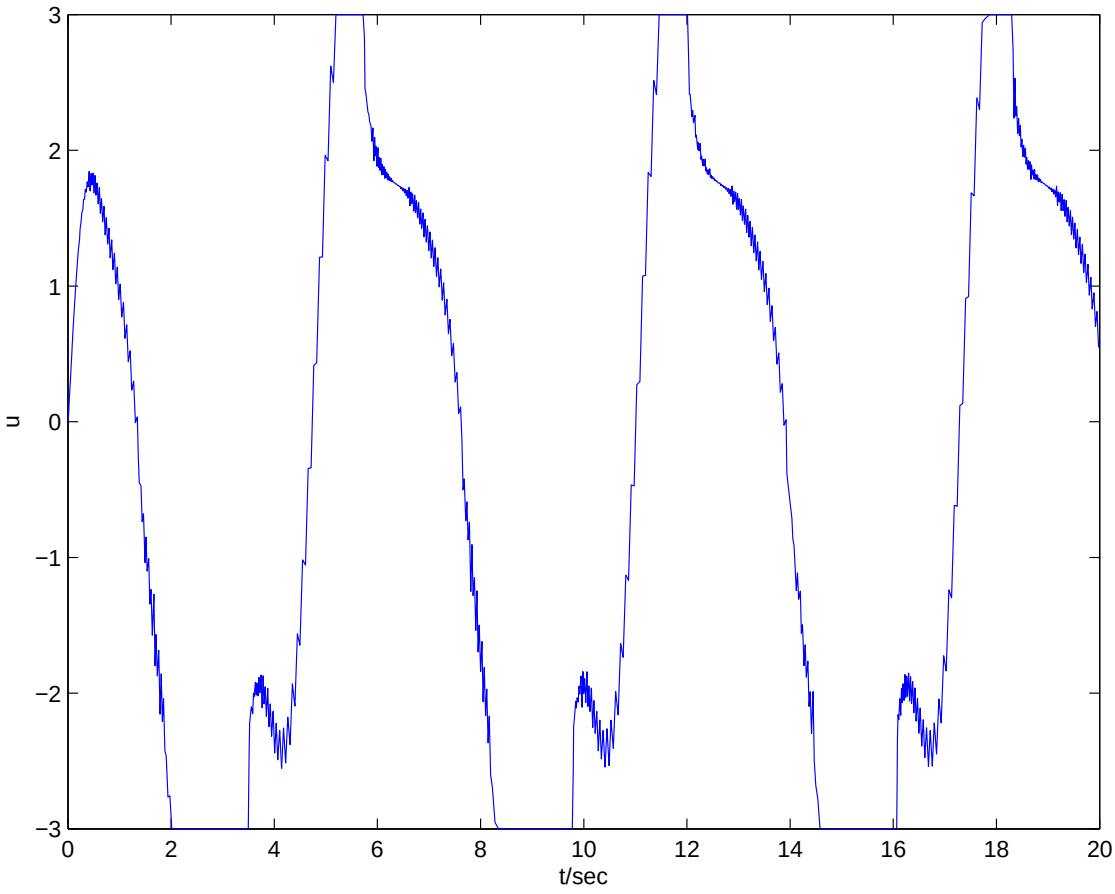

(b) Control signal saturated at ±3.0.

Figure 3.10: Tracking control result for Theorem 3.2 with $\sigma_1 = 3.7067$ and $\sigma_2 = 0.26733$.

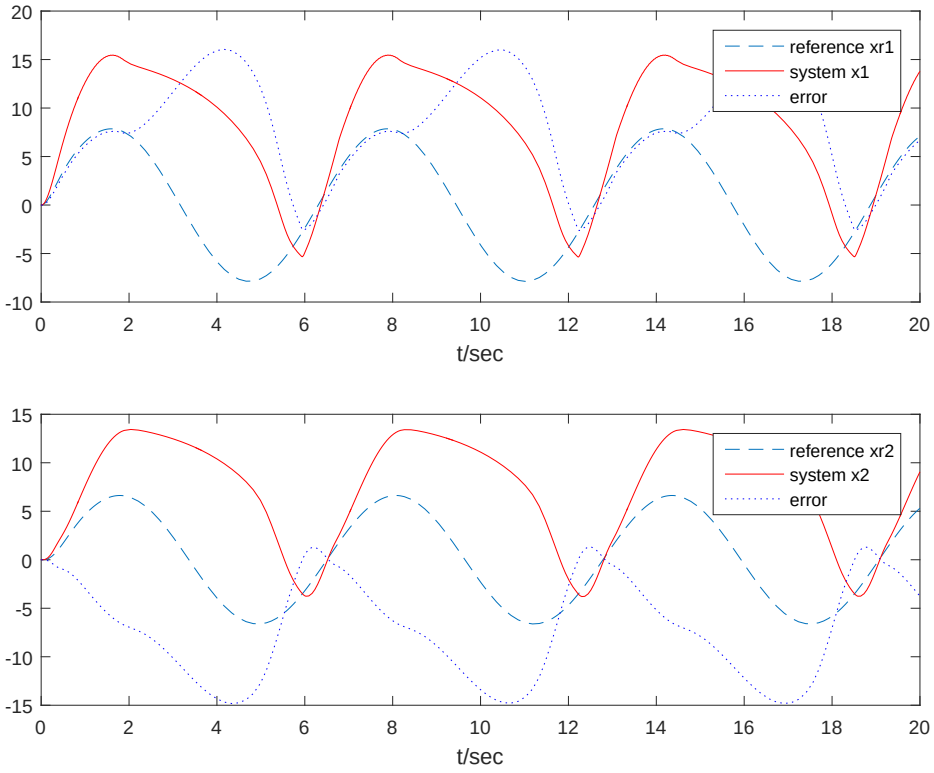

(a) State tracking result and tracking error.

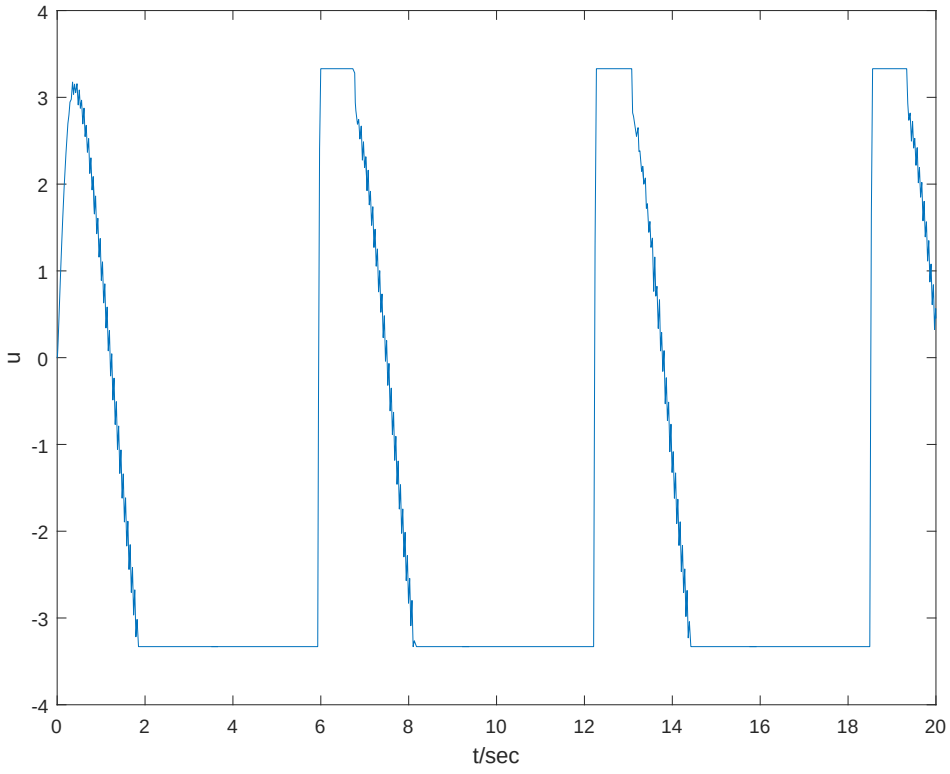

(b) Control signal saturated at ± 3.3.

Figure 3.11: Tracking control result for Theorem 3.1 with $\sigma_1 = 10$ and $\sigma_2 = 10$.

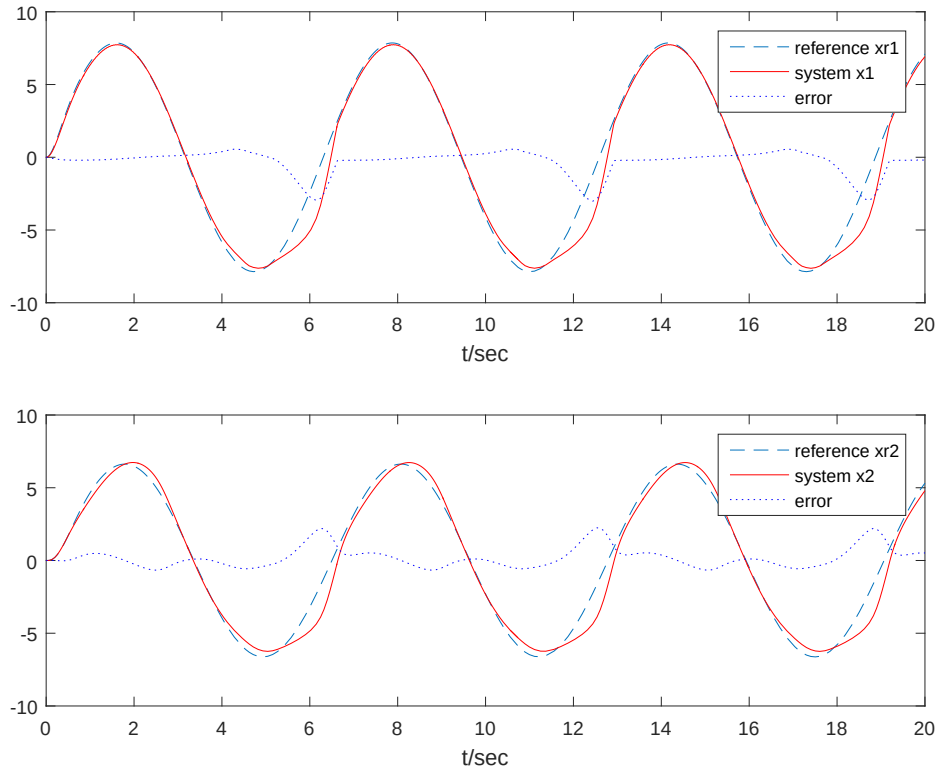

(a) State tracking result and tracking error.

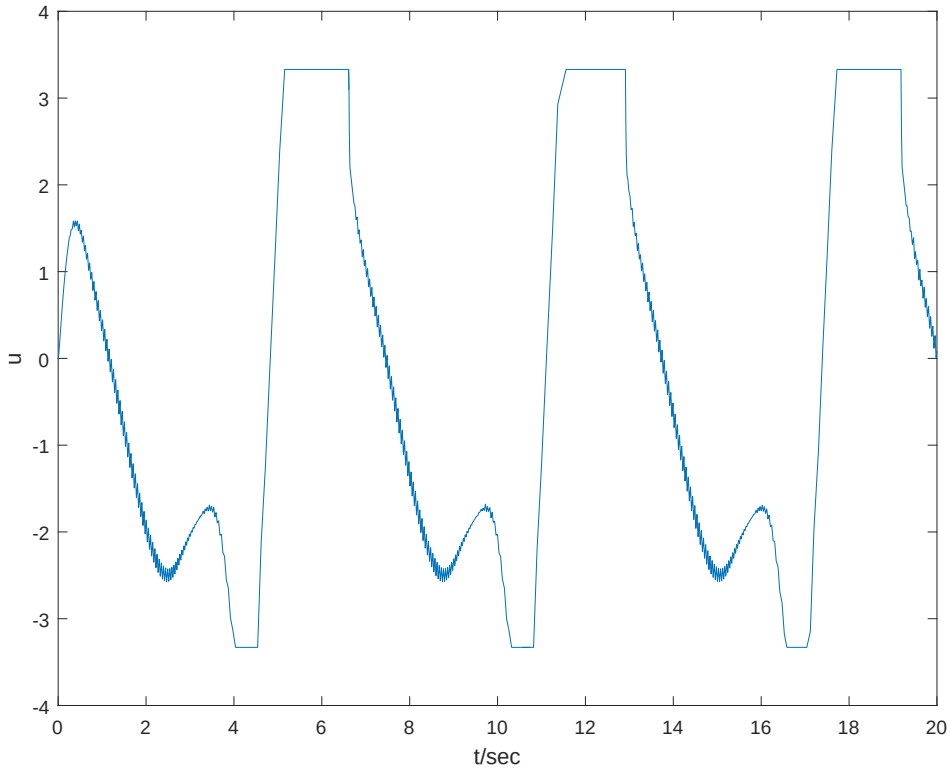

(b) Control signal saturated at ±3.3.

Figure 3.12: Tracking control result for Theorem 3.1 with $\sigma_1 = 4.0872$ and $\sigma_2 = 0.51569$.

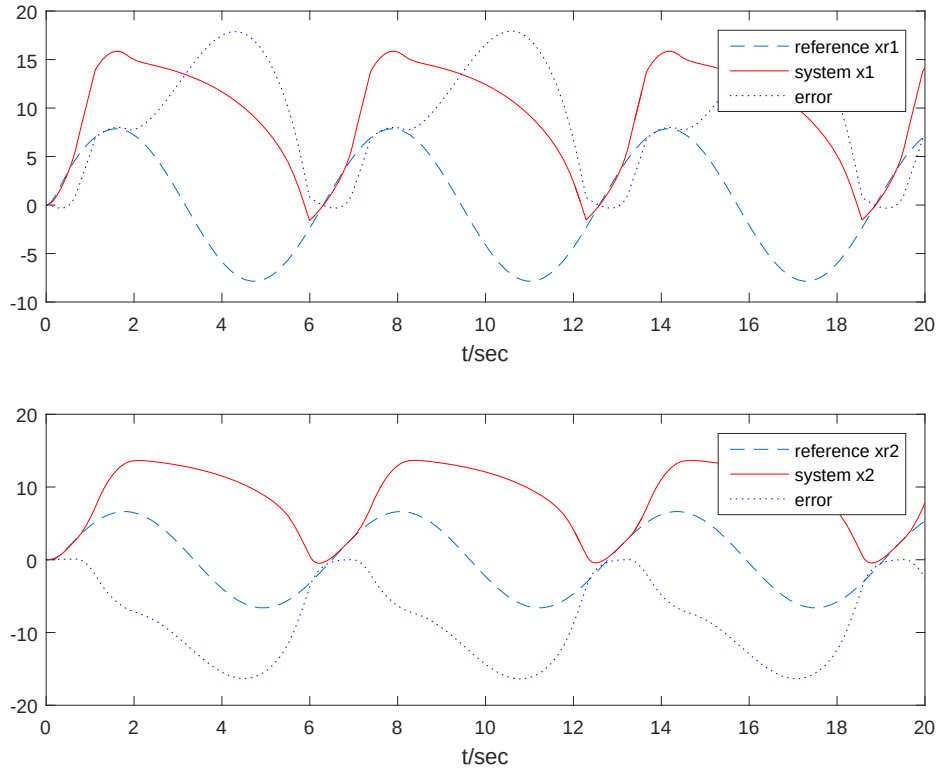

(a) State tracking result and tracking error.

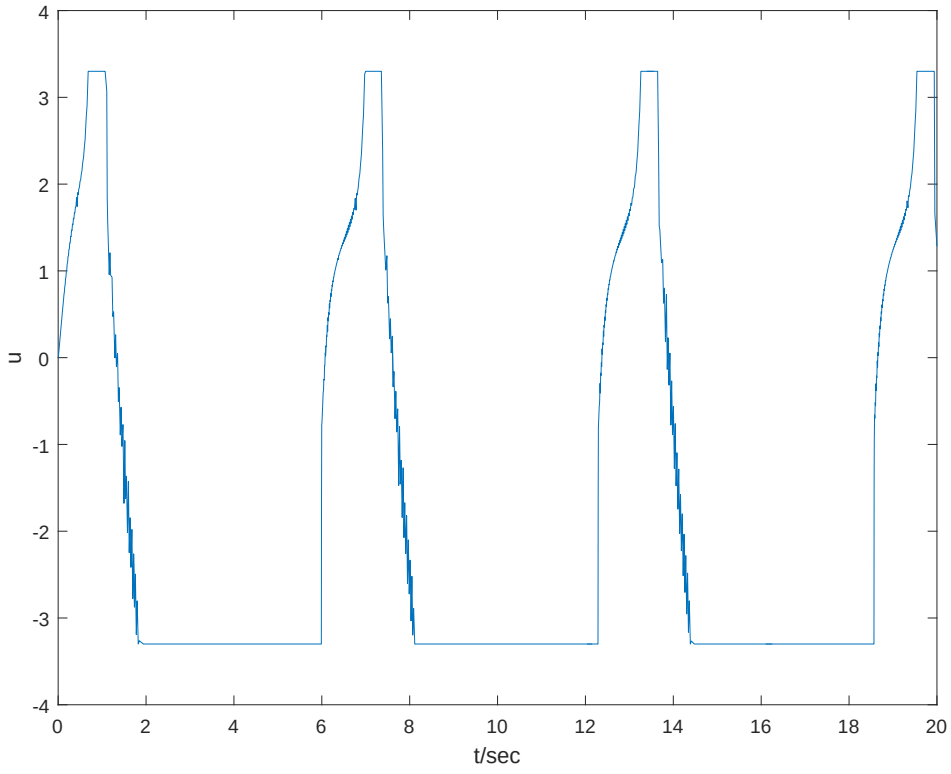

(b) Control signal saturated at ± 3.3.

Figure 3.13: Tracking control result for Theorem 3.2 with $\sigma_1 = 10$ and $\sigma_2 = 10$.

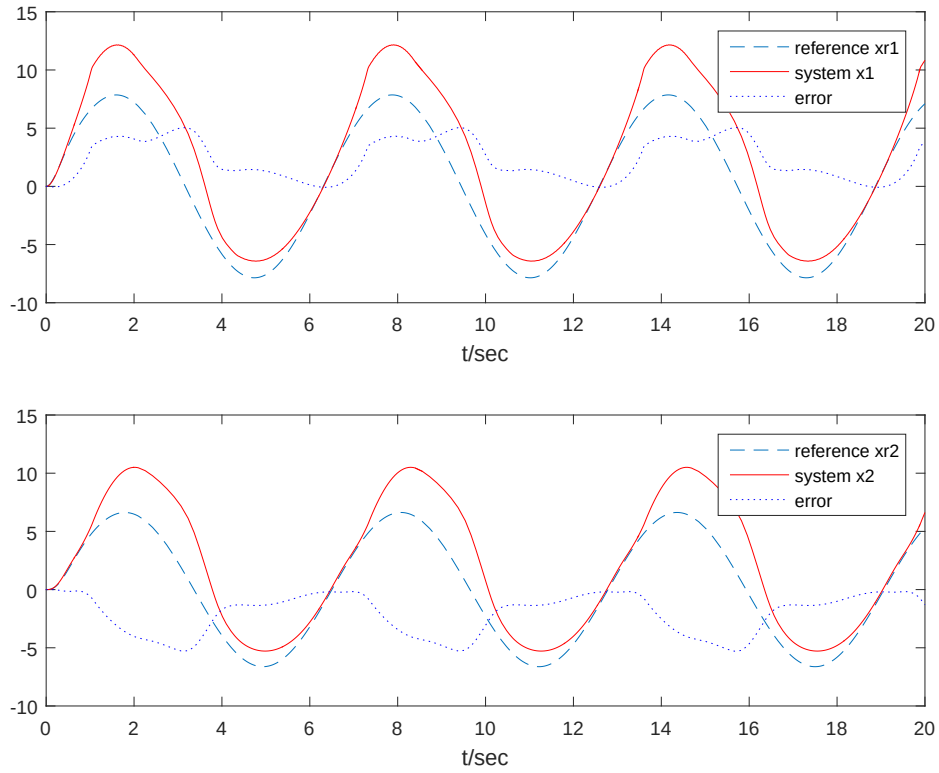

(a) State tracking result and tracking error.

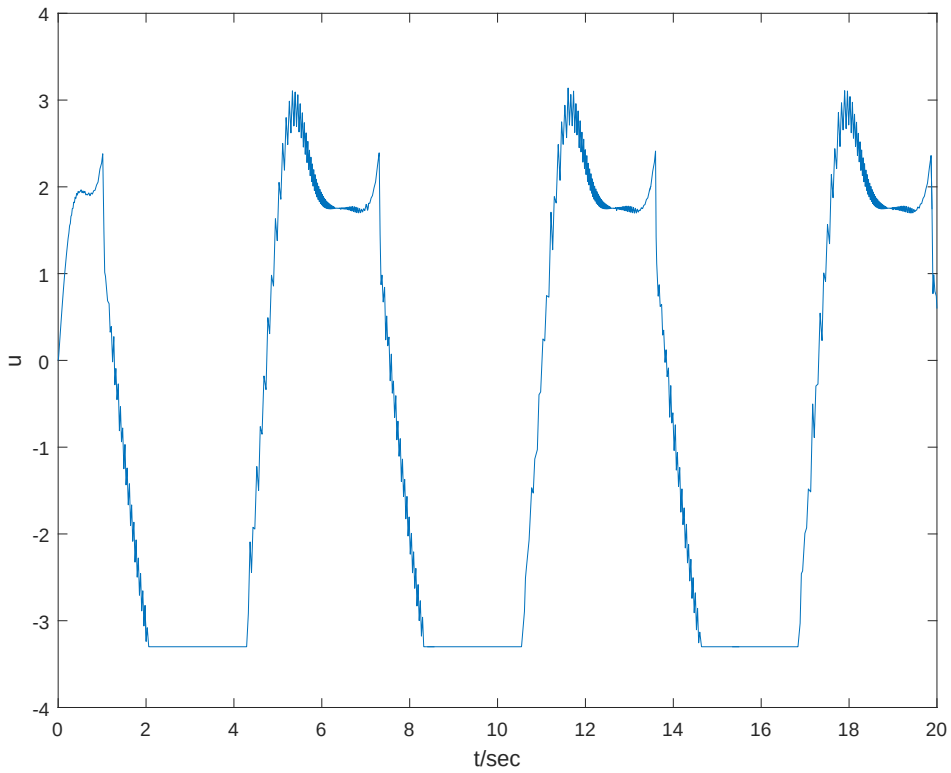

(b) Control signal saturated at ±3.3.

Figure 3.14: Tracking control result for Theorem 3.2 with $\sigma_1 = 3.6982$ and $\sigma_2 = 0.22660$.

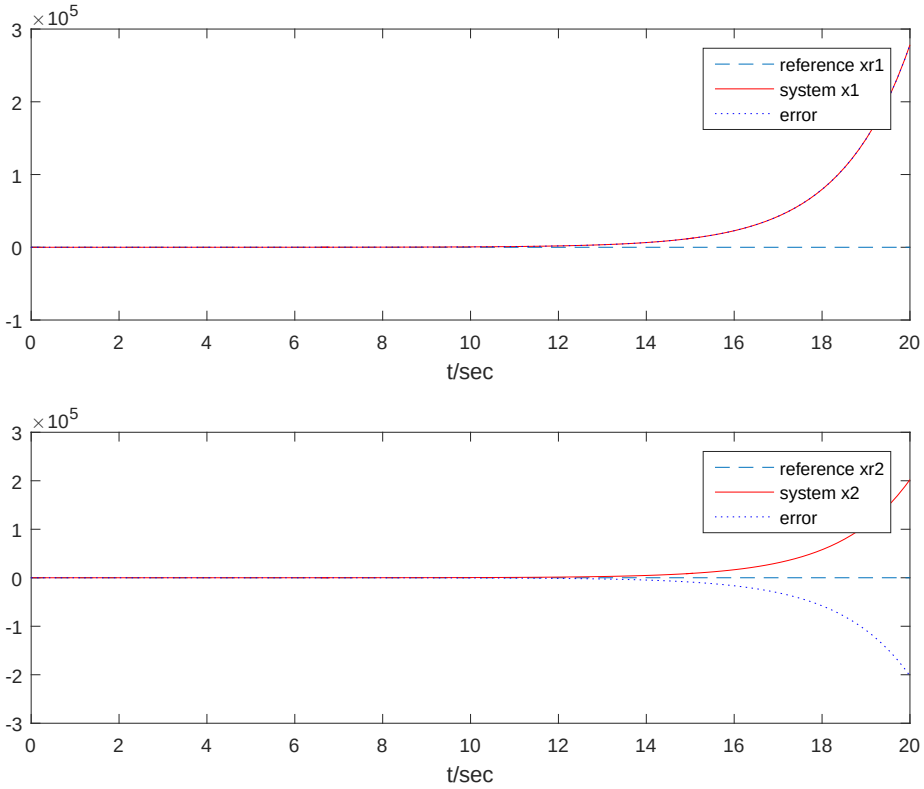

(a) State tracking result and tracking error.

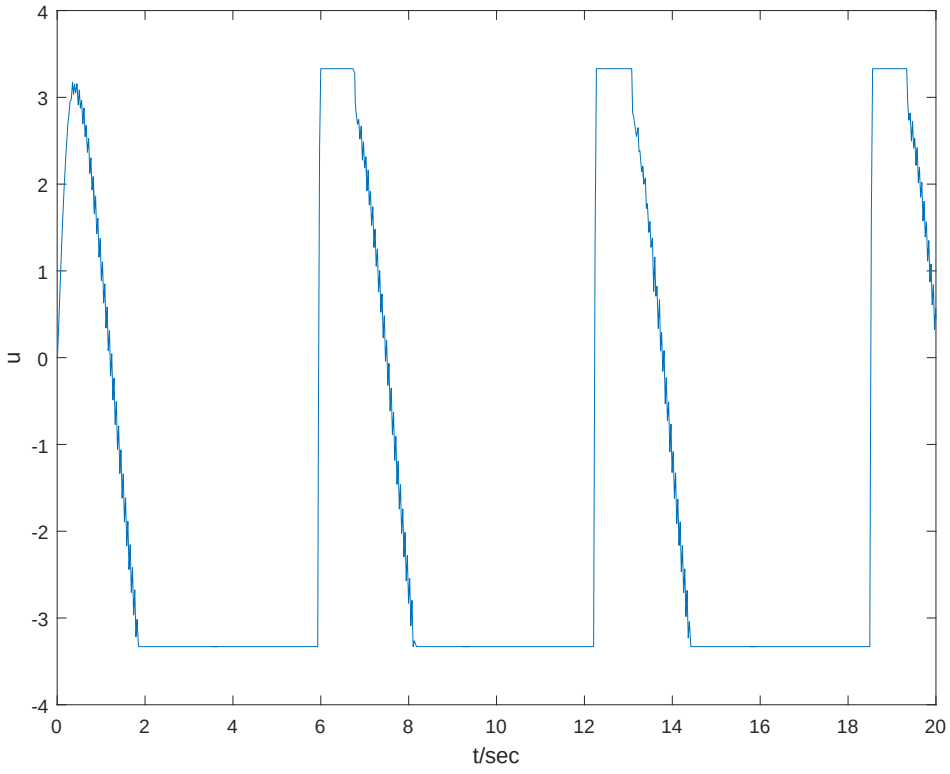

(b) Control signal saturated at ± 2.6.

Figure 3.15: Tracking control result for Theorem 3.1 with $\sigma_1 = 10$ and $\sigma_2 = 10$.

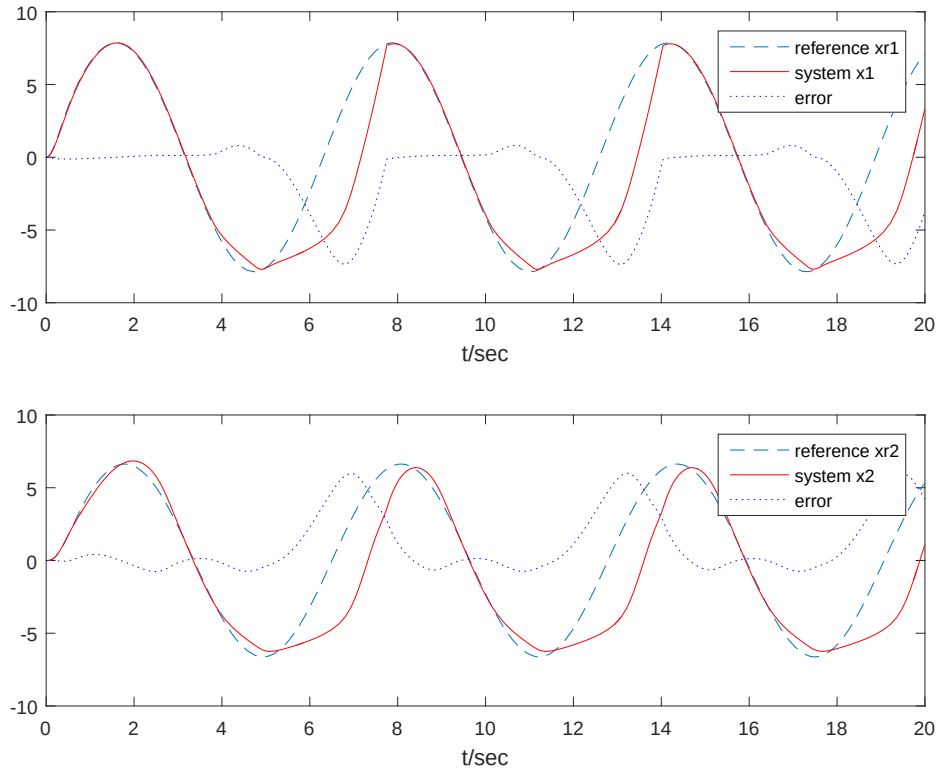

(a) State tracking result and tracking error.

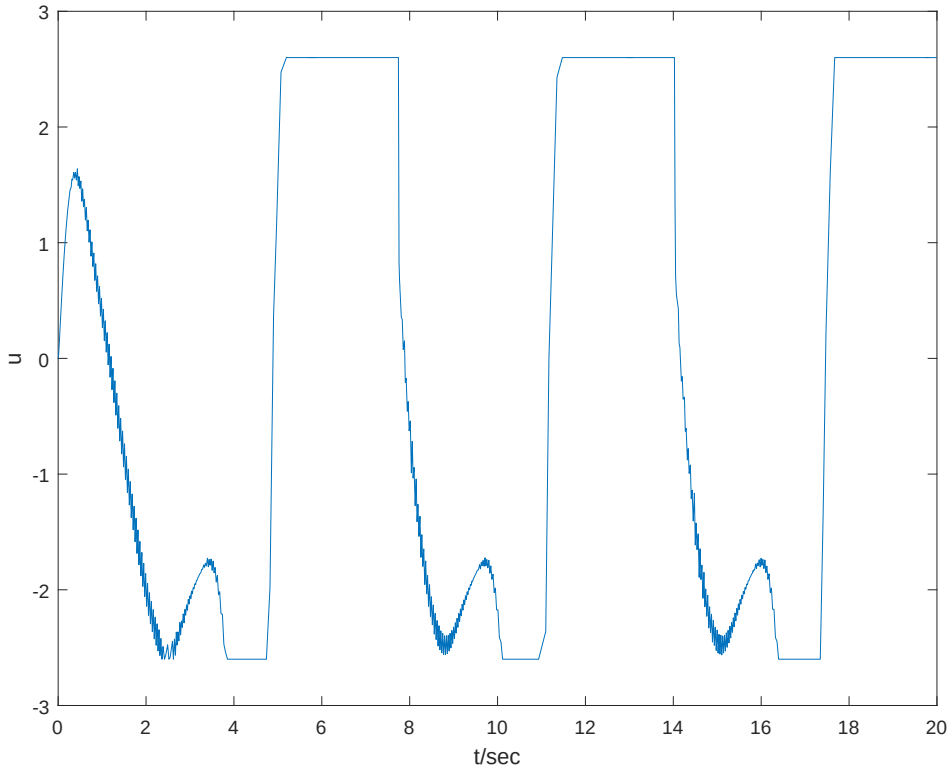

(b) Control signal saturated at ± 2.6.

Figure 3.16: Tracking control result for Theorem 3.1 with $\sigma_1 = 4.1799$ and $\sigma_2 = 0.53704$.

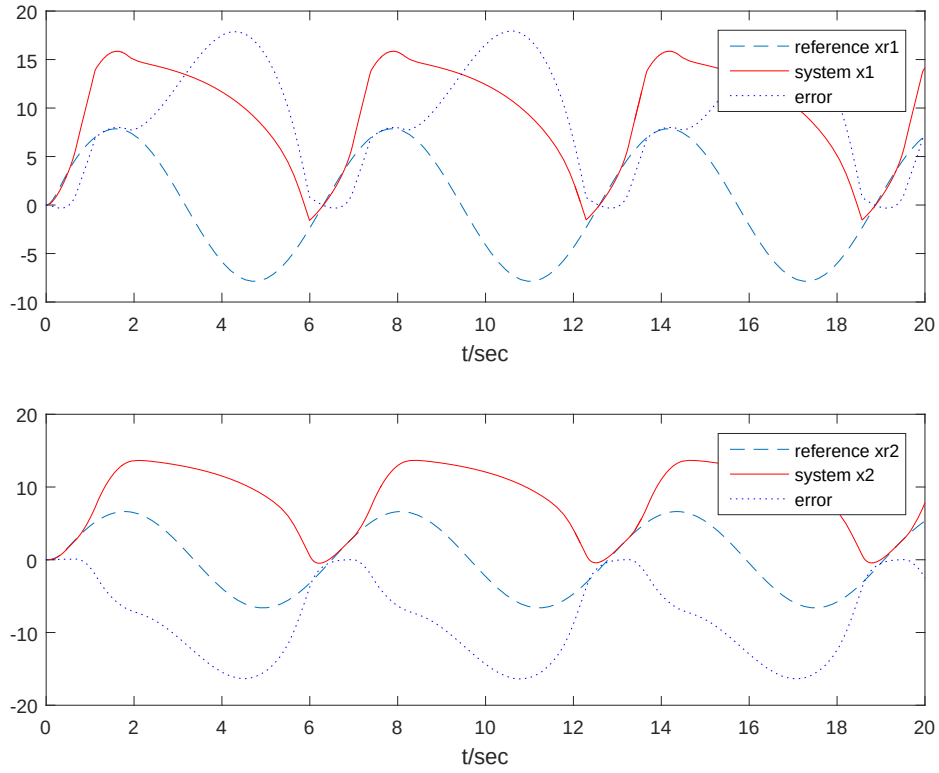

(a) State tracking result and tracking error.

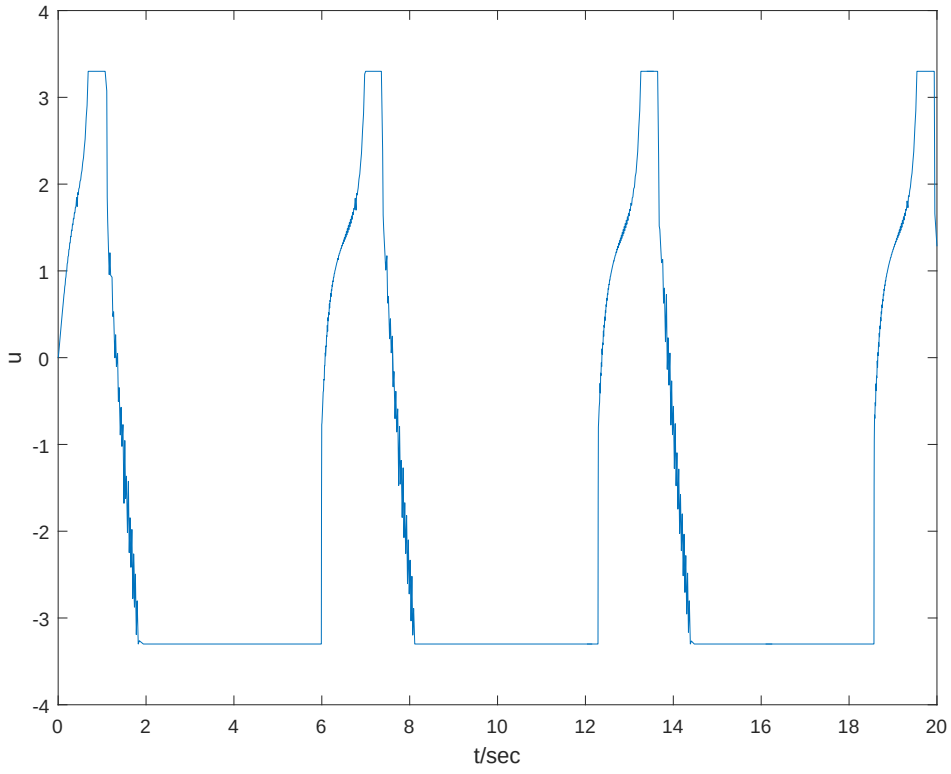

(b) Control signal saturated at ± 2.6.

Figure 3.17: Tracking control result for Theorem 3.2 with $\sigma_1 = 10$ and $\sigma_2 = 10$.

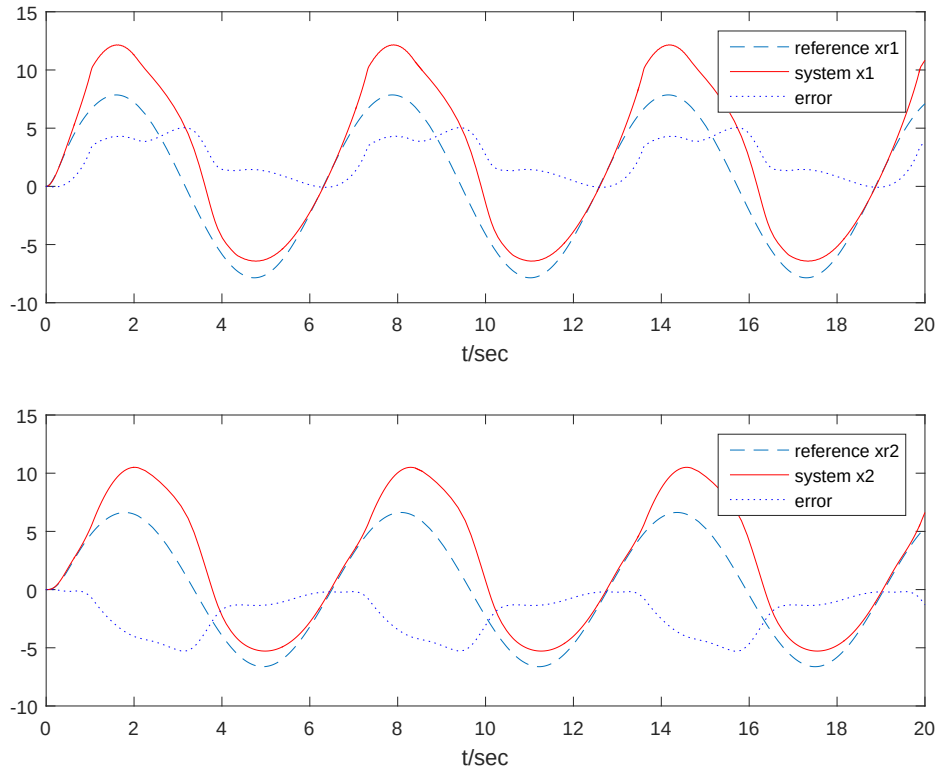

(a) State tracking result and tracking error.

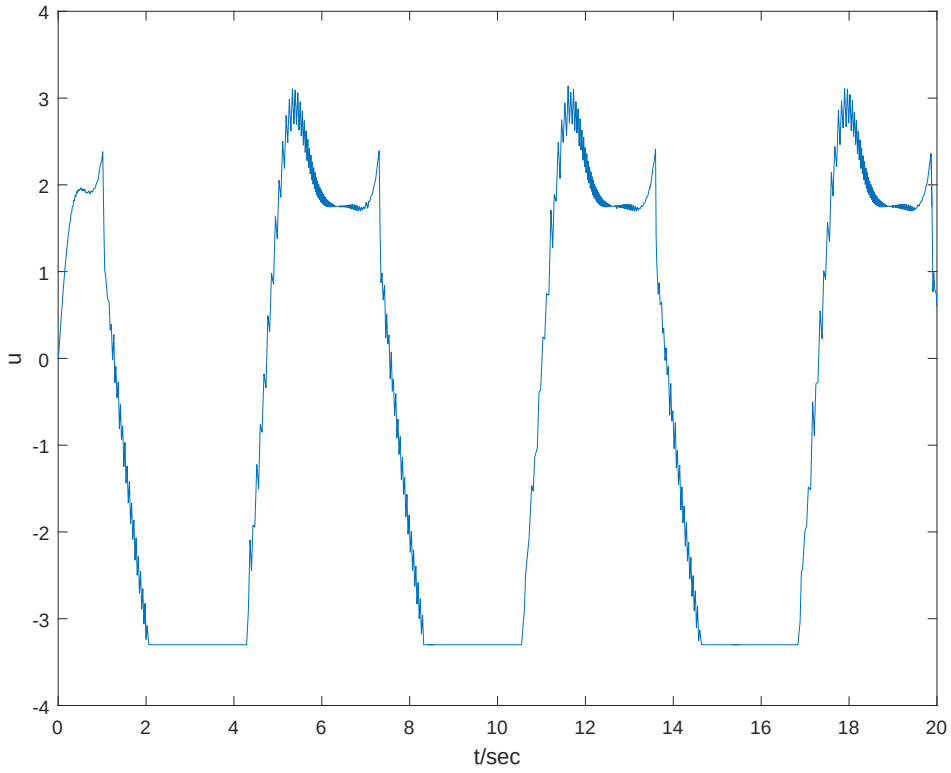

(b) Control signal saturated at ±3.3.

Figure 3.18: Tracking control result for Theorem 3.2 with $\sigma_1 = 3.7959$ and $\sigma_2 = 0.29619$.

Table 3.1: Simulation parameters for $\mathbf{H}_1 = [0.8]$ and $\mathbf{H}_2 = [1.0]$.

(a) $\tilde{\mathbf{u}}_{\max\,/\,\min} = \pm 20, \mathbf{u}_{\max\,/\,\min} = \pm 16$.

	σ_1	σ_2	**Figure**
Theorem 1	10	10	Fig. 3.3
	4.1323	0.51299	Fig. 3.4
Theorem 2	10	10	Fig. 3.5
	3.7067	0.26733	Fig. 3.6

(b) $\tilde{\mathbf{u}}_{\max\,/\,\min} = \pm 3.7, \mathbf{u}_{\max\,/\,\min} = \pm 3.0$.

	σ_1	σ_2	**Figure**
Theorem 1	10	10	Fig. 3.7
	4.1323	0.51299	Fig. 3.8
Theorem 2	10	10	Fig. 3.9
	3.7067	0.26733	Fig. 3.10

Table 3.2: Simulation parameters for $\mathbf{H}_2 = [1.0]$ and $\tilde{\mathbf{u}}_{\max\,/\,\min} = \pm 3.7$.

(a) $\mathbf{H}_1 = [0.9], \mathbf{u}_{\max\,/\,\min} = \pm 3.3$.

	σ_1	σ_2	**Figure**
Theorem 1	10	10	Fig. 3.11
	4.0872	0.51569	Fig. 3.12
Theorem 2	10	10	Fig. 3.13
	3.6982	0.22660	Fig. 3.14

(b) $\mathbf{H}_1 = [0.7], \mathbf{u}_{\max\,/\,\min} = \pm 2.6$.

	σ_1	σ_2	**Figure**
Theorem 1	10	10	Fig. 3.15
	4.1799	0.53704	Fig. 3.16
Theorem 2	10	10	Fig. 3.17
	3.7959	0.29619	Fig. 3.18

Table 3.3: Feedback gains for Table 3.1.

Figure	$\mathbf{F}_1$	$\mathbf{F}_2$	$\mathbf{G}_1$	$\mathbf{G}_2$	**X**
Fig.3.3	-14.039	-14.039	13.155	13.155	$\begin{bmatrix} 3.6974 & 0 \\ 0 & 3.1815 \end{bmatrix}$
Fig.3.4	-14.928	-14.928	-0.2549	-0.2549	$\begin{bmatrix} 2.9393 & 0 \\ 0 & 3.2280 \end{bmatrix}$
Fig.3.5	-58.644	-18.521	-36.909	18.508	$\begin{bmatrix} 2.9253 & 0 \\ 0 & 3.4489 \end{bmatrix}$
Fig.3.6	-27.082	-14.536	-5.5138	4.4844	$\begin{bmatrix} 2.6365 & 0 \\ 0 & 3.6732 \end{bmatrix}$
Fig.3.7	-14.039	-14.039	13.155	13.155	$\begin{bmatrix} 3.6974 & 0 \\ 0 & 3.1815 \end{bmatrix}$
Fig.3.8	-14.928	-14.928	-0.2549	-0.2549	$\begin{bmatrix} 2.9393 & 0 \\ 0 & 3.2280 \end{bmatrix}$
Fig.3.9	-58.644	-18.521	-36.909	18.508	$\begin{bmatrix} 2.9253 & 0 \\ 0 & 3.4489 \end{bmatrix}$
Fig.3.10	-27.082	-14.536	-5.5138	4.4844	$\begin{bmatrix} 2.6365 & 0 \\ 0 & 3.6732 \end{bmatrix}$

Table 3.4: Feedback gains for Table 3.2.

Figure	$\mathbf{F}_1$	$\mathbf{F}_2$	$\mathbf{G}_1$	$\mathbf{G}_2$	**X**
Fig.3.11	-13.240	-13.240	12.532	12.532	$\begin{bmatrix} 3.7171 & 0 \\ 0 & 3.1850 \end{bmatrix}$
Fig.3.12	-13.957	-13.957	-0.35649	-0.35649	$\begin{bmatrix} 2.9385 & 0 \\ 0 & 3.2413 \end{bmatrix}$
Fig.3.13	-56.533	-17.413	-35.654	17.482	$\begin{bmatrix} 2.9220 & 0 \\ 0 & 3.4484 \end{bmatrix}$
Fig.3.14	-33.143	-13.658	-8.2062	7.2653	$\begin{bmatrix} 2.7441 & 0 \\ 0 & 4.1272 \end{bmatrix}$
Fig.3.15	-14.140	-14.140	14.529	14.529	$\begin{bmatrix} 3.6539 & 0 \\ 0 & 3.0509 \end{bmatrix}$
Fig.3.16	-15.908	-15.908	-0.13290	-0.13290	$\begin{bmatrix} 2.9562 & 0 \\ 0 & 3.2087 \end{bmatrix}$
Fig.3.17	-59.574	-19.963	-37.263	-19.738	$\begin{bmatrix} 2.9320 & 0 \\ 0 & 3.4497 \end{bmatrix}$
Fig.3.18	-34.431	-15.027	-7.8749	7.9213	$\begin{bmatrix} 2.7771 & 0 \\ 0 & 3.9744 \end{bmatrix}$

Chapter 4

Membership-Function-Dependent Stability Analysis and Control Synthesis of Guaranteed Cost Fuzzy-Model-Based Control System

In this chapter, we focuses on the guaranteed-cost stability analysis of FMB control systems. Representing the nonlinear plant using a T-S fuzzy model, a fuzzy controller is employed to close the feedback loop. A weighted linear quadratic cost function is considered as the cost index to measure the performance of the closed-loop fuzzy system in terms of the system states, system outputs and control signals. The stability of the FMB control system is investigated by the Lyapunov stability theory subject to the minimization of cost index for performance realization. A membership-function-dependent approach using the PLMFs approach is employed to include the information of membership functions into the stability analysis. Membership-function-dependent stability conditions in terms of LMIs are obtained to determine the system stability and feedback gains with the consideration of the system performance measured by the cost function. A simulation example is provided to illustrate the effectiveness and merits of the proposed approach.

4.1 Introduction

T-S fuzzy model was first developed by Takagi and Sugeno in 1985 [24], which provided an effective model to represent nonlinear plants which facilitates the system analysis and control synthesis. Based on the T-S fuzzy model, a fuzzy controller is proposed to close the feedback loop which forms a FMB control system for feedback control [72]. Since then, the T-S FMB control systems have drawn the attention of

fuzzy control researchers for more than 20 years due to its effectiveness on handling nonlinear control systems [108, 109]. In particular, the issues of stability analysis and control synthesis have been investigated extensively and fruitful results can be found in [34, 68, 75, 77–80, 82, 83, 110, 111] and the references there in.

The Lyapunov based approach is a popular method used to investigate the stability of T-S FMB control systems. Through the Lyapunov stability theory, basic stability conditions of T-S FMB control systems can be achieved in terms of LMIs. With the PDC [110] design approach, the stability conditions can be relaxed and some further related works can be found in [34, 68, 75–80, 110]. The work in [75] used the symmetry property of the membership functions of the T-S fuzzy model and fuzzy controller in the analysis and then managed to relax the LMI-based stability conditions. Inspired by the work in [75], various techniques have been proposed to gather the membership functions in the stability analysis [68, 76–80]. The work in [76] combined all the LMIs used in [75] to form a large symmetric matrix resulting in further reducing the conservativeness of stability conditions. The work in [34] generalize the stability conditions with the consideration of the permutations of membership functions using the Pólya theorem.

One of the main difficulties to bring the information of membership functions into the analysis is the continuity property of the membership functions. When we consider continuous membership functions, the number of LMIs will reach infinity so it is impractical to apply numerical techniques to solve the solution to the stability conditions. Hence, approximations of membership functions is one of the methods to circumvent this difficulty by approximating the infinite number of stability conditions with finite ones. Staircase membership functions were proposed in [39] to approximate the original membership functions of the FMB control system in the stability analysis. With the consideration of the approximation error, the stability of the FMB control system is implied by the stability of the FMB control systems having the membership grades at the flat regions of the staircase membership functions. Along this line, PLMFs [40] and Taylor-series membership functions [112] were proposed to facilitate the stability analysis.

The performance of FMB control systems is another important issue to be considered during the controller design, and the index of performance can be the transient response and constrains on system variables (input, output and control) [68]. The guaranteed performance control aims at not only stabilizing the system, but also guaranteeing the specific cost of the system through pre-defined cost function [48, 113]. Also there is a guaranteed cost approach introduced by works in [46], which is able to provide an upper bound on a given performance index and the performance of the system is guaranteed to be less than the boundary. This approach has been applied on T-S fuzzy systems with time delays in [47] and this approach has also been adopted in the stability analysis of polynomial fuzzy systems in works

in [114]. In this research, we define a weighted cost function as the performance criteria in the controller design. Through the guaranteed cost approach, we manage to stabilise the control system meanwhile maintain a constrained input, output, control cost, which depends on the weighted cost function we choose.

In this chapter, we consider a FMB control system where the T-S fuzzy model and fuzzy controller do not share the same premise rules. Consequently, the fuzzy controller demonstrates a greater design flexibility by choosing its own number of rules and membership functions. PLMFs are adopted to approximate the original membership functions in a favorable form to facilitate the stability analysis. The PLMFs carrying the information of the original membership functions can be brought into the stability conditions so that the stability conditions become membership function dependent [34, 68, 75–80, 110]. Furthermore, we consider a cost function to describe the system performance on top of the stability analysis. By taking the cost function on board along with the PLMFs, membership-function-dependent guaranteed cost stability conditions are obtained for the design of stable FMB control system.

4.2 Preliminaries

4.2.1 Fuzzy Controller

A fuzzy controller with c rules of the following format is employed to control the nonlinear plant represented by the T-S fuzzy model (2.5). The IF-THEN rule is described as follows:

$$\begin{aligned} \text{Rule } j\text{: IF } & g_1(\mathbf{x}(t)) \text{ is } N_1^j \text{ AND } \cdots \text{ AND } g_\Omega(\mathbf{x}(t)) \text{ is } N_\Omega^j \\ & \text{THEN } \mathbf{u}(t) = \mathbf{G}_j\mathbf{x}(t), \end{aligned} \tag{4.1}$$

where N_β^j is a fuzzy term of rule j corresponding to the function $g_\beta(\mathbf{x}(t))$, $\beta = 1, 2, \ldots, \Omega$; $j = 1, 2, \ldots, c$; Ω is a positive integer; $\mathbf{G}_j \in \Re^{m\times n}$, $j = 1, 2, \ldots, c$, are constant feedback gains to be determined.

The fuzzy controller is defined as follows

$$\mathbf{u}(t) = \sum_{j=1}^{c} m_j(\mathbf{x}(t))\mathbf{G}_j\mathbf{x}(t), \tag{4.2}$$

where

$$m_j(\mathbf{x}(t)) \geq 0 \; \forall \; j, \sum_{j=1}^{c} m_j(\mathbf{x}(t)) = 1, \tag{4.3}$$

$$m_j(\mathbf{x}(t)) = \frac{\prod_{l=1}^{\Omega} \mu_{N_l^j}(g_l(\mathbf{x}(t)))}{\sum_{k=1}^{c} \prod_{l=1}^{\Omega} \mu_{N_l^k}(g_l(\mathbf{x}(t)))} \quad \forall\, j, \tag{4.4}$$

where $m_j(\mathbf{x}(t))$, $j = 1, 2, \ldots, c$, are the normalized grades of membership, $\mu_{N_\alpha^j}(g_\alpha(\mathbf{x}(t)))$, $\beta = 1, 2, \ldots, \Omega$, are the grades of membership corresponding to the fuzzy term N_β^j.

4.2.2 Fuzzy-Model-Based Control System

Considering the T-S fuzzy model (2.5) and the fuzzy controller (4.2) connected in a closed loop, with the property of the membership functions that $\sum_{i=1}^{p} w_i(\mathbf{x}(t)) = \sum_{j=1}^{c} m_j(\mathbf{x}(t)) = \sum_{i=1}^{p}\sum_{j=1}^{c} w_i(\mathbf{x}(t)) m_j(\mathbf{x}(t)) = 1$, the FMB control system is obtained as follows,

$$\begin{aligned}\dot{\mathbf{x}}(t) &= \sum_{i=1}^{p} w_i(\mathbf{x}(t))(\mathbf{A}_i\mathbf{x}(t) + \mathbf{B}_i \sum_{j=1}^{c} m_j(\mathbf{x}(t))\mathbf{G}_j\mathbf{x}(t)) \\ &= \sum_{i=1}^{p}\sum_{j=1}^{c} w_i(\mathbf{x}(t)) m_j(\mathbf{x}(t))(\mathbf{A}_i + \mathbf{B}_i\mathbf{G}_j)\mathbf{x}(t). \end{aligned} \tag{4.5}$$

The control objective is to drive the system state vector $\mathbf{x}(t)$ to the origin by determining the feedback gains $\mathbf{G}_j$. As the premise membership functions of the T-S fuzzy model and fuzzy controller are not the same, the analysis results with the PDC design [34] cannot be applied to check for the stability of the FMB control system (4.5).

4.3 Stability Analysis

In this section, we will investigate the system stability of the FMB control system considering a guaranteed cost fuzzy controller in the form of (4.2) through a cost measuring the system performance. For brevity, the time t for variables is dropped for the situation without ambiguity.

4.3.1 Lyapunov Function

The following quadratic Lyapunov function candidate is employed for the stability analysis of the FMB control system (4.5).

$$V = \mathbf{x}^T\mathbf{P}\mathbf{x}, \tag{4.6}$$

where $0 < \mathbf{P} = \mathbf{P}^T \in \Re^{n\times n}$. In the following analysis, for brevity, the time t associated with the variables is dropped for situation without ambiguity, e.g., $\mathbf{x}(t)$

is denoted as $\mathbf{x}$.

Denote $\mathbf{z} = \mathbf{P}^{-1}\mathbf{x}$ and $\mathbf{X} = \mathbf{P}^{-1}$. Define the feedback gains $\mathbf{G}_j = \mathbf{N}_j\mathbf{X}^{-1}$ where $\mathbf{N}_j \in \Re^{m\times n}$, $j = 1, 2, \ldots, c$, are matrices to be determined. From (4.5) and (4.6), we have,

$$\begin{aligned}\dot{V} &= \dot{\mathbf{x}}^T\mathbf{P}\mathbf{x} + \mathbf{x}^T\mathbf{P}\dot{\mathbf{x}} \\ &= \sum_{i=1}^{p}\sum_{j=1}^{c} w_i(\mathbf{x})m_j(\mathbf{x})\mathbf{x}^T\big((\mathbf{A}_i + \mathbf{B}_i\mathbf{G}_j)^T\mathbf{P} \\ &\quad + \mathbf{P}(\mathbf{A}_i + \mathbf{B}_i\mathbf{G}_j)\big)\mathbf{x} \\ &= \sum_{i=1}^{p}\sum_{j=1}^{c} w_i(\mathbf{x})m_j(\mathbf{x})\mathbf{x}^T\mathbf{Q}_{ij}\mathbf{x}.\end{aligned} \tag{4.7}$$

4.3.2 Weighting Matrix

$$J = \int_t^\infty \begin{bmatrix}\mathbf{x}\\ \mathbf{y}\\ \mathbf{u}\end{bmatrix}^T \mathbf{W} \begin{bmatrix}\mathbf{x}\\ \mathbf{y}\\ \mathbf{u}\end{bmatrix} dt \tag{4.8}$$

where $0 \leq \mathbf{W} \in \Re^{(n+l+m)\times(n+l+m)}$ is a pre-defined weighting matrix.

Remark 4.1. *The cost $J > 0$ (except for $\mathbf{x} = \mathbf{0}$) is employed to measure the system performance. It can be considered as the energy consumed by the system state $\mathbf{x}$, the system output $\mathbf{y}$ and the control signal $\mathbf{u}$. With regard to the same weighting matrix $\mathbf{W}$, a smaller value of J implies a better system performance in terms of less energy consumption contributed by the combination of $\mathbf{x}$, $\mathbf{y}$ and $\mathbf{u}$, which will eventually affect the transient behaviour of the FMB control system (4.5) such as rise time, settling time, overshoot, undershoot, etc. The performance object is to suppress the value of J as much as possible through the design of the feedback gains $\mathbf{G}_j$ subject to the system stability.*

Remark 4.2. *The weighting matrix $\mathbf{W}$ plays an important role to the system performance. A special case is to choose $\mathbf{W} = \begin{bmatrix}\mathbf{W}_x & \mathbf{0} & \mathbf{0}\\ \mathbf{0} & \mathbf{W}_y & \mathbf{0}\\ \mathbf{0} & \mathbf{0} & \mathbf{W}_u\end{bmatrix}$ where $0 \leq \mathbf{W}_x \in \Re^{n\times n}$ is the weighting matrix controlling the energy consumed by the system state $\mathbf{x}$; $0 \leq \mathbf{W}_y \in \Re^{l\times l}$ is the weighting matrix controlling the energy consumed by the system output $\mathbf{y}$; and $0 \leq \mathbf{W}_u \in \Re^{m\times m}$ is the weighting matrix controlling the energy consumed by the control signal $\mathbf{u}$.*

From (2.5), (4.2) and (4.8), we have

$$J = \int_t^\infty \mathbf{x}^T \begin{bmatrix} \mathbf{I} \\ \sum_i^p w_i \mathbf{C}_i \\ \sum_j^c m_j \mathbf{G}_j \end{bmatrix}^T \mathbf{W} \begin{bmatrix} \mathbf{I} \\ \sum_i^p w_i \mathbf{C}_i \\ \sum_j^c m_j \mathbf{G}_j \end{bmatrix} \mathbf{x} dt \tag{4.9}$$

where $\mathbf{I}$ is the identify matrix of compatible dimensions.

From (4.9) and (4.7), we have

$$\begin{aligned} \dot{V} \leq & \sum_{i=1}^p \sum_{j=1}^c w_i(\mathbf{x}) m_j(\mathbf{x}) \mathbf{x}^T \big((\mathbf{A}_i + \mathbf{B}_i \mathbf{G}_j)^T \mathbf{P} + \mathbf{P}(\mathbf{A}_i + \mathbf{B}_i \mathbf{G}_j) \big) \mathbf{x} \\ & + \mathbf{x}^T \begin{bmatrix} \mathbf{I} \\ \sum_i^p w_i \mathbf{C}_i \\ \sum_j^c m_j \mathbf{G}_j \end{bmatrix}^T \mathbf{W} \begin{bmatrix} \mathbf{I} \\ \sum_i^p w_i \mathbf{C}_i \\ \sum_j^c m_j \mathbf{G}_j \end{bmatrix} \mathbf{x} \\ = & \sum_{i=1}^p \sum_{j=1}^c w_i(\mathbf{x}) m_j(\mathbf{x}) \mathbf{z}^T \mathbf{Q}_{ij} \mathbf{z} \\ & + \mathbf{z}^T \begin{bmatrix} \mathbf{X} \\ \sum_i^p w_i \mathbf{C}_i \mathbf{X} \\ \sum_j^c m_j \mathbf{N}_j \end{bmatrix}^T \mathbf{W} \begin{bmatrix} \mathbf{X} \\ \sum_i^p w_i \mathbf{C}_i \mathbf{X} \\ \sum_j^c m_j \mathbf{N}_j \end{bmatrix} \mathbf{z} \end{aligned} \tag{4.10}$$

where $\mathbf{X} = \mathbf{P}^{-1}$; $\mathbf{z} = \mathbf{X}^{-1}\mathbf{x}$, $\mathbf{Q}_{ij} = \mathbf{A}_i\mathbf{X} + \mathbf{X}\mathbf{A}_i^T + \mathbf{B}_i\mathbf{N}_j + \mathbf{N}_j^T\mathbf{B}_i^T$; $\mathbf{G}_j = \mathbf{N}_j\mathbf{X}^{-1}$; $\mathbf{N}_j \in \Re^{m\times n}$ is a matrix to be determined for all j.

It is required that $\dot{V} \leq 0$ (equality holds when $\mathbf{x} = \mathbf{0}$) for system stability which can be achieved by

$$\begin{aligned} & \sum_{i=1}^p \sum_{j=1}^c w_i(\mathbf{x}) m_j(\mathbf{x}) \mathbf{Q}_{ij} \\ & + \begin{bmatrix} \mathbf{X} \\ \sum_i^p w_i \mathbf{C}_i \mathbf{X} \\ \sum_j^c m_j \mathbf{N}_j \end{bmatrix}^T \mathbf{W} \begin{bmatrix} \mathbf{X} \\ \sum_i^p w_i \mathbf{C}_i \mathbf{X} \\ \sum_j^c m_j \mathbf{N}_j \end{bmatrix} < 0. \end{aligned} \tag{4.11}$$

By Schur complement, the inequality (4.11) is equivalent to

$$\sum_{i=1}^p \sum_{j=1}^c w_i(\mathbf{x}) m_j(\mathbf{x}) \mathbf{H}_{ij} < 0 \tag{4.12}$$

where $\mathbf{H}_{ij} = \begin{bmatrix} \mathbf{Q}_{ij} & \mathbf{T}_{ij}^T \\ \mathbf{T}_{ij} & \mathbf{W}^{-1} \end{bmatrix}$; $\mathbf{T}_{ij} = \begin{bmatrix} \mathbf{X} \\ \mathbf{C}_i\mathbf{X} \\ \mathbf{N}_j \end{bmatrix}$.

As a result, it can be proved by the Lyapunov stability theory that the system

stability is implied by $V > 0$ and $\dot{V} < 0$ (excluding $\mathbf{x} = \mathbf{x}$). The cost (4.8) reflects the system performance. Following from the fact $J > 0$ in (4.9) and assuming that the FMB control system (4.5) is stable, we have

$$\dot{V} \leq -\mathbf{x}^T \begin{bmatrix} \mathbf{I} \\ \sum_i^p w_i \mathbf{C}_i \\ \sum_j^c m_j \mathbf{G}_j \end{bmatrix}^T \mathbf{W} \begin{bmatrix} \mathbf{I} \\ \sum_i^p w_i \mathbf{C}_i \\ \sum_j^c m_j \mathbf{G}_j \end{bmatrix} \mathbf{x}. \tag{4.13}$$

Taking integration on both sides of (4.13) from 0 to ∞ and using the fact that $\mathbf{x}(\infty) \to \mathbf{0}$, we have

$$\mathbf{x}(0)^T \mathbf{P} \mathbf{x}(0) > J. \tag{4.14}$$

Remark 4.3. *It can be seen from* (4.14) *that* $\mathbf{x}(0)^T\mathbf{P}\mathbf{x}(0)$*, where* $\mathbf{x}(0)$ *is the initial condition, is the upper bound of* J*. By suppressing* $\mathbf{x}(0)^T\mathbf{P}\mathbf{x}(0)$*, the upper bound of* J *can be reduced reflecting a better system performance.*

Let $\mathbf{x}(0)^T\mathbf{P}\mathbf{x}(0) \leq \alpha \mathbf{x}(0)^T\mathbf{x}(0)$ which gives

$$\mathbf{P} < \alpha \mathbf{I}. \tag{4.15}$$

By minimizing the value of α, the upper bound of J, i.e. $\mathbf{x}(0)^T\mathbf{P}\mathbf{x}(0)$, can be minimized. By Schur complement, the inequality (4.15) is equivalent to the following:

$$\begin{bmatrix} \alpha \mathbf{I} & \mathbf{I} \\ \mathbf{I} & \mathbf{X} \end{bmatrix} > 0. \tag{4.16}$$

Theorem 4.1. *The FMB control system* (4.5) *formed by a nonlinear system represented by the fuzzy model* (2.5) *and the fuzzy controller* (4.2) *connected in a closed-loop is asymptotically stable and the system performance satisfies the cost* (4.8) *which is bound by a pre-determined value of* $\alpha > 0$ *if there exist decision matrix variables* $\mathbf{N}_j \in \Re^{m \times n}$ *and* $\mathbf{X} \in \Re^{n \times n}$*, and pre-defined weighting matrix* $0 \leq \mathbf{W} \in \Re^{(n+l+m)\times(n+l+m)}$ *such that the following LMIs are satisfied:*

$$\begin{bmatrix} \alpha \mathbf{I} & \mathbf{I} \\ \mathbf{I} & \mathbf{X} \end{bmatrix} > 0;$$

$$\mathbf{H}_{ij} < 0, \forall\, i, j$$

where $\mathbf{Q}_{ij} = \mathbf{A}_i\mathbf{X} + \mathbf{X}\mathbf{A}_i^T + \mathbf{B}_i\mathbf{N}_j + \mathbf{N}_j^T\mathbf{B}_i^T$*;* $\mathbf{H}_{ij} = \begin{bmatrix} \mathbf{Q}_{ij} & \mathbf{T}_{ij}^T \\ \mathbf{T}_{ij} & \mathbf{W}^{-1} \end{bmatrix}$*;* $\mathbf{T}_{ij} = \begin{bmatrix} \mathbf{X} \\ \mathbf{C}_i\mathbf{X} \\ \mathbf{N}_j \end{bmatrix}$*;*

and the feedback gain is given as $\mathbf{G}_j = \mathbf{N}_j\mathbf{X}^{-1}$ *for all* j*.*

Remark 4.4. *The conditions* $\mathbf{X} > 0$ *is omitted in Theorem 4.1 which is implied by* $\begin{bmatrix} \alpha\mathbf{I} & \mathbf{I} \\ \mathbf{I} & \mathbf{X} \end{bmatrix} > 0.$

Remark 4.5. *The stability conditions in Theorem 4.1 are membership-function-dependent which does not consider the information of membership functions* w_i *and* m_j *in the stability analysis resulting in conservative stability analysis result.*

4.3.3 Piecewise Linear Membership Functions

In the following, we attempt to include the information of membership functions into the stability conditions to relax the stability analysis result. We approximate the membership function $h_{ij}(\mathbf{x}) \equiv w_i(\mathbf{x})m_j(\mathbf{x})$ using the PLMFs [115]. The basic idea of constructing the PLMFs is to first sample the original membership functions. Linear interpolation is then employed to approximate the grades of the original membership functions based on the sample points. Details are given as follows. The state space of interest Φ is first divided into q connected sub-state spaces Φ_k, $k = 1, 2, \ldots, q$. Consequently, we have $\Phi = \bigcup_{k=1}^{q} \Phi_k$. Mathematically, the PLMFs $\hat{h}_{ij}(\mathbf{x})$ approximating the original membership function $h_{ij}(\mathbf{x})$ can be expressed as follows:

$$\hat{h}_{ij}(\mathbf{x}) = \sum_{k=1}^{q} \sum_{i_1=1}^{2} \cdots \sum_{i_n=1}^{2} \prod_{r=1}^{n} v_{ri_rk}(x_r)\delta_{iji_1i_2\cdots i_nk}, \quad \forall\, i, j, k, \tag{4.17}$$

$$0 \leq \hat{h}_{ijl}(\mathbf{x}) \leq 1, \tag{4.18}$$

$$0 \leq \delta_{iji_1i_2\cdots i_nk} \leq 1, \tag{4.19}$$

where $\delta_{iji_1i_2\cdots i_nk}$ is a constant scalar to be determined which is in general a sample point of the original membership function $h_{ij}(\mathbf{x})$ at a chosen point $\mathbf{x}$; $0 \leq v_{ri_sk}(x_r(t)) \leq 1$ and $v_{r1k}(x_r(t)) + v_{r2k}(x_r(t)) = 1$ for $r, s = 1, 2, \ldots, n$; $i_r = 1, 2$; $\mathbf{x}(t) \in \Phi_k$; otherwise, $v_{ri_sk}(x_r(t)) = 0$. As a result of the above settings, we have the following property:

$$\sum_{k=1}^{q} \sum_{i_1=1}^{2} \sum_{i_2=1}^{2} \cdots \sum_{i_n=1}^{2} \prod_{r=1}^{n} v_{ri_rk}(x_r(t)) = 1. \tag{4.20}$$

The approximation error satisfies

$$\Delta\underline{h}_{ij} \leq h_{ij}(\mathbf{x}) - \hat{h}_{ij}(\mathbf{x}) \leq \Delta\overline{h}_{ij} \tag{4.21}$$

where $\Delta\underline{h}_{ij}$ and $\Delta\overline{h}_{ij}$ are constant scalars to be determined.

From (4.21), it follows that

$$0 \leq h_{ij}(\mathbf{x}) - \hat{h}_{ij}(\mathbf{x}) - \Delta\underline{h}_{ij} \leq \Delta\overline{h}_{ij} - \Delta\underline{h}_{ij}. \tag{4.22}$$

From (4.12) and (4.17), we have

$$\begin{aligned}
&\sum_{i=1}^{p}\sum_{j=1}^{c} h_{ij}(\mathbf{x})\mathbf{H}_{ij} \\
&= \sum_{i=1}^{p}\sum_{j=1}^{c} \hat{h}_{ij}(\mathbf{x})\mathbf{H}_{ij} + \sum_{i=1}^{p}\sum_{j=1}^{c}(h_{ij}(\mathbf{x}) - \hat{h}_{ij}(\mathbf{x}))\mathbf{H}_{ij} \\
&= \sum_{i=1}^{p}\sum_{j=1}^{c}(\hat{h}_{ij}(\mathbf{x}) + \Delta\underline{h}_{ij})\mathbf{H}_{ij} + \sum_{i=1}^{p}\sum_{j=1}^{c}(h_{ij}(\mathbf{x}) - \hat{h}_{ij}(\mathbf{x}) - \Delta\underline{h}_{ij})\mathbf{H}_{ij} \\
&\leq \sum_{i=1}^{p}\sum_{j=1}^{c}(\hat{h}_{ij}(\mathbf{x}) + \Delta\underline{h}_{ij})(\mathbf{x})\mathbf{H}_{ij} + \sum_{i=1}^{p}\sum_{j=1}^{c}(\Delta\overline{h}_{ij} - \Delta\underline{h}_{ij})\mathbf{Y}_{ij}
\end{aligned} \tag{4.23}$$

where $0 \leq \mathbf{Y}_{ij} = \mathbf{Y}_{ij}^T \in \Re^{(n+l+m)\times(n+l+m)}$ and $\mathbf{Y}_{ij} \geq \mathbf{H}_{ij}$ for all i and j.

Expanding $\hat{h}_{ij}(\mathbf{x})$ in (4.23), we have

$$\begin{aligned}
&\sum_{i=1}^{p}\sum_{j=1}^{c} h_{ij}(\mathbf{x})\mathbf{H}_{ij} \\
&\leq \sum_{i=1}^{p}\sum_{j=1}^{c}\sum_{k=1}^{q}\sum_{i_1=1}^{2}\cdots\sum_{i_n=1}^{2}\prod_{r=1}^{n} v_{ri_rk}(x_r) \times (\delta_{iji_1i_2\cdots i_nk} + \Delta\underline{h}_{ij})\mathbf{H}_{ij} \\
&+ \sum_{i=1}^{p}\sum_{j=1}^{c}(\Delta\overline{h}_{ij} - \Delta\underline{h}_{ij})\mathbf{Y}_{ij} \\
&= \sum_{k=1}^{q}\sum_{i_1=1}^{2}\cdots\sum_{i_n=1}^{2}\prod_{r=1}^{n} v_{ri_rk}(x_r) \\
&\times \sum_{i=1}^{p}\sum_{j=1}^{c}\Big((\delta_{iji_1i_2\cdots i_nk} + \Delta\underline{h}_{ij})\mathbf{H}_{ij} + (\Delta\overline{h}_{ij} - \Delta\underline{h}_{ij})\mathbf{Y}_{ij}\Big).
\end{aligned} \tag{4.24}$$

Given the property (4.20), the satisfaction of $\sum_{i=1}^{p}\sum_{j=1}^{c}\Big((\delta_{iji_1i_2\cdots i_nk}+\Delta\underline{h}_{ij})\mathbf{H}_{ij}+(\Delta\overline{h}_{ij}-\Delta\underline{h}_{ij})\mathbf{Y}_{ij}\Big) < 0$ implies the satisfaction of (4.12) which further implies $\dot{V} \leq 0$ except $\mathbf{x} = \mathbf{0}$. The stability analysis result obtained through PLMFs is summarized in the following Theorem.

Theorem 4.2. *The FMB control system* (4.5) *formed by a nonlinear system represented by the fuzzy model* (2.5) *and the fuzzy controller* (4.2) *connected in a closed-loop is asymptotically stable and the system performance satisfies the cost* (4.8) *which is bound by a pre-determined value of* $\alpha > 0$ *if there exist decision matrix variables*

$\mathbf{N}_j \in \Re^{m\times n}$, $\mathbf{X} \in \Re^{n\times n}$ *and* $\mathbf{Y}_{ij} = \mathbf{Y}_{ij}^T \in \Re^{(n+l+m)\times(n+l+m)}$, *and pre-defined weighting matrix* $0 \leq \mathbf{W} \in \Re^{(n+l+m)\times(n+l+m)}$ *such that the following LMIs are satisfied:*

$$\begin{bmatrix} \alpha\mathbf{I} & \mathbf{I} \\ \mathbf{I} & \mathbf{X} \end{bmatrix} > 0;$$

$$\mathbf{Y}_{ij} > 0, \forall\, i, j;$$

$$\mathbf{Y}_{ij} > \mathbf{H}_{ij}, \forall\, i, j;$$

$$\sum_{i=1}^{p}\sum_{j=1}^{c}\left((\delta_{iji_1i_2\cdots i_nk} + \Delta\underline{h}_{ij})\mathbf{H}_{ij} + (\Delta\overline{h}_{ij} - \Delta\underline{h}_{ij})\mathbf{Y}_{ij}\right) < 0,$$
$$\forall\, i, j, k, i_1, i_2, \cdots, i_n$$

where $\mathbf{Q}_{ij} = \mathbf{A}_i\mathbf{X} + \mathbf{X}\mathbf{A}_i^T + \mathbf{B}_i\mathbf{N}_j + \mathbf{N}_j^T\mathbf{B}_i^T$; $\mathbf{H}_{ij} = \begin{bmatrix} \mathbf{Q}_{ij} & \mathbf{T}_{ij}^T \\ \mathbf{T}_{ij} & \mathbf{W}^{-1} \end{bmatrix}$; $\mathbf{T}_{ij} = \begin{bmatrix} \mathbf{X} \\ \mathbf{C}_i\mathbf{X} \\ \mathbf{N}_j \end{bmatrix}$; $\delta_{iji_1i_2\cdots i_nk}$ *is a sample point of the original membership function* $h_{ij}(\mathbf{x})$ *at a chosen point* $\mathbf{x}$; $\Delta\underline{h}_{ij}$ *and* $\Delta\overline{h}_{ij}$ *are constant scalars satisfying* $\Delta\underline{h}_{ij} \leq h_{ij}(\mathbf{x}) - \hat{h}_{ij}(\mathbf{x}) \leq \Delta\overline{h}_{ij}$ *for all* i *and* j; *and the feedback gain is given as* $\mathbf{G}_j = \mathbf{N}_j\mathbf{X}^{-1}$ *for all* j.

Remark 4.6. *The problem of minimizing the value of* α *subject to the stability conditions in Theorems 4.1 and 4.2 can be formulated as a a generalized eigenvalue problem that the solution can be solved numerically, say, using existing scientific engineering software package such as MATLAB.*

4.4 Simulation Examples

A simulation example is given to verify the analysis results in terms of stability and performance. A 3-rule T-S fuzzy model inspired from [80] in the form of (2.5) is considered where the system, input and output matrices are chosen as $\mathbf{A}_1 = \begin{bmatrix} 1.59 & -7.29 \\ 0.01 & 0 \end{bmatrix}$, $\mathbf{A}_2 = \begin{bmatrix} 0.02 & -4.64 \\ 0.35 & 0.21 \end{bmatrix}$, $\mathbf{A}_3 = \begin{bmatrix} -3.25 & -4.33 \\ 0 & -0.05 \end{bmatrix}$, $\mathbf{B}_1 = \begin{bmatrix} 1 \\ 0 \end{bmatrix}$, $\mathbf{B}_2 = \begin{bmatrix} 8 \\ 0 \end{bmatrix}$, $\mathbf{B}_3 = \begin{bmatrix} 4 \\ -1 \end{bmatrix}$, $\mathbf{C}_1 = \begin{bmatrix} 1.21 & -3.65 \end{bmatrix}$, $\mathbf{C}_2 = \begin{bmatrix} 3.15 & 6.37 \end{bmatrix}$, $\mathbf{C}_3 = \begin{bmatrix} -2.25 & 1.66 \end{bmatrix}$, $\mathbf{x} = [x_1 \quad x_2]^T$. The membership functions are chosen as follows.

$$w_1(x_1) = \mu_{M_1^1}(x_1) = \begin{cases} 1 & \text{for } x_1 < -10 \\ \frac{-x_1+2}{12} & \text{for } -10 \leq x_1 \leq 2 \\ 0 & \text{for } x_1 > 2 \end{cases}; \tag{4.25}$$

$$w_2(x_1) = \mu_{M_1^2}(x_1) = 1 - w_1(x_1) - w_3(x_1); \tag{4.26}$$

$$w_3(x_1) = \mu_{M_1^3}(x_1) = \begin{cases} 0 & \text{for } x_1 < -2 \\ \frac{x_1+2}{12} & \text{for } -2 \leq x_1 \leq 10 \\ 1 & \text{for } x_1 > 10 \end{cases}. \tag{4.27}$$

The 3-rule T-S fuzzy model is obtained as follows:

$$\dot{\mathbf{x}} = \sum_{i=1}^{3} w_i(x_1)(\mathbf{A}_i\mathbf{x} + \mathbf{B}_i u) \tag{4.28}$$

and its output is obtained as

$$y = \sum_{i=1}^{3} w_i(x_1)\mathbf{C}_i\mathbf{x}. \tag{4.29}$$

We consider a 2-rule fuzzy controller in the form of (4.2) is employed to close the feedback loop. The membership functions of the fuzzy controller are chosen as follows

$$m_1(x_1) = \mu_{N_1^1}(x_1) = 1 - \frac{1}{e^{\frac{-x_1}{2}}}; \tag{4.30}$$

$$m_2(x_1) = \mu_{N_1^2}(x_1) = 1 - m_1(x_1). \tag{4.31}$$

The 2-rule fuzzy control is obtained as follows:

$$u = \sum_{j=1}^{2} m_j(x_1)\mathbf{G}_j\mathbf{x}. \tag{4.32}$$

Unlike the fuzzy controller using PDC design, the fuzzy controller uses different number of rules and shape of membership functions different from those of the T-S fuzzy model.

In order to investigate the impact of the weighting matrix on different signals, namely the system states $\mathbf{x}$, the system outputs $\mathbf{y}$ and the control signals $\mathbf{u}$, the weighting matrix $\mathbf{W}$ is chosen as shown in Remark 4.2. As the off-diagonal block entries of $\mathbf{W}$ are all set as zero, so that the mutual influence between $\mathbf{x}$, $\mathbf{y}$ and $\mathbf{u}$ are eliminated. The influence from the weighting matrices $\mathbf{W}_x$, $\mathbf{W}_y$ and $\mathbf{W}_u$ to the system states $\mathbf{x}$, the system outputs $\mathbf{y}$ and the control signals $\mathbf{u}$, respectively, is more significant.

In this simulation, the system is tested by applying different weighting matrices $\mathbf{W}_x$, $\mathbf{W}_y$ and $\mathbf{W}_u$ as given in Table 4.1 that we take 1 as the reference and 0.01/100 as small/large value for the weighting matrices resulting in 9 cases in total. For cases 1 to 3, we only change $\mathbf{W}_x$ but keep $\mathbf{W}_y$ and $\mathbf{W}_u$ unchanged to investigate

how $\mathbf{W}_x$ influences the system states in particular x_1. Similarly, for cases 4 to 6, we only change $\mathbf{W}_y$ but keep $\mathbf{W}_x$ and $\mathbf{W}_u$ unchanged to investigate how $\mathbf{W}_y$ influences the system output y. For cases 7 to 9, we only change $\mathbf{W}_u$ but keep $\mathbf{W}_x$ and $\mathbf{W}_y$ unchanged to investigate how $\mathbf{W}_u$ influences the control signal u.

Table 4.1: Weighting matrices $\mathbf{W}_x$, $\mathbf{W}_y$ and $\mathbf{W}_u$ for the 9 cases.

Case	$\mathbf{W}_x$	$\mathbf{W}_y$	$\mathbf{W}_u$
1	$\begin{bmatrix} 0.01 & 0 \\ 0 & 1 \end{bmatrix}$	1	1
2	$\begin{bmatrix} 1 & 0 \\ 0 & 1 \end{bmatrix}$	1	1
3	$\begin{bmatrix} 100 & 0 \\ 0 & 1 \end{bmatrix}$	1	1
4	$\begin{bmatrix} 1 & 0 \\ 0 & 1 \end{bmatrix}$	0.01	1
5	$\begin{bmatrix} 1 & 0 \\ 0 & 1 \end{bmatrix}$	1	1
6	$\begin{bmatrix} 1 & 0 \\ 0 & 1 \end{bmatrix}$	100	1
7	$\begin{bmatrix} 1 & 0 \\ 0 & 1 \end{bmatrix}$	1	0.01
8	$\begin{bmatrix} 1 & 0 \\ 0 & 1 \end{bmatrix}$	1	1
9	$\begin{bmatrix} 1 & 0 \\ 0 & 1 \end{bmatrix}$	1	100

To apply Theorem 4.2, we need to defined the PLMFs as in (4.17). As the membership functions of both T-S fuzzy model and fuzzy controller depends on x_1, the PLMFs can be constructed by considering only x_1. Considering $x_1 \in [-10, 10]$, δ_{iji_1k} is set as $h_{ij}(x_1)$ by considering the sample points of x_1 at $\{-10, -9.5, \ldots, 9.5, 10\}$, e.g., $\delta_{iji_11} = h_{ij}(-10)$, $\delta_{iji_12} = h_{ij}(-9.5)$ and so on. The function $v_{11k}(x_1) = \frac{x_1 - \underline{x}_{1k}}{\overline{x}_{1k} - \underline{x}_{1k}}$ and $v_{12k}(x_1) = 1 - v_{11k}(x_1)$ where $\overline{x}_{1k}$ and $\underline{x}_{1k}$ denote the lower and upper end points of x_1 at the k-th region, e.g., $\overline{x}_{1k} = -10$ and $\underline{x}_{1k} = -9.5$ when $k = 1$, $\overline{x}_{1k} = -9.5$ and $\underline{x}_{1k} = -9$ when $k = 2$ and so on. It should be noted that $v_{11k}(x_1) = 0$ and $v_{12k}(x_1) = 0$ when x_1 is outside the k-th region. According to the chosen original membership functions and PLMFs, it is found numerically that $\Delta\underline{h}_{11} = \Delta\underline{h}_{32} = -2.4426 \times 10^{-3}$, $\Delta\underline{h}_{12} = \Delta\underline{h}_{31} = -6.7708 \times 10^{-4}$, $\Delta\underline{h}_{21} = \Delta\underline{h}_{22} = -1.7826 \times 10^{-3}$, $\Delta\overline{h}_{11} = \Delta\overline{h}_{32} = 1.7839 \times 10^{-3}$, $\Delta\overline{h}_{12} = \Delta\overline{h}_{31} = 1.3139 \times 10^{-3}$, $\Delta\overline{h}_{21} = \Delta\overline{h}_{22} = 2.4622 \times 10^{-3}$ satisfying the inequality. (4.21). For comparison

purposes, we employ Theorem 4.1 to check the system stability. However, no feasible solution is found which indicates that the stability conditions in Theorem 2 are more relaxed thanks to the stability analysis using the PLMFs.

From the above settings, Theorem 4.2 is employed to check the system stability and determine the feedback gains. Table 4.2 tabulates the feedback gains $\mathbf{G}_j$ and $\mathbf{X}$ for the 9 cases. The 9 fuzzy controllers are employed to stabilize the T-S fuzzy model. The time responses of x_1, x_2, y and u are shown in Figs. 4.1 to 4.12. It can be seen from the figures that all fuzzy controllers are able to stabilize the T-S fuzzy model that the system states x_1 and x_2 approach the origin.

To facilitate comparison among cases, we define the following performance indexes J_{x_1}, J_y and J_u which are the integral of squared signals.

$$J_{x_1} = \int_t^\infty {x_1}^T x_1 dt = \int_t^\infty {x_1}^2 dt \tag{4.33}$$

$$J_y = \int_t^\infty y^T y dt = \int_t^\infty {y_1}^2 dt \tag{4.34}$$

$$J_u = \int_t^\infty u^T u dt = \int_t^\infty u^2 dt \tag{4.35}$$

A smaller value of performance index indicates a smaller consumption implying a better performance. Table 4.3 tabulates J_{x_1}, J_y and J_u for the 9 cases in Table 4.1. In cases 1 to 3, the cost J_{x_1} decreases (increases) when placing heavier (lighter) weight on x_1. Referring to Figs. 4.1 to 4.4, the effect on different weights on x_1 can be seen that the response of state x_1 demonstrates a faster (slower) transient response with shorter (longer) settling time and smaller (larger) steady-state error with the increase (decrease) of weight on x_1. In cases 4 to 6, we place different weights on y. It can be seen from Table 4.1 that cost J_y decreases (increases) when placing heavier (lighter) weight on $\mathbf{y}$. Referring to Figs. 4.5 to 4.8, it demonstrates that a faster (slower) transient response with shorter (longer) settling time and smaller (larger) steady-state error with the increase (decrease) of weight on y. Similarly, in cases 7 to 9, we place different weights on u to investigate how it is influenced. It is found that the cost J_u decreases (increases) when placing heavier (lighter) weight on u. Furthermore, Figs. 4.9 to 4.12 shows that a smaller (larger) control signal is required to stabilize the T-S fuzzy model corresponding to a heavier (lighter) weight on u.

In addition, among the three system indexes considered in weighting matrix $\mathbf{W}$, namely $\mathbf{x}$, $\mathbf{y}$, and $\mathbf{u}$, if only consider two of them, for example $\mathbf{W}_x$ and $\mathbf{W}_u$ or $\mathbf{W}_y$ and $\mathbf{W}_u$, theoretically it means less conservativeness when searching for the

feasible solutions for controller which implies a better system performance with lower index cost J. However, according to further simulation results (not included in this thesis), the system performance improvement under this assumption is very limited compared with three indexes in weighting matrix $\mathbf{W}$. Therefore, in order to keep integrity on the consideration of system indexes, the three indexes $\mathbf{x}$, $\mathbf{y}$, and $\mathbf{u}$ are all included in the stability analysis in this research.

Through this example, we can conclude that Theorem 4.2 offers relaxed stability conditions using the PLMFs in the stability analysis. Furthermore, with the consideration of cost function in the stability analysis, it offers an effective way to realize the system performance improvement and the cost control of system index.

4.5 Conclusion

In this chapter, the T-S FMB control system equipped with different fuzzy rules of model and controller is investigated in terms of both stability and performance based on Lyapunov theory. In addition, the information of membership function of T-S FMB control systems has been included into the analysis through a PLMFs approach to further relax the stability conditions. Furthermore, the weighted cost function is introduced into the analysis to improve the system performance by adjusting the weight of cost index and suppress the system cost within the certain range of requirement. The stability conditions are derived in terms of LMIs and solved in the simulation examples to show the effectiveness of the proposed approach.

Table 4.2: Feedback gains $\mathbf{G}_j$ for the 9 cases.

Case	$\mathbf{G}_j$	$\mathbf{X}$
1	$\mathbf{G}_1 = \begin{bmatrix} -7.1875 & -2.0128 \times 10^1 \end{bmatrix}$ $\mathbf{G}_2 = \begin{bmatrix} 2.2165 & 1.1649 \times 10^1 \end{bmatrix}$	$\begin{bmatrix} 6.6355 \times 10^{-3} & -6.1887 \times 10^{-4} \\ -6.1887 \times 10^{-4} & 1.4083 \times 10^{-4} \end{bmatrix}$
2	$\mathbf{G}_1 = \begin{bmatrix} -7.2042 & -2.0077 \times 10^1 \end{bmatrix}$ $\mathbf{G}_2 = \begin{bmatrix} 2.2159 & 1.1600 \times 10^1 \end{bmatrix}$	$\begin{bmatrix} 6.0729 \times 10^{-3} & -5.6668 \times 10^{-4} \\ -5.6668 \times 10^{-4} & 1.2963 \times 10^{-4} \end{bmatrix}$
3	$\mathbf{G}_1 = \begin{bmatrix} -7.6533 & -2.0301 \times 10^1 \end{bmatrix}$ $\mathbf{G}_2 \begin{bmatrix} 2.2846 & 1.1299 \times 10^1 \end{bmatrix}$	$\begin{bmatrix} 6.2224 \times 10^{-4} & -5.9669 \times 10^{-5} \\ -5.9669 \times 10^{-5} & 1.4643 \times 10^{-5} \end{bmatrix}$
4	$\mathbf{G}_1 = \begin{bmatrix} -7.1438 & -1.9815 \times 10^1 \end{bmatrix}$ $\mathbf{G}_2 = \begin{bmatrix} 2.1967 & 1.1502 \times 10^1 \end{bmatrix}$	$\begin{bmatrix} 8.7972 \times 10^{-3} & -8.1453 \times 10^{-4} \\ -8.1453 \times 10^{-4} & 1.8623 \times 10^{-4} \end{bmatrix}$
5	$\mathbf{G}_1 = \begin{bmatrix} -7.2042 & -2.0077 \times 10^1 \end{bmatrix}$ $\mathbf{G}_2 = \begin{bmatrix} 2.2159 & 1.1600 \times 10^1 \end{bmatrix}$	$\begin{bmatrix} 6.0729 \times 10^{-3} & -5.6668 \times 10^{-4} \\ -5.6668 \times 10^{-4} & 1.2963 \times 10^{-4} \end{bmatrix}$
6	$\mathbf{G}_1 = \begin{bmatrix} -7.2999 & -2.0494 \times 10^1 \end{bmatrix}$ $\mathbf{G}_2 = \begin{bmatrix} 2.2447 & 1.1755 \times 10^1 \end{bmatrix}$	$\begin{bmatrix} 1.8854 \times 10^{-4} & -1.7815 \times 10^{-5} \\ -1.7815 \times 10^{-5} & 4.0800 \times 10^{-6} \end{bmatrix}$
7	$\mathbf{G}_1 = \begin{bmatrix} -7.3229 & -2.0407 \times 10^1 \end{bmatrix}$ $\mathbf{G}_2 = \begin{bmatrix} 2.2455 & 1.1690 \times 10^1 \end{bmatrix}$	$\begin{bmatrix} 1.4841 \times 10^{-2} & -1.4005 \times 10^{-3} \\ -1.4005 \times 10^{-3} & 3.2333 \times 10^{-4} \end{bmatrix}$
8	$\mathbf{G}_1 = \begin{bmatrix} -7.2042 & -2.0077 \times 10^1 \end{bmatrix}$ $\mathbf{G}_2 = \begin{bmatrix} 2.2159 & 1.1600 \times 10^1 \end{bmatrix}$	$\begin{bmatrix} 6.0729 \times 10^{-3} & -5.6668 \times 10^{-4} \\ -5.6668 \times 10^{-4} & 1.2963 \times 10^{-4} \end{bmatrix}$
9	$\mathbf{G}_1 = \begin{bmatrix} -7.3032 & -2.0649 \times 10^1 \end{bmatrix}$ $\mathbf{G}_2 = \begin{bmatrix} 2.2667 & 1.1893 \times 10^1 \end{bmatrix}$	$\begin{bmatrix} 9.7268 \times 10^{-5} & -9.1494 \times 10^{-6} \\ -9.1494 \times 10^{-6} & 2.0800 \times 10^{-6} \end{bmatrix}$

Table 4.3: Costs J, J_{x_1}, J_y and J_u for the 9 cases.

Case	J	J_{x_1}	J_y	J_u
1	2.5571×10^2	1.2001×10^1	2.4745×10^2	8.0823
2	2.6746×10^2	1.1999×10^1	2.4730×10^2	8.0972
3	1.4423×10^3	1.1895×10^1	2.4411×10^2	8.6622
4	2.2564×10^1	1.2021×10^1	2.4769×10^2	8.0079
5	2.6746×10^2	1.1999×10^1	2.4730×10^2	8.0972
6	2.4691×10^4	1.1968×10^1	2.4671×10^2	8.2355
7	2.5861×10^2	1.1964×10^1	2.4650×10^2	8.2608
8	2.6746×10^2	1.1999×10^1	2.4730×10^2	8.0972
9	1.0875×10^3	1.1939×10^1	2.4667×10^2	8.2883

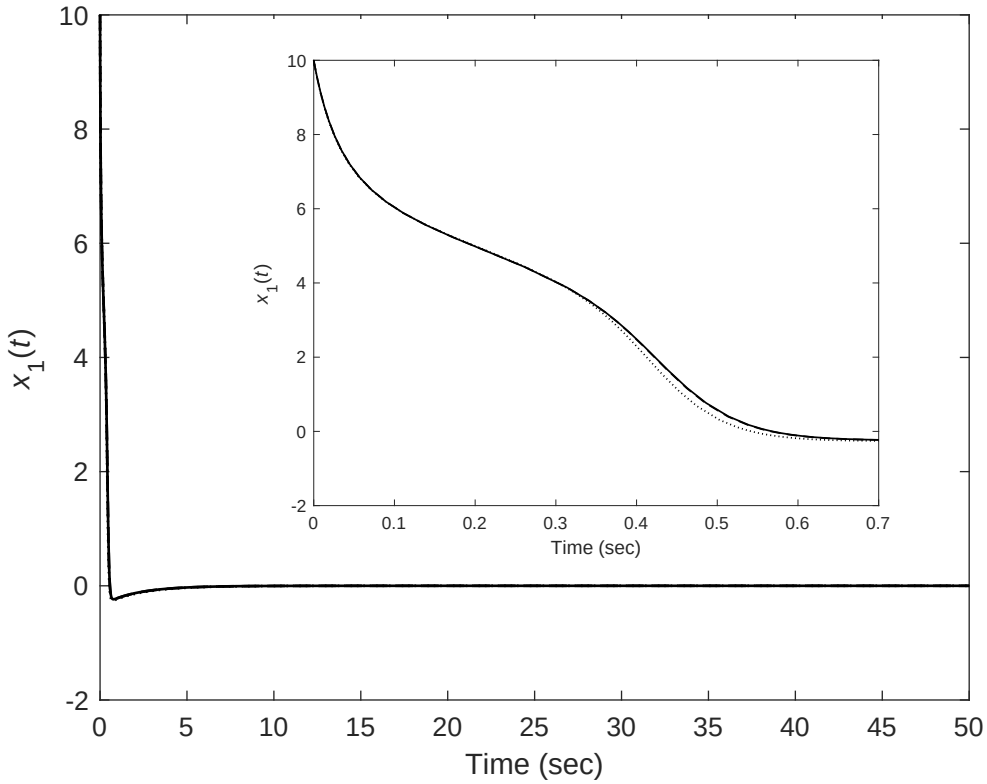

Figure 4.1: Response of state $x_1(t)$ for Cases 1 (solid line), 2 (dashed line) and 3 (dotted line).

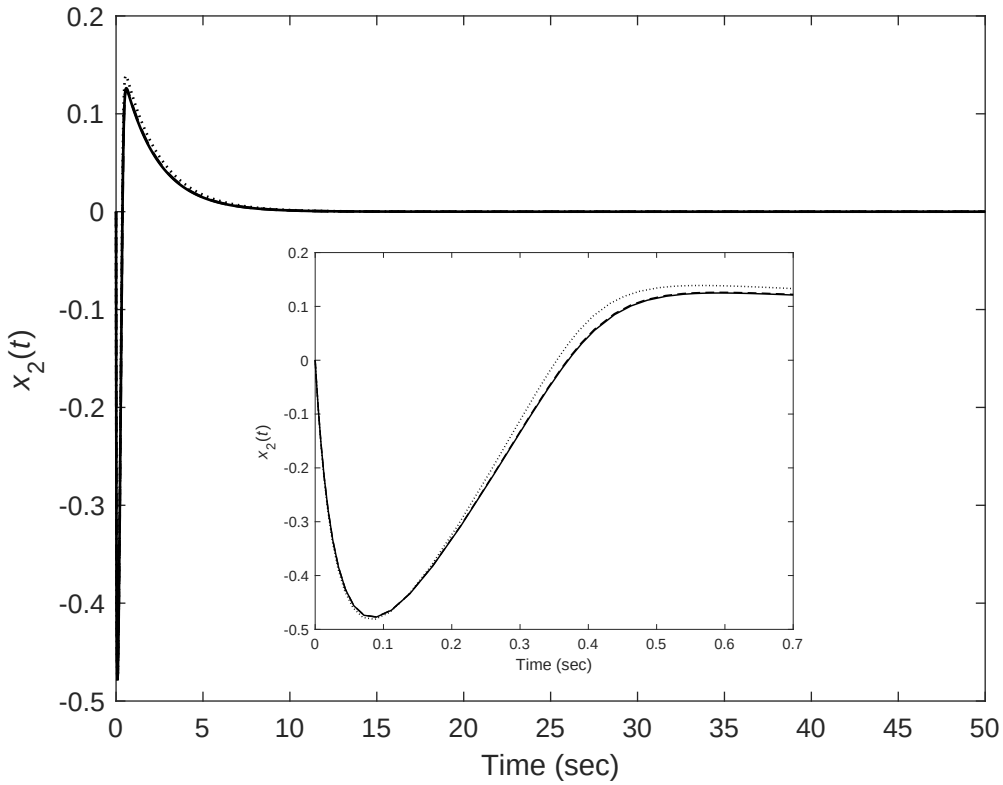

Figure 4.2: Response of state $x_2(t)$ for Cases 1 (solid line), 2 (dashed line) and 3 (dotted line).

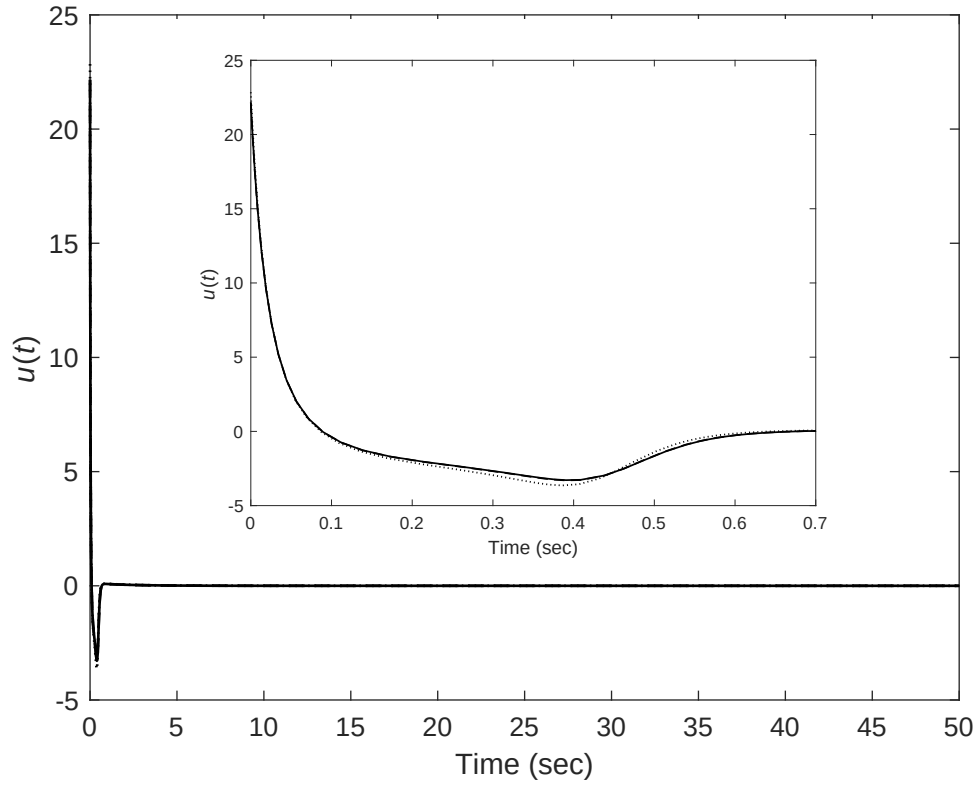

Figure 4.3: Control signal $u(t)$ for Cases 1 (solid line), 2 (dashed line) and 3 (dotted line).

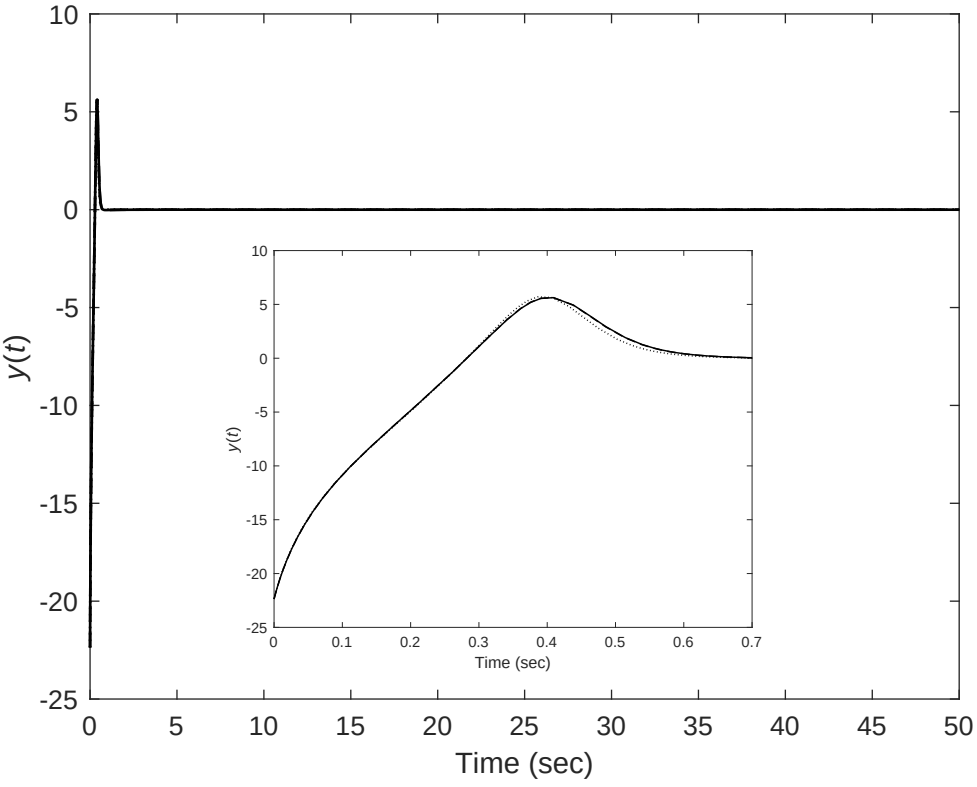

Figure 4.4: Response of output $y(t)$ for Cases 1 (solid line), 2 (dashed line) and 3 (dotted line).

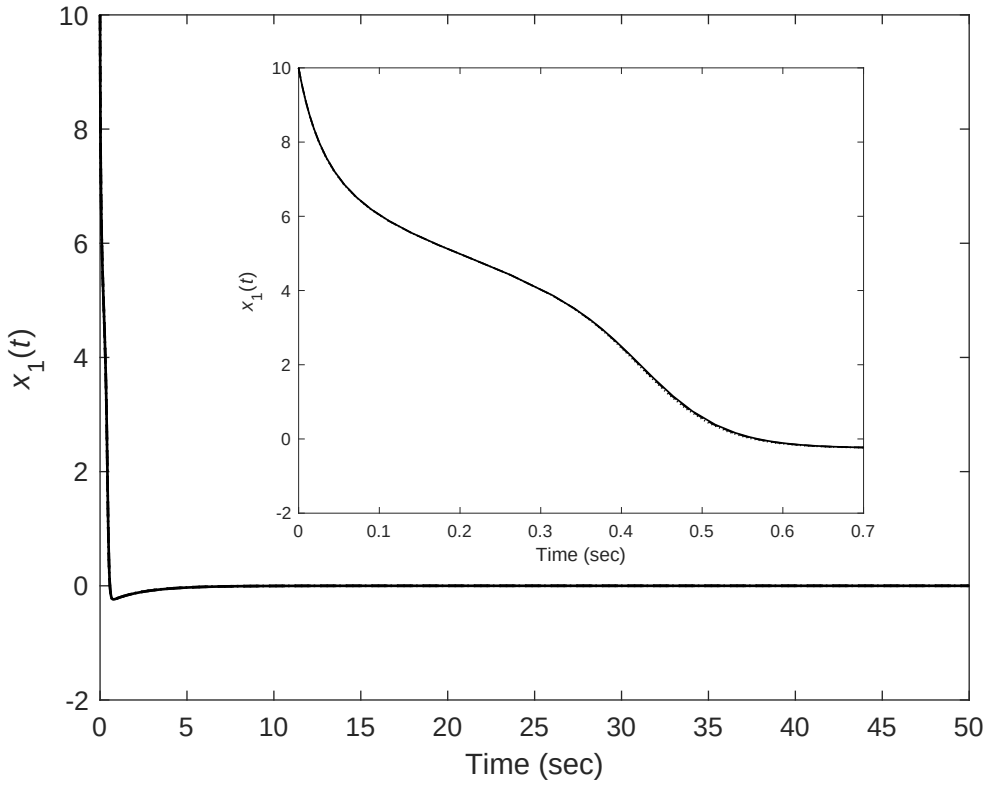

Figure 4.5: Response of state $x_1(t)$ for Cases 4 (solid line), 5 (dashed line) and 6 (dotted line).

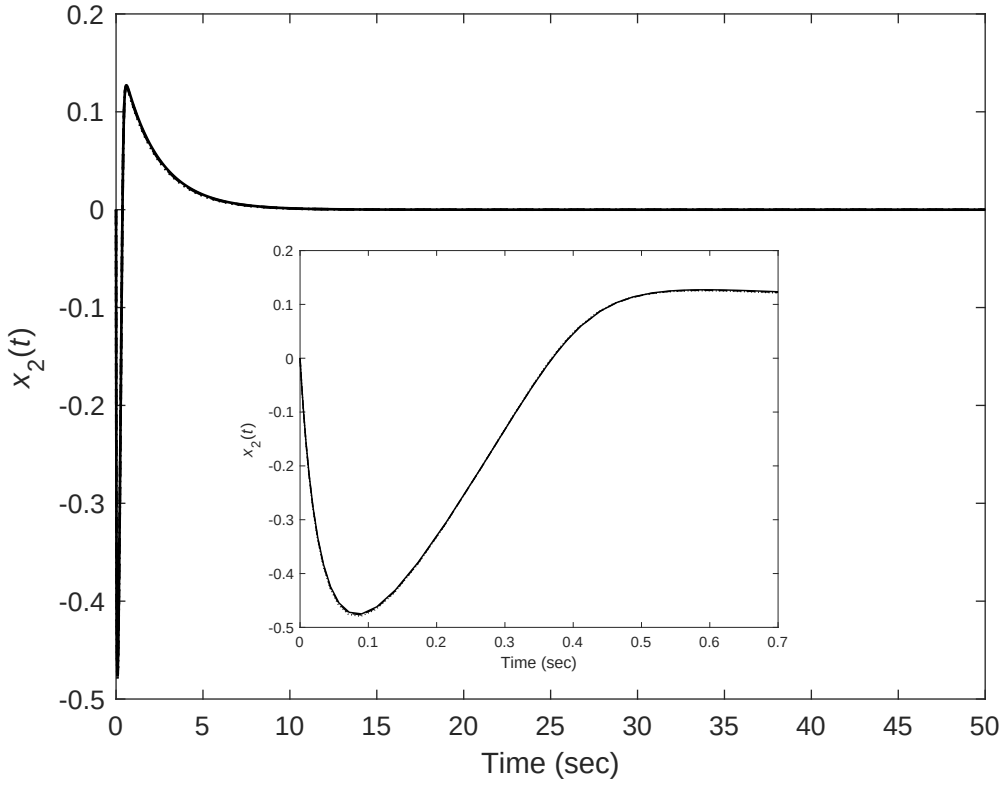

Figure 4.6: Response of state $x_2(t)$ for Cases 4 (solid line), 5 (dashed line) and 6 (dotted line).

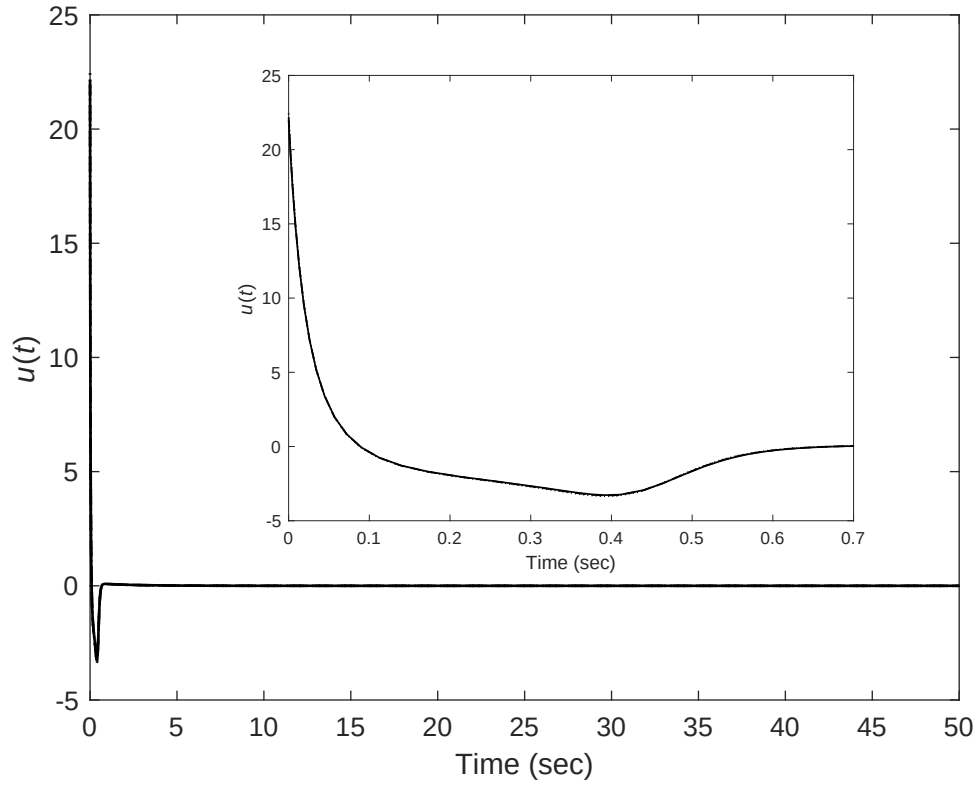

Figure 4.7: Control signal $u(t)$ for Cases 4 (solid line), 5 (dashed line) and 6 (dotted line).

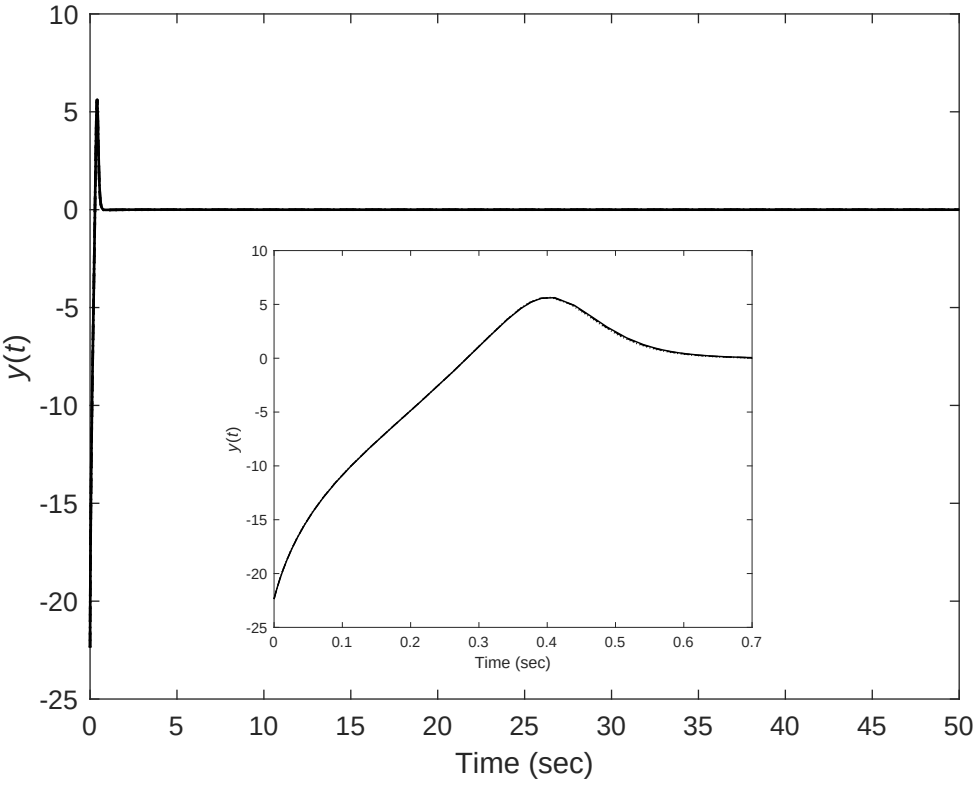

Figure 4.8: Response of output $y(t)$ for Cases 4 (solid line), 5 (dashed line) and 6 (dotted line).

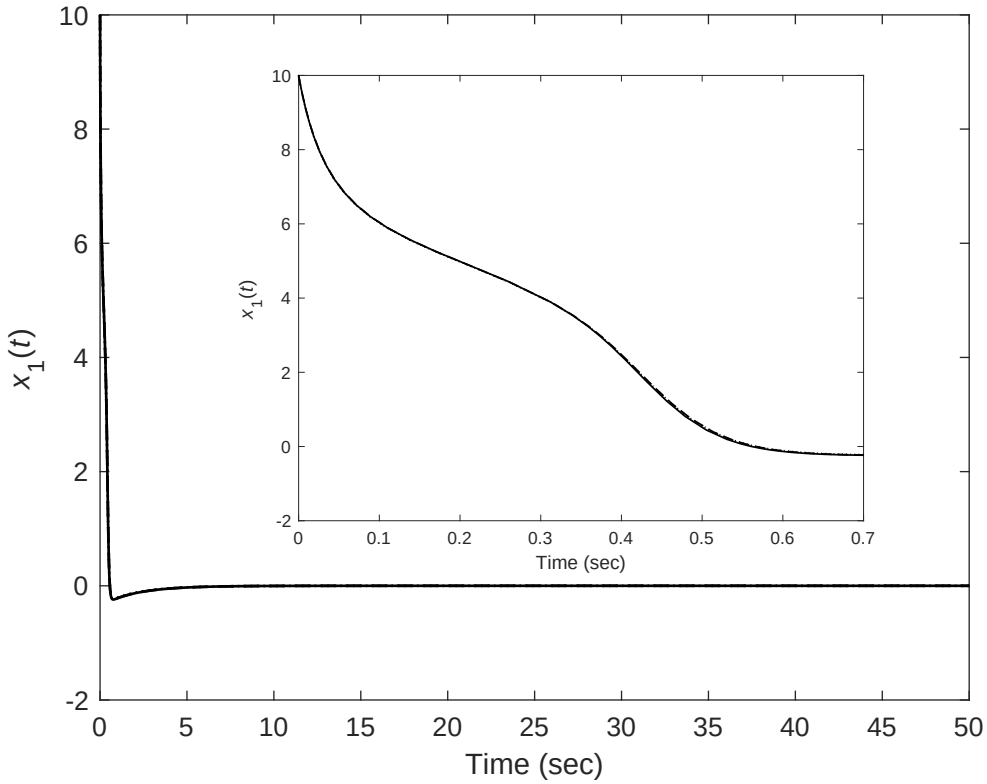

Figure 4.9: Response of state $x_1(t)$ for Cases 7 (solid line), 8 (dashed line) and 9 (dotted line).

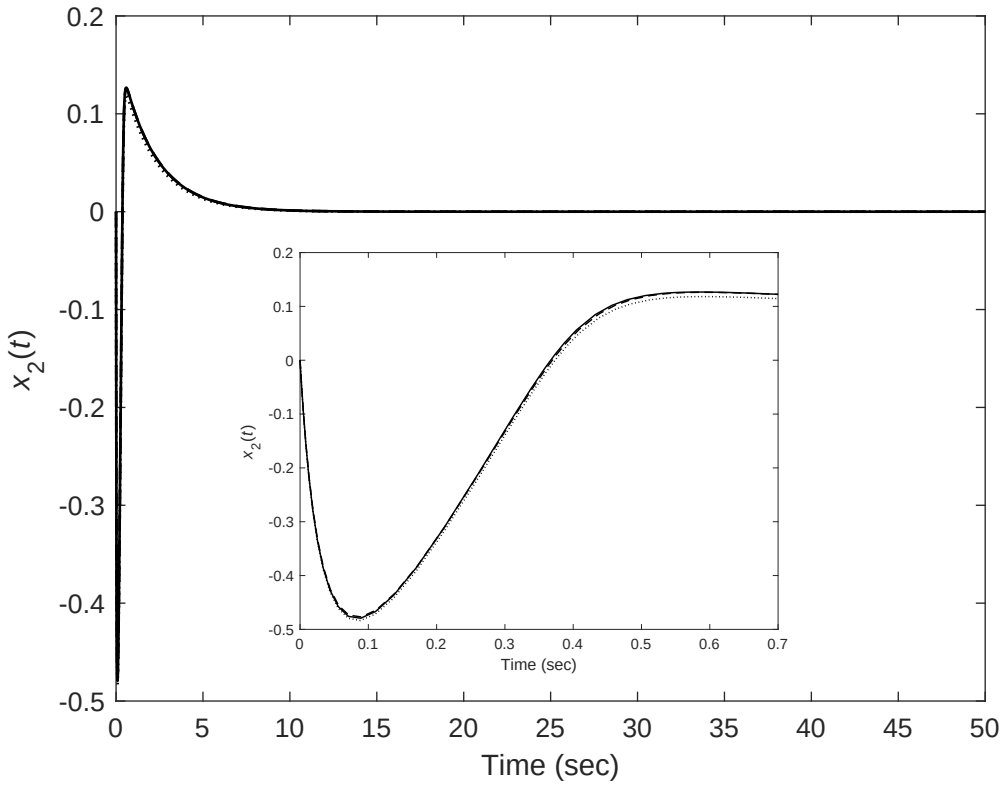

Figure 4.10: Response of state $x_2(t)$ for Cases 7 (solid line), 8 (dashed line) and 9 (dotted line).

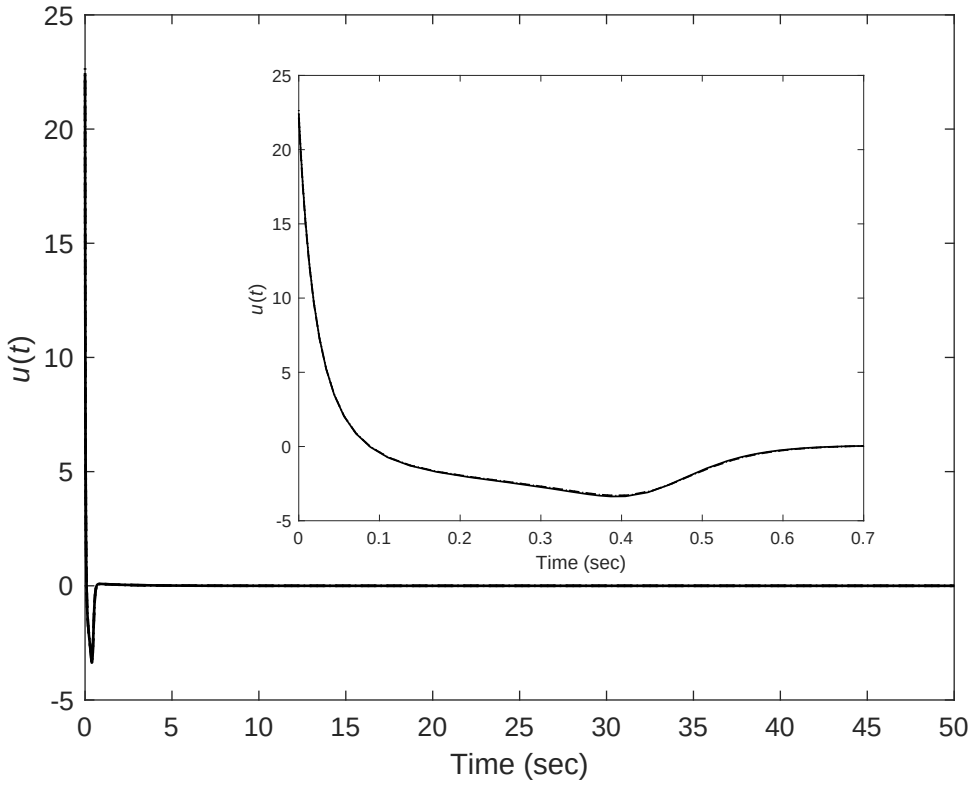

Figure 4.11: Control signal $u(t)$ for Cases 7 (solid line), 8 (dashed line) and 9 (dotted line).

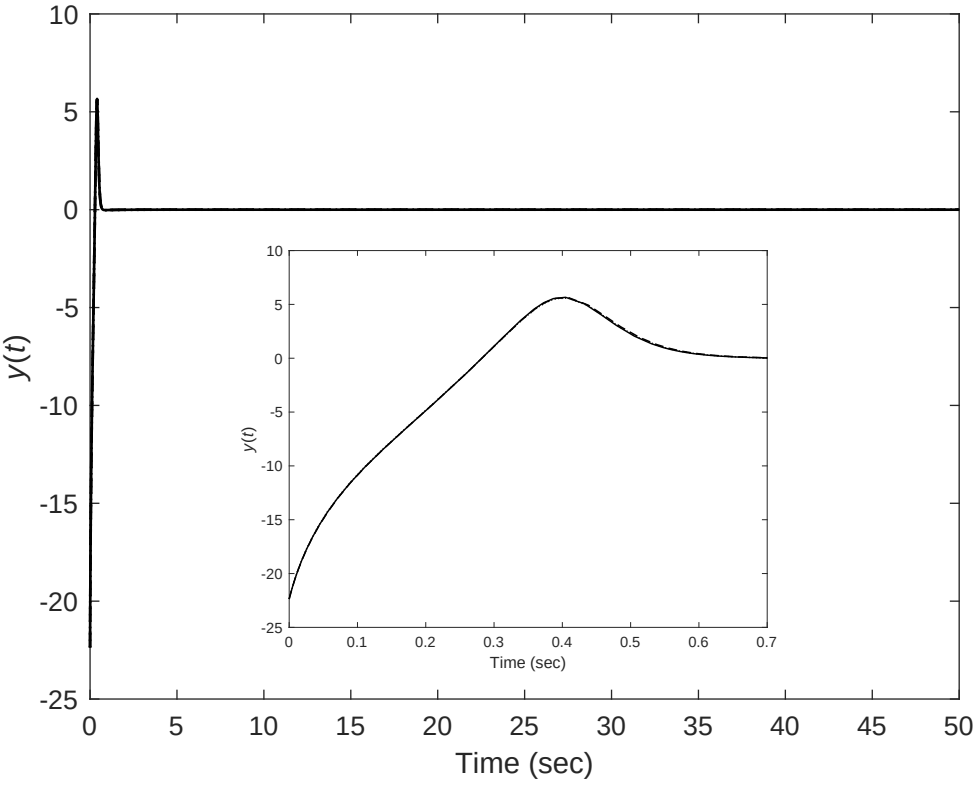

Figure 4.12: Response of output $y(t)$ for Cases 7 (solid line), 8 (dashed line) and 9 (dotted line).

Chapter 5

Applications of Fuzzy Logic and Fuzzy-Model-Based Control to a Continuum Manipulator

In this chapter, the dynamic model of continuum manipulator is used as an example of applications for the implementation of fuzzy logic and FMB control methods. The continuum manipulator considered in this chapter possess both bending and contractile capabilities. Based on curve geometry under the Frenet frame, the kinematics of continuum manipulator can be established. Then, the kinetic energy and potential energy are calculated as the integration of the energies in each slice perpendicular to the backbone. Thus, the dynamic model of continuum manipulator can be developed by applying the Euler-Lagrangian equation of motion to the obtained kinetic and potential energies. Based on the dynamic model of continuum manipulator, two nonlinear control methods, namely inverse dynamic control and sliding mode control, are implemented to realize the tracking control on bending and contractile action of the manipulator. In order to improve the system performance, the fuzzy logic is applied to traditional sliding mode control method proposing fuzzy sliding mode control which significantly alleviates the chattering problem in the output performance in sliding mode control method. Before applying FMB control methods, the nonlinear dynamic model of robot manipulator has to be transformed into fuzzy model with necessary simplifications. The fuzzy model of two-link rigid manipulator is developed first by using sector nonlinearity approach. The polynomial fuzzy model of continuum manipulator is derived with much more complex calculation where advanced computation techniques are needed. Simulation process has been produced in MATLAB Simulink environment for the verification of effectiveness and comparison purposes.

5.1 Introduction

The robot manipulator has now been largely developed and utilized to improve human's living convenience and productive efficiency, not only in manufacture industry but also, just to name a few, in agriculture [116], education [117] and medical industry [118]. Inspired by natural biological features, such as elephant trunks and squid tentacles, the first continuum robot manipulator, called "Scripps Tensor Arm", was invented by Anderson in 1968 [119]. Compared with conventional rigid-link manipulators, the continuum manipulator, also known as snake-like robots, has its unique compliant structure with high number of degrees of freedom. Due to its strong manoeuvrability, the continuum manipulators are capable of working in various special environmental conditions where conventional rigid-link robots may be incompetent. Therefore, in recent years, more and more attention has been drawn on the development of continuum manipulators. With the booming research in this field, continuum manipulators have been developed for many industrial and medical applications [120].

One of the notable continuum manipulator – Sensei X robotic catheter system – manufactured by Hansen Medical Inc. [121], gives a great contribution to the surgical operation. By using Sensei X continuum robotic device, physicians are able to accurately control the tip position of the curving manipulator, such that the surgical tools can reach the targets through a smaller incision compared to rigid-link devices. Motivated by the stunning performance of Sensei X robotic catheter system, many researchers have proposed relative analysis on the snake-like continuum robots.

In previous research, the dynamic characteristics and control strategies for rigid-link manipulators have been comprehensively studied [122]. Based on the knowledge of rigid-link manipulator model, the kinematics of a hyper-redundant manipulator was firstly presented by Chirikjian in [60] in 1994 and then extended in [61]. Straight after that, a study on dynamics of the hyper-redundant manipulator based on a modal model was published [62]. However, the hyper-redundant manipulator model established in the above papers were all treated as actuated by infinite numbers of motors. Thus, this dynamic model is derived in an approximated method and restricted within a small acting region. In 2002, Mochiyama and Suzuki proposed a more intuitive modelling method to study the cable-like hyper-flexible manipulators in [63] and [123]. The continuum manipulator was considered to be composed of infinite number of slices in 3D space and each slice was viewed as an infinitesimal-width rigid link. It established a general framework to study the arbitrary curve geometry of continuum and its kinematic features. However, the work is limited to a type of constant-length continuum manipulators which can not extend or contract the body. Based upon [63], Tatliciogku and Walker [124] further presented the dynamic model for the "Octarm" continuum manipulator which possesses both bending and extensibility. Then, in [125], the potential energy was taken into ac-

count for dynamic analysis. Recently, Walker wrote a review article about current research achievements on continuous backbone robot manipulators in [126], mainly concludes the aspects of design principles, kinematics, and dynamics.

After obtaining the dynamic model of continuum manipulator, control strategy is able to be conducted accordingly. In [122], fundamental control methods were presented for the conventional rigid-link robot manipulators, such as feedforward control and feedback linearisation strategies. In [127] and [128], researchers applied a control strategy to snake-like robot system dynamics, but the model was approximated as serial rigid-link robots. Kapadia provided a task-space control and sliding mode control based on the "Octarm" system dynamics in [129] and [130]. In [131], Shafiei combined sliding model control, fuzzy logic and neural network approaches for manipulator control. However, these methods are still applied to a rigid-link style robot.

In the respect of control strategies for robot manipulator, the sliding mode control has for long been recognized as an effective control method to deal with system uncertainties and external disturbances. As a complex and highly nonlinear system, the robot manipulator's parameters are decided by material, structure and payload, which means it could be difficult to guarantee the accuracy of obtained parameters. Therefore, sliding mode control becomes a useful technique to tackle control problems for robot manipulators. However, it is hard to use a systematic way to determine the sliding mode control feedback gains and sliding surface. Moreover, the sliding mode control may need feedback gains with high magnitude and discontinuous switching control signals in order to compensate the uncertainties and guarantee the system stability. This may cause chattering problem in control system which may deteriorate the system performance. Therefore, there must be a trade-off between system robustness and the attenuation of chattering problem.

One of the effective approaches to tackle chattering problem is by introducing saturation function to control signals [132]. Although the chattering problem can be addressed, this method may cause a steady-state error in the tracking control and the reduction of robustness. Another approach to dealing with chattering problem is to combine fuzzy logic theory to nonlinear control methods. Fuzzy logic control theory can solve complex and highly nonlinear control problems by designing its own fuzzy rules and membership functions such that the sliding mode controller can be more adaptive for tracking control problem.

Fuzzy sliding mode control method uses fuzzy logic to tune the control feedback gains adaptively such that the chattering problem can be tackled without losing system robustness. In [133], the fuzzy logic was used to implement on both unknown system dynamic model and control feedback gains, which obviously required large and complex computation process. [134] considered fuzzy sliding mode control to design the controller for a two degree-of-freedom rigid-link robot manipulator, while

[128] used fuzzy sliding mode control on a two-link robot manipulator. Although both of them successfully verify the effectiveness of fuzzy sliding mode control on solving chattering problem and reducing steady-state error, they are still limited on the models of rigid-link manipulators. [135] proposed parallel fuzzy inference system compensator to a continuum manipulator. However the feedback gains are decided only by the value of sliding surface s, which can be further improved.

5.2 Dynamic Model of Rigid Manipulator

As the technology improves, there are many types of robot manipulator model proposed for practical use, such as multi-link robot manipulators [136], continuum manipulators [137] and flexible robot manipulators [138]. In order to design the control system for the robot manipulator, it is necessary to obtain a mathematically expression of the dynamic model of robot manipulator. In this thesis, we construct the dynamic model of manipulator by applying kinetic energy and potential energy to Euler-Lagrangian equation of motion.

The two-link rigid robot manipulator shown in Fig. 5.1 is a classic and representative example to be studied, such that many other advanced dynamic models of robot manipulators can be investigated as its extensions, including the continuum manipulator. The research of continuum manipulator can be inspired from the process of deriving the dynamic model of two-link rigid manipulator. The length of links 1 and 2 are l_1 and l_2 respectively. The joint variables are the two angles, where $\mathbf{q} = \begin{bmatrix} \theta_1 & \theta_2 \end{bmatrix}^T$. Assume the mass centre of each link is at the middle weighted as m_1 and m_2. For calculation simplicity, let $a_1 = \frac{1}{2}l_1$ and $a_2 = \frac{1}{2}l_2$.

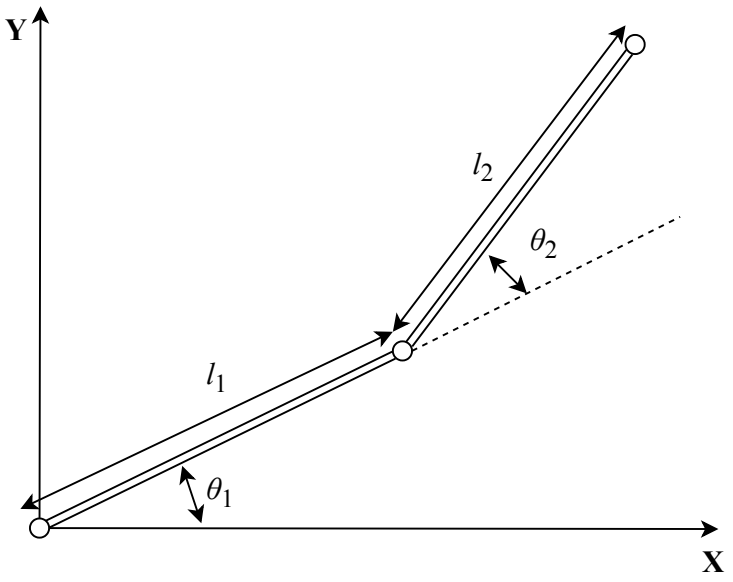

Figure 5.1: Two-link robot arm.

For link 1, the kinetic energy yields $K_1 = \frac{1}{2}m_1 a_1^2 \dot{\theta}^2$ and the potential energy

yields $P_1 = m_1 g a_1 \sin\theta_1$.

For link 2, the position of mass centre can be expressed by (x_2, y_2) where

$$x_2 = 2a_1 \cos\theta_1 + a_2 \cos(\theta_1 + \theta_2); \tag{5.1}$$

$$y_2 = 2a_1 \sin\theta_1 + a_2 \sin(\theta_1 + \theta_2). \tag{5.2}$$

Thus, the kinetic energy for link 2: $K_2 = \frac{1}{2} m_2 v_2^2 = \frac{1}{2} m_2 (\dot{x}_2^2 + \dot{y}_2^2)$ and the potential energy for link 2: $P_2 = m_2 g y_2$ can be obtained.

The Lagrangian operator for the entire arm can be written as

$$L = K - P = K_1 + K_2 - P_1 - P_2. \tag{5.3}$$

By presenting Euler-Lagrangian equation of motion in the following form

$$\frac{d}{dt}\frac{\partial L}{\partial \dot{q}} - \frac{\partial L}{\partial q} = \tau, \tag{5.4}$$

the dynamic function of two-link rigid manipulator is given as

$$\mathbf{M_r}(\mathbf{q})\ddot{\mathbf{q}} + \mathbf{C_r}(\mathbf{q}, \dot{\mathbf{q}})\dot{\mathbf{q}} + \mathbf{G_r}(\mathbf{q}) = \tau, \tag{5.5}$$

where $\mathbf{M_r}(\mathbf{q}) \in \mathbb{R}^{2\times 2}$ is the inertia matrix of two-link rigid manipulator, $\mathbf{C_r}(\mathbf{q}, \dot{\mathbf{q}}) \in \mathbb{R}^{2\times 2}$ is the centrifugal and Coriolis matrix, $\mathbf{G_r}(\mathbf{q}) \in \mathbb{R}^2$ is the gravitational matrix and $\tau \in \mathbb{R}^2$ is the force vector.

The detail of each matrix is presented as follows [122]:

$$\mathbf{M_r}(\mathbf{q}) = \begin{bmatrix} (m_1 + 4m_2)a_1^2 + m_2 a_2^2 + 4m_2 a_1 a_2 \cos\theta_2 & m_2 a_2^2 + 2m_2 a_1 a_2 \cos\theta_2 \\ m_2 a_2^2 + 2m_2 a_1 a_2 \cos\theta_2 & m_2 a_2^2 \end{bmatrix}; \tag{5.6}$$

$$\mathbf{C_r}(\mathbf{q}, \dot{\mathbf{q}}) = \begin{bmatrix} -2m_2 a_1 a_2 \dot{\theta}_2 \sin\theta_2 & -2m_2 a_1 a_2 (\dot{\theta}_1 + \dot{\theta}_2) \sin\theta_2 \\ 2m_2 a_1 a_2 \dot{\theta}_1 \sin\theta_2 & 0 \end{bmatrix}; \tag{5.7}$$

$$\mathbf{G_r}(\mathbf{q}) = \begin{bmatrix} (m_1 + 2m_2) g a_1 \cos\theta_1 + m_2 g a_2 \cos(\theta_1 + \theta_2) \\ m_2 g a_2 \cos(\theta_1 + \theta_2) \end{bmatrix}. \tag{5.8}$$

5.3 Kinematics of Continuum Manipulator

Based on the discussion of two-link rigid manipulator in previous section, the continuum manipulator can be considered with rigid-property slice σ of infinitesimal width and being perpendicular along the backbone curve. This methodology has been developed in [63] and [123]. The kinematic equations below are developed in the coordinate frames wherein the z-axis is tangent to the backbone.

The orientation matrix of the extended Frenet frame ${}^0\Phi(\sigma, t)$ at slice σ respec-

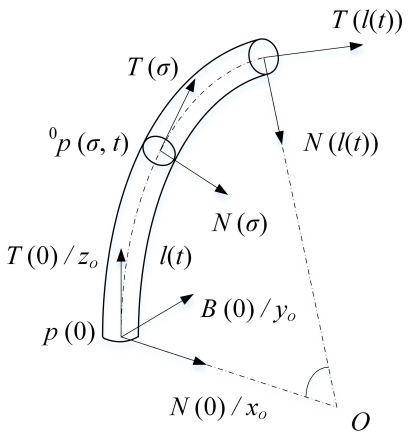

Figure 5.2: Diagram of a continuum manipulator bending geometry in 3D space with coordinate frames illustrated.

tive to the base frame $\{x_0y_0z_0\}$ which corresponds to the Frenet frame $\{NBT\}$, is expressed as follows

$$
{}^0\Phi(\sigma,t) = \begin{bmatrix} \cos(\sigma\kappa(\sigma,t)) & 0 & \sin(\sigma\kappa(\sigma,t)) \\ 0 & 1 & 0 \\ -\sin(\sigma\kappa(\sigma,t)) & 0 & \cos(\sigma\kappa(\sigma,t)) \end{bmatrix}. \tag{5.9}
$$

The change of the above orientation matrix along the backbone of a continuum manipulator can be characterized by [63], [123]

$$
\frac{\partial^0\Phi(\sigma,t)}{\partial\sigma} = {}^0\Phi(\sigma,t)a^{\times}(\sigma,t), \tag{5.10}
$$

where $a(\sigma,t) \in \mathbb{R}^3$ represents the frame rate vector at slice σ and $a^{\times}(\sigma,t) \in \mathbb{R}^{3\times3}$ is the product of $a(\sigma,t)$ after a linear operation. The details of $a(\sigma,t)$ and the corresponding linear operator $[\cdot]^{\times}$ are defined as follows

$$
a(\sigma,t) = \begin{bmatrix} 0 \\ \kappa(\sigma,t) \\ 0 \end{bmatrix}, \tag{5.11}
$$

$$
[i]^{\times} = \begin{bmatrix} 0 & -i_z & i_y \\ i_z & 0 & -i_x \\ -i_y & i_x & 0 \end{bmatrix}, \tag{5.12}
$$

where $i = \begin{bmatrix} i_x & i_y & i_z \end{bmatrix}^T \in \mathbb{R}^3$.

Therefore, we have

$$a^{\times}(\sigma,t)=\begin{bmatrix} 0 & 0 & \kappa(\sigma,t) \\ 0 & 0 & 0 \\ -\kappa(\sigma,t) & 0 & 0 \end{bmatrix}. \tag{5.13}$$

The position vector ${}^0p(\sigma,t)\in\mathbb{R}^3$ stands for the direction viewing from the origin $p(0)$ to the slice σ. By applying the orientation matrix, the position vector can be derived as

$${}^0p(\sigma,t)=\int_0^{\sigma}{}^0\Phi(\eta,t)e_z d\eta, \tag{5.14}$$

where $e_z:=\begin{bmatrix}0 & 0 & 1\end{bmatrix}^T$.

Then we define the orientation matrix at point η relating to ${}^0\Phi(\sigma,t)$ as [63], [123]

$${}^{\sigma}\Phi(\eta,t)={}^0\Phi^T(\sigma,t){}^0\Phi(\eta,t). \tag{5.15}$$

And also we define the position vector ${}^{\sigma}p(\eta,t)\in\mathbb{R}^3$, viewing from one slice σ to another slice η, as follows

$${}^{\sigma}p(\eta,t)={}^0\Phi^T(\sigma,t){}^0p(\eta,t). \tag{5.16}$$

Let $\theta(\sigma,t)\in\mathbb{R}^3$ be the internal variable vector, containing the contraction $l(\sigma,t)$, curvature $\kappa(\sigma,t)$ and direction angle $\alpha(\sigma,t)$ at slice σ. It can be written as

$$\theta(\sigma,t)=\begin{bmatrix} l(\sigma,t) \\ \kappa(\sigma,t) \\ \alpha(\sigma,t) \end{bmatrix}. \tag{5.17}$$

Based on the internal variable vector at σ, the extended axis matrix $\bar{A}(\theta(\sigma,t))\in\mathbb{R}^{6\times 2}$ is defined as follows. For more details regarding the axis matrix and the extended axis matrix, please refer to [63], [123].

$$\bar{A}(\theta(\sigma,t))=\begin{bmatrix} 0 & 0 & 1 & 0 & 0 & 0 \\ 0 & 0 & 0 & 0 & 1 & 0 \end{bmatrix}^T. \tag{5.18}$$

In the above development, we assume that the continuum manipulator has no torsion along the backbone. The internal variables are only defined in the bending plane. The convention utilized in this section are adopted from [63] and [123]. Equivalent results are also found in [124], but in different coordinate systems. We expect the work summarized above giving a more clarified illustration to the slice-based methodology for continuum dynamics.

5.4 Dynamic Model of Continuum Manipulator

In this section, the dynamic model of continuum manipulator is developed in the form of Euler-Lagrange equation of motion, where the kinetic and potential energies need to be obtained complying to the curved continuum manipulator.

5.4.1 Kinetic Energy

The kinetic energy $K(\sigma, t)$ of slice σ is expressed as follows

$$K(\sigma,t) = \frac{1}{2}m(\sigma)\frac{\partial p_c^T(\sigma,t)}{\partial t}\frac{\partial p_c(\sigma,t)}{\partial t} + \frac{1}{2}\omega(\sigma,t)^T I(\sigma)\omega(\sigma,t), \tag{5.19}$$

where $I(\sigma)$ and $m(\sigma)$ are the rotational inertia and translational inertia, respectively.

The angular velocity $\omega(\sigma, t)$ at slice σ can be calculated by

$$\omega(\sigma,t) = \int_0^\sigma {}^\sigma\Phi(\eta,t)\frac{\partial a}{\partial t}(\eta,t)d\eta. \tag{5.20}$$

Then, the kinetic energy $K(\sigma, t)$ can be rewritten as

$$\begin{aligned} K(\sigma,t) &= \frac{1}{2}v^T(\sigma,t)M(\sigma)v(\sigma,t) \\ &= \frac{1}{2}\int_0^\sigma\int_0^\sigma \frac{\partial\theta^T(\eta,t)}{\partial t}\bar{A}^T(\eta,t)Ad^T_{g(\sigma,\eta,t)}M(\sigma) \\ &\quad Ad_{g(\sigma,\xi,t)}\bar{A}(\xi,t)\frac{\partial\theta(\xi,t)}{\partial t}d\eta d\xi, \end{aligned} \tag{5.21}$$

where the adjoint matrix $Ad_{g(\sigma,\eta,t)} \in \mathbb{R}^{6\times6}$ in terms of rigid body transformation and the inertia matrix $M(\sigma) \in \mathbb{R}^{6\times6}$ at slice σ can be expressed as follows

$$Ad_{g(\sigma,\eta,t)} = \begin{bmatrix} {}^\sigma\Phi(\eta,t) & ({}^\sigma p^\times(\eta,t) - {}^\sigma p^\times(\sigma,t)){}^\sigma\Phi(\eta,t) \\ 0_{3\times3} & {}^\sigma\Phi(\eta,t) \end{bmatrix}, \tag{5.22}$$

$$M(\sigma) = \begin{bmatrix} m(\sigma)I_3 & -m(\sigma)\Delta p^\times(\sigma) \\ m(\sigma)\Delta p^\times(\sigma) & I(\sigma) \end{bmatrix}, \tag{5.23}$$

where $\Delta p(\sigma)$ means the distance between geometric center and center of mass at slice σ, which in our case is zero.

$I_3 \in \mathbb{R}^{3\times3}$ is the identity matrix and $I(\sigma) \in \mathbb{R}^{3\times3}$ is the inertial tensor of the slice which can be written as

$$I(\sigma) = \frac{mr^2}{4l(t)}\begin{bmatrix} 0 & 0 & 0 \\ 0 & 1 & 0 \\ 0 & 0 & 0 \end{bmatrix}. \tag{5.24}$$

Thus, the inertial matrix of slice σ can be written as

$$M(\sigma) = diag\{\frac{m}{l(t)}, \frac{m}{l(t)}, \frac{m}{l(t)}, 0, \frac{mr^2}{4l(t)}, 0\}. \tag{5.25}$$

Therefore, the total kinetic energy of continuum manipulator is calculated as

$$K(t) = \int_0^{l(t)} K(\sigma, t) d\sigma. \tag{5.26}$$

5.4.2 Potential Energy

In the continuum manipulator, the potential energy consists of three parts, namely gravitational potential energy and elastic potential energy due to bending and contraction.

5.4.2.1 Gravitational Potential Energy

The gravitational potential energy of the slice σ can be expressed as

$$P_g(\sigma, t) = -m(\sigma)^{\sigma} g^T(\sigma, t) p(\sigma, t), \tag{5.27}$$

where ${}^{\sigma}g(\sigma, t) \in \mathbb{R}^3$ is defined by

$${}^{\sigma}g(\sigma, t) = {}^{\sigma}\Phi^T(0, t) \begin{bmatrix} 0 & 0 & -g \end{bmatrix}^T, \tag{5.28}$$

where $g \in \mathbb{R}$ is constant representing the gravitational acceleration.

Regarding to (5.9) and (5.14), the gravitational potential energy of slice σ can be written as

$$P_g(\sigma, t) = \frac{mg}{l(t)\kappa(\sigma, t)} \sin(\sigma\kappa(\sigma, t)). \tag{5.29}$$

Therefore, the total gravitational potential energy of the continuum manipulator is calculated as the integration of the energy in each slice and can be written as

$$P_g(t) = \int_0^{l(t)} P_g(\sigma, t) d\sigma. \tag{5.30}$$

5.4.2.2 Elastic Potential Energy due to Bending

According to the contractible continuum manipulator model [139], the elastic potential energy should be considered in two part: bending and contraction. The total bending potential energy is calculated as

$$P_b(t) = \frac{1}{2} \int_0^{l(t)} k_b(\sigma) \beta^2(\sigma, t) d\sigma, \tag{5.31}$$

where $k_b(\sigma) \in \mathbb{R}$ is the bending spring constant and $\beta(\sigma, t)$ is defined as

$$\beta(\sigma, t) = \pi - \frac{1}{2}\sigma\kappa(\sigma, t). \tag{5.32}$$

5.4.2.3 Elastic Potential Energy due to Contraction

The elastic potential energy attributed by contraction can be obtained by

$$P_e(t) = \frac{1}{2}k_e[d^* - l(t)]^2, \tag{5.33}$$

where $k_e \in \mathbb{R}$ is the spring constant associated with contraction and d^* is the relaxed length of manipulator.

Thus, the total potential energy of continuum manipulator is the sum of gravitational potential energy and elastic potential energy due to bending and contraction, which is calculated as

$$P(t) = P_g(t) + P_b(t) + P_e(t). \tag{5.34}$$

5.4.3 Lagrange Representation

The system Lagrangian operator $L(t)$ is defined as follows

$$L(t) = K(t) - P(t), \tag{5.35}$$

where $K(t)$ and $P(t)$ are total kinetic and potential energy obtained from (5.30) and (5.34) respectively.

The Euler-Lagrangian equation of motion is defined as

$$\frac{d}{dt}\frac{\partial L}{\partial \dot{q}} - \frac{\partial L}{\partial q} = \tau, \tag{5.36}$$

where $q(t) \in \mathbb{R}^2$ is the configuration-space joint position variable and defined as follows

$$\mathbf{q}(t) = \begin{bmatrix} l(t) & \kappa(t) \end{bmatrix}^T. \tag{5.37}$$

For brevity, t in the time varying variables can be omitted. The process of developing dynamic model of continuum manipulator by using Euler-Lagrangian equation of motion is presented in Fig. 5.3.

Thus, the dynamic model of continuum manipulator is expressed as

$$\mathbf{M}(\mathbf{q})\ddot{\mathbf{q}} + \mathbf{C}(\mathbf{q}, \dot{\mathbf{q}})\dot{\mathbf{q}} + \mathbf{G}(\mathbf{q}) = \tau, \tag{5.38}$$

where $\mathbf{q} \in \mathbb{R}^2$ is the configuration space variable defined as $\mathbf{q} = \begin{bmatrix} l & \kappa \end{bmatrix}^T$, $\mathbf{M}(\mathbf{q}) \in \mathbb{R}^{2\times2}$ is the inertia matrix, $\mathbf{C}(\mathbf{q}, \dot{\mathbf{q}}) \in \mathbb{R}^{2\times2}$ is the matrix relating to centrifugal

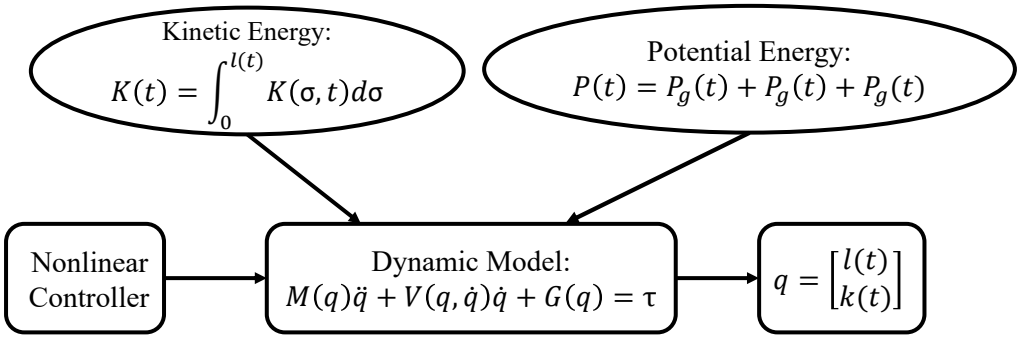

Figure 5.3: The process of developing dynamic model of continuum manipulator.

Coriolis force, $\mathbf{G}(\mathbf{q}) \in \mathbb{R}^2$ is the matrix of gravitational force and $\tau \in \mathbb{R}^2$ is the force.

For brevity, matrices $\mathbf{M}(\mathbf{q})$, $\mathbf{C}(\mathbf{q}, \dot{\mathbf{q}})$ and $\mathbf{G}(\mathbf{q})$ are written as $\mathbf{M}$, $\mathbf{C}$ and $\mathbf{G}$.

Remark 5.1. *The inertia matrix* $\mathbf{M}$ *is symmetric and positive definite, bounded by the existence of its inverse matrix.*

Remark 5.2. *The matrix* $\dot{\mathbf{M}} - 2\mathbf{C}$ *is a skew-symmetric matrix, which means the following condition is satisfied*

$$\xi^T(\dot{\mathbf{M}} - 2\mathbf{C})\xi = \mathbf{0}, \forall \xi \in \mathbb{R}^2_{\neq 0}. \tag{5.39}$$

Remark 5.3. *Considering about the mathematical calculation complexity, the configuration space joint position variable* $\theta = \begin{bmatrix} l & \kappa & \alpha \end{bmatrix}^T \in \mathbb{R}^3$ *considered in Section 5.3 is simplified to two dimensional variable* $q = \begin{bmatrix} l & \kappa \end{bmatrix}^T \in \mathbb{R}^2$ *for dynamic model and control theory development.*

Based on the parameters listed in Table 5.2, the dynamic model for the continuum manipulator derived from Section 5.4 can be obtained as follows:

$$\mathbf{M}\ddot{\mathbf{q}} + \mathbf{C}\dot{\mathbf{q}} + \mathbf{G} = \tau, \tag{5.40}$$

where $\mathbf{M} = \begin{bmatrix} m_{11} & m_{12} \\ m_{21} & m_{22} \end{bmatrix}$, $\mathbf{C} = \begin{bmatrix} c_{11} & c_{12} \\ c_{21} & c_{22} \end{bmatrix}$ and $\mathbf{G} = \begin{bmatrix} g_{11} \\ g_{12} \end{bmatrix}$. The details of each matrix element is presented as below:

$$m_{11} = -0.1l^{-1}\kappa^{-3}\sin(l\kappa) + 0.1\kappa^{-2}; \tag{5.41}$$

$$\begin{aligned} m_{12} \;=\; & -0.025l^{-1}\kappa^{-4}\cos(l\kappa)\sin(l\kappa) + 0.05\kappa^{-3}\cos^2(l\kappa) + 0.25l^{-1}\kappa^{-4}\sin(l\kappa) \\ & -0.15\kappa^{-3}\cos(l\kappa) - 0.125\kappa^{-3}; \end{aligned} \tag{5.42}$$

$$m_{21} = m_{12}; \tag{5.43}$$

$$\begin{aligned} m_{22} &= 0.1l^{-1}\kappa^{-4}\cos(l\kappa)\sin(l\kappa) - 0.1l^{-1}\kappa^{-3}\cos(l\kappa)\sin(l\kappa) + 0.2\kappa^{-4}\cos^2(l\kappa) \\ &\quad -0.4l^{-1}\kappa^{-5}\sin(l\kappa) + 0.3\kappa^{-4}\cos(l\kappa) + 0.05l^2\kappa^{-2} + 0.2\kappa^{-4}; \end{aligned} \tag{5.44}$$

$$\begin{aligned} c_{11} &= \dot{\kappa}\Big(-0.1l^{-1}\kappa^{-3}\cos^2(l\kappa) + 0.3l^{-1}\kappa^{-4}\sin(l\kappa) - 0.1\kappa^{-3}\cos(l\kappa) - 0.2k^{-3}\Big) \\ &\quad +\dot{l}\Big(0.05\kappa^{-3}l^{-2}\sin(l\kappa) - 0.05l^{-1}\kappa^{-2}\cos(l\kappa)\Big); \end{aligned} \tag{5.45}$$

$$\begin{aligned} c_{12} &= \dot{\kappa}\Big(\cos(l\kappa)\sin(l\kappa)(-0.1l\kappa^{-3} + 0.1l^{-1}\kappa^{-5} - 0.15\kappa^{-3} + 0.05l^{-2}\kappa^{-5}) \\ &\quad + \cos^2(l\kappa)(-0.2\kappa^{-4} - 0.1l^{-1}\kappa^{-4} + 0.1l\kappa^{-2}) \\ &\quad + \sin(l\kappa)(-l^{-1}\kappa^{-5} + 0.15l\kappa^{-3} - 0.2l^{-2}\kappa^{-5} + 0.15\kappa^{-3}) \\ &\quad + \cos(l\kappa)(0.7\kappa^{-4} + 0.2l^{-1}\kappa^{-4}) \\ &\quad +0.4\kappa^{-4} - 0.1l\kappa^{-2} + 0.05l^{-1}\kappa^{-4}\Big); \end{aligned} \tag{5.46}$$

$$\begin{aligned} c_{21} &= \dot{\kappa}\Big(\cos(l\kappa)\sin(l\kappa)(0.3\kappa^{-3} - 0.1l^{-2}\kappa^{-5} + 0.1l^{-1}\kappa^{-5} - 0.1l^{-1}k^{-6}) \\ &\quad + \cos^2(l\kappa)(0.2l^{-1}\kappa^{-4} - 0.2l\kappa^{-2}) + \sin(l\kappa)(0.4l^{-2}\kappa^{-5} - 0.3\kappa^{-3}) \\ &\quad + \cos(l\kappa)(-0.4l^{-1}\kappa^{-4}) + 0.2l\kappa^{-2} - 0.1l^{-1}\kappa^{-4}\Big) \\ &\quad +\dot{l}\Big(\cos(l\kappa)\sin(l\kappa)(-0.1\kappa^{-2} + 0.025l^{-2}\kappa^{-4}) \\ &\quad + \cos^2(l\kappa)(-0.05l^{-1}\kappa^{-3}) + \sin(l\kappa)(-0.25l^{-2}\kappa^{-4} + 0.15l\kappa^{-2} - 0.15l^{-1}\kappa^{-4}) \\ &\quad + \cos(l\kappa)(0.25l^{-1}\kappa^{-3} + 0.05\kappa^{-3}) - 0.1\kappa^{-3}\Big); \end{aligned} \tag{5.47}$$

$$\begin{aligned} c_{22} &= \dot{\kappa}\Big(\cos(l\kappa)\sin(l\kappa)(0.35l\kappa^{-4} - 0.25l^{-1}\kappa^{-6}) + \cos^2(l\kappa)(0.5\kappa^{-5} - 0.1l^2\kappa^{-3}) \\ &\quad + \sin(l\kappa)(l^{-1}\kappa^{-6} - 0.15l\kappa^{-4}) + \cos(l\kappa)(-0.8\kappa^{-5}) - 0.45\kappa^{-5}\Big); \end{aligned} \tag{5.48}$$

$$g_{11} = 0.49l^{-2}\kappa^{-2} + 0.49l^{-2}\kappa^{-2}\cos(l\kappa) + 1 - 10l + 0.49l^{-1}\kappa^{-1}\sin(l\kappa); \quad (5.49)$$

$$g_{21} = 0.49\kappa^{-2}\sin(l\kappa) + 0.98l^{-1}\kappa^{-3}\cos(l\kappa) + 0.98l^{-1}\kappa^{-3}. \quad (5.50)$$

5.5 Nonlinear Control Method

Having the dynamic model that has been developed in (5.38), we can see that the continuum manipulator is a complex nonlinear system. In this section, we attempt to apply two nonlinear control strategies, namely inverse dynamic control and sliding mode control, to the manipulator system. The control system block diagram is shown in Fig. 5.4.

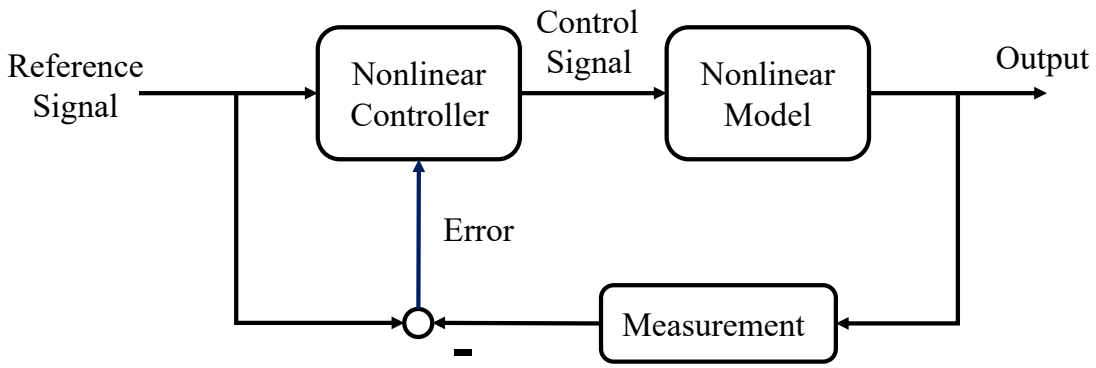

Figure 5.4: Block diagram of nonlinear control system.

5.5.1 Inverse Dynamic Control

First, define $\mathbf{e} \in \mathbb{R}^2$ as the configuration space error

$$\mathbf{e} = \mathbf{q} - \mathbf{q_d}, \quad (5.51)$$

where $\mathbf{q_d} \in \mathbb{R}^2$ is the desired configuration space trajectory.

The purpose of our control is to choose a suitable control input $\mathbf{u} \in \mathbb{R}^2$ to converge the tracking error $\mathbf{e}$ to zero.

Theorem 5.1. *The inverse dynamic controller is chosen as follows*

$$\tau = \mathbf{M}(\ddot{\mathbf{q}}_\mathbf{d} - K_p\mathbf{e} - K_d\dot{\mathbf{e}}) + \mathbf{C}\dot{\mathbf{q}} + \mathbf{G}, \quad (5.52)$$

where K_p and K_d are the proportional and derivative constant control gains. $\ddot{\mathbf{q}}_\mathbf{d} \in \mathbb{R}^2$ is the second derivative value of the desired trajectory. By choosing a set of

appropriate gain values of K_p and K_d, the configuration variables of the closed-loop system is able to track the desired trajectory and minimize the error $\mathbf{e}$.

Proof. Let the control input $\mathbf{u}$ be constructed as [119]

$$\mathbf{u} = \mathbf{M}\mathbf{a_q} + \mathbf{C}\dot{\mathbf{q}} + \mathbf{G}, \tag{5.53}$$

where $\mathbf{a_q} \in \mathbb{R}^2$ stands for a new input for control signal $\mathbf{u}$. By substituting (5.53) to the dynamic model in (5.38), where the inertia matrix $\mathbf{M}$ is invertible, hereby, the closed-loop system becomes in a linear form as

$$\ddot{\mathbf{q}} = \mathbf{a_q}. \tag{5.54}$$

The nonlinear control law presented in (5.53)) is the so-called inverse dynamic control. As we all known that nonlinear system is comparatively difficult to control due to its complex nonlinearity. However, the inverse dynamic control converts the nonlinear manipulator dynamics into a closed-loop linear system, therefore, many linear control methods can be applied.

Choose a new input $\mathbf{a_q}$ in the following form:

$$\mathbf{a_q} = -K_p\mathbf{q} - K_d\dot{\mathbf{q}} + \mathbf{r}, \tag{5.55}$$

where $\mathbf{r} \in \mathbb{R}^2$ is the reference input. For a desired trajectory $\mathbf{q_d} \in \mathbb{R}^2$, the reference input is defined by [129]

$$\mathbf{r} = \ddot{\mathbf{q}}_\mathbf{d} + K_p\mathbf{q_d} + K_d\dot{\mathbf{q}}_\mathbf{d}. \tag{5.56}$$

If taking (5.54)-(5.56) into consideration, we can have the tracking error $\mathbf{e}$ satisfying

$$\ddot{\mathbf{e}} + K_d\dot{\mathbf{e}} + K_p\mathbf{e} = 0; \tag{5.57}$$

and then combining (5.53)-(5.56), we can conclude the control input τ as

$$\tau = \mathbf{M}(\ddot{\mathbf{q}}_\mathbf{d} - K_p\mathbf{e} - K_d\dot{\mathbf{e}}) + \mathbf{C}\dot{\mathbf{q}} + \mathbf{G}. \tag{5.58}$$

□

5.5.2 Sliding Mode Control

Different from the above mentioned inverse dynamic control, sliding mode control is a nonlinear control method that utilizes the discontinuous control signal to make the system sliding along the hyper-surface.

Theorem 5.2. *The sliding mode controller is set as*

$$\tau_{smc} = \mathbf{M}\ddot{\mathbf{q}}_\mathbf{r} + \mathbf{C}\dot{\mathbf{q}}_\mathbf{r} + \mathbf{G} - \mathbf{K}\,\mathrm{sgn}(\mathbf{s}), \tag{5.59}$$

where $\ddot{\mathbf{q}}_\mathbf{r} \in \mathbb{R}^2$ *and* $\dot{\mathbf{q}}_\mathbf{r} \in \mathbb{R}^2$ *are the reference acceleration and velocity vector respectively.* $\mathrm{sgn}(\mathbf{s})$ *is the sign function that extracts the sign of a real number.* $\mathbf{s} \in \mathbb{R}^2$ *is the hyper surface of sliding mode controller, which can be chosen as [131]*

$$\mathbf{s} = \dot{\mathbf{e}} + \lambda \mathbf{e}, \tag{5.60}$$

where $\mathbf{e}$ *is the error vector as defined in* (5.51) *and* $\lambda \in \mathbb{R}^{2\times 2}$ *is a selected symmetric positive definite matrix.* $\mathbf{K} \in \mathbb{R}^2$ *is a diagonal matrix and*

$$\mathrm{sgn}(\mathbf{s}) = \begin{cases} 1\ , & \text{if } \mathbf{s} > 0; \\ 0\ , & \text{if } \mathbf{s} = 0; \\ -1, & \text{if } \mathbf{s} < 0. \end{cases}$$

Proof. Define the reference velocity vector as

$$\dot{\mathbf{q}}_\mathbf{r} = \dot{\mathbf{q}}_\mathbf{d} - \lambda \mathbf{e}. \tag{5.61}$$

By applying (5.51) and (5.60), the hyper surface can be interpreted in the form of

$$\mathbf{s} = \dot{\mathbf{q}} - \dot{\mathbf{q}}_\mathbf{r}. \tag{5.62}$$

The sliding mode control law is expressed as follows

$$\tau = \hat{\tau} - \mathbf{K}\,\mathrm{sgn}(\mathbf{s}), \tag{5.63}$$

where $\hat{\tau}$ is defined by [131]

$$\hat{\tau} = \mathbf{M}\ddot{\mathbf{q}}_\mathbf{r} + \mathbf{C}\dot{\mathbf{q}}_\mathbf{r} + \mathbf{G}. \tag{5.64}$$

Then we consider the Lyapunov function candidate as follows

$$V = \frac{1}{2}\mathbf{s}^T\mathbf{M}\mathbf{s}. \tag{5.65}$$

As the inertia matrix $\mathbf{M}$ is symmetric and positive definite, for $\mathbf{s} \neq 0$, we have $V > 0$. Then we consider the derivative form of Lyapunov function as

$$\dot{V} = \dot{\mathbf{s}}^T\mathbf{M}\mathbf{s} + \frac{1}{2}\mathbf{s}^T\dot{\mathbf{M}}^T\mathbf{s}. \tag{5.66}$$

Taking (5.62) into consideration, it shows

$$\begin{aligned} \dot{V} &= \mathbf{s}^T\mathbf{M}\ddot{\mathbf{q}} - \mathbf{s}^T\mathbf{M}\ddot{\mathbf{q}}_\mathbf{r} + \frac{1}{2}\mathbf{s}^T\dot{\mathbf{M}}^T\mathbf{s} \\ &= \mathbf{s}^T(\tau - \mathbf{M}\ddot{\mathbf{q}}_\mathbf{r} - \mathbf{C}\dot{\mathbf{q}} - \mathbf{G}) + \frac{1}{2}\mathbf{s}^T\dot{\mathbf{M}}^T\mathbf{s} \end{aligned}$$

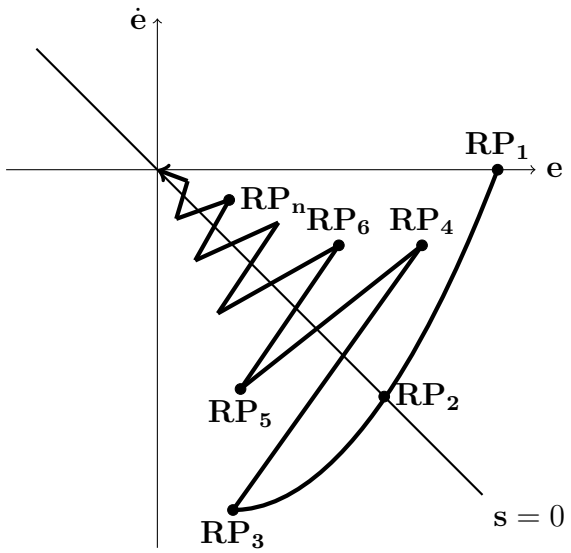

Figure 5.5: Sliding mode control in error state-space.

$$\begin{aligned} &= \mathbf{s}^T(\tau - \mathbf{M}\ddot{\mathbf{q}}_\mathbf{r} - \mathbf{C}\dot{\mathbf{q}}_\mathbf{r} - \mathbf{G}) - \mathbf{s}^T\mathbf{C}(\dot{\mathbf{q}} - \dot{\mathbf{q}}_\mathbf{r}) + \frac{1}{2}\mathbf{s}^T\dot{\mathbf{M}}^T\mathbf{s} \\ &= \mathbf{s}^T(\tau - \mathbf{M}\ddot{\mathbf{q}}_\mathbf{r} - \mathbf{C}\dot{\mathbf{q}}_\mathbf{r} - \mathbf{G}) + \frac{1}{2}\mathbf{s}^T(\dot{\mathbf{M}}^T - 2\mathbf{C})\mathbf{s}. \end{aligned} \tag{5.67}$$

Recall the property in Remark 5.2, we have

$$\dot{V} = \mathbf{s}^T(\tau - \mathbf{M}\ddot{\mathbf{q}}_\mathbf{r} - \mathbf{C}\dot{\mathbf{q}}_\mathbf{r} - \mathbf{G}). \tag{5.68}$$

Thus, the stability analysis in classic sliding mode control becomes

$$\begin{aligned} \dot{V}_{smc} &= -\mathbf{s}^T\mathbf{K}\,\mathrm{sgn}(\mathbf{s}) \\ &\leq -\sum_{i=1}^{2}\eta_i|\mathbf{s}_i|, \end{aligned} \tag{5.69}$$

where $\eta_i \in \mathbb{R}$ is positive, $\mathbf{s}_i$ is the ith element of $\mathbf{s}$. This means that the nonlinear sliding mode control stability condition can be satisfied by the chosen Lyapunov function. □

The sliding mode control is well-known for its capability of tackling uncertain nonlinear system problems. Let **RP** be the representative point of system in error state-space and $\mathbf{s}$ be the sliding surface. Fig. 5.5 [134] illustrates the process of **RP** moving to neighbouring predetermined sliding surface and finally leading to $\mathbf{s} = 0$ under ideal condition. Each $\mathbf{RP_n}$ represents the system instant position in the error state-space. In order to overcome the uncertainty problem, it may need high feedback gains to force the system sliding along the surface to guarantee the stability. However, as shown in Fig. 5.5, the high gains may drive the system swinging around $\mathbf{s} = 0$. Thus, the chattering problem occurs. In order words, there must be a trade-off between system robustness and chattering problem.

Fuzzy sliding mode control solves the chattering problem by designing the feedback gains adaptively varying to the manipulator configuration and applying large gains only when it is necessary.

5.6 Application of Fuzzy Logic to Sliding Mode Control

5.6.1 Fuzzy Sets

Fuzzy Logic uses a set of membership functions to assign any possible values between 0 and 1 to the variables. The linguistic variables are used to fuzzify all numerical variables into the expression of membership functions and IF-THEN rules. The membership functions are commonly defined as triangle or trapezoid-shaped curves, which describes each value experiences a rising and falling process. Then the IF-THEN rules map the input variables to output values based on human experience and desire.

A two-input-single-output fuzzy system IF-THEN rules can be expressed as

$$\text{Rule } i\text{: IF } x_1 \text{ is } A_i \text{ AND } x_2 \text{ is } B_i \text{ THEN } z \text{ is } Z_i, \tag{5.70}$$

where x_1 and x_2 are the input variables to the fuzzy system; z is the output variable; A_i, B_i and Z_i are the linguistic values of the input variables, $i = 1, 2, \ldots, N$, where N is the number of rules.

After executing all applicable rules and membership functions, the fuzzy output functions can be obtained. Then, the final step is to defuzzify the fuzzy output functions to a crisp value which can be used by control system. The Sugeno fuzzy inference output computed by weighted average method is presented as below

$$z = \frac{\sum_{i=1}^{N} w_i z_i}{\sum_{i=1}^{N} w_i}, \tag{5.71}$$

where w_i is the truth value of the ith rule, which is decided by the engineer experience.

5.6.2 Stability Analysis

Although the classic sliding mode control can guarantee the system stability following the above derivations, it is difficult to choose the feedback gains $\mathbf{K}$ balancing between system robustness and chattering problem.

On the contrary, fuzzy sliding mode control can propose an algorithm to tune the feedback gains $\mathbf{K}$, such that when $\mathbf{s}$ is far from $\mathbf{s} = 0$, a higher gain applies; when $\mathbf{s}$ is close to $\mathbf{s} = 0$, a lower gain works instead. Therefore, the IF-THEN rules to determine the feedback gains can be written as

$$\text{Rule } i\text{: IF } \mathbf{s} \text{ is } A_i \text{ AND } \dot{\mathbf{s}} \text{ is } B_i \text{ THEN } \mathbf{K} \text{ is } \mathbf{Z}_i. \tag{5.72}$$

In order to ensure the fuzzy sliding mode control with a speedy and effective fuzzy inference, the linguistic variables of $\mathbf{s}$ and $\dot{\mathbf{s}}$ are detailed into five fuzzy sets:

$$\mathbf{s} = \dot{\mathbf{s}} = \begin{cases} \text{Positive Big} & \text{(PB)}; \\ \text{Positive Medium} & \text{(PM)}; \\ \text{Zero} & \text{(ZO)}; \\ \text{Negative Medium} & \text{(NM)}; \\ \text{Negative Big} & \text{(NB)}. \end{cases}$$

The linguistic output variables describing output feedback gains $\mathbf{K}$ can be defined as

$$\mathbf{K} \in \{\text{N6, N5, N4, N3, N2, N1, ZO, P1, P2, P3, P4, P5, P6}\},$$

where $N_i, ZO, P_i,\ i = 1,\ 2,\ \ldots,\ 6$ are the fuzzy output values of $\mathbf{K}$ selected by engineer experience.

Thus, the 25 control rules for a two-input-single-output fuzzy system can be concluded in look-up table in Table 5.1.

Remark 5.4. *Although the values of two inputs and one output linguistic variables are often determined by engineer's experience, a good way to choose such values can be designing the fuzzy sets referring to the corresponding classic sliding mode control system. In this way, fuzzy sliding mode control can be a significant improvement from sliding mode control method.*

The fuzzy sliding mode control law can be written as

$$\tau = \mathbf{M}\ddot{\mathbf{q}}_\mathbf{r} + \mathbf{C}\dot{\mathbf{q}}_\mathbf{r} + \mathbf{G} - \sum_{i=1}^{25} w_i \mathbf{Z}_i. \tag{5.73}$$

According to the fuzzy rules in Table 5.1, it can be known that $\sum_{i=1}^{25} w_i \mathbf{Z}_i$ and $\mathbf{K}\,\mathrm{sgn}(\mathbf{s})$ are congruent matrices, which indicates the following relation exists

$$\mathbf{P}^T \mathbf{K}\,\mathrm{sgn}(\mathbf{s})\mathbf{P} = \sum_{i=1}^{25} w_i \mathbf{Z}_i, \tag{5.74}$$

Table 5.1: The rule table for fuzzy sliding mode control.

$\mathbf{s}/\dot{\mathbf{s}}$	**PB**	**PM**	**ZO**	**NM**	**NB**
PB	P6	P5	P4	P3	P2
PM	P5	P4	P3	P2	P1
ZO	P2	P1	ZO	N1	N2
NM	N1	N2	N3	N4	N5
NB	N2	N3	N4	N5	N6

where $\mathbf{P} \in \mathbb{R}^{2\times 2}$ is an invertible matrix.

Thus, the stability analysis of fuzzy sliding mode control can be written as

$$\begin{aligned} \dot{V} &= -\mathbf{s}\sum_{i=1}^{25} w_i \mathbf{Z}_i \\ &= -\mathbf{s}\mathbf{P}^T\mathbf{K}\,\mathrm{sgn}(\mathbf{s})\mathbf{P} \\ &= \mathbf{P}^T\dot{V}_{smc}\mathbf{P} \leq 0. \end{aligned} \tag{5.75}$$

Consequently, we have $V > 0$ and $\dot{V} \leq 0$, which implies that the fuzzy sliding control law in (5.73) can converge $\mathbf{s} \to 0$ and guarantee the system stability.

5.7 Fuzzy Model of Robot Manipulator

In previous sections, the dynamic model of continuum manipulator has been presented in (5.38). Three nonlinear control methods are proposed to control the system states to follow a reference signal, namely inverse dynamic control, sliding mode control and fuzzy sliding mode control. Note that the proposed three nonlinear control methods are all developed and implemented based on the full knowledge of the dynamic characteristics of continuum manipulator. However, due to the complicated dynamic characteristics of continuum manipulator, it is very limited and difficult to measure the dynamics and apply control strategies explicitly. Also the model uncertainties can bring challenges to the control system as well.

Based on the above consideration, it is necessary to consider another way to realize the control of this complex dynamic continuum manipulator. Fuzzy-model-based control is a good ideal to be proposed on the continuum manipulator model, since it can fuzzify the smooth nonlinear system and formulate to weighted sum of linear subsystems. In order to apply the FMB control method, the first step is to obtain the fuzzy model of the continuum manipulator. Then the fuzzy controller can be designed to stabilize the fuzzy system by using Lyapunov stability conditions.

5.7.1 Fuzzy Model of Rigid Manipulator

In order to develop the fuzzy model of continuum manipulator, it is instructive to first build the fuzzy model of a traditional rigid manipulator. Referring to the dynamic function derived in (5.5), the nonlinear model of the two-link rigid manipulator operating in the horizontal plane ($\mathbf{G_r}(\mathbf{q}) = 0$) can be written as:

$$\mathbf{M_r}(\mathbf{q})\ddot{\mathbf{q}} + \mathbf{C_r}(\mathbf{q}, \dot{\mathbf{q}})\dot{\mathbf{q}} = \tau, \tag{5.76}$$

where

$$\mathbf{M_r}(\mathbf{q}) = \begin{bmatrix} P_1 + P_2 + 2P_3\cos\theta_2 & P_2 + P_3\cos\theta_2 \\ P_2 + P_3\cos\theta_2 & P_2 \end{bmatrix}; \tag{5.77}$$

$$\mathbf{C_r}(\mathbf{q}, \dot{\mathbf{q}}) = \begin{bmatrix} b_1 - P_3\dot{\theta}_2\sin\theta_2 & -P_3(\dot{\theta}_1 + \dot{\theta}_2)\sin\theta_2 \\ P_3\dot{\theta}_1\sin\theta_2 & b_2 \end{bmatrix}, \tag{5.78}$$

where b_1 and b_2 are the damping in the first and the second joint respectively; $P_1 = (m_1 + 4m_2)a_1^2$, $P_2 = m_2a_2^2$ and $P_3 = 2m_2a_1a_2$. For brevity, matrices $\mathbf{M_r}(\mathbf{q})$ and $\mathbf{C_r}(\mathbf{q}, \dot{\mathbf{q}})$ are written as $\mathbf{M_r}$ and $\mathbf{C_r}$.

Then the mathematical dynamic model can be transformed into a state-space form as follows:

$$\dot{\mathbf{x}} = \mathbf{A}(\theta_1, \theta_2)\mathbf{x} + \mathbf{B}(\theta_1, \theta_2)\tau, \tag{5.79}$$

where $\mathbf{x} = \begin{bmatrix} \dot{\theta}_1 & \dot{\theta}_2 & \theta_1 & \theta_2 \end{bmatrix}^T$, $\mathbf{A}(\theta_1, \theta_2) = \begin{bmatrix} -\mathbf{M_r}^{-1}\mathbf{C_r} & 0 \\ \mathbf{I} & 0 \end{bmatrix}$ and $\mathbf{B}(\theta_1, \theta_2) = \begin{bmatrix} \mathbf{M_r}^{-1} \\ 0 \end{bmatrix}$. The details of matrices $\mathbf{A}(\theta_1, \theta_2)$ and $\mathbf{B}(\theta_1, \theta_2)$ is written as follows [140]:

$$\mathbf{A}(\theta_1, \theta_2) = \begin{bmatrix} A_{11} & A_{12} & 0 & 0 \\ A_{21} & A_{22} & 0 & 0 \\ 1 & 0 & 0 & 0 \\ 0 & 1 & 0 & 0 \end{bmatrix}, \tag{5.80}$$

$$\mathbf{B}(\theta_1, \theta_2) = \begin{bmatrix} -\frac{P_2}{P_3^2\cos^2\theta_2 - P_1P_2} & \frac{P_2 + P_3\cos\theta_2}{P_3^2\cos^2\theta_2 - P_1P_2} \\ \frac{P_2 + P_3\cos\theta_2}{P_3^2\cos^2\theta_2 - P_1P_2} & -\frac{P_1 + P_2 + 2P_3\cos\theta_2}{P_3^2\cos^2\theta_2 - P_1P_2} \\ 0 & 0 \\ 0 & 0 \end{bmatrix}, \tag{5.81}$$

where

$$A_{11} = \frac{P_2(b_1 - P_3\dot{\theta}_2\sin\theta_2) - P_3\dot{\theta}_2\sin\theta_2(P_2 + P_3\cos\theta_2)}{P_3^2\cos^2\theta_2 - P_1P_2}; \tag{5.82}$$

$$A_{12} = -\frac{b_2(P_2 + P_3\cos\theta_2) - P_2P_3\sin\theta_2(\dot{\theta}_1 + \dot{\theta}_2)}{P_3^2\cos\theta_2^2 - P_1P_2}; \tag{5.83}$$

$$A_{21} = -\frac{P_3\dot{\theta}_2 \sin\theta_2(P_1 + P_2 + 2P_3\cos\theta_2) - (P_2 + P_3\cos\theta_2)(b_1 - P_3\theta_2\dot{\sin}\theta_2)}{P_3^2\cos\theta_2^2 - P_1P_2}; \tag{5.84}$$

$$A_{22} = \frac{b_2(P_1 + P_2 + 2P_3\cos\theta_2) + P_3\sin\theta_2(P_2 + P_3\cos\theta_2)(\dot{\theta}_1 + \dot{\theta}_2)}{P_3^2\cos\theta_2^2 - P_1P_2}. \tag{5.85}$$

The state-space form (5.79) indicates the presence of following 6 nonlinear terms:

$$\begin{aligned}
z_1 &= \frac{1}{P_3^2\cos^2\theta_2 - P_1P_2};\\
z_2 &= \frac{\cos\theta_2}{P_3^2\cos^2\theta_2 - P_1P_2};\\
z_3 &= \frac{\dot{\theta}_2\sin\theta_2}{P_3^2\cos^2\theta_2 - P_1P_2};\\
z_4 &= \frac{\dot{\theta}_2\sin\theta_2\cos\theta_2}{P_3^2\cos^2\theta_2 - P_1P_2};\\
z_5 &= \frac{\dot{\theta}_1\sin\theta_2}{P_3^2\cos^2\theta_2 - P_1P_2};\\
z_4 &= \frac{\dot{\theta}_1\sin\theta_2\cos\theta_2}{P_3^2\cos^2\theta_2 - P_1P_2}.
\end{aligned} \tag{5.86}$$

This requires $2^6 = 64$ fuzzy rules to describe the nonlinear dynamic system by using sector nonlinearity approach, which is too complicated for calculation.

One of the methods to reduce the number of fuzzy rules and simplify the fuzzy model is by neglecting the Coriolis and centrifugal forces, which makes $\mathbf{C_r} = \begin{bmatrix} b_1 & 0 \\ 0 & b_2 \end{bmatrix}$. The details of state-space form matrices $\mathbf{A}(\theta_1, \theta_2)$ and $\mathbf{B}(\theta_1, \theta_2)$ can be simplified as follows:

$$\mathbf{A}(\theta_1, \theta_2) = \begin{bmatrix} \frac{P_2 b_1}{P_3^2\cos^2\theta_2 - P_1P_2} & -\frac{b_2(P_2 + P_3\cos\theta_2)}{P_3^2\cos^2\theta_2 - P_1P_2} & 0 & 0 \\ -\frac{b_1(P_2 + P_3\cos\theta_2)}{P_3^2\cos^2\theta_2 - P_1P_2} & \frac{b_2(P_1 + P_2 + 2P_3\cos\theta_2)}{P_3^2\cos^2\theta_2 - P_1P_2} & 0 & 0 \\ 1 & 0 & 0 & 0 \\ 0 & 1 & 0 & 0 \end{bmatrix}, \tag{5.87}$$

$$\mathbf{B}(\theta_1, \theta_2) = \begin{bmatrix} -\frac{P_2}{P_3^2\cos^2\theta_2 - P_1P_2} & \frac{P_2 + P_3\cos\theta_2}{P_3^2\cos^2\theta_2 - P_1P_2} \\ \frac{P_2 + P_3\cos\theta_2}{P_3^2\cos^2\theta_2 - P_1P_2} & -\frac{P_1 + P_2 + 2P_3\cos\theta_2}{P_3^2\cos^2\theta_2 - P_1P_2} \\ 0 & 0 \\ 0 & 0 \end{bmatrix}. \tag{5.88}$$

Thus, the simplified state-space form has only 2 nonlinear terms z_1 and z_2:

$$z_1 = \frac{1}{P_3^2\cos^2\theta_2 - P_1P_2}; \tag{5.89}$$

$$z_2 = \frac{1}{P_3^2 \cos^2\theta_2 - P_1 P_2}. \tag{5.90}$$

The matrices $\mathbf{A}(\theta_1, \theta_2)$ and $\mathbf{B}(\theta_1, \theta_2)$ can be represented by the following form:

$$\mathbf{A}(z_1, z_2) = \begin{bmatrix} P_2 b_1 z_1 & -P_2 b_2 z_1 - P_3 b_2 z_2 & 0 & 0 \\ -P_2 b_1 z_1 - P_3 b_1 z_2 & b_2 z_1 (P_1 + P_2) + 2 P_3 b_2 z_2 & 0 & 0 \\ 1 & 0 & 0 & 0 \\ 0 & 1 & 0 & 0 \end{bmatrix}; \tag{5.91}$$

$$\mathbf{B}(z_1, z_2) = \begin{bmatrix} -P_2 z_1 & P_2 z_1 + P_3 z_2 \\ P_2 z_1 + P_3 z_2 & 2 P_3 z_2 + z_1 (P_1 + P_2) \\ 0 & 0 \\ 0 & 0 \end{bmatrix}. \tag{5.92}$$

The two nonlinear terms z_1 and z_2 indicates $2^2 = 4$ fuzzy rules to represent the nonlinear dynamic model of two-link rigid manipulator by using sector nonlinearity approach as follows ($\mathbf{C} = \mathbf{I}^{4\times 4}$):

Rule 1: IF z_1 is $z_{1\,\min}$ AND z_2 is z_{2min} THEN

$$\begin{aligned} \dot{\mathbf{x}} &= \mathbf{A}(z_{1\,\min}, z_{2\,\min})\mathbf{x} + \mathbf{B}(z_{1\,\min}, z_{2\,\min})\mathbf{u}; \\ \mathbf{y} &= \mathbf{C}\mathbf{x}, \end{aligned} \tag{5.93}$$

where

$$\mathbf{A}(z_{1\,\min}, z_{2\,\min}) = \begin{bmatrix} P_2 b_1 z_{1\,\min} & -P_2 b_2 z_{1\,\min} - P_3 b_2 z_{2\,\min} & 0 & 0 \\ -P_2 b_1 z_{1\,\min} - P_3 b_1 z_{2\,\min} & b_2 z_{1\,\min}(P_1 + P_2) + 2 P_3 b_2 z_{2\,\min} & 0 & 0 \\ 1 & 0 & 0 & 0 \\ 0 & 1 & 0 & 0 \end{bmatrix}; \tag{5.94}$$

$$\mathbf{B}(z_{1\,\min}, z_{2\,\min}) = \begin{bmatrix} -P_2 z_{1\,\min} & P_2 z_{1\,\min} + P_3 z_{2\,\min} \\ P_2 z_{1\,\min} + P_3 z_{2\,\min} & 2 P_3 z_{2\,\min} + z_{1\,\min}(P_1 + P_2) \\ 0 & 0 \\ 0 & 0 \end{bmatrix}. \tag{5.95}$$

Rule 2: IF z_1 is $z_{1\,\min}$ AND z_2 is $z_{2\,\max}$ THEN

$$\begin{aligned} \dot{\mathbf{x}} &= \mathbf{A}(z_{1\,\min}, z_{2\,\max})\mathbf{x} + \mathbf{B}(z_{1\,\min}, z_{2\,\max})\mathbf{u}; \\ \mathbf{y} &= \mathbf{C}\mathbf{x}, \end{aligned} \tag{5.96}$$

where

$$\mathbf{A}(z_{1\,\min}, z_{2\,\max}) = \begin{bmatrix} P_2 b_1 z_{1\,\min} & -P_2 b_2 z_{1\,\min} - P_3 b_2 z_{2\,\max} & 0 & 0 \\ -P_2 b_1 z_{1\,\min} - P_3 b_1 z_{2\,\max} & b_2 z_{1\,\min}(P_1 + P_2) + 2P_3 b_2 z_{2\,\max} & 0 & 0 \\ 1 & 0 & 0 & 0 \\ 0 & 1 & 0 & 0 \end{bmatrix}; \tag{5.97}$$

$$\mathbf{B}(z_{1\,\min}, z_{2\,\max}) = \begin{bmatrix} -P_2 z_{1\,\min} & P_2 z_{1\,\min} + P_3 z_{2\,\max} \\ P_2 z_{1\,\min} + P_3 z_{2\,\max} & 2P_3 z_{2\,\max} + z_{1\,\min}(P_1 + P_2) \\ 0 & 0 \\ 0 & 0 \end{bmatrix}. \tag{5.98}$$

Rule 3: IF z_1 is $z_{1\,\max}$ AND z_2 is $z_{2\,\min}$ THEN

$$\begin{aligned} \dot{\mathbf{x}} &= \mathbf{A}(z_{1\,\max}, z_{2\,\min})\mathbf{x} + \mathbf{B}(z_{1\,\max}, z_{2\,\min})\mathbf{u}; \\ \mathbf{y} &= \mathbf{C}\mathbf{x}, \end{aligned} \tag{5.99}$$

where

$$\mathbf{A}(z_{1\,\max}, z_{2\,\min}) = \begin{bmatrix} P_2 b_1 z_{1\,\max} & -P_2 b_2 z_{1\,\max} - P_3 b_2 z_{2\,\min} & 0 & 0 \\ -P_2 b_1 z_{1\,\max} - P_3 b_1 z_{2\,\min} & b_2 z_{1\,\max}(P_1 + P_2) + 2P_3 b_2 z_{2\,\min} & 0 & 0 \\ 1 & 0 & 0 & 0 \\ 0 & 1 & 0 & 0 \end{bmatrix}; \tag{5.100}$$

$$\mathbf{B}(z_{1\,\max}, z_{2\,\min}) = \begin{bmatrix} -P_2 z_{1\,\max} & P_2 z_{1\,\max} + P_3 z_{2\,\min} \\ P_2 z_{1\,\max} + P_3 z_{2\,\min} & 2P_3 z_{2\,\min} + z_{1\,\max}(P_1 + P_2) \\ 0 & 0 \\ 0 & 0 \end{bmatrix}. \tag{5.101}$$

Rule 4: IF z_1 is $z_{1\,\max}$ AND z_2 is $z_{2\,\max}$ THEN

$$\begin{aligned} \dot{\mathbf{x}} &= \mathbf{A}(z_{1\,\max}, z_{2\,\max})\mathbf{x} + \mathbf{B}(z_{1\,\max}, z_{2\,\max})\mathbf{u}; \\ \mathbf{y} &= \mathbf{C}\mathbf{x}, \end{aligned} \tag{5.102}$$

where

$$\mathbf{A}(z_{1\max}, z_{2\max}) = \begin{bmatrix} P_2 b_1 z_{1\max} & -P_2 b_2 z_{1\max} - P_3 b_2 z_{2\max} & 0 & 0 \\ -P_2 b_1 z_{1\max} - P_3 b_1 z_{2\max} & b_2 z_{1\max}(P_1 + P_2) + 2P_3 b_2 z_{2\max} & 0 & 0 \\ 1 & 0 & 0 & 0 \\ 0 & 1 & 0 & 0 \end{bmatrix}; \tag{5.103}$$

$$\mathbf{B}(z_{1\max}, z_{2\max}) = \begin{bmatrix} -P_2 z_{1\max} & P_2 z_{1\max} + P_3 z_{2\max} \\ P_2 z_{1\max} + P_3 z_{2\max} & 2P_3 z_{2\max} + z_{1\max}(P_1 + P_2) \\ 0 & 0 \\ 0 & 0 \end{bmatrix}. \tag{5.104}$$

The membership functions can be expressed by the local minimum and maximum values of the nonlinearities z_1 and z_2 as follows:

$$w_{11}(z_1) = \frac{z_{1\max} - z_1}{z_{1\max} - z_{1\min}}; \tag{5.105}$$

$$w_{12}(z_1) = \frac{z_1 - z_{1\min}}{z_{1\max} - z_{1\min}}; \tag{5.106}$$

$$w_{21}(z_2) = \frac{z_{2\max} - z_2}{z_{2\max} - z_{2\min}}; \tag{5.107}$$

$$w_{22}(z_2) = \frac{z_2 - z_{2\min}}{z_{2\max} - z_{2\min}}. \tag{5.108}$$

5.7.2 Fuzzy Model of Continuum Manipulator

Inspired by the process of developing the fuzzy model of rigid manipulator in Section 5.7.1, the investigation of fuzzy model of continuum manipulator starts as follows. First, consider transforming the dynamic model of continuum manipulator in (5.38) to polynomial fuzzy model by using sector nonlinearity approach. The nonlinear terms in (5.38) can be listed as below:

$$\begin{aligned} z_1 &= \cos(l\kappa)\sin(l\kappa); \\ z_2 &= \cos^2(l\kappa); \\ z_3 &= \cos(l\kappa); \\ z_4 &= \sin((l\kappa)); \\ z_5 &= \dot{l}\cos(l\kappa)\sin(l\kappa); \\ z_6 &= \dot{l}\cos^2(l\kappa); \\ z_7 &= \dot{l}\cos(l\kappa); \\ z_8 &= \dot{l}\sin((l\kappa)); \\ z_9 &= \dot{\kappa}\cos(l\kappa)\sin(l\kappa); \end{aligned}$$

$$
\begin{aligned}
z_{10} &= \dot{\kappa}\cos^2(l\kappa);\\
z_{11} &= \dot{\kappa}\cos(l\kappa);\\
z_{12} &= \dot{\kappa}\sin((l\kappa)).
\end{aligned} \tag{5.109}
$$

Since there are 12 nonlinear terms, the polynomial fuzzy model for the continuum manipulator would require $2^{12} = 4096$ rules.

A simplified nonlinear model for the continuum manipulator can be proposed by neglecting the Coriolis and centrifugal forces, similar as the process in rigid manipulator in (5.87) and (5.88).

According to the formula of arc length, we have

$$
l = r\theta, \tag{5.110}
$$

where l is the arc length, r is the radius of the arc which can be written as $r = \frac{1}{\kappa}$, and θ is the central angle of the arc in radians. Thus, we can obtain the following relationship from the arc formula in (5.110):

$$
l\kappa = \theta. \tag{5.111}
$$

Since the Coriolis force is proportional to the rotation rate $\dot{\theta}$ and the centrifugal force is proportional to the square of rotation rate $\dot{\theta}^2$ (not considered in this model), we can assume that

$$
\dot{\kappa}l + \dot{l}\kappa = 0, \tag{5.112}
$$

which means

$$
\dot{\kappa}(\dot{\kappa}l + \dot{l}\kappa) = 0; \tag{5.113}
$$

$$
\dot{l}(\dot{\kappa}l + \dot{l}\kappa) = 0. \tag{5.114}
$$

By applying the assumption in (5.112) to (5.38) the dynamic model of the continuum manipulator can be simplified and the matrix $\mathbf{C}$ can be updated in the following form:

$$
\mathbf{C_{new}} = \begin{bmatrix} c_{new11} & c_{new12} \\ c_{new21} & c_{new22} \end{bmatrix}, \tag{5.115}
$$

where

$$
c_{new11} = \dot{\kappa}\Big(0.25l^{-1}\kappa^{-4}\sin(l\kappa) - 0.05\kappa^{-3}\cos(l\kappa) - 0.2k^{-3}\Big); \tag{5.116}
$$

$$
c_{new12} = \dot{\kappa}\Big(\cos(l\kappa)\sin(l\kappa)(-0.1l\kappa^{-3} + 0.1l^{-1}\kappa^{-5} - 0.15\kappa^{-3} + 0.05l^{-2}\kappa^{-5})
$$

$$
\begin{aligned}
&+\cos^2(l\kappa)(-0.1\kappa^{-4}-0.1l^{-1}\kappa^{-4}+0.1l\kappa^{-2})\\
&+\sin(l\kappa)(-l^{-1}\kappa^{-5}+0.15l\kappa^{-3}-0.2l^{-2}\kappa^{-5}+0.15\kappa^{-3})\\
&+\cos(l\kappa)(0.7\kappa^{-4}+0.2l^{-1}\kappa^{-4})\\
&+0.4\kappa^{-4}-0.1l\kappa^{-2}+0.05l^{-1}\kappa^{-4}\Big); \qquad (5.117)
\end{aligned}
$$

$$
\begin{aligned}
c_{new21} &= \dot{\kappa}\Big(\cos(l\kappa)\sin(l\kappa)(0.075l^{-1}\kappa^{-5}-0.1l^{-1}k^{-6})+\cos^2(l\kappa)(-0.1l\kappa^{-2})\\
&\quad+\sin(l\kappa)(-0.15\kappa^{-3})+\cos(l\kappa)(-0.4l^{-1}\kappa^{-4})+0.2l\kappa^{-2}\Big)\\
&\quad+\dot{l}\Big(\cos(l\kappa)\sin(l\kappa)(-0.1\kappa^{-2})+\cos^2(l\kappa)(-0.05l^{-1}\kappa^{-3})\\
&\quad+\sin(l\kappa)(-0.25l^{-2}\kappa^{-4}+0.15l\kappa^{-2}-0.15l^{-1}\kappa^{-4})\\
&\quad+\cos(l\kappa)(0.25l^{-1}\kappa^{-3}+0.05\kappa^{-3})-0.1\kappa^{-3}\Big); \qquad (5.118)
\end{aligned}
$$

$$
\begin{aligned}
c_{new22} &= \dot{\kappa}\Big(\cos(l\kappa)\sin(l\kappa)(0.05l\kappa^{-4}-0.1l^{-1}\kappa^{-6})+\cos^2(l\kappa)(0.3\kappa^{-5})\\
&\quad+\sin(l\kappa)(0.6l^{-1}\kappa^{-6})+\cos(l\kappa)(-0.4\kappa^{-5})-0.35\kappa^{-5}\Big). \qquad (5.119)
\end{aligned}
$$

5.7.3 Application of Fuzzy-model-based Control to Continuum Manipulator

Through the simplification process of neglecting Coriolis and centrifugal forces, the nonlinear terms in the rigid manipulator dynamic model have been reduced from 6 which requires 64 fuzzy rules to 2 which needs only 4 fuzzy rules to use fuzzy model to represent the simplified nonlinear model. However, according to the simplification process in Section 5.7.2, although the total number of nonlinear terms in continuum manipulator dynamic model is reduced by applying the same simplification method, it still requires 4096 rules in the polynomial fuzzy model of continuum manipulator due to 12 nonlinear terms listed in (5.109). Therefore, some other simplification or mathematical transformation techniques are required to further reduce the number of rules into a feasible level.

After using polynomial fuzzy model to represent the nonlinear dynamic model of the continuum manipulator, the FMB control methods can be implemented to control the continuum manipulator and investigate the stability conditions. The block diagram of polynomial FMB control system is described in Fig. 5.6. It is advantageous to apply fuzzy-model-based control methods such as mentioned in Chapters 3 and 4 to the continuum manipulator compared with traditional linear

or nonlinear control methods. The complex and nonlinear system like the dynamic model of continuum manipulator can bring many challenges when applying traditional control methods, for example the robustness issue in inverse dynamic control and how to choose proper sliding mode surface for the nonlinear system. The FMB control methods not only can investigate the system stability by using Lyapunov stability condition, but also are able to involve practical issues into the stability condition such as control input saturation and guaranteed cost on system index. The main challenge of applying FMB control system on the nonlinear model of continuum manipulator is difficult to use a feasible number of fuzzy rules to represent the nonlinear model. Currently, the dynamic model of continuum manipulator is represented by 4096 fuzzy rules which certainly involves large amount and highly complex calculation process. To make the application of FMB control feasible, it either requires more advanced computation capability or simplified fuzzy model of continuum manipulator.

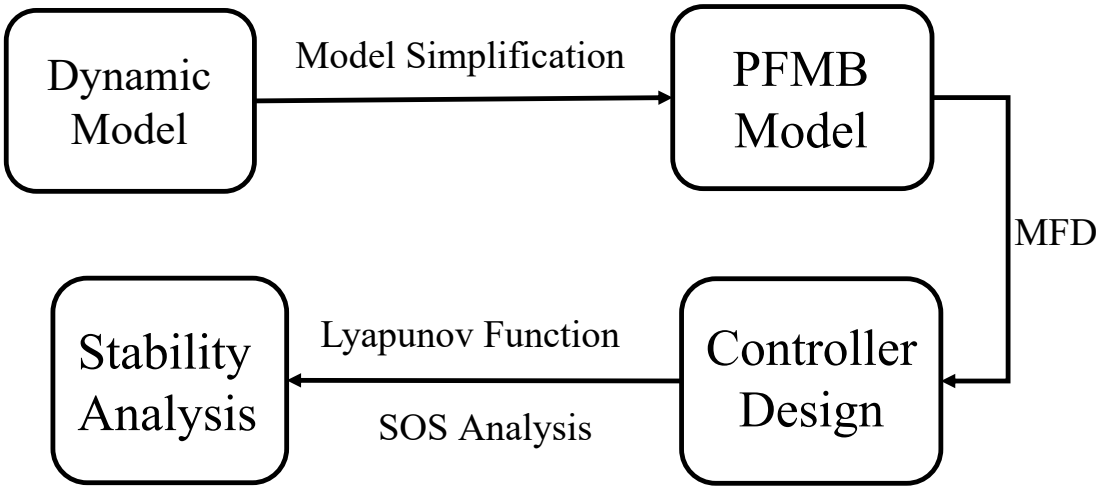

Figure 5.6: Block diagram of polynomial fuzzy model control system for continuum manipulator.

5.8 Simulation Results

The simulation process has two main purposes: one is to verify the effectiveness of proposed three control methods, namely inverse dynamic control, sliding mode control and fuzzy sliding mode control, to realize the tracking control of continuum manipulator on configuration state-space $\mathbf{q} = \begin{bmatrix} l & \kappa \end{bmatrix}^T$; another purpose is to make the comparison of the system performances between these three control methods to analyze and conclude the better control method for the control system of continuum manipulator.

The simulation is run under MATLAB Simulink environment. The dynamic sys-

tem of continuum manipulator aims to follow the trajectory of desired configuration variables $\mathbf{q_d} = \begin{bmatrix} l_d & \kappa_d \end{bmatrix}^T$. In order to avoid the singularities, the initial conditions of system states are chosen as $\mathbf{q_0} = \begin{bmatrix} 0.08 & 10 \end{bmatrix}^T$. The necessary parameters of the continuum manipulator is listed in Table 5.2.

Table 5.2: The continuum manipulator parameter setting.

Name and notation	Value with unit
Relaxed length d^*	0.1 m
Gravitational acceleration g	9.8 N/kg
Cross-section radius r	0.01 m
Mass m	0.05 kg
Bending spring constant k_b	0.001
Elastic spring constant k_e	10

The simulation process for the continuum manipulator control system is described as follows. First, a step response is used as a reference signal to test the system performance, where the stepping time is $10s$ and the final values are $\mathbf{q_f} = \begin{bmatrix} 0.05 & 15 \end{bmatrix}^T$. In the second test, the reference is a sinusoidal signal where the bias is $\mathbf{q_{sin}} = \begin{bmatrix} 0.06 & 12.5 \end{bmatrix}^T$, the amplitude is $\begin{bmatrix} 0.03 & 2.5 \end{bmatrix}^T$ and the frequency is 0.5 rad/sec. The third test considers the effect of measurement noise in the dynamic control of continuum manipulator. The amplitude of measurement noise is maximum 5% of stepping amplitude with the characteristics of white Gaussian noise. Fig. 5.7 represents the block diagram of the control system of continuum manipulator with measurement noise.

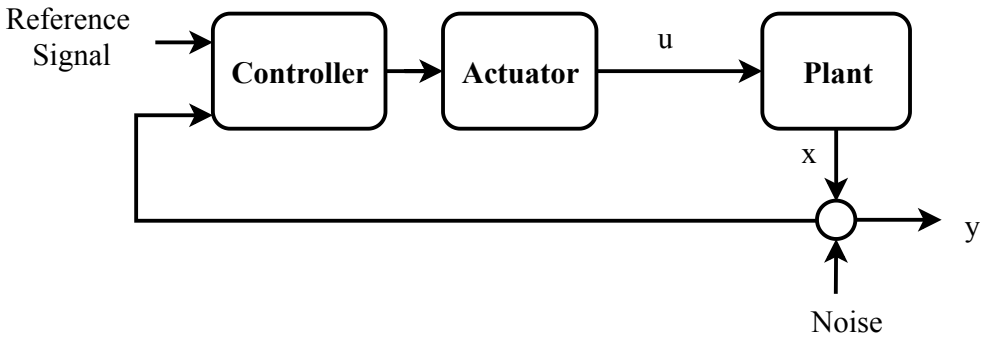

Figure 5.7: Block diagram of continuum manipulator control system with noise.

For the simulation test of inverse dynamic control, Fig. 5.8 shows the Simulink block diagram of the closed-loop inverse dynamic control system. The inverse dynamic controller is built based on (5.52), where the plant represents the physical model of continuum manipulator dynamics and the integrators are used to obtain the configuration-space velocity and position (these values are expected to be obtained from sensor data). Applied with the pre-tuned controller parameters $K_p = 0.3$

and $K_d = 2.4$, the closed-loop system simulation results are captured and plotted in Figs. 5.9, 5.10 and 5.11. It can be seen from Fig. 5.9 that the output signals of the length l and curvature κ reach the reference signals without oscillation and overshoot. The final values settle down in about 35 seconds. This owes to the closed-loop system being tuned in an over-damped condition. According to the sinusoidal signal tracking result in Fig. 5.10, the system states start from different values and follow the reference signal at about 17 seconds. However, when the measurement noise is involved in the control system, the system performance significantly deteriorates, especially on the step response of length. This reflects that the good performance of inverse dynamic control system heavily relies on the correct and accurate mathematical model of continuum manipulator. The unexpected factors may significantly affect the stability of inverse dynamic control system, such as measurement noise, external disturbance and system uncertainty.

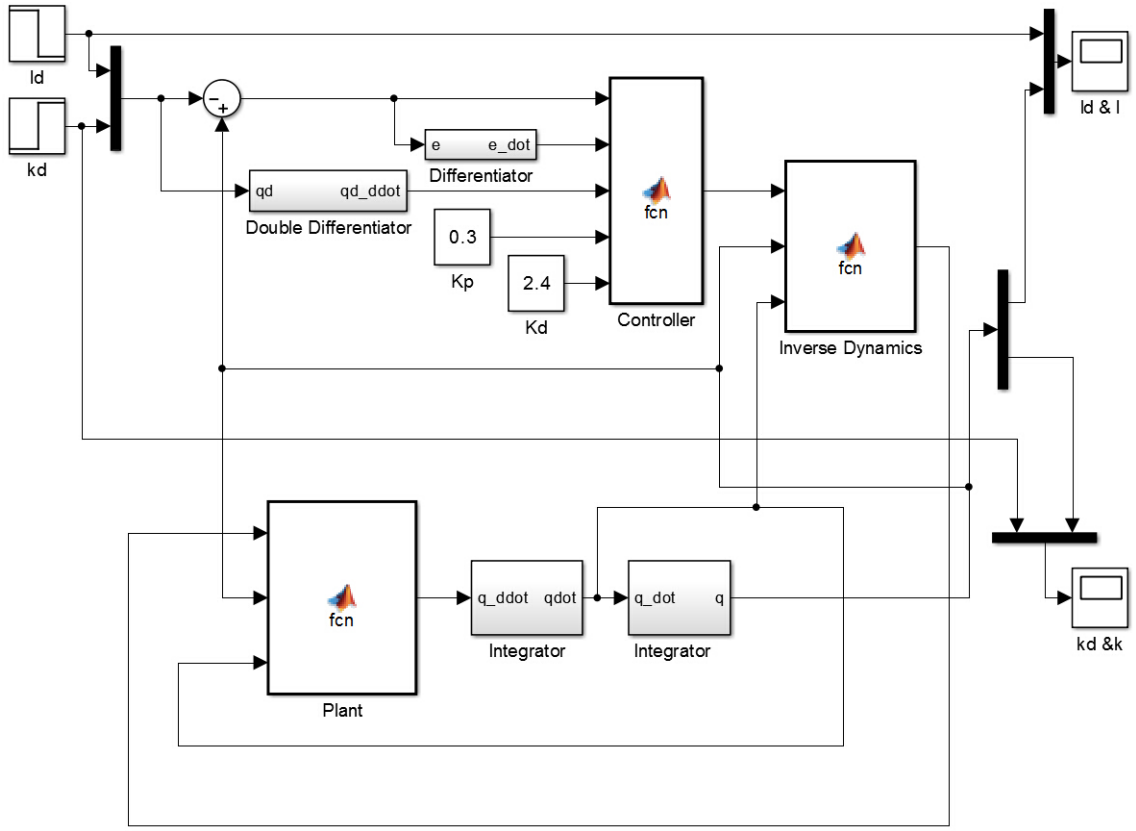

Figure 5.8: Block diagram of the closed-loop inverse dynamic control system in MATLAB Simulink environment.

For the simulation test of sliding mode control, Fig. 5.12 gives the block diagram of the closed-loop sliding mode control system in Simulink. The sliding mode controller is constructed based on the sliding mode control law (5.59). Applied with appropriate values of the positive definite diagonal matrices $\lambda = \begin{bmatrix} 1 & 0 \\ 0 & 1 \end{bmatrix}$ and $\mathbf{K} = \begin{bmatrix} 1 \times 10^{-4} & 0 \\ 0 & 3 \times 10^{-6} \end{bmatrix}$, the simulation results are obtained and shown in Figs.

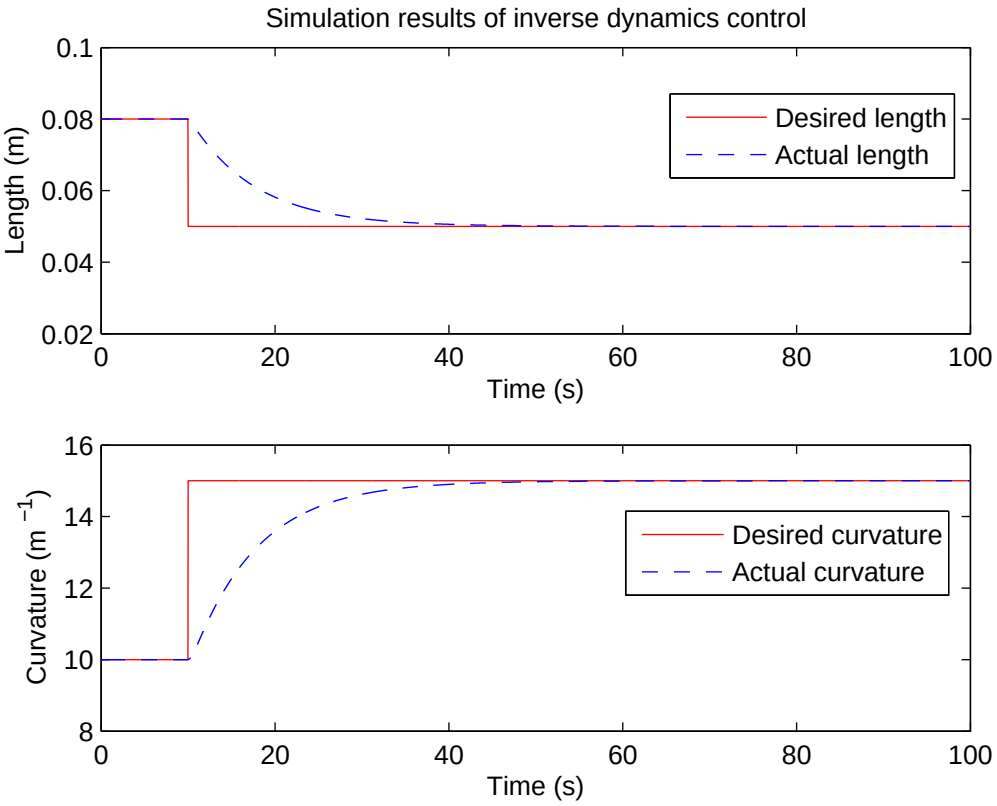

Figure 5.9: The step response of the inverse dynamic control.

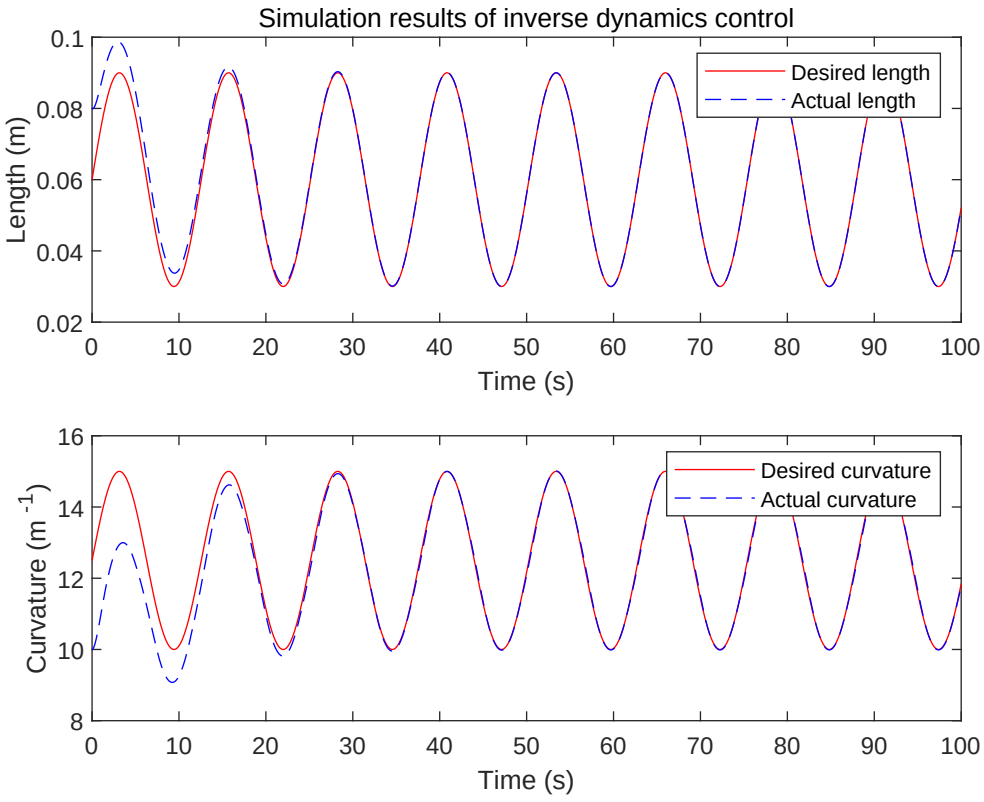

Figure 5.10: The sine wave response of the inverse dynamic control.

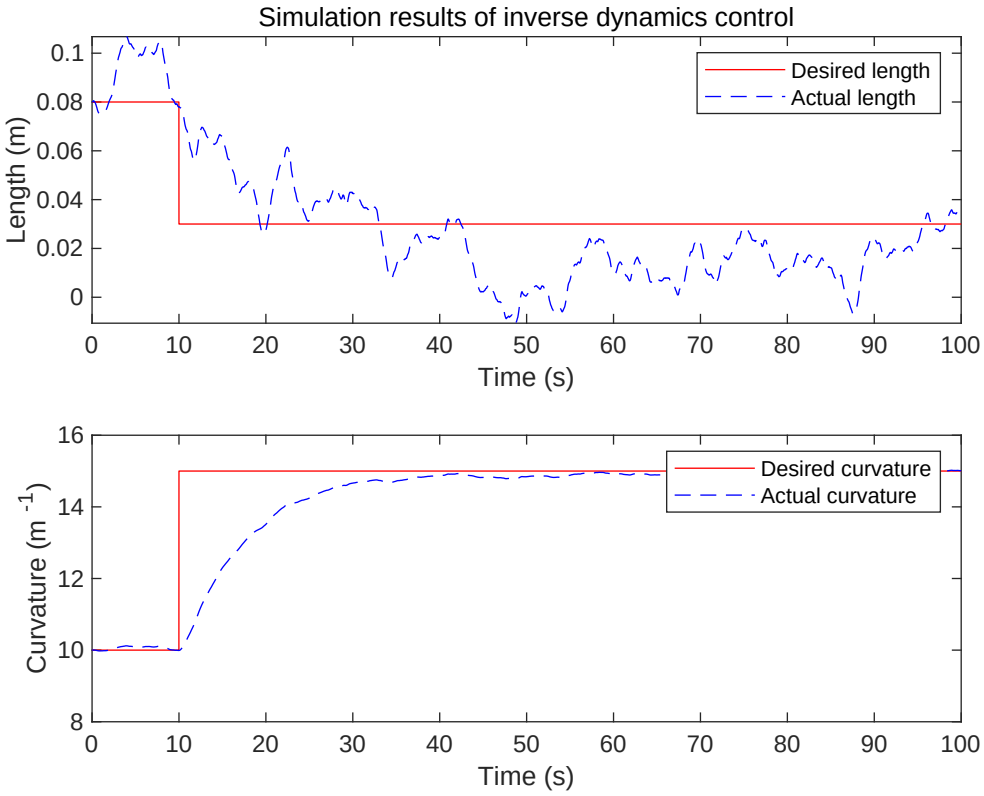

Figure 5.11: The step response of the inverse dynamic control with noise.

5.13, 5.14 and 5.15, respectively. According to the step response, the configuration-space variables are able to be controlled to reach at the final value of the reference signals. Note that the system settling time of sliding mode controller is about 5 seconds, which is significantly reduced compared with inverse dynamic control system. However, we can see from the step response in Fig. 5.13 that the chattering problem affects the system performance, especially for the length l. The chattering problem is a common issue for sliding mode control, which has been discussed in Section 5.5.2. The high frequency chattering is caused by the instantaneously switching control signals in sliding mode control. Although the chattering problem shown in Fig. 5.13 does not affect the system stability, the high frequency chattering may cause problem in practical applications. In the sinusoidal signal test, Fig. 5.14 shows the sliding mode control produces a better tracking performance with faster reaction than inverse dynamic control in Fig. 5.10. More importantly, Fig. 5.15 shows that the system performance of sliding mode control can be much better than that of inverse dynamic control in Fig. 5.11 when the measurement noise is considered. Since the Gaussian white noise is zero-mean symmetric signal, the noise can only affect the switching frequency of the control signal such that the system performance can be affected very little. This shows the advantage of robustness in sliding mode control compared with inverse dynamic control.

For the fuzzy sliding mode control, the membership functions of the two input

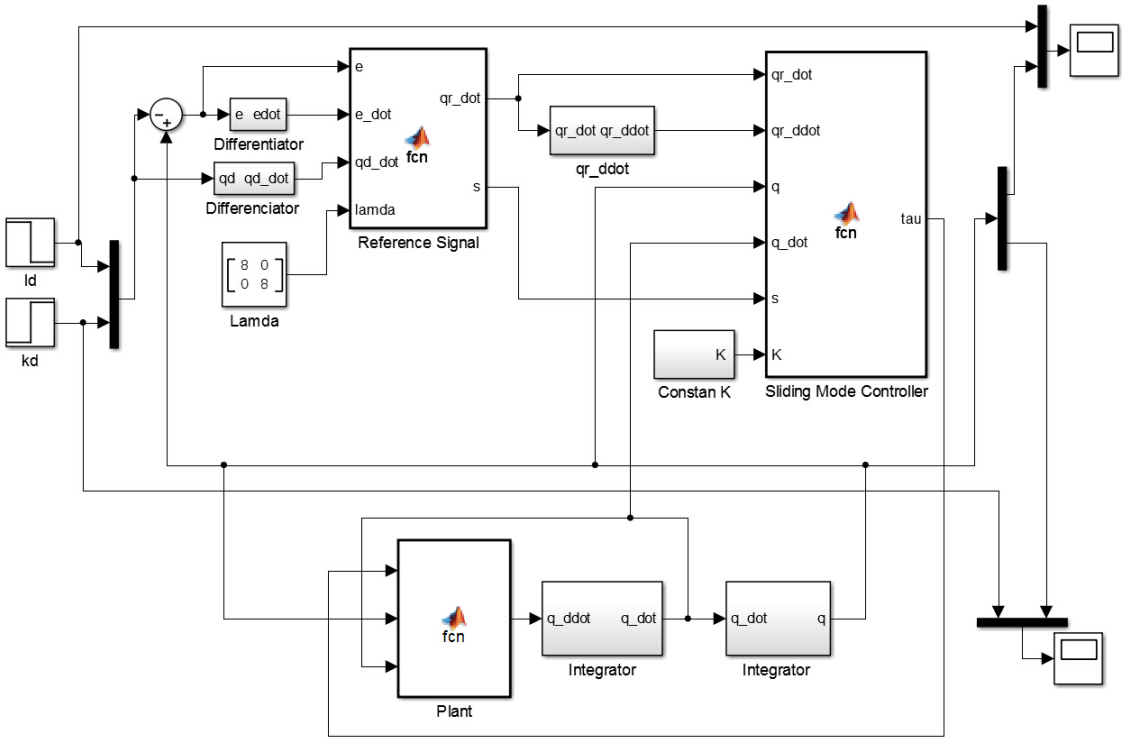

Figure 5.12: Block diagram of the closed-loop sliding mode control system in MATLAB Simulink environment.

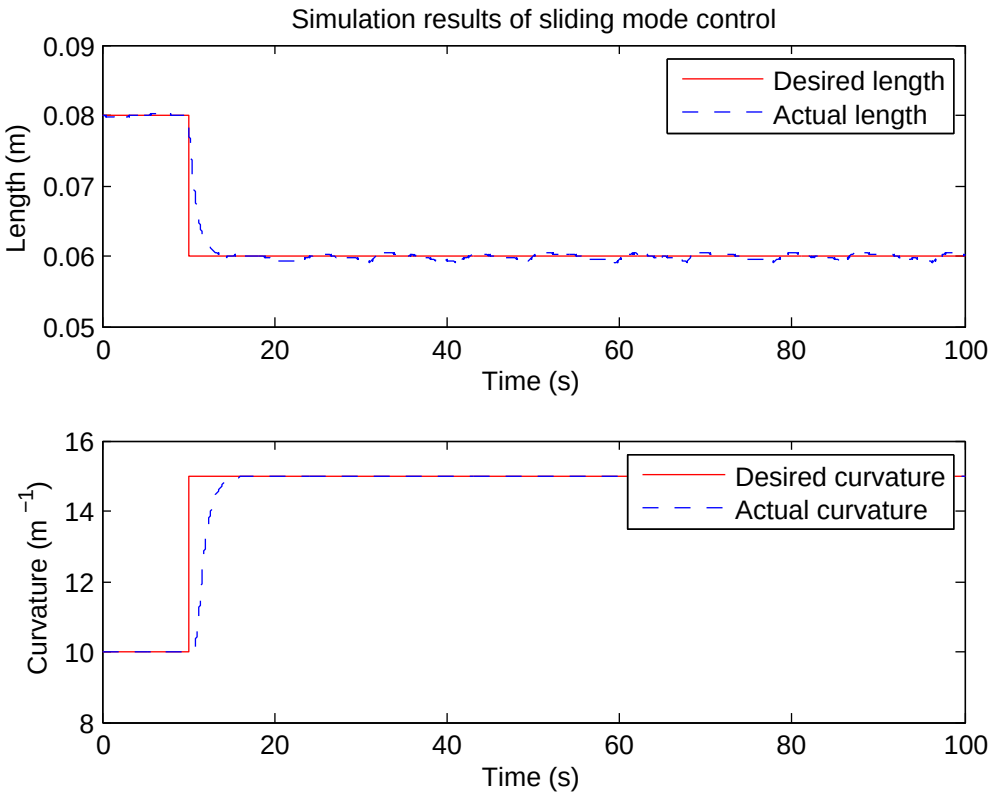

Figure 5.13: The step response results of the sliding mode control.

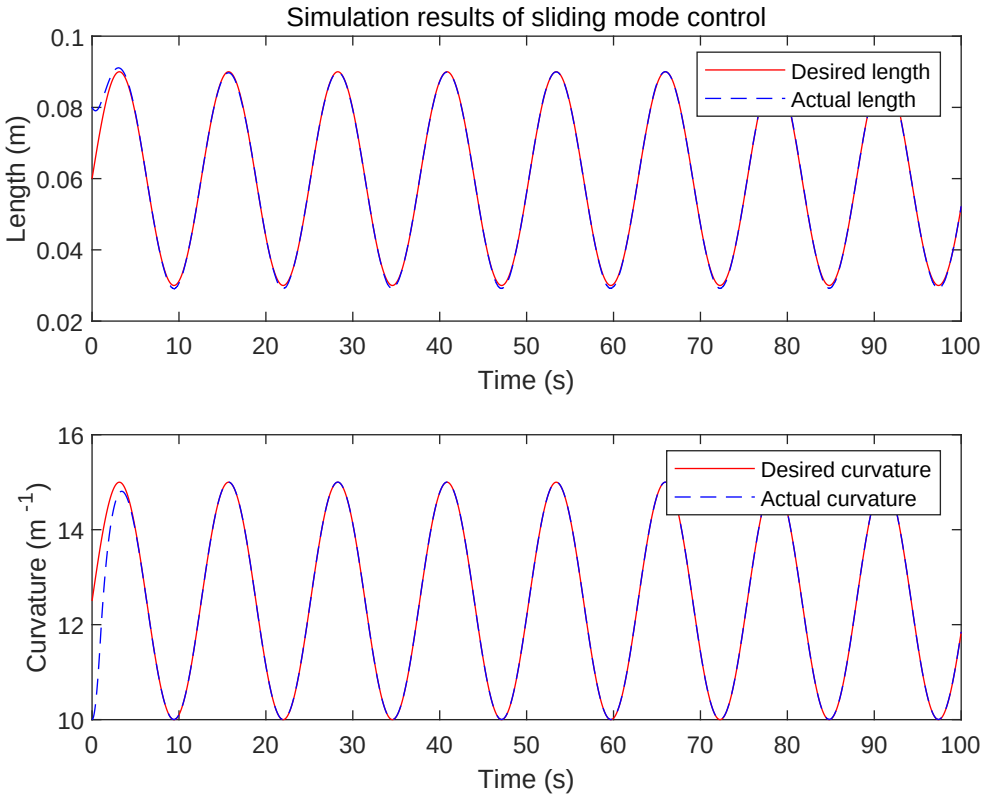

Figure 5.14: The sine wave response results of the sliding mode control.

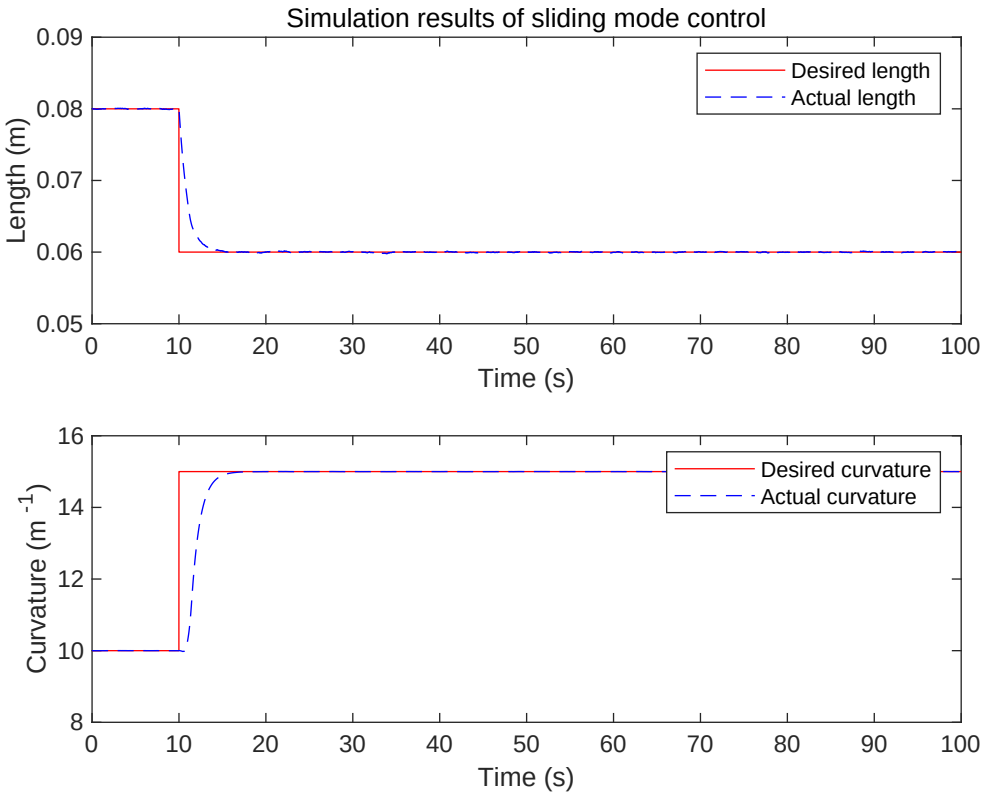

Figure 5.15: The step response results of the sliding mode control with noise.

Table 5.3: Fuzzy output value gains for $\mathbf{K}$.

N6	N5	N4	N3	N2	N1	ZO	P1	P2	P3	P4	P5	P6
-2	-1.8	-1.6	-1.4	-1.2	-1	0	1	1.2	1.4	1.6	1.8	2

linguistic variables $\mathbf{s} \in \mathbb{R}^2$ and $\dot{\mathbf{s}} \in \mathbb{R}^2$ are presented in Figs. 5.16 to 5.19. The output fuzzy value gains for $\mathbf{K}$ are listed in Table 5.3. Choose $\lambda = \begin{bmatrix} 1 & 0 \\ 0 & 1 \end{bmatrix}$. As mentioned in Remark 5.4, the decision of linguistic variables' values is referred to the simulation results of sliding mode control. The output fuzzy inference is designed in Sugeno type. Different from Mamdani type of fuzzy inference, the Sugeno type of membership functions are either constant or linear.

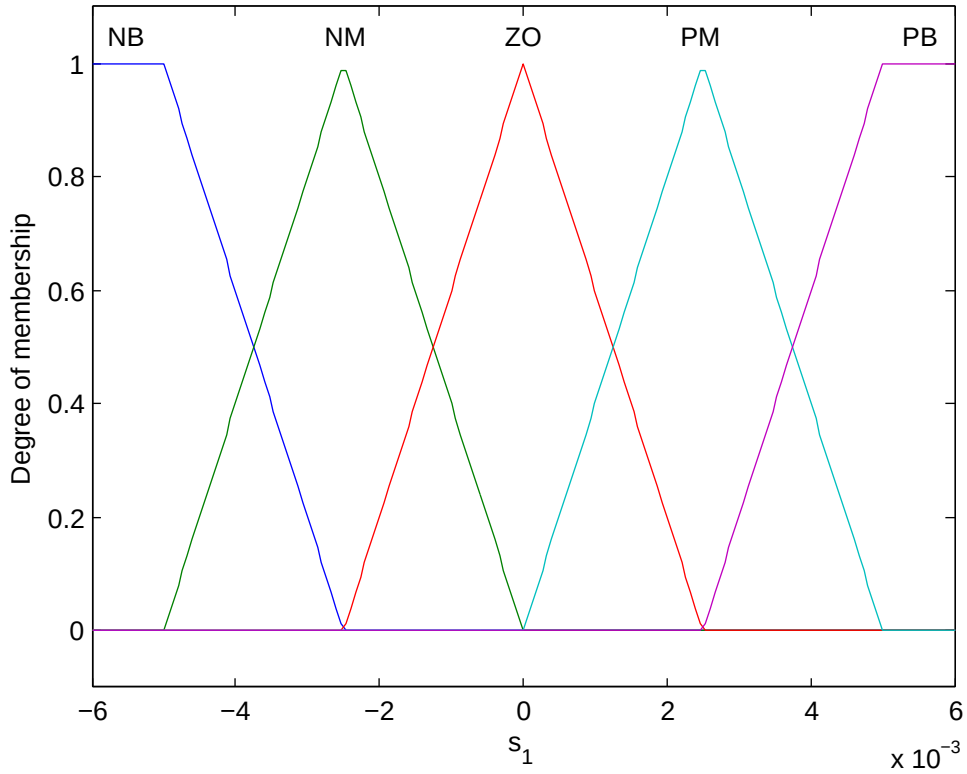

Figure 5.16: Fuzzy sliding mode control membership function of s_1.

Figs. 5.21, 5.22 and 5.23 show the reference signal as step signal, sinusoidal signal and sinusoidal with measurement noise for fuzzy sliding mode control system respectively. Obviously, the fuzzy sliding mode controller proposes an effective control to guarantee the system stability and drive the manipulator configuration variables to follow the reference signals towards desired value. The sliding mode control and fuzzy sliding mode control show some similar characteristics according to the simulation results. For example, the rising times are almost the same and they both perform well when the system is affected by measurement noise where it is an obvious advantage over the inverse dynamic control method. However, the chattering problem clearly exists in sliding mode control result, where the length l suffers

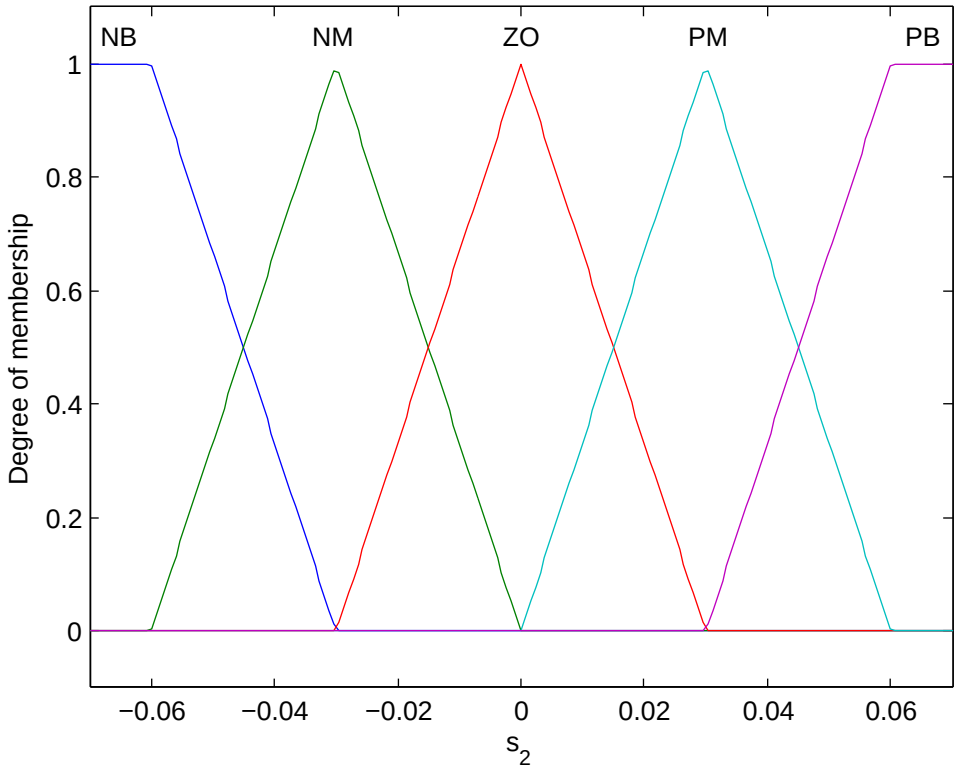

Figure 5.17: Fuzzy sliding mode control membership function of s_2.

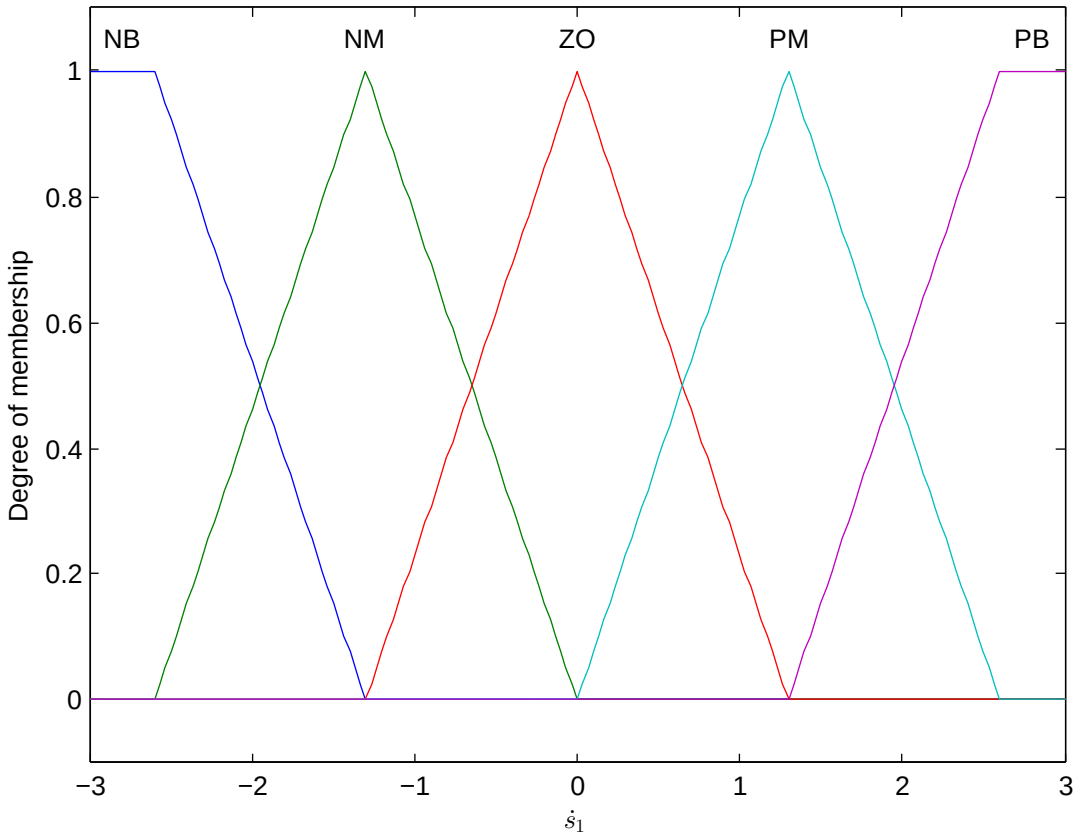

Figure 5.18: Fuzzy sliding mode control membership function of $\dot{s}_1$.

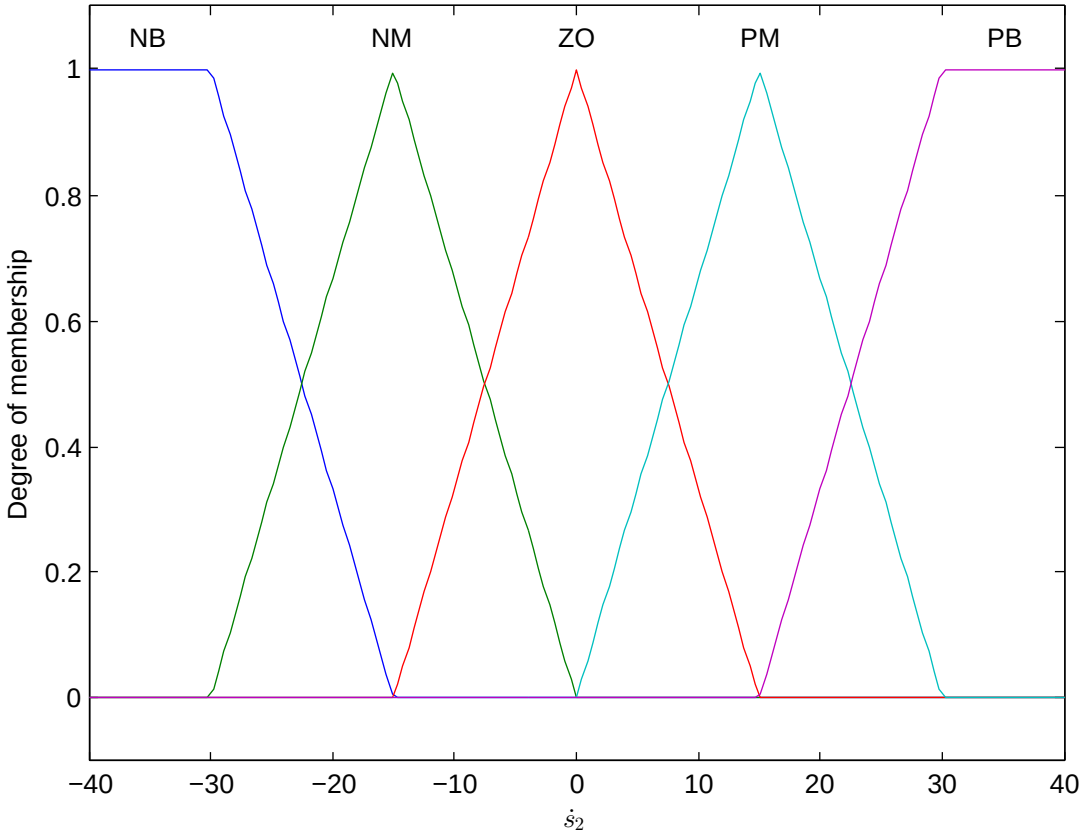

Figure 5.19: Fuzzy sliding mode control membership function of $\dot{s}_2$.

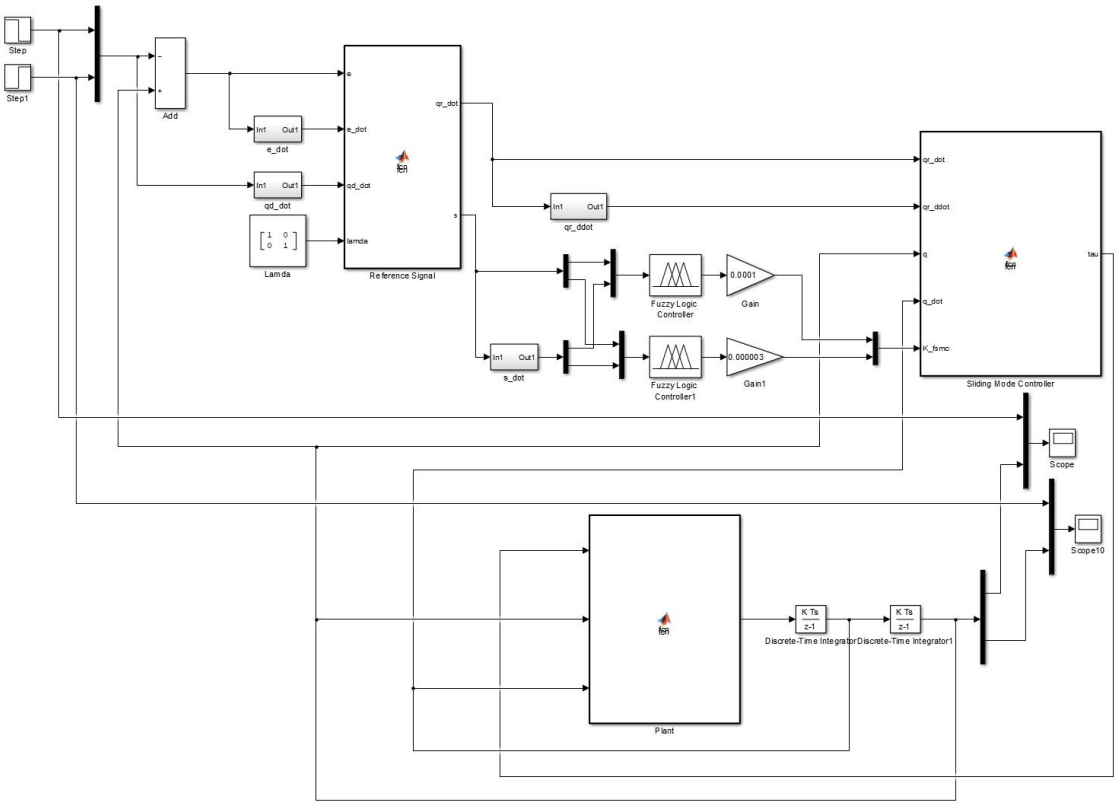

Figure 5.20: Block diagram of the closed-loop fuzzy sliding mode control system in MATLAB Simulink environment.

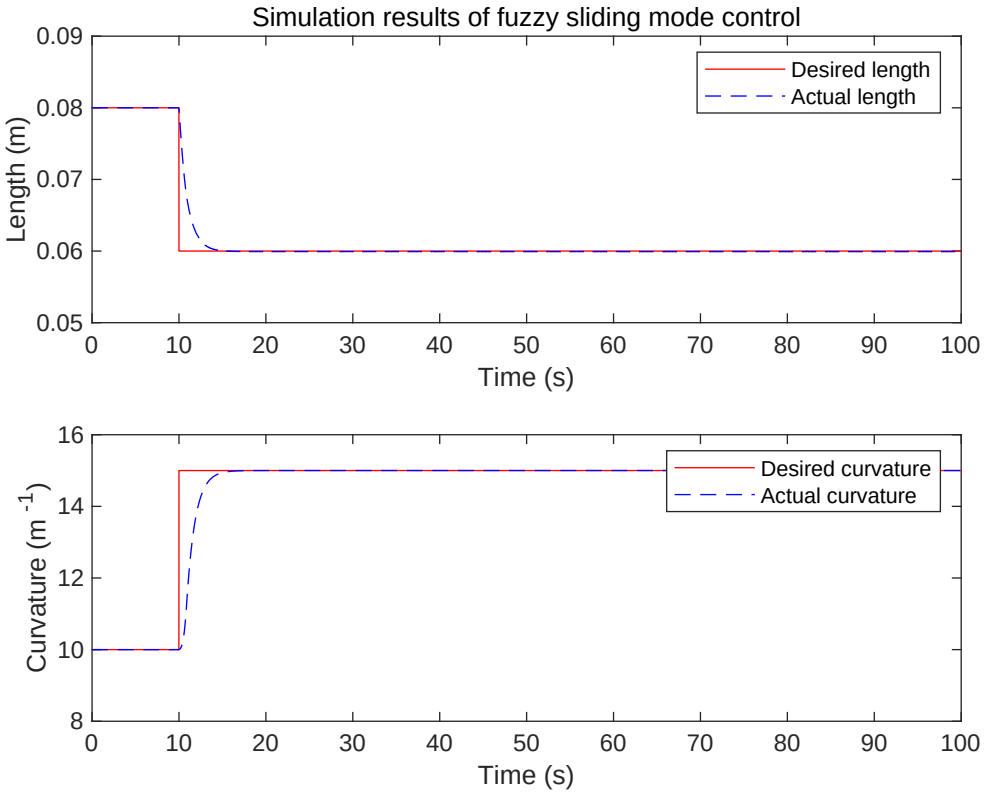

Figure 5.21: The step response of fuzzy sliding mode control.

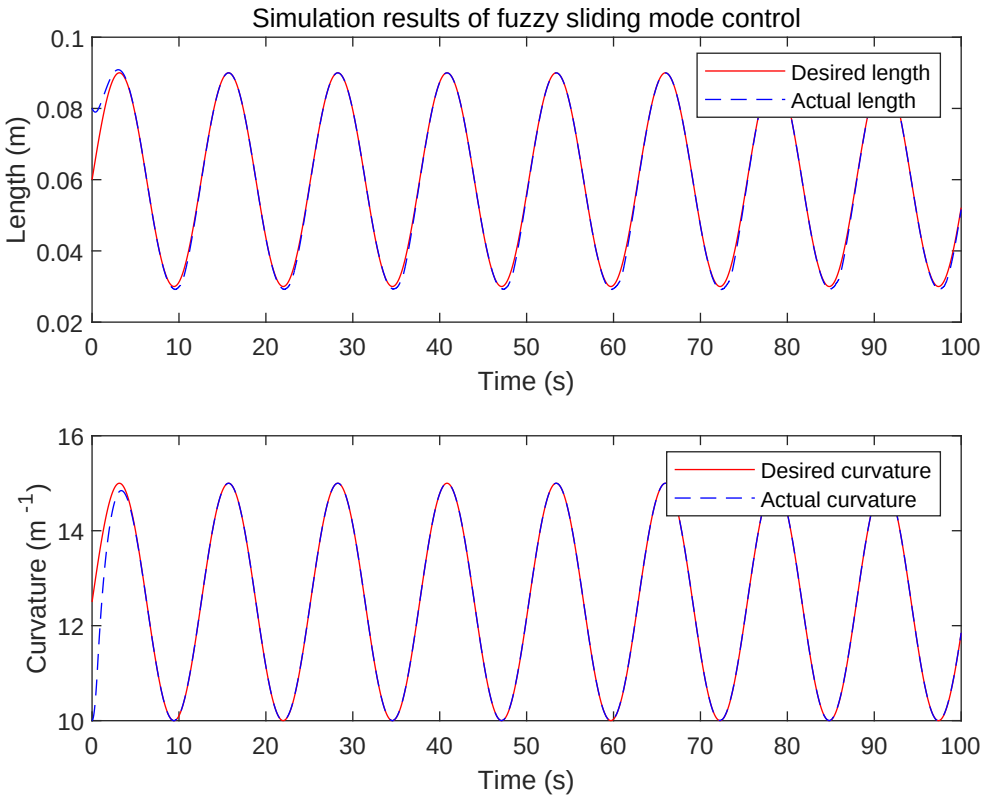

Figure 5.22: The sine wave response of fuzzy sliding mode control.

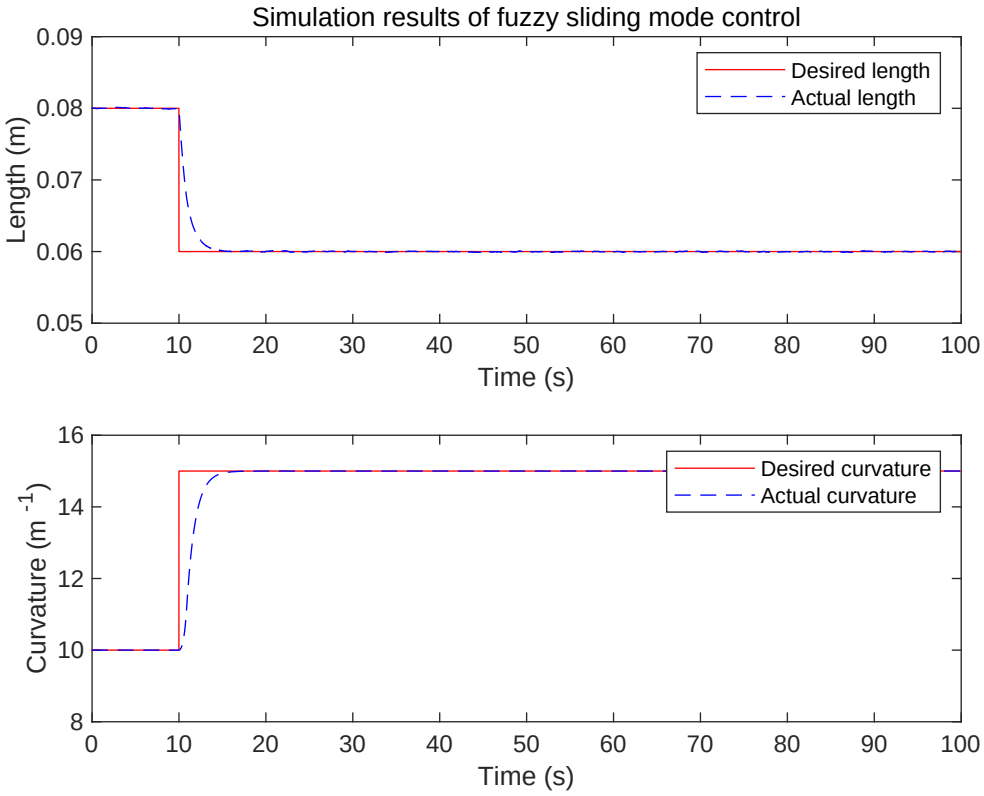

Figure 5.23: The step response of fuzzy sliding mode control with noise.

most. Therefore, the advantage of applying fuzzy sliding mode control is obvious that the chattering problem can be significantly eliminated. The fuzzy sliding mode control improves the system performance by instantly tuning the feedback gains to meet the system requirement. The high gains are used to guarantee to the system stability and overcome uncertainty problems when $\mathbf{s}$ is far from the surface $\mathbf{s} = 0$. When $\mathbf{s}$ becomes closer to the surface $\mathbf{s} = 0$, the lower gains are applied which can effectively avoid the chattering problem. Therefore, compared with inverse dynamic control and sliding mode control, fuzzy sliding mode control can keep the advantage of robustness, in the meantime of eliminating the chattering problem.

5.9 Conclusions

In this chapter, the dynamic model of continuum robot manipulator has been derived by using Lagrangian equation of motion. Based on the study of the dynamic model of two-link rigid robot manipulator, we treat the continuum manipulator as a serial of rigid-body slices such that the continuum kinetic and potential energies can be derived by using integral action. Then, we can apply the energy terms to Euler-Lagrangian equation of motion to obtain the dynamic model of continuum manipulator.

Based on the nonlinear model of continuum manipulator, three control strategies

are proposed to realize the control and stabilization of the dynamic system, which are namely inverse dynamic control, sliding mode control and fuzzy sliding mode control. Specifically, the inverse dynamic controller equivalently transforms the nonlinear dynamic system into a new second-order linear system with PID controller applied. Thus, the complex nonlinear system can be treated as linear system where linear control strategies are able to be implemented. Different from inverse dynamic control, the sliding mode controller uses the discontinuous control signal to force the system sliding along the hyper surface with stability. Based on sliding mode control method, the fuzzy logic theory is applied to adaptively change the nonlinear feedback gains varying to the system condition. The two-input-one-output IF-THEN rules are proposed to build a connection between instant system condition and feedback gains. Then the value of three linguistic variables, namely $\mathbf{s}$, $\dot{\mathbf{s}}$ and output $\mathbf{K}$, are chosen based on the engineer's experience to fuzzify numerical input. After processing a 25-rule fuzzy sets, the fuzzy output signal is then defuzzified by weighted average method to be applied as fuzzy sliding mode control feedback gains.

In order to implement the fuzzy-model-based control method, the fuzzy model of continuum manipulator needs to be investigated. First, a simpler example, the fuzzy model of two-link rigid manipulator operating in the horizontal plane, is developed which requires 64 fuzzy rules to represent the nonlinear model of rigid manipulator. The number of fuzzy rules is then reduced to 4 by neglecting the Coriolis and centrifugal forces. Then, the polynomial fuzzy model of continuum manipulator is investigated and simplified with similar techniques as used in two-link rigid manipulator. However, it requires 4096 fuzzy rules to represent the dynamic model of continuum manipulator which is currently not feasible for computation.

The simulation process of continuum manipulator is developed in MATLAB Simulink environment. According to the simulation results, the proposed three closed-loop control methods are all able to stabilize the system and track the reference configuration-space states, which means that the continuum manipulator can be operated to the desired length and curvature.

Specifically, the sliding mode control and fuzzy sliding mode control achieve better tracking performance in shorter settling time than the inverse dynamic control method. Since the inverse dynamic control equivalently changes the system into a decoupled linear second-order system, linear control methods can be further implemented to improve the performance. However, it requires full and accurate knowledge of the nonlinear system. When the measurement noise is introduced into the system, the inverse dynamic control shows the lack of robustness and the system performance is severely deteriorated. In contrary, the sliding mode control demonstrates itself with strong robustness to the system by instantaneously switching control signal according to the system condition. This gives the system a great advantage to minimize the affect of measurement noise. The drawbacks of the sliding

mode control is the existence of chattering problem, where the fuzzy sliding mode control has significant improvement at this point. The fuzzy sliding mode control uses fuzzy logic theory to apply suitable high/low gains through feedback control to attenuate the chattering problem but also inherits the advantage of robustness in traditional sliding mode control.

Future work first aims to continue to investigate the polynomial fuzzy model of continuum manipulator and apply the FMB control methods, such as in Chapters 3 and 4. Due to the high complexity and nonlinear property, the FMB control methods may have more possibility to perform good control on continuum manipulator. Another direction of future work is to implement the proposed control systems on practical applications. The configuration space may need to be switched to other practical control state-space, for example endpoint position coordinates or overall gestures. The practical application may necessarily involve uncertainties and disturbances. Therefore, the robustness of the control system should be drawn with more attention.

Chapter 6

Conclusion and Future Work Plans

6.1 Conclusion

In this thesis, the stability analysis of T-S FMB control system has been successfully investigated with the extensions of practical issues, such as output feedback control, control input saturation and guaranteed cost of system index. The stability conditions have been relaxed through PLMFs of MFD technique. Due to the complex and nonlinear characteristics in the dynamic model, the continuum manipulator is used as the application to implement the fuzzy logic theory to the configuration-space control. The proposed fuzzy sliding model control is proved to output better performance on the continuum manipulator compared to traditional nonlinear control methods. In order to apply the FMB control, the polynomial fuzzy model of the continuum manipulator is proposed with the simplification of neglecting Coriolis and centrifugal forces.

In Chapter 3, the stability analysis of T-S FMB output feedback tracking control is investigated with the extension of considering control input saturation. The T-S fuzzy controller is employed to drive the system states following the reference system states. The $\mathcal{H}_\infty$ performance is introduced to minimize the system tracking error and optimize the system performance. The nonlinear control input saturation problem is tackled by creating a linear sector from local linear upper and lower bounds to include the operating saturation area. Thus, the nonlinear saturation problem can be represented by linear equations to be involved in the stability analysis. The imperfectly matched premises of membership functions and MFD technique are used to relax the stability conditions. Through the verification by simulation examples, the linear sector can be adjusted accordingly to realize the output feedback tracking control for T-S FMB control system stability conditions with control input saturation. The simulation results verify the effectiveness of the proposed output feedback tracking control system to tackle the control input saturation problem and optimize

the system performance subject to the $\mathcal{H}_\infty$ performance.

In Chapter 4, the guaranteed cost of system index, including the system states, outputs and control signals, is considered in the stability analysis of T-S FMB control system in the form of weighted quadratic cost functions. The system stability conditions are obtained by employing Lyapunov stability theory subject to the minimization of the weighted cost index. In order to relax the system stability conditions, the information of membership functions has been included in the stability analysis by using PLMFs approach. The simulation results demonstrate that the system performance can be improved by adjusting the weight of cost function.

In Chapter 5, the dynamic model of continuum manipulator is developed referring to the model of two-link rigid manipulator. The kinetic and potential energies are obtained by considering the continuum manipulator composed of infinite number of slices and applied with integral action. Thus, the dynamic model of continuum manipulator can be obtained through Euler-Lagrangian equation of motion. In order to realize the configuration-space control, two nonlinear control methods are employed to the dynamic model of the continuum manipulator, namely inverse dynamic control and sliding mode control. Both nonlinear control systems are successfully designed and capable of driving the system states to follow the states of the reference system. In order to solve the chattering problem in sliding mode control, fuzzy logic theory is applied to develop fuzzy sliding mode control such that the feedback gains varying adaptively to the system conditions. The test of introducing measurement noise into the control system indicates that the inverse dynamic control requires accurate knowledge of the dynamic system and the system performance can be severely deteriorated by the measurement noise. Therefore, the inverse dynamic control has weaker robustness than the sliding mode control. The fuzzy sliding mode control demonstrates superior robustness property than the classic sliding mode control and also effectively attenuates the chattering problem by applying adaptive low/high gains according to system status. Then, in order to implement the FMB control to the continuum manipulator, the polynomial fuzzy model of continuum manipulator is proposed referring to the fuzzy model of two-link rigid manipulator operating in the horizontal plane. The dynamic model is simplified by neglecting Coriolis and centrifugal forces such that the number of nonlinear items in the state-space form can be reduced. However, it still requires 4096 fuzzy rules to transform the dynamic model of continuum manipulator to the polynomial fuzzy model due to the existence of 12 nonlinear items.

In conclusion, the thesis successfully investigates the stability analysis of T-S FMB control system with the extension of control input saturation and guaranteed cost of system index. The stability conditions are relaxed by using MFD approach with PLMFs technique. The research results are verified by numerical examples in the environment of MATLAB simulation. The continuum manipulator is considered

as an application to implement the fuzzy logic to nonlinear control method. According to the simulation results in MATLAB SIMULINK, the fuzzy sliding mode control provides the control system with better robustness than inverse dynamic control and effectively eliminates the chattering problem in classic sliding mode control. Then, the polynomial fuzzy model of continuum manipulator is developed in a process of simplification in order to further apply FMB control methods in future.

6.2 Future Work

Although considerable works have been achieved in this thesis, there are still plenty of improvement and further research topics can be extended. The future work extended from this thesis mainly relates to two parts of research.

One is the further extension of FMB control system stability analysis. Specifically, it is perspectively to extend the current research work to the polynomial-fuzzy-model-based (PFMB) control system [40]. As an extension of T-S fuzzy model, the polynomial fuzzy model has recently attracted many attentions from researchers due to its compatibility of polynomial terms in fuzzy model design. When considering a complex nonlinear dynamic model, it is sometimes more applicable to contain polynomial terms in fuzzy model, rather than restricted in linear terms as in T-S fuzzy model. In fact, the T-S fuzzy model is a special case of polynomial fuzzy model when the polynomial terms are zero-th order polynomials. However, it also brings the complexity in handling polynomial terms in stability analysis when using polynomial fuzzy model, which needs to be dealt with SOS technique [41].

Another aspect for future work locates on the fuzzy model design of the continuum manipulator. According to currently work, it is very challenging to build the fuzzy model of continuum manipulator due to its high nonlinearity. Although some simplification has been applied where the Coriolis and centrifugal forces are neglected, the dynamic model of continuum manipulator still requests as many as 4096 fuzzy rules to present the polynomial fuzzy model. Therefore, there is still many work needs to be done in order to reduce the number of fuzzy rules and simplify the polynomial fuzzy model of continuum manipulator. Additionally, the control of configuration space variables in this thesis also can be extended to other control state-space, such as endpoint position coordinates [141] or overall gestures which are more applicable in practical applications. After obtaining the polynomial fuzzy model of continuum manipulator, the PFMB control system stability analysis and further extension techniques can be investigated to improve the system performance.

Appendix A

Awarded Poster

Fuzzy Control of Continuum Manipulator

Yan Yu, Qian Shi, and H.K. Lam

Centre for Robotics Research, Department of Informatics, King's College London

INTRODUCTION

The continuum manipulator is inspired by some natural biological features, such as elephant trunks and tentacles. The continuum manipulator has its particular advantages which traditional rigid-link manipulator does not have. Its unique compliant structure enables the manipulator with high number of degrees of freedom. Thus, the continuum manipulator is capable of working in different environments where the rigid-link manipulator cannot achieve.

H. Yahya, T. Mossman. "Biomimetics, Technology imitates nature", *Global Pub.*, 2006.

P. Ben-Tzvi, P. Moubarak," A Mechatronic Perspective on Robotic Arms and End-Effectors", *Intelligent Mechatronics.*

A fuzzy model proposed by Takagi and Sugeno, namely T-S fuzzy model, can facilitate that any smooth nonlinear control systems is able to be approximated by linear rule consequence and formulated by weighted sum of linear subsystems. Each linear subsystem features one characteristic of the local nonlinear system, where the corresponding weight is determined by membership functions.

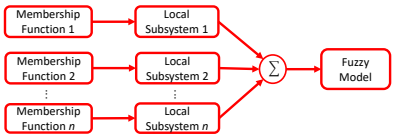

BACKGROUND KNOWLEDGE

The dynamic model of continuum manipulator [1] can be considered as infinite number of rigid-property slices σ with infinitesimal width and being perpendicular along the backbone curve. It can be obtained by presenting the system kinetic energy and potential energy in the form of Euler-Lagrange representation, where $q(t) = [l(t) \quad k(t)]^T$, $l(t)$ and $k(t)$ represent the contraction and curvature, respectively.

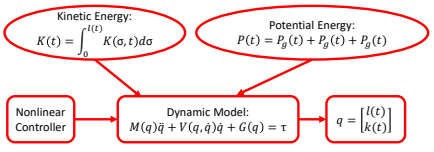

Due to the complexity in dynamic model of continuum manipulator, it is very challenging to apply nonlinear control methods directly to the system. Based on the dynamic model, paper [2] proposes two nonlinear control strategies, namely inverse dynamic control and sliding mode control. However, either of them needs the exact mathematical model of dynamic system or performs critical oscillation in the results

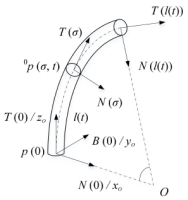

Previous control method [2] applied:

- Inverse Dynamic Control

Exact Mathematical Model Required

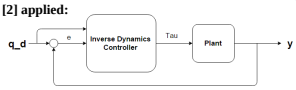

- Sliding Mode Control

Oscillation Exists

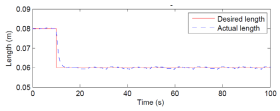

METHODOLOGY

- **T-S Fuzzy-Model-Based (FMB) Control**

It is notable that an effective way to represent a complex nonlinear system is the T-S FMB approach [3] which can approximate smooth nonlinear system by linear rule consequence and formulate with weighted sum of linear subsystems. However, due to the high nonlinearity, it is still very difficult to use T-S fuzzy model to represent the dynamic system which could involve more than 2^{16} number of rules for linear subsystems.

- **Polynomial-Fuzzy-Model-Based (PFMB) Control**

Due to the difficult shown from T-S FMB control, the research method has been extended to the PFMB control system [3]. Different from TS FMB approach, PFMB approach allows polynomial terms to exist in the model and the stability analysis which can effectively reduce the complexity of fuzzy system.

- **Model Simplification**

Some simplification can be applied to alleviate the pressure of calculation during this process. For example, the term $\dot{l}(t) \cdot \dot{k}(t)$ can be assumed as zero, which means the movement of contraction and curving cannot happen at same time. It can be seen as a decomposition of continuum manipulator's movement.

- **System Stability Analysis**

After obtained the PFMB dynamic model of the continuum manipulator, the stability analysis can be proceeded in the forms of sum of squares (SOS) and the solution to the stability conditions can be solved numerically. In order to reduce the conservativeness of analysis results, membership-function-dependant (MFD) approach will be used to include the information of membership functions to the stability conditions.

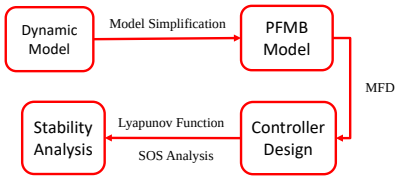

REFERENCES

1. P. Qi, C. Liu, H. K. Lam, and K. Althoefer, "Kinematic control of continuum manipulators using a fuzzy-model-based approach," *IEEE Trans. Industrial Electronics*, vol. 63, no. 8, pp. 5022–5035, 2016.
2. Y. Yu, P. Qi, K. Althoefer, and H. K. Lam, "Lagrangian dynamics and nonlinear control of a continuum manipulator," *IEEE Conf. Robotics and Biomimetics (ROBIO)*, pp. 1912–1917, 2015.
3. H. K. Lam, "A review on stability analysis of continuous-time fuzzy-model-based control systems: From membership-function-independent to membership-function-dependent analysis," *Engineering Applications of Artificial Intelligence*, vol. 67, pp. 390–408, 2018.

yan.yu@kcl.ac.uk

Bibliography

[1] H. K. Lam, "A review on stability analysis of continuous-time fuzzy-model-based control systems: From membership-function-independent to membership-function-dependent analysis," *Engineering Applications of Artificial Intelligence*, vol. 67, pp. 390–408, 2018.

[2] H. K. Lam and S. H. Tsai, "Stability analysis of polynomial-fuzzy-model-based control systems with mismatched premise membership functions," *IEEE Trans. Fuzzy Syst.*, vol. 22, no. 1, pp. 223–229, 2014.

[3] H. A. Antosiewicz, "Linear control systems," *Archive for Rational Mechanics and Analysis*, pp. 313–324, 1963.

[4] H. Kwakernaak and R. Sivan, *Linear Optimal Control Systems*. New York: Wiley-Interscience, 1972.

[5] Z. Sun and S. Ge, "Analysis and synthesis of switched linear control systems," *Automatica*, vol. 41, no. 2, pp. 181–195, 2005.

[6] T. Hu, R. Andrew, and Z. Luca, "Anti-windup synthesis for linear control systems with input saturation: Achieving regional, nonlinear performance," *Automatica*, vol. 44, no. 2, pp. 512–519, 2008.

[7] K. Ogata, *Designing Linear Control Systems with MATLAB*. Englewood Cliffs, NJ: Prentice Hall, 1994.

[8] P. Caines, *Linear Stochastic Systems*. SIAM, 2018.

[9] G. Goodwin, F. Stefan, and E. Mario, *Control System Design*. Upper Saddle River, 2001.

[10] H. Khalil, *Nonlinear Control*. New York: Pearson, 2015.

[11] M. Farza, "State observation of a nonlinear system: Application to (bio) chemical processes," *AIChE Journal*, vol. 45, no. 1, pp. 93–106, 1999.

[12] G. Meyer, R. Su, and R. Louis, "Application of nonlinear transformations to automatic flight control," *Automatica*, vol. 20, no. 1, pp. 103–107, 1984.

[13] R. Wallen, "System theory and practical applications of biomedical signals," *Biomedical Instrumentation and Technology*, vol. 38, no. 3, pp. 220–220, 2004.

[14] P. Kumar and P. Dwarka, "Recent philosophies of automatic generation control strategies in power systems," *IEEE Trans. Power Systems*, vol. 20, no. 1, pp. 346–357, 2005.

[15] R. Olfati-Saber, "Nonlinear control of underactuated mechanical systems with application to robotics and aerospace vehicles," *Diss. Massachusetts Institute of Technology*, 2001.

[16] Z. Dygadlo and A. Krzyanowski, "Dynamics of non-autonomous spatial motion of an aeroplane with deformable control systems," *Technical Physics*, vol. 25, no. 1, 1984.

[17] L. Zadeh, "Fuzzy sets," *Information and Control*, vol. 8, no. 3, pp. 338–353, 1965.

[18] ——, "Outline of a new approach to the analysis of complex systems and decision processes," *IEEE Trans. Syst., Man., and Cybern.*, vol. 1, pp. 24–44, 1973.

[19] ——, "The concept of a linguistic variable and its application to approximate reasoning—i," *Information Sciences*, vol. 8, no. 3, pp. 199–249, Jun. 2011.

[20] M. Braae and D. Rutherford, "A fuzzy relations in a control setting," *Kybernetes*, vol. 7, no. 3, pp. 185–188, 1978.

[21] N. Mandic, E. Scharf, and E. Mamdani, "Practical application of a heuristic fuzzy rule-based controller to the dynamic control of a robot arm," *IEEE Proc. of the D-Control Theory and Applications*, vol. 132, no. 4, 1985.

[22] J. Han, "Control theory, is it a model analysis approach or a direct control approach?" *Journal of Syst. Science and Mathematical Science*, vol. 9, no. 4, pp. 328–335, 1989.

[23] T. Johansen, "Fuzzy model based control: Stability, robustness, and performance issues," *IEEE Trans. Fuzzy Syst.*, vol. 2, no. 3, pp. 221–234, 1994.

[24] T. Takagi and M. Sugeno, "Fuzzy identification of systems and its applications to modelling and control," *IEEE Trans. Syst., Man., and Cybern.,*, vol. 15, no. 1, pp. 116–132, Jan. 1985.

[25] H. O. Wang, K. Tanaka, and M. F. Griffin, "Parallel distributed compensation of nonlinear systems by Takagi-Sugeno fuzzy model," *Proc. of the IEEE Int. Conf. on Fuzzy Syst.*, vol. 2, pp. 531–538, 1995.

[26] H. K. Lam and J. Lauber, "Membership-function-dependent stability analysis of fuzzy-model-based control systems using fuzzy Lyapunov functions," *Information Sciences*, vol. 232, pp. 253–266, 2013.

[27] M. Bernal, T. M. Guerra, and A. Kruszewski, "A membership-function-dependent approach for stability analysis and controller synthesis of Takagi-Sugeno models," *Fuzzy Sets and Syst.*, vol. 160, no. 19, pp. 2776–2795, 2009.

[28] A. M. Lyapunov, "Polynomial fuzzy-model-based control systems: stability analysis via piecewise-linear membership functions," *Int. Journal of Control*, vol. 55, no. 3, pp. 531–534, 1992.

[29] E. Kalman, "Lyapunov functions for the problem of Lur'e in automatic control," *Proc. of the The National Academy of Sciences*, vol. 49, no. 2, pp. 201–205, 1963.

[30] W. Tan and P. Andrew, "Stability region analysis using polynomial and composite polynomial Lyapunov functions and sum-of-squares programming," *IEEE Trans. Automatic Control*, vol. 53, no. 2, p. 565, 2008.

[31] X. Koutsoukos and J. Panos, "Design of stabilizing switching control laws for discrete-and continuous-time linear systems using piecewise-linear Lyapunov functions," *Int. Journal of Control*, vol. 75, no. 12, pp. 932–945, 2002.

[32] K. Tanaka, O. Hiroshi, and H. O. Wang, "A descriptor system approach to fuzzy control system design via fuzzy Lyapunov functions," *IEEE Trans. Fuzzy Syst.*, vol. 15, no. 3, pp. 333–341, 2007.

[33] O. F. A. Dembo and T. Kailath, "High-order absolutely stable neural networks," *IEEE Trans. Fuzzy Syst.*, vol. 38, no. 1, pp. 57–65, 1991.

[34] A. Sala and C. Ariño, "Asymptotically necessary and sufficient conditions for stability and performance in fuzzy control: Applications of Polya's theorem," *Fuzzy Sets Syst.*, vol. 158, no. 24, pp. 2671–2686, Jul. 2007.

[35] V. Montagner, R. Oliveira, and P. Pedro, "Convergent LMI relaxations for quadratic stabilizability and H_∞ control of Takagi-Sugeno fuzzy systems," *IEEE Trans. Fuzzy Syst.*, vol. 17, no. 4, pp. 863–873, 2009.

[36] F. Delmotte, K. Mohamed, and A. Ellouz, "Comparison between Pólya's theorem and sum-of squares approaches for relaxing conditions in fuzzy control," *Int. Journal of Sciences and Techniques of Automatic Control and Computer Engineering*, vol. 4, no. 2, pp. 1420–1437, 2010.

[37] M. Narimani and H. K. Lam, "Relaxed LMI-based stability conditions for Takagi-Sugeno fuzzy control systems using regional-membership-function-shape-dependent analysis approach," *IEEE Trans. Fuzzy Syst.*, vol. 17, no. 5, pp. 1221–1228, Oct 2009.

[38] T. G. M. Bernal and A. Kruszewski, "A membership-function-dependent stability analysis of Takagi-Sugeno models," *IFAC Proceedings Volumes*, vol. 41, no. 2, pp. 5611–5616, 2008.

[39] H. K. Lam and M. Narimani, "Quadratic-stability analysis of fuzzy-model-based control systems using staircase membership functions," *IEEE Trans. Fuzzy Syst.*, vol. 18, no. 1, pp. 125–137, 2010.

[40] H. K. Lam, "Polynomial fuzzy-model-based control systems: stability analysis via piecewise-linear membership functions," *IEEE Trans. Fuzzy Syst.*, vol. 19, no. 3, pp. 588–593, Jun. 2011.

[41] M. Narimani and H. K. Lam, "SOS-based stability analysis of polynomial fuzzy-model-based control systems via polynomial membership functions," *IEEE Trans. Fuzzy Syst.*, vol. 18, no. 5, pp. 862–871, 2010.

[42] H. K. Lam and L. Seneviratne, "Stability analysis of polynomial fuzzy-model-based control systems under perfect/imperfect premise matching," *IET Control Theory and Applications*, vol. 5, no. 15, pp. 1689–1697, 2011.

[43] B. Wei and Y. Kuo, "Pevaluation of fuzzy operators with membership function translation approach," *IEEE Proc. of the Computational Intelligence Conf.*, 1994.

[44] X. Li, H. K. Lam, F. Liu, and X. Zhao, "Stability and stabilization analysis of positive polynomial fuzzy systems with time delay considering piecewise membership functions," *IEEE Trans. Fuzzy Syst.*, vol. 25, no. 4, pp. 958–971, 2017.

[45] H. K. Lam, "Stabilization of nonlinear systems using sampled-data output-feedback fuzzy controller based on polynomial-fuzzy-model-based control approach," *IEEE Trans. Syst., Man., and Cybern., Part B: Cybern.*, vol. 42, no. 1, pp. 258–267, 2012.

[46] S. S. Chang and T. Peng, "Adaptive guaranteed cost control of systems with uncertain parameters," *IEEE Trans. Automatic Control*, vol. 17, no. 4, pp. 474–483, 1972.

[47] X. Guan and C. Chen, "Delay-dependent guaranteed cost control for Takagi-Sugeno fuzzy systems with time delays," *IEEE Trans. Fuzzy Syst.*, vol. 12, no. 2, pp. 236–249, 2004.

[48] L. Yu and J. Chu, "An LMI approach to guaranteed cost control of linear uncertain time-delay systems," *Automatica*, vol. 35, no. 6, pp. 1155–1159, 1999.

[49] J. Slotine and S. Sastry, "Tracking control of non-linear systems using sliding surfaces, with application to robot manipulators," *Int. Journal of Control*, vol. 38.

[50] T. Clmen and P. Stephen, "Nonlinear optimal tracking control with application to super-tankers for autopilot design," *Automatica*, vol. 40, no. 11, pp. 1845–1863, 2004.

[51] T. Kim, "A novel maximum power point tracking control for photovoltaic power system under rapidly changing solar radiation," *Proc. of the ISIE*, vol. 2, 2001.

[52] X. Jia, "Fuzzy H_∞ tracking control for nonlinear networked control systems in T–S fuzzy model," *IEEE Trans. Syst., Man., and Cybern., Part B: Cybern.*, vol. 39, no. 4, pp. 1073–1079, 2009.

[53] X. Sun, Y. Gao, and C. Wu, "Output tracking control for a class of continuous-time t–s fuzzy systems," *Neurocomputing*, vol. 152, pp. 199–208, 2015.

[54] C. S. Tseng, B. S. Chen, and H. J. Uang, "Fuzzy tracking control design for nonlinear dynamic systems via TS fuzzy model," *IEEE Trans. Fuzzy Syst.*, vol. 9, no. 3, pp. 381–392, 2001.

[55] L. Xie, "Output feedback H_∞ control of systems with parameter uncertainty," *Int. Journal of control*, vol. 63, no. 4, pp. 741–750, 1996.

[56] Y. Cao and M. Paul, "Analysis and synthesis of nonlinear time-delay systems via fuzzy control approach," *IEEE Trans. Fuzzy Syst.*, vol. 8, no. 2, pp. 200–211, 2000.

[57] Y. Liu, "Fuzzy approximation-based adaptive backstepping optimal control for a class of nonlinear discrete-time systems with dead-zone," *IEEE Trans. Fuzzy Syst.*, vol. 24, no. 1, pp. 16–28, 2016.

[58] H. Su, "Semi-global leader-following consensus of linear multi-agent systems with input saturation via low gain feedback," *IEEE Trans. Circuit and Syst.*, vol. 60, no. 7, pp. 1881–1889, 2013.

[59] S. Ferrari and F. Robert, "Smooth function approximation using neural networks," *IEEE Trans. Neural Networks*, vol. 16, no. 1, pp. 24–38, 2005.

[60] G. S. Chirikjian and J. W. Burdick, "A hyper-redundant manipulator," *IEEE Robotics and Automation Magazine*, vol. 1, no. 4, pp. 22–29, 1994.

[61] ——, "A modal approach to hyper-redundant manipulator kinematics," *IEEE Trans. Robotics and Automation*, vol. 10, no. 3, pp. 343–354, 1994.

[62] G. S. Chirikjian, "Hyper-redundant manipulator dynamics: a continuum approximation," *Advanced Robotics*, vol. 9, no. 3, pp. 217–243, 1994.

[63] H. Mochiyama and T. Suzuki, "Dynamical modelling of a hyper-flexible manipulator," *Proc. of the 41st SICE Annual Conf.*, vol. 3, pp. 1505–1510, 2002.

[64] T. Yoshimura, "Active suspension of vehicle systems using fuzzy logic," *Int. Journal of Syst. Sciences*, vol. 27, no. 2, pp. 215–219, 1996.

[65] A. R. Frisancho, *Human Adaptation and Accommodation.* University of Michigan Press, 1993.

[66] K. Derinkuyu and C. Mustafa, "On the s-procedure and some variants," *Mathematical Methods of Operations Research*, vol. 64, no. 1, pp. 55–77, 2006.

[67] F. Zhang, *The Schur Complement and Its Applications.* Springer Science and Business Media, 2006.

[68] K. Tanaka and H. O. Wang, *Fuzzy Control Systems Design and Analysis: A Linear Matrix Inequality Approach.* John Wiley & Sons, 2004.

[69] Y. W. Liang, S. D. Xu, and L. W. Ting, "T-S model-based SMC reliable design for a class of nonlinear control systems," *IEEE Trans. Industrial Electronics*, vol. 56, no. 9, pp. 3286–3295, 2009.

[70] K. Tanaka, H. Ohtake, and H. O. Wang, "A practical design approach to stabilization of a 3-DOF RC helicopter," *IEEE Trans. Control Syst. Technology*, vol. 12, no. 2, pp. 315–325, 2004.

[71] Y. A. Almatheel and A. Abdelrahman, "Speed control of DC motor using fuzzy logic controller," in *IEEE Int. Conf. Communication, Control, Computing and Electronics Engineering (ICCCCEE), 2017*, 2017, pp. 1–8.

[72] K. Tanaka and M. Sugeno, "Stability analysis and design of fuzzy control systems," *Fuzzy sets and syst.*, vol. 45, no. 2, pp. 135–156, Jan. 1992.

[73] I. Alaayed, H. El Bahja, and P. Vega, "A sliding mode based on fuzzy logic control for photovoltaic power system using DC-DC boost converter," in *IEEE Int. Conf. Syst. and Control (ICSC), 2013*, 2013, pp. 320–325.

[74] H. O. Wang, K. Tanaka, and M. F. Griffin, "An approach to fuzzy control of nonlinear systems: Stability and design issues," *IEEE Trans. Fuzzy Syst.*, vol. 4, no. 1, pp. 14–23, Feb. 1996.

[75] K. Tanaka, T. Ikeda, and H. O. Wang, "Fuzzy regulators and fuzzy observers: Relaxed stability conditions and LMI-based designs," *IEEE Trans. Fuzzy Syst.*, vol. 6, no. 2, pp. 250–265, May 1998.

[76] E. Kim and H. Lee, "New approaches to relaxed quadratic stability condition of fuzzy control systems," *IEEE Trans. Fuzzy Syst.*, vol. 8, no. 5, pp. 523–534, 2000.

[77] X. Liu and Q. Zhang, "New approaches to H_∞ controller designs based on fuzzy observers for Takagi-Sugeno fuzzy systems via LMI," *Automatica*, vol. 39, no. 9, pp. 1571–1582, 2003.

[78] ——, "Approaches to quadratic stability conditions and H_∞ control designs for Takagi-Sugeno fuzzy systems," *IEEE Trans. Fuzzy Syst.*, vol. 11, no. 6, pp. 830–839, Dec. 2003.

[79] M. C. Teixeira, E. Assuncao, and R. G. Avellar, "On relaxed LMI-based designs for fuzzy regulators and fuzzy observers," *IEEE Trans. Fuzzy Syst.*, vol. 11, no. 5, pp. 613–623, Oct. 2003.

[80] C. Fang, Y. S. Liu, S. W. Kau, L. Hong, and C. H. Lee, "A new LMI-based approach to relaxed quadratic stabilization of Takagi-Sugeno fuzzy control systems," *IEEE Trans. Fuzzy Syst.*, vol. 14, no. 3, pp. 386–397, Jun. 2006.

[81] H. K. Lam, "Stability analysis of sampled-data fuzzy controller for nonlinear systems based on switching T-S fuzzy model," *Nonlinear Analysis: Hybrid Systems*, vol. 3, no. 4, pp. 418–432, 2009.

[82] X. Su, P. Shi, L. Wu, and Y. Song, "A novel control design on discrete-time Takagi–Sugeno fuzzy systems with time-varying delays," *IEEE Trans. Fuzzy Syst.*, vol. 21, no. 4, pp. 655–671, 2013.

[83] H. Li, J. Yu, C. Hilton, and H. Liu, "Adaptive sliding-mode control for nonlinear active suspension vehicle systems using T-S fuzzy approach," *IEEE Trans. Industrial Electronics*, vol. 60, no. 8, pp. 3328–3338, 2013.

[84] S. P. Boyd, *Linear Matrix Inequalities in System and Control theory*. Society for Industrial and Applied Mathematics (SIAM), 1994.

[85] K. Zhang, B. Jiang, and P. Shi, "Fault estimation observer design for discrete-time Takagi-Sugeno fuzzy systems based on piecewise Lyapunov functions," *IEEE Trans. Fuzzy Syst.*, vol. 20, no. 1, pp. 192–200, 2012.

[86] J. Qiu, G. Feng, and H. Gao, "Static-Output-Feedback H_∞ control of continuous-time T-S fuzzy affine systems via piecewise Lyapunov functions," *IEEE Trans. Fuzzy Syst.*, vol. 21, no. 2, pp. 245–261, 2013.

[87] H. K. Lam and F. H. F. Leung, "Stability analysis of fuzzy control systems subject to uncertain grades of membership," *IEEE Trans. Syst., Man., and Cybern., Part B: Cybern.*, vol. 35, no. 6, pp. 1322–1325, Dec. 2005.

[88] H. K. Lam and M. Narimani, "Stability analysis and performance deign for fuzzy-model-based control system under imperfect premise matching," *IEEE Trans. Fuzzy Syst.*, vol. 17, no. 4, pp. 949–961, Aug 2009.

[89] H. K. Lam, B. Xiao, Y. Yu, X. Yin, H. Han, S. H. Tsai, and C. S. Chen, "Membership-function-dependent stability analysis and control synthesis of guaranteed cost fuzzy-model-based control systems," *Int. Journal of Fuzzy Syst.*, vol. 18, no. 4, pp. 537–549, 2016.

[90] H. K. Lam, C. Liu, L. Wu, and X. Zhao, "Polynomial fuzzy-model-based control systems: Stability analysis via approximated membership functions considering sector nonlinearity of control input," *IEEE Trans. Fuzzy Syst.*, vol. 23, no. 6, pp. 2202–2214, 2015.

[91] T. Lee, M. Leoky, and N. H. McClamroch, "Geometric tracking control of a quadrotor UAV on SE(3)," in *IEEE Conf. Decision and Control (CDC), 2010*, 2010, pp. 5420–5425.

[92] H. F. Ho, Y. K. Wong, and A. B. Rad, "Robust fuzzy tracking control for robotic manipulators," *Simulation Modelling Practice and Theory*, vol. 15, no. 7, pp. 801–816, 2007.

[93] H. K. Lam, "Output-feedback tracking control for polynomial fuzzy model-based control systems," in *Polynomial Fuzzy Model-Based Control Systems*. Springer, 2016, pp. 175–196.

[94] T. Hu and Z. Lin, *Control Systems with Actuator Saturation: Analysis and Design*. Springer Science & Business Media, 2001.

[95] F. Yang and Y. Li, "Set-membership filtering for systems with sensor saturation," *Automatica*, vol. 45, no. 8, pp. 1896–1902, 2009.

[96] F. L. Lewis, J. Campos, and R. Selmic, *Neuro-Fuzzy Control of Industrial Systems with Actuator Nonlinearities*. SIAM, 2002.

[97] S. Sui, Y. Li, and S. Tong, "Adaptive fuzzy control design and applications of uncertain stochastic nonlinear systems with input saturation," *Neurocomputing*, vol. 156, pp. 42–51, 2015.

[98] Y. Cao and Z. Lin, "Robust stability analysis and fuzzy-scheduling control for nonlinear systems subject to actuator saturation," *IEEE Trans. Fuzzy Syst.*, vol. 11, no. 1, pp. 57–67, 2003.

[99] Y. Zhao and H. Gao, "Fuzzy-model-based control of an overhead crane with input delay and actuator saturation," *IEEE Trans. Fuzzy Syst.*, vol. 20, no. 1, pp. 181–186, 2012.

[100] N. Kapoor, A. R. Teel, and P. Daoutidis, "An anti-windup design for linear systems with input saturation," *Automatica*, vol. 34, no. 5, pp. 559–574, 1998.

[101] Q. Zhou, L. Wang, C. Wu, H. Li, and H. Du, "Adaptive fuzzy control for nonstrict-feedback systems with input saturation and output constraint," *IEEE Syst., Man., and Cybern.*, vol. 47, no. 1, pp. 1–12, 2017.

[102] Y. Li, S. Tong, and T. Li, "Adaptive fuzzy output-feedback control for output constrained nonlinear systems in the presence of input saturation," *Fuzzy Sets and Syst.*, vol. 248, pp. 138–155, 2014.

[103] Y. Liu, X. Ban, F. Wu, and H. K. Lam, "Gain-scheduling control of TS fuzzy systems with actuator saturation," *Journal of Intelligent & Fuzzy Syst.*, vol. 32, no. 3, pp. 2579–2589, 2017.

[104] M. Sugeno and G. T. Kang, "Structure identification of fuzzy model," *Fuzzy sets and syst.*, vol. 28, no. 1, pp. 15–33, Oct. 1988.

[105] W. Lu and J. Doyle, "H_∞ control of nonlinear systems via output feedback: a class of controllers," *IEEE Conf. Decision and Control*, pp. 166–171, 1993.

[106] I. Petersen, V. Ugrinovskii, and A. Savkin, *Robust Control Design Using H_∞ Methods*. Springer Science & Business Media, 2012.

[107] H. K. Lam, *Polynomial Fuzzy Model-Based Control Systems: Stability Analysis and Control Synthesis Using Membership Function Dependent Techniques*. Springer, 2016.

[108] G. Feng, "A survey on analysis and design of model-based fuzzy control systems," *IEEE Trans. Fuzzy Syst.*, vol. 14, no. 5, pp. 676–697, 2006.

[109] A. Sala, T. M. Guerra, and R. Babuška, "Perspectives of fuzzy systems and control," *Fuzzy Sets and Syst.*, vol. 156, no. 3, pp. 432–444, Dec. 2005.

[110] H. O. Wang, K. Tanaka, and M. F. Griffin, "An approach to fuzzy control of nonlinear systems: stability and design issues," *IEEE Trans. Fuzzy Syst.*, vol. 4, no. 1, pp. 14–23, 1996.

[111] E. Kim and H. Lee, "New approaches to relaxed quadratic stability condition of fuzzy control systems," *IEEE Trans. Fuzzy Syst.*, vol. 8, no. 5, pp. 523–534, 2000.

[112] C. Liu, H. K. Lam, X. Zhang, H. Li, and S. H. Ling, "Relaxed stability conditions based on Taylor series membership functions for polynomial fuzzy-model-based control systems," pp. 2111–2118, 2014.

[113] S. H. Esfahani, S. R. Moheimani, and I. R. Petersen, "LMI approach to suboptimal guaranteed cost control for uncertain time-delay systems," in *IEE Proc. of the Control Theory and Applications*, vol. 145, no. 6, 1998, pp. 491–498.

[114] K. Tanaka, H. Ohtake, and H. O. Wang, "Guaranteed cost control of polynomial fuzzy systems via a sum of squares approach," *IEEE Trans. Syst., Man., and Cybern., Part B: Cybern.*, vol. 39, no. 2, pp. 561–567, 2009.

[115] H. K. Lam, H. Li, C. Deters, E. L. Secco, H. A. Wurdemann, and K. Althoefer, "Control design for interval type-2 fuzzy systems under imperfect premise matching," *IEEE Trans. Industrial Electronics*, vol. 61, no. 2, pp. 956–968, Feb. 2014.

[116] M. F. Robinette and R. Manseur, "Systems engineering of agricultural robot design," *IEEE Trans. Syst., Man., and Cybern., Part B: Cybern.*, vol. 24, no. 8, pp. 1259–1265, 1994.

[117] Y. Edan and G. E. Miles, "Robot-draw, an internet-based visualization tool for robotics education," *IEEE Trans. Education*, vol. 44, no. 1, pp. 29–34, 2001.

[118] P. Qi, C. Liu, L. Zhang, S. Wang, H. Lam, and K. Althoefer, "Fuzzy logic control of a continuum manipulator for surgical applications," *IEEE Int. Conf. Robotics and Biomimetics (ROBIO)*, pp. 413–418, 2014.

[119] V. C. Anderson and R. C. Horn, "Tensor arm manipulator design," *Trans. the ASME*, vol. 67, no. 57, pp. 1–12, 1967.

[120] P. Qi, C. Qiu, H. Liu, J. S. Dai, L. Seneviratne, and K. Althoefer, "A novel continuum-style robot with multilayer compliant modules," *Proc. of the IEEE/RSJ Int. Conf. on Intelligent Robots and Systems (IROS)*, pp. 3175–3180, 2014.

[121] "Hansen medical inc." *From http://www.hansenmedical.com.*

[122] M. W. Spong and M. Vidyasagar, "Robot Dynamics and Control," 2008.

[123] H. Mochiyama and T. Suzuki, "Kinematics and dynamics of a cable-like hyper-flexible manipulator," *IEEE Int. Conf. Robotics and Automation (ICRA)*, pp. 3672–3677, 2003.

[124] E. Tatlicioglu, I. D. Walker, and D. M. Dawson, "Dynamic modelling for planar extensible continuum robot manipulators," *IEEE Int. Conf. Robotics and Automation (ICRA)*, pp. 1357–1362, 2007.

[125] ——, "New dynamic models for planar extensible continuum robot manipulators," *Proc. of the IEEE/RSJ Int. Conf. on Intelligent Robots and Systems (IROS)*, pp. 1485–1490, 2007.

[126] I. D. Walker, "Continuous backbone "continuum" robot manipulators," *ISRN Robotics*, 2013.

[127] W. Khalil, G. Gallot, and F. Boyer, "Dynamic modeling and simulation of a 3-D serial eel-like robot," *IEEE Trans. Systems, Man, and Cybern., Part C: Applications and Reviews*, vol. 37, no. 6, pp. 1259–1268, 2007.

[128] F. Matsuno and H. Sato, "Trajectory tracking control of snake robots based on dynamic model," *IEEE Int. Conf. Robotics and Automation (ICRA)*, pp. 3029–3034, 2005.

[129] A. Kapadia and I. D. Walker, "Task-space control of extensible continuum manipulators," *Proc. of the IEEE/RSJ Int. Conf. Intelligent Robots and Systems (IROS)*, pp. 1087–1092, 2011.

[130] A. Kapadia, I. D. Walker, D. M. Dawson, and E. Tatlicioglu, "A new approach to extensible continuum robot control using the sliding-mode," *Computer Science and Technology*, vol. 2, no. 4, pp. 293–300, 2011.

[131] S. E. Shafiei, "Sliding mode control of robot manipulators via intelligent approaches," *INTECH*, 2010.

[132] J. Slotine and W. Li, "Applied Nonlinear Control," 1991.

[133] F. Y. Hsu and L. C. Fu, "Nonlinear control of robot manipulators using adaptive fuzzy sliding mode control," *IEEE Int. Conf. Intelligent Robots and Syst. 95.'Human Robot Interaction and Cooperative Robots'*, vol. 1, pp. 156–161, 1995.

[134] S. B. Choi and J. Kim, "A fuzzy-sliding mode controller for robust tracking of robotic manipulators," *Mechatronics*, vol. 7, no. 2, pp. 199–216, 1997.

[135] S. Heidari, F. Piltan, and M. Shamsodini, "Design new nonlinear controller with parallel fuzzy inference system compensator to control of continuum robot manipulator," *IEEE Conf. Control and Automation*, vol. 3, pp. 2174–2179, 2003.

[136] E. Bayo, "Inverse dynamics and kinematics of multi-link elastic robots: An iterative frequency domain approach," *The Int. Journal of Robotics Research*, vol. 8, no. 6, pp. 49–62, 1989.

[137] D. Camarillo, "Mechanics modeling of tendon-driven continuum manipulators," *IEEE Trans. Robotics*, pp. 1262–1273, 2008.

[138] M. Siddique and G. Irwin, "Flexible Robot Manipulators," 2008.

[139] P. Qi, H. Liu, L. Seneviratne, and K. Althoefer, "Design, kinematics and prototype of a flexible robot arm with planar springs," *ASME 2015 Int. Design Engineering Technical Conf. Computers and Information*, 2015.

[140] S. B. Nagesh, "Adaptive fuzzy observer and robust controller for a 2-DOF robot arm," *IEEE Int. Conf. Fuzzy Syst.*, pp. 1–7, 2012.

[141] D. Xiao, "Sensor-based hybrid position/force control of a robot manipulator in an uncalibrated environment," *IEEE Trans. Control Syst. Technology*, vol. 8, no. 4, pp. 635–645, 2000.